
Climate Change Initiative Extension (CCI+) Phase 1
New Essential Climate Variables (NEW ECVS)
High-Resolution Land Cover ECV (HR_LandCover_cci)

Product Validation and Intercomparison Report
(PVIR)

Part B – Validation Report

Prepared by:

Università degli Studi di Trento
Fondazione Bruno Kessler
Università degli Studi di Pavia
Università degli Studi di Genova
Université Catholique de Louvain
Politecnico di Milano
Université de Versailles Saint Quentin
CREAF
e-GEOS s.p.a.
Planetek Italia
GeoVille



	Ref	CCI_HRLC_Ph1-D4.1_PVIRb		
	Issue	Date	Page	
	2.rev.2	10/02/2023	1	

Changelog

Issue	Changes	Date
1.0	First version.	17/07/2020
1.1	Second version with the results of the visual qualitative assessment of the RR prototypes	18/08/2020
1.2	The third version includes a section on the quantitative assessment of the RR prototypes for Africa and a section on the qualitative assessment of Amazon and Siberia. It also includes results of inter-comparison with existing land cover for all RR prototypes and static maps in Siberia and Amazon.	18/11/2020
1.3	Updated version according to CCI_HRLC_Ph1_AR2_RID-ESA.xlsx Sections 4.2.2 and 4.2.3 were updated to include results of inter-comparison with Atlas of Urban Expansion as suggested during AR2.	07/12/2020
1.4	Updated with the quantitative assessment of the RR prototypes for Amazonia and Siberia, and update of the quantitative assessment of the RR prototype for Africa. Also includes a qualitative assessment of the African zoom area and Amazonian historical maps.	04/02/2021
2.0	Version of the document for the final review. In this issue the intercomparison analysis (PVIR-Part A) has been separated from the validation one (PVIR-Part B). This document refers to validation report (PVIR-Part B), only.	10/11/2022
2.1	Section 2.2 was updated to take into account changes in the legend of the static LC products v202212 provided mid-December. Section 3 was updated to reflect the augmentation of the number of validation samples. Sections 4.1.1.2, 4.1.2.2, and 4.1.3.2 about the results of the quantitative assessment were also updated accordingly.	23/12/2022
2.2	The qualitative assessment sections were updated to take into account the improvements of the products brought after the final meeting. Updates were made to reporting accuracy figures with the confidence interval. Correction of Table 3. Details were added to the description of the validation database.	10/02/2023

Detailed Change Record

Issue	RID	Description of discrepancy	Sections	Change
1.3	FR-01	It does not match the document version. It should be 'CCI_HRLC_Ph1-PVIR_1.2' instead of 'CCI_HRLC_Ph1-PVIR_2.1'.		The filename of version v1.2 is fixed.
	FR-02	The 'No Data' class (0 value) is not present in the table reporting the new legend	Section 2	Updated Table 1.

	Ref	CCI_HRLC_Ph1-D4.1_PVIRb		
	Issue	Date	Page	
	2.rev.2	10/02/2023	2	

Contents

1	Executive summary	4
1	Introduction	5
1.1	Purpose and scope	5
1.2	Applicable documents	6
1.3	Reference documents	6
1.4	Acronyms and abbreviations	6
2	The CCI HR LC products	7
2.1	Overview	7
2.2	Class codes associated with the CCI HR LC Legend	8
3	Specific validation databases	9
4	Results of the accuracy assessment	11
4.1	Static 10-m sub-continental LC maps 2019	11
4.1.1	Siberia	11
4.1.2	Amazonia	16
4.1.3	Africa	21
4.2	Historical 30-m regional dynamic LC Best Class and change detection maps	24
4.2.1	Siberia	24
4.2.2	Amazonia	27
4.2.3	Africa	30
5	ANNEX –The CCI HRLC hierarchical approach of the legend	36
6	ANNEX – Area-based confusion matrices for the static LC maps v202212	37
6.1	Siberia	37
6.2	Amazonia	38
6.3	Africa	39
7	ANNEX – Results of the previous validation exercises	39
7.1	RR prototypes	40
7.1.1	Visual quality assessment	40
7.1.2	Quantitative quality assessment	65
7.2	Preliminary HRLC static LC map 2019 over a zoom area	89
7.2.1	Visual quality assessment	89
7.3	Quantitative assessment of the previous LC static maps	108
7.3.1	Siberia v20220624	108
7.4	First visual quality assessment of the Amazonia historic LC maps	110
7.4.1	Processing artefacts	110
7.4.2	Area of stable LC	110
7.4.3	Area of LC change	111

	Ref	CCI_HRLC_Ph1-D4.1_PVIRb		
	Issue	Date	Page	
	2.rev.2	10/02/2023	3	

7.4.4 Concluding remarks..... 113

	Ref	CCI_HRLC_Ph1-D4.1_PVIRb		
	Issue	Date	Page	
	2.rev.2	10/02/2023	4	

1 Executive summary

The Product Validation and Intercomparison Report (PVIR) is a living document that describes and presents all activities aimed at evaluating the quality of the various Climate Change Initiative (CCI) High Resolution Land Cover (HR LC) products visually and quantitatively. The benchmarking with other existing LC maps was done in a second version of the PVIR.

After the introduction (Section 1), we briefly describe the CCI HRLC products that were validated (Section 2). Specific validation databases were built by photointerpretation of high and very-high resolution imagery (Section 3). Results of these qualitative and quantitative assessments are detailed in Section 4. Annexes 5 to 7 provide complementary information about the hierarchy of the classes in the legend, the detailed confusion matrices of the products quantitatively validated in Section 4 and the qualitative and quantitative results of the previous validation exercises.

Systematic visual qualitative assessments were performed on each version of the product. This task provides useful complementary insights on the macroscopic errors to quantitative accuracy assessment. The main issues observed in the static LC maps relate to tiles and sensor swath borders affecting the spatial consistency of the classifications. Similar processing artefacts were observed in the historical LC maps.

Specific validations were conducted to estimate the accuracy of the static regional LC maps and historical LC map series. Unlike most quantitative validation exercises reported in the literature, this one is completely independent in terms of the people responsible for production and validation and of the data sources used for processing and validation. This is a requirement from the CEOS-LPVS. This certainly removes the positive bias that might favour the accuracy estimates of maps when a validation sample is obtained as a subset of a larger training sample ensemble or when the same EO time series is used for training and validation. This strict independence must be considered when making comparisons between the accuracy estimates of CCI HRLC maps and maps validated using other protocols, typically less independent.

For the static maps, we evaluated the presence/absence of a LC class at a specific location as described in the PVP [AD6]. For the validation of the historical products, we considered change as a LC transition between pairs of Best Class layers of consecutive periods. Although the validation database includes the year of change, we decided to evaluate only the presence/absence of at least a LC transition over the full period. LC transition is referred to a permanent modification of the LC – and not of the seasonality of the surface – in comparison with baseline status. The validation results provided here should be interpreted in light of this choice. The historical CCI HR LC products consist of several layers (see section 2.1) that could also be validated according to the climate modellers priorities, and given a proper understanding of the definition of the change they represent.

A total of 4546 consolidated samples were retained to build six specific validation databases covering 3 regions and two types of LC products. This consolidation step took place in order to increase the confidence in the obtained results by enhancing the validation sampling. The additional sampling allowed to consider the most recent LC products version provided in December 2022. Samples were interpreted based on HR and VHR imagery, and a long series of NDVI profiles were available through the Collect Earth, Google Earth and Glovis interfaces.

The guidelines described by the CEOS-LPVS also recommend using the map classes for stratification in the case of stratified random sampling. Such stratified random samplings derived from the LC static classes or the LC change detection strata were used for the quantitative validation of the static and historical maps, respectively. Post-stratification cannot be properly performed for missing LC classes in the map, like the class "Aquatic or regularly flooded woody vegetation" in Africa. For the sake of simplicity, this class was not quantitatively validated.

The change detection product was chosen for stratification to focus on high-priority changes from the perspective of climate modellers [AD6], and not necessarily the most obvious changes for classification. This choice is allowed from a statistical point of view but might have biased the sampling on a reduced amount of change and maybe the most difficult landscapes. Another data source for stratification (e.g. the Dynamic LC maps) might have yielded other accuracy estimates. This impact should be further investigated.

Several precautions have been taken to ensure maximum robustness in the reference data. Of all the photo-interpreted samples, only fully homogeneous footprints for which the interpreter was certain of his interpretation were retained for validation. In the case of change validation, erosion was applied to the change stratum so that only change hotspots with a minimum area of 0.81 ha were retained. On the one hand, this increases our certainty about the photointerpretation of large changes. But on the other hand, this has a positive

	Ref	CCI_HRLC_Ph1-D4.1_PVIRb		
	Issue	Date	Page	
	2.rev.2	10/02/2023	5	

effect on the final accuracy since only significantly large change is considered in the confusion matrices. The selection of homogenous samples and the focus on the hot spot of LC change also aim at reducing the issue of geolocation between the reference datasets and the HR LC products.

We first quantitatively evaluated the static LC maps with their original legend of 15-16 LC classes depending on the region. In Siberia, the distinction between the leaf seasonality of evergreen and deciduous shrubs could not be photointerpreted with certainty. The two types of shrubs were merged into a single "Shrub Cover" class for validation. We also performed a second assessment using an aggregated legend where shrubs and trees are grouped into a woody vegetation class and where the woody and grassland vegetations are grouped into an aquatic or regularly flooded vegetation class. The first grouping is justified by the current absence of shrub PFT in the ORCHIDEE scheme. The last grouping is to highlight the ability of the maps to detect the wetness of a landscape rather than the vegetation type.

Great improvements in the accuracies of the classifications were demonstrated since the intermediary products (see Section 7) and the final version of the HR LC products over zoom areas. The final area-based overall accuracies range from $70.1 \pm 3.7 \%$ to $81.7 \pm 2.9 \%$ for the static LC maps with the class grouping, and from $57.8 \pm 4.3 \%$ to $67.9 \pm 3.5 \%$ for the static maps in their full legend. The Amazonia static map yields the best accuracy figures, probably due to the presence of compact LC patterns with few dominant and contrasted mapped LC classes. The Siberia and Africa static LC maps show closer accuracy estimates around 70% and 60%. These lower estimates are not surprising given the complexity of both landscapes. In all maps, misclassifications between forest types and between forest and shrubs types were observed. Grasslands seem to be overestimated in each product.

Large-scale LC classification and LC change detection remain challenging tasks at high resolution. We observed strong discrepancies between the validation database and the maps, especially in the evaluation of LC change. The reasons could be the heterogeneous quality of the EO time series, the robustness of the validation database, the amount and uncertainty associated with the validation and classification sources, the common understanding of the definition of LC change, the minimum mapping unit of the change detection in the LC change algorithm and the validation database, etc. Investigating specifically the reasons of these discrepancies are expected to pave the way to improve the products accuracy performances.

We strongly recommend that several additional analyses be performed to better understand the above-mentioned results. For example, the definition of LC change in the CCI HR LC products could be more precisely specified and, in turn, the reference validation database should be updated. Similarly, it would be interesting to reduce the current stratification bias towards climate modelling priorities. The different quantity of missing images through the years and a sensitivity analysis of the land cover change probability could also bring additional insights to better understand the current discrepancies and possibly increase the robustness of the accuracy estimates of the change class. Accurate large-scale high-resolution LC mapping and more specifically long-term LC change seem to remain a scientific challenge when validated with strictly independent protocols as recommended by CEOS-LPVS.

This document (PVIR-Part B) only includes validation analysis. For the intercomparison analysis, please refer to the PVIR – Part A.

1 Introduction

1.1 Purpose and scope

The Product Validation and Intercomparison Report Part A and B gives a complete report of the activities executed to assess the quality of the following CCI HR Land Cover products:

- HRLC prototypes on limited spatial extents dedicated to a Round Robin (RR) assessment.
- An HRLC map at the zoom level at a spatial resolution of 10m, precursor to the HRLC maps at the subcontinental level.
- An HRLC map at the subcontinental level at a spatial resolution of 10m as reference static input to the climate models.
- A long-term record of regional HRLC maps at a spatial resolution of 30m in sub-regions of the static input for historical analysis every 5 years.
- The change information at 30 m and yearly scale for HRLC map update.

	Ref	CCI_HRLC_Ph1-D4.1_PVIRb		
	Issue	Date	Page	
	2.rev.2	10/02/2023	6	

1.2 Applicable documents

Ref. Title, Issue/Rev, Date, ID

- [AD1] CCI HR Technical Proposal, v1.1, 16/03/2018
 [AD2] CCI Extension (CCI+) Phase 1 – New ECVs – Statement of Work, v1.3, 22/08/2017, ESA-CCI-PRGM-EOPS-SW-17-0032
 [AD3] Data Standards Requirements for CCI Data Producers, v2.0, 17/09/2018, CCI-PRGM-EOPS-TN-13-0009
 [AD4] CCI_HRLC_Ph1-D1.1_URD, the latest version
 [AD5] CCI Extension (CCI+) Phase 1 – Product User Guide (PUG) – v1.1, 04/05/2020, ESA-CCI-HRLC
 [AD6] CCI_HRLC_Ph1-D2.5_PVP, the latest version

1.3 Reference documents

Ref. Title, Issue/Rev, Date, ID

- [RD1] World Meteorological Organization (WMO); United Nations Educational, Scientific and Cultural Organization; Intergovernmental Oceanographic Commission; United Nations Environment Programme; International Science Council, (ISC). The 2022 GCOS ECVs Requirements. GCOS- No. 245. 2022.
 [RD2] Bartsch, Annett; Widhalm, Barbara; Pointner, Georg; Ermokhina, Ksenia; Leibman, Marina; Heim, Birgit (2019): Landcover derived from Sentinel-1 and Sentinel-2 satellite data (2015-2018) for subarctic and arctic environments. Zentralanstalt für Meteorologie und Geodynamik, Wien, GLOBPERMAFROST, <https://doi.org/10.1594/GLOBPERMAFROST.897916>

1.4 Acronyms and abbreviations

CCI	Climate Change Initiative
DN	Digit Number
ESA	European Space Agency
FAO	Food and Agriculture Organization
HR	High Resolution
ISC	International Science Council
LC	Land cover
LCC	Land cover change
LCCS	Land cover classification system
LOGP	Logarithmic opinion pool decision fusion
LSTM	Long Short-Term Memory
LSTM – MC	LSTM Monthly Composite
LSTM – TS	LSTM Time Series
MRF	Markov Random Field decision fusion
NDVI	Normalized Vegetation Index
OA	Overall accuracy
PA	Producer’s accuracy
PVIR	Product Validation and Intercomparison Report
PVP	Product Validation Plan
RF	Random Forest classification algorithm
RR	Round Robin
S2	Sentinel-2
SAR	Synthetic Aperture Radar
SVM	Support Vector Machine classification algorithm
UA	User’s accuracy
UTM	Universal Transverse Mercator coordinate system
VHR	Very High Resolution
WGS84	World Geodetic System 1984
WMO	World Meteorological Organization

2 The CCI HR LC products

2.1 Overview

Three main types of products were generated and validated thematically within the ESA CCI HRLC project:

- **Static 10-m sub-continental LC maps for 2019.** The algorithms from the RR exercise with the best accuracy figures were selected and applied at the sub-continental scale
- **Historical 30-m regional dynamic LC maps** in the **1990-2019** period, generated every five years for the period on reduced areas inside the sub-continental static LC maps. Yet, land cover change was detected on an annual basis among these five-year intervals. **We evaluated the LC transitions between pairs of Best Class layers of consecutive periods.**
- **Historical 30-m change detection maps for 1990-2015** obtained from Landsat 5, 7 and 8 products at a spatial resolution of 30m covering the same extents as the historical 30-m regional LC maps. The change map was produced based on Landsat acquisitions for 1 year from 1990-2019. Each historical change detection map is composed of 4 layers:
 - *Year*: the value is the year in which the pixel has changed and 0 for no-change.
 - *Probability*: the probability of change from 0 to 100
 - *Temporal reliability*: temporal distance between years in which the change has been calculated
 - *PCC*: 1 for the low priority of changes and 2 for the high priority of change.

Each type of product was delivered in the form of tiles and mosaics. The mosaic format was assessed in priority, although the tiles were also checked to some extent for comparison.

In addition, two types of intermediary products were received and validated:

- 10-m Round Robin local LC prototypes for the year 2019, produced through a Round Robin (RR) exercise during which optical and SAR classifications were benchmarked using a quantitative validation scheme.
- a spatial sub-set of the 10-m static sub-continental LC maps for the year 2019

The products will be generated over three areas selected through key users' consultation, with varying extents (Figure 1). The RR sites, in grey, cover 4 Sentinel-2 (S2) tiles located in the Amazonian region (21KUQ, 21KXT), Siberia (42WXS), and Sahel (37PCP). The static LC maps, in green, cover the extended regions in Amazon (including Mato Grosso), Sahel and Siberia. The historical LC maps are restricted to the orange areas.

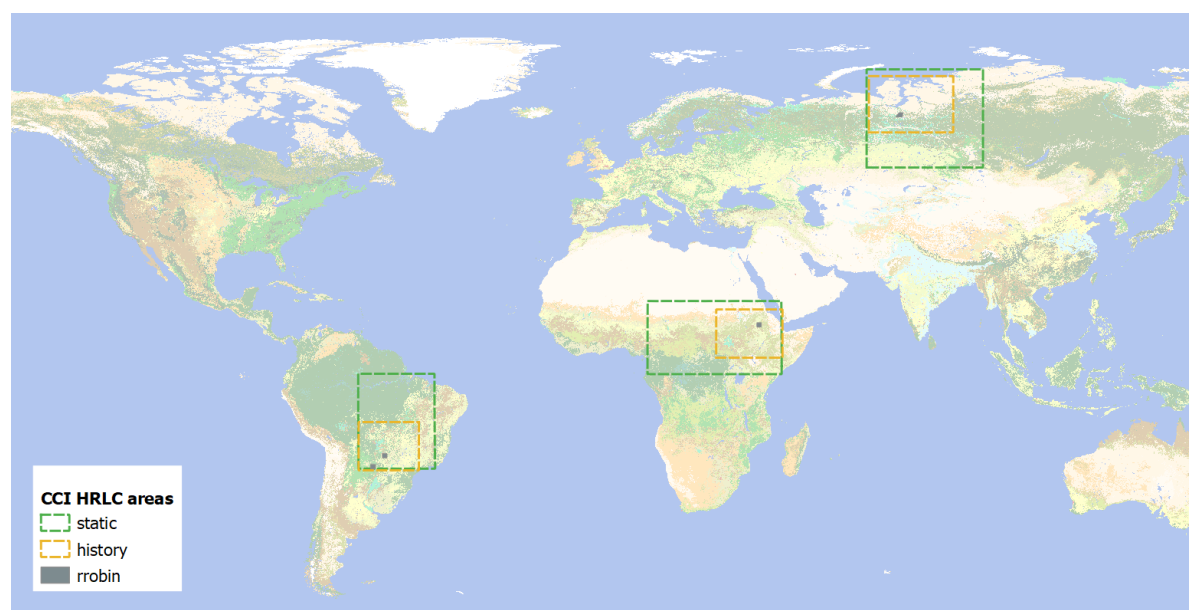


Figure 1: Distribution of the study sites per type of CCI HR LC product.

The geographical coordinates of the three selected regions are the following:

Africa:

- Static map: (0.1°S – 18.1°N; 9.9°E – 43.3°E)

- Historical LC and LCC map: (3.5°N – 16.3°N; 27.0°E – 43.3°E)

Amazonia:

- Static map: (23.6°S - 0°S; 42.9°W – 62.1°W)
- Historical LC and LCC map: (23.6°S – 11.7°S; 46.7°W – 62.1°W)

Siberia:

- Static map: (51.3°N – 75.7°N; 64.4°E – 93.4°E),
- Historical LC and LCC map: (59.4°N – 73.9°N; 64.8°E – 87.4°E).

As the production of the LC map was an iterative process, so were the validation exercises. Table 1 details the date of versions, bands and dates of the products for which validation is presented. Section 4.1 and Section 4.2 detail the results of the quantitative assessment of the last version of static LC products (v202212), and dynamic products respectively. Accuracy figures of the previous validated products can be found in Section 7.

Table 1: Summary of the versions of the products used for validation.

	Static maps 2019	Historic maps, Land cover dynamic
Siberia	v202212, v24062022	v22082022, Best Class layer
Amazonia	v202212, v14042022	v01092022, Best Class layer
Africa	v202212, v27102022	v06102022, Best Class layer

2.2 Class codes associated with the CCI HR LC Legend

Figure 2 details the codes associated with the land cover class labels of the CCI HRLC products. Land cover classes are described using the conventions of the Food and Agriculture Organization (FAO) Land Cover Classification System (LCCS). Static maps of Amazonia and Africa include 16 classes including a distinction of permanent and seasonal water. These DNs are used both for the classification of the static map and for historical maps [AD5].

HRLC CLASSES			
CODE	DESCRIPTION		
0	No data		
10	Tree cover evergreen broadleaf		
20	Tree cover evergreen needleleaf		
30	Tree cover deciduous broadleaf		
40	Tree cover deciduous needleleaf		
50	Shrub cover evergreen		
60	Shrub cover deciduous		
70	Grasslands		
80	Croplands		
90	Woody vegetation aquatic or regularly flooded		
100	Grassland vegetation aquatic or regularly flooded		
110	Lichens and mosses		
120	Bare areas		
130	Built-up		
140	Open water	141	Open water seasonal
		142	Open water permanent
150	Permanent snow and/or ice		

Figure 2. The CCI HR LC legend includes 16 main land cover classes for Africa and Amazonia. Sub-classes “Open Water seasonal” and “Open Water permanent” are merged into “Open Water” in Siberia.

3 Specific validation databases

A total of 4546 consolidated samples, i.e. fully homogeneous and interpreted with high certainty, were retained to build six specific validation databases covering 3 regions and two types of LC products (Table 2).

Table 2. Number of consolidated samples forming the validation databases of each product

Number of consolidated samples	Siberia	Amazonia	Africa	Total
Static LC maps	549	857	748	2154
Historical LC maps	627	970	795	2392

The class "Aquatic or regularly flooded woody vegetation" is absent from the static map of Africa. The initial few reference samples belonging to this class could not be increased using the stratification approach based on the map classes. Therefore, the class was removed from the quantitative accuracy assessment. In Siberia, the distinction between shrub evergreen and deciduous leaf seasonalities could not be photointerpreted with certainty. Both shrub types were merged into a unique "Shrub cover" class for validation.

Table 3, Table 4 and Table 5 detail the number of certain and homogeneous samples by class of the 2019 static maps of Siberia, Amazon, and Africa. Selecting certain and homogeneous samples aims at ensuring the maximum robustness in the reference data despite the possible geolocation errors of the reference VHR imagery, and the potential uncertainty in evaluating the proportions of land surface elements in heterogeneous landscapes. The ratio of retained certain and homogeneous samples to the total number of samples is 82.8, 73.6 and 77.7% for Siberia, Amazon and Africa, respectively. The total number of samples corresponds to the sum of original and augmented samples as described in section 5.2.2 in [AD6].

Table 3. Siberia static class area (m²) and the number of certain and homogeneous samples from the perspective of the reference and the map. Total of samples: 549.

Code	Class label	Area	REF	MAP
20	Tree cover evergreen needleleaf	5.9909E+11	72	73
30	Tree cover deciduous broadleaf	4.7982E+11	48	68
40	Tree cover deciduous needleleaf	1.1759E+11	27	14
50	Shrub cover	9.3333E+10	77	22
70	Grassland	1.0022E+12	110	99
80	Croplands	2.8987E+11	61	64
90	Woody vegetation aquatic or regularly flooded	1.9595E+11	4	35
100	Grassland vegetation aquatic or regularly flooded	1.7079E+11	19	33
110	Lichen and mosses	4.0976E+10	29	33
120	Bare areas	4.6924E+10	26	38
130	Built-up	6451053109	25	21
140	Open Water permanent	3.094E+11	51	49

Table 4. Amazonia static class area (m²) and the number of certain and homogeneous samples from the perspective of the reference and the map. Total of samples: 857.

Code	Class label	Area	REF	MAP
10	Tree cover evergreen broadleaf	2.15E+12	241	237
30	Tree cover deciduous broadleaf	4.05E+11	60	55
50	Shrub cover evergreen	1.07E+11	82	41
60	Shrub cover deciduous	1.34E+11	29	30
70	Grassland	1.77E+12	132	168
80	Croplands	5.26E+11	100	102
90	Woody vegetation aquatic or regularly flooded	6950000000	25	33
100	Grassland vegetation aquatic or regularly flooded	2.58E+10	22	25
120	Bare areas	2.64E+10	24	30
130	Built-up	1.86E+10	36	42
141	Open Water seasonal	6990000000	3	24
142	Open Water permanent	1.48E+11	103	70

Table 5. Africa static class area (m²) and the number of certain and homogeneous samples from the perspective of the reference and the map. Total of samples: 748.

Code	Class label	Area	REF	MAP
------	-------------	------	-----	-----

10	Tree cover evergreen broadleaf	1.16E+12	88	79
30	Tree cover deciduous broadleaf	5.22E+11	43	44
50	Shrub cover evergreen	646000000	32	23
60	Shrub cover deciduous	8.2E+11	56	57
70	Grassland	2.39E+12	126	183
80	Croplands	9E+11	68	69
100	Grassland vegetation aquatic or regularly flooded	2.46E+10	42	46
120	Bare areas	1.31E+12	118	78
130	Built-up	1.19E+10	36	36
141	Open Water seasonal	4260000000	19	50
142	Open Water permanent	2.03E+11	120	83

Figure 3 illustrates various characteristics of the samples used for the validation of the historic CCI HR LC maps for Siberia (a – c), Amazonia (d – f), and Africa (g – i). The certainty of interpretation and homogeneity of the footprints relate to the full validation database while the proportion of stable and change samples describes the final validation database including only certain and homogeneous samples.

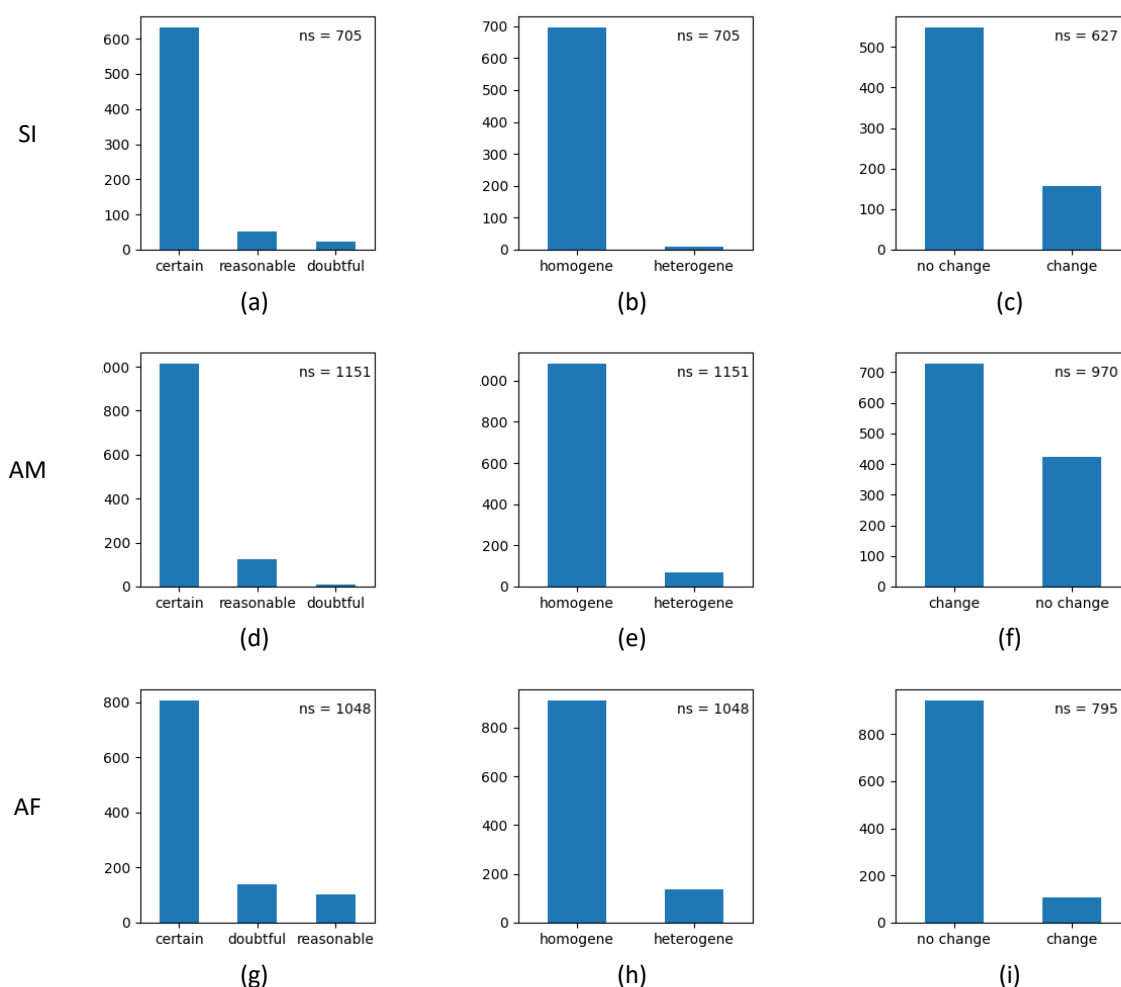


Figure 3. Summary information about the validation database used for the validation of the historical CCI HRLC products. (a-c) Siberia database with (a) the proportion of samples for the three certainty levels of the photointerpretation, (b) the proportion of homogeneous and heterogeneous samples, and (c) the proportion of stable and changed samples among the homogeneous and certain samples forming the final validation database. A similar explanation for Amazonia (d – f) and Africa (g – i). ns is the total number of samples.

	Ref	CCI_HRLC_Ph1-D4.1_PVIRb		
	Issue	Date	Page	
	2.rev.2	10/02/2023	11	

4 Results of the accuracy assessment

4.1 Static 10-m sub-continental LC maps 2019

4.1.1 Siberia

Despite some lingering tile effects, the map looks good, and the water is well delineated, but the major problem is the large amount of grassland that contaminates some classes. Some urban and water pixels contaminate bare areas. Bare areas were sometimes contaminating lakes but this problem has been fixed. The following sections illustrate and detail these problems.

4.1.1.1 Visual qualitative assessment

This section presents the qualitative assessment of the Siberia map (Figure 4). As expected no pixel is classified as “tree cover evergreen broadleaf”. However, the classes “Open water” and “Permanent snow and ice” are missing. Despite some tile effects, the map looks good, and the water is well delimited, but the major problem is the important part of grassland that contaminates some classes.

According to the reference data observed, a lot of areas are covered by snow for around 9 months, sometimes less, sometimes more. According to the definition of the legend, 10 months of snow cover define the permanent snow and ice class (5 - Annex). The representation of the landscape in the Northern latitudes without snow is thus correct in the Siberia maps.

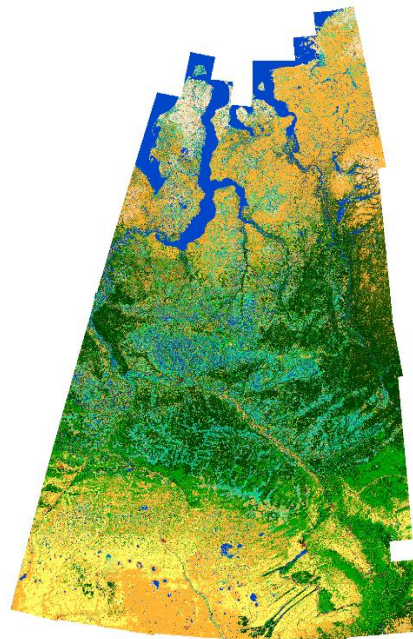


Figure 4. Mosaic of the Siberia static map (WGS84, UTM45N).

4.1.1.1.1 Tile effect

Tile effects were visible all around the 45XWC tiles and led to large differences in identical vegetation patterns in the v17012022 static map. The v24062022 static map is improved as this tile effect disappears, although a small error remains in the north-western part of the map (Figure 5).

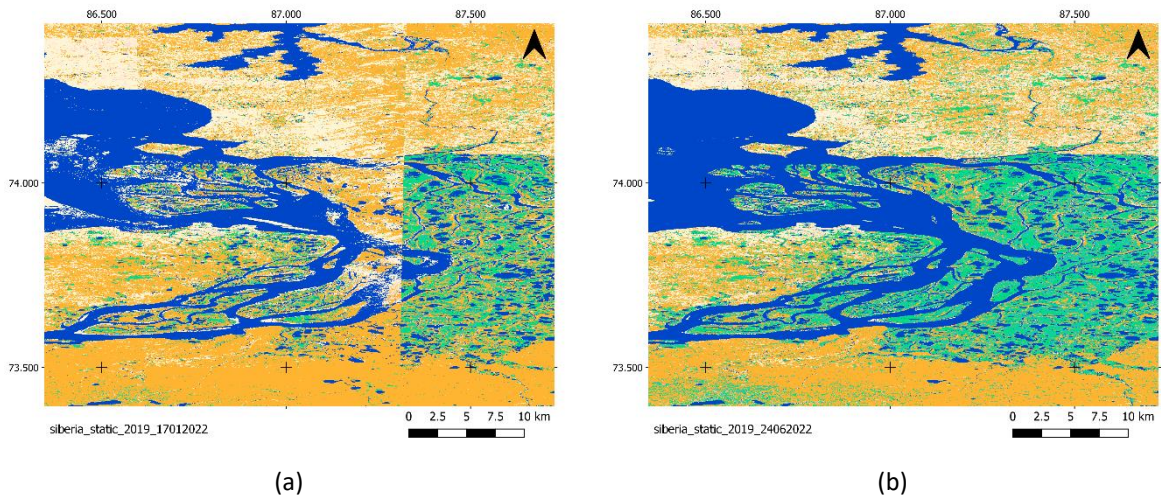


Figure 5. Illustration of an improvement of the tile effect between (a) the static map v17012022 and (b) the static map v24062022.

4.1.1.1.2 Differentiation cropland grassland

Figure 6 shows a good distinction between fields and grasslands. Lakes, urban and forest patches are also well delineated.

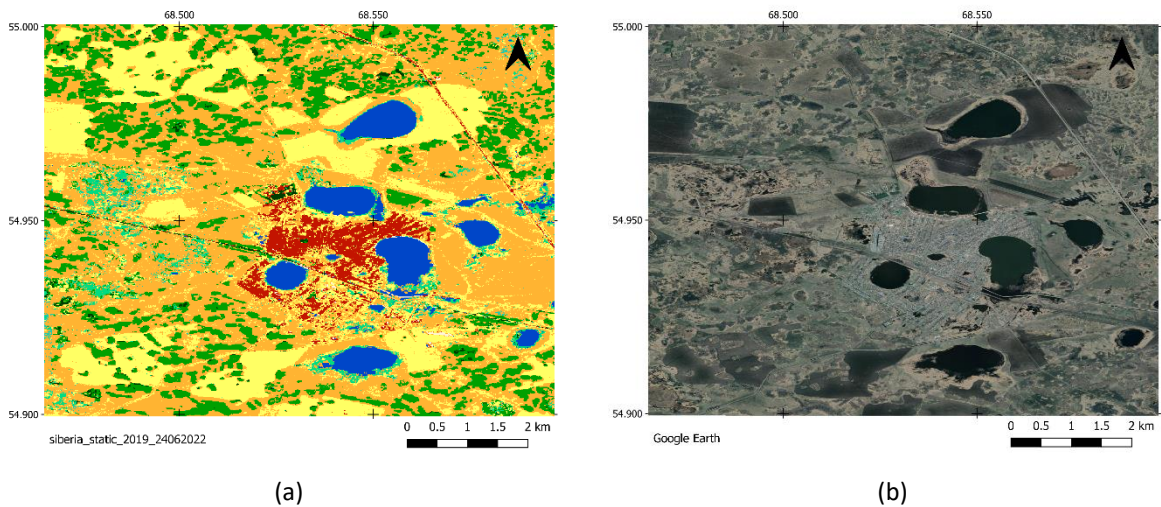


Figure 6. Crop and grassland delineation (a) on the static map v24062022 and (b) on Google Earth.

4.1.1.1.3 Shrub

There are large areas where the static map and the GlobPermafrost map [RD1] disagree for low vegetation areas (Figure 7). The static map tends to place grasslands while the GlobPermafrost map places shrubs. In general, the GlobPermafrost map is correct, as shown by the Google Earth zoom in Figure 7 (d-f).

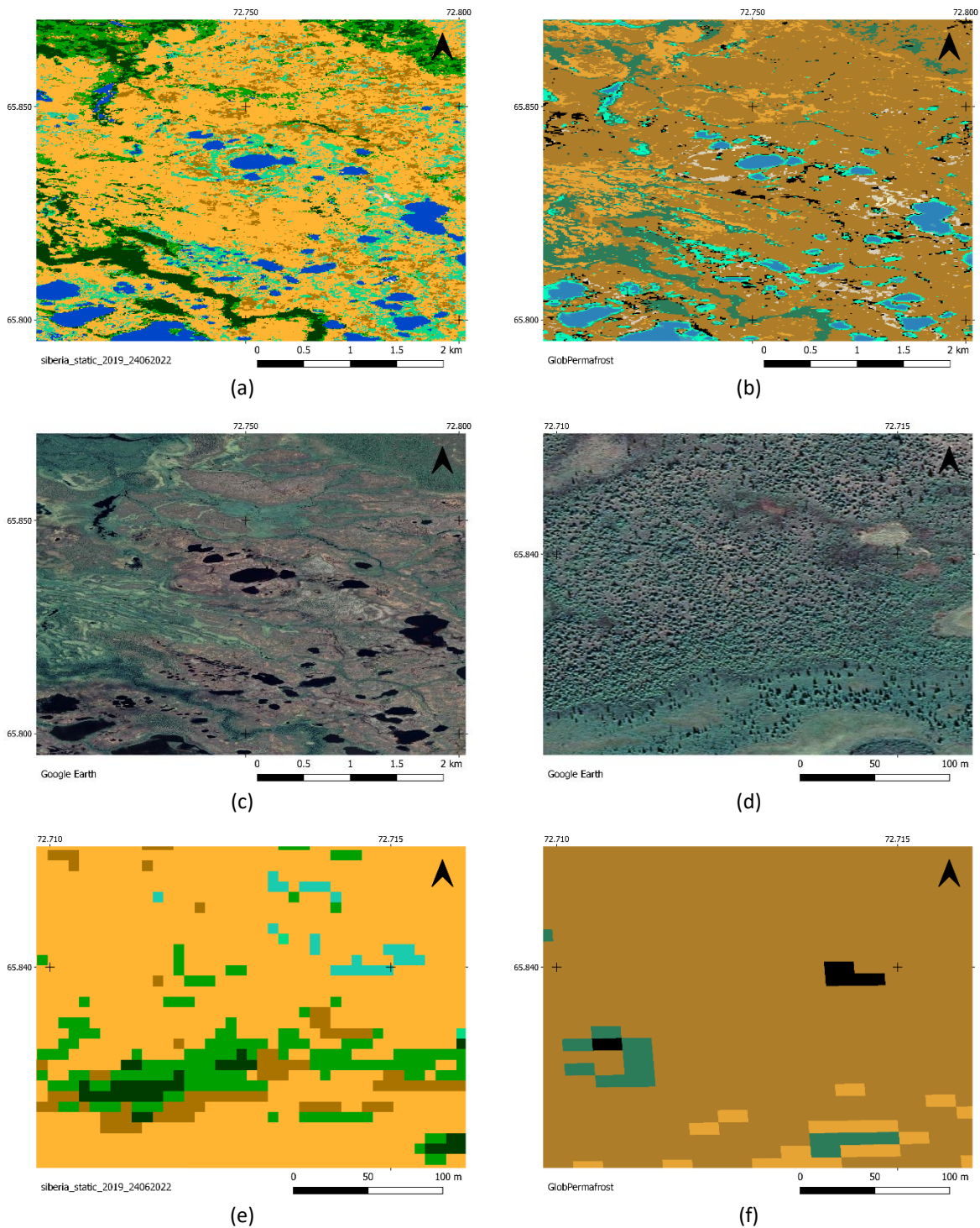


Figure 7. Illustration of the overestimation of grasslands versus shrubs by comparing (a) the static map v24062022, (b) the GlobPermafrost map and (c) Google Earth. Zooming in on the shrubs gives a better view of the problem (d-e-f).

4.1.1.1.4 Trees

The difference between evergreen and deciduous needleleaf trees is sometimes doubtful. Figure 8 shows a straight line delimitation between a majority of deciduous needleleaf in the North and a majority of evergreen in the South while the high-resolution imagery indicates similar vegetation, mostly composed of deciduous trees. The misclassification of the leaf seasonality may be engendered by the tiling effect.

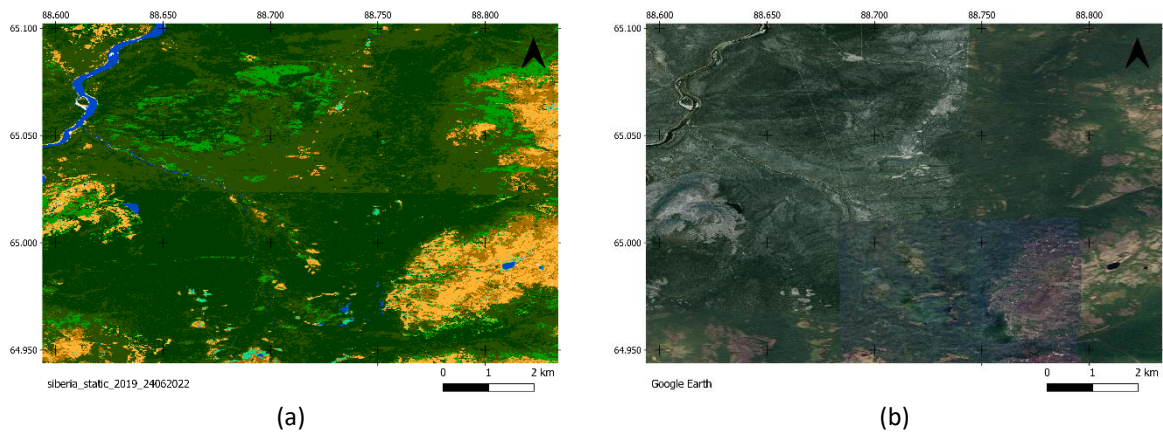


Figure 8: Errors to separate the different forest types.

4.1.1.1.5 Bare areas

According to the legend of the project, extraction sites are supposed to be classified as bare soil but the v24062022 static map systematically classifies them as built-up areas. The new version of the map (v202212) corrects this error and allows for a more accurate classification of mining sites as bare soil.

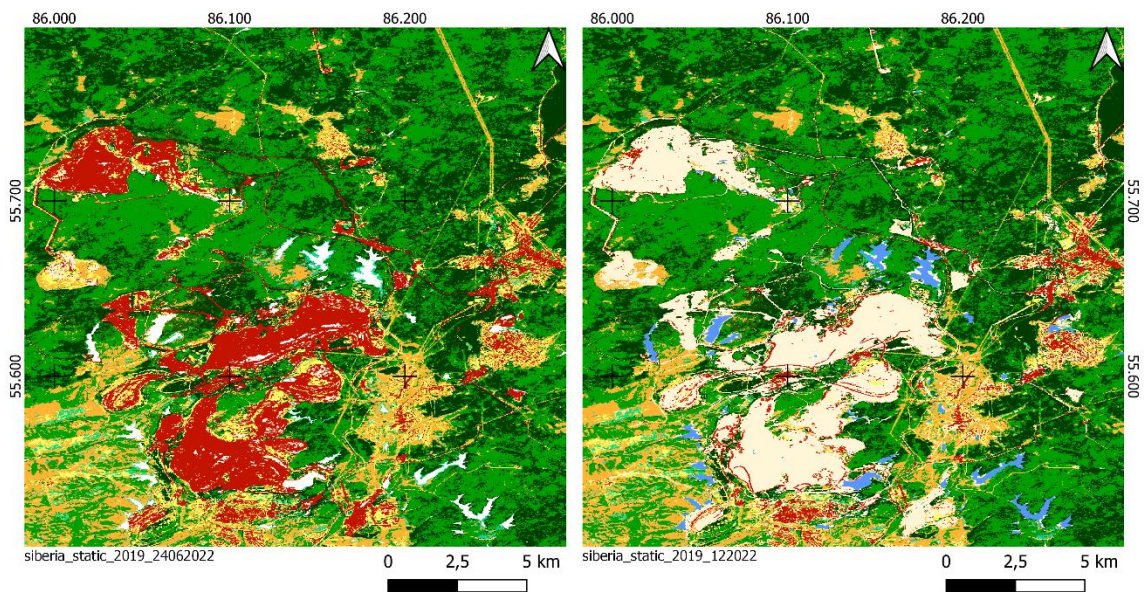


Figure 9: Illustration of a mine that is classified as bare soil in the v202212 map.

4.1.1.1.6 Water bodies

Water bodies are well detected, as shown here with the lakes and with the meanders of a river well defined. (Figure 10). The classification is improved in the v24062022 static map compared to the v17012022 static map since the lake is well classified as a water body and no longer as bare soil (Figure 11).

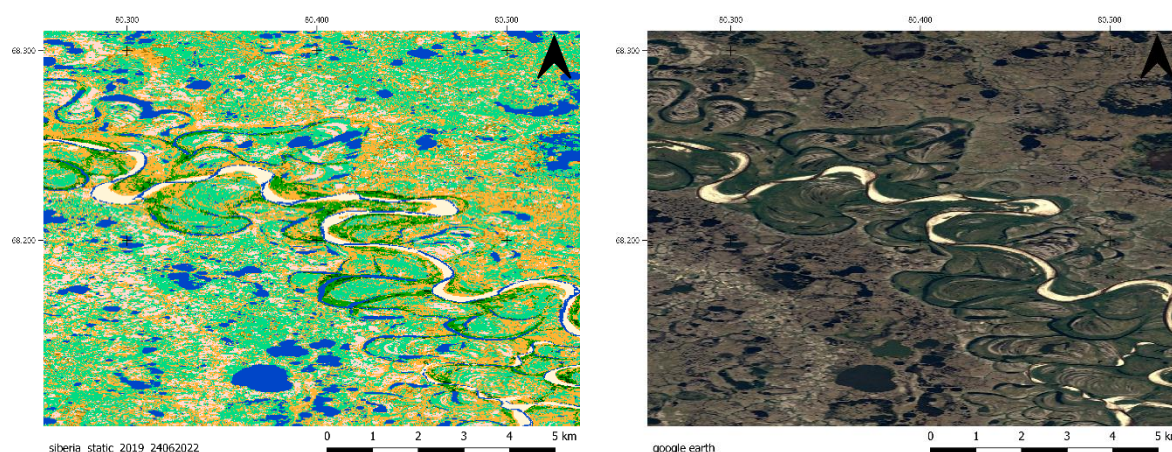


Figure 10. Illustration of wetland and water body detection.

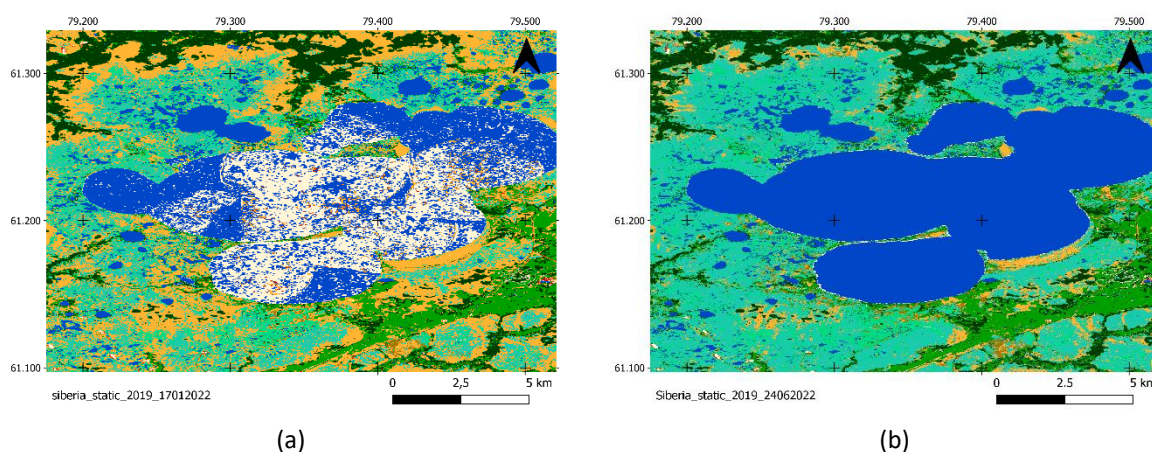


Figure 11. Illustration of improved classification for lakes. (a) the Siberia static map v17012022 (b) the Siberia static map v2.

4.1.1.2 Quantitative assessment

The accuracy estimates of the Siberia static map obtained with the 549 homogeneous and certain samples and the grouping of the original legend show an OA of $70.1 \pm 3.7\%$ (Table 6). This estimate is 12 % higher than the overall accuracy obtained using a legend with a grouping of the shrub types only ($57.8 \pm 4.3\%$, Table 7). This significant difference confirms the difficulty of distinguishing, in the classification and photo-interpretation exercises, tree types, trees from shrubs and shrubs from grasses in an area with dwarf woody vegetation. Area-based confusion matrices are detailed in Section 6.

Along the woody vegetation, the best-classified classes are the “Open Water” and “Croplands” with PA and UA above 90 % (UA = $95.9 \pm 5.7\%$, PA = $93.1 \pm 7.3\%$) and 70 % (UA = $81.2 \pm 9.8\%$; PA = $72.7 \pm 12.7\%$), respectively. The built-up class is well-classified from a user perspective (UA = $85.7 \pm 15.3\%$) but shows high rates of omissions. This version of the static map of Siberia reduces the proportion of the grassland class in favour of the wetland classes (trees or grass) which, according to our samples increases their respective commission error (see Section 7.3 for the assessment of the previous version of the map).

Class “Lichens and mosses” is poorly classified and shows high omission errors (PA = $22.2 \pm 12.5\%$). It is mixed with short vegetation and wetlands (woody and herbaceous). Not surprisingly, robust training and reference data for this class, mostly present at high latitudes, are difficult to obtain. The lack of valid, cloud-free, well-distributed EO data throughout the year may also explain the reduced accuracy of the “Vegetation aquatic or regularly flooded” estimates (UA = $20.6 \pm 9.6\%$ and PA = $51.8 \pm 20.4\%$) for which temporal estimation is critical by definition. Bare areas are the least precise class showing both omissions and commissions.

Table 6. The area-based accuracy estimates of the Siberia static map v202212 with a grouping of the original legend were derived using 549 homogeneous samples photo-interpreted with certainty. Accuracy figures are reported in % with a 95 % confidence interval. OA, PA and UA stand for overall, producer, and user accuracy.

Label	OA (%)	UA (%)	PA (%)
Woody vegetation		88.7 ± 4.7	76 ± 4.5
Grassland		55.6 ± 9.8	69.3 ± 7.1
Croplands		81.2 ± 9.6	72.7 ± 12.7
Vegetation aquatic or regularly flooded	70.1 ± 3.7	20.6 ± 9.6	51.8 ± 20.4
Lichens and mosses		48.5 ± 17.2	22.2 ± 12.5
Bare areas		34.2 ± 15.3	12.9 ± 8.0
Built-up		85.7 ± 15.3	13.2 ± 10.4
Open Water		95.9 ± 5.7	93.1 ± 7.3

Table 7. The area-based accuracy estimates of the Siberia static map v202212 with a grouping of the shrub classes were derived using 549 homogeneous samples photo-interpreted with certainty. Accuracy figures are reported in % with a 95% confidence interval. OA, PA and UA stand for overall, producer, and user accuracy.

Label	OA (%)	UA (%)	PA (%)
Tree cover evergreen needleleaf		68.5 ± 10.8	72.2 ± 8.2
Tree cover deciduous broadleaf		54.4 ± 12.0	76 ± 11.6
Tree cover deciduous needleleaf		42.9 ± 26.9	23.6 ± 13.3
Shrub cover		59.1 ± 21.0	13.8 ± 5.3
Grassland		55.6 ± 9.8	70.5 ± 6.9
Croplands		81.2 ± 9.6	72.8 ± 12.7
Woody vegetation aquatic or regularly flooded	57.8 ± 4.3	2.9 ± 5.7	18.8 ± 34.7
Grassland vegetation aquatic or regularly flooded		15.2 ± 12.3	23.5 ± 17.4
Lichens and mosses		48.5 ± 17.2	22.2 ± 12.5
Bare areas		34.2 ± 15.3	12.9 ± 8.0
Built-up		85.7 ± 15.3	13.2 ± 10.4
Open Water		95.9 ± 5.7	93.2 ± 7.3

4.1.2 Amazonia

4.1.2.1 Visual qualitative assessment

This section shows the qualitative assessment of the Amazonia static map (Figure 12). In general, the map seems quite accurate, at least more accurate than the static map of Siberia.

As expected, no pixels were classified in the categories “Tree cover deciduous needleleaf”, “Lichen and mosses” and “Permanent snow and/or ice”. Some pixels have been classified as “Tree cover evergreen needleleaf”, which was not foreseen but seems correct as needleleaf tree plantations were found in this area. No satellite swaths or tile effects are visible on the map.



Figure 12. Mosaic of the Amazonia Static map (EPSG4326).

As in the Siberian map, grasslands tend to contaminate the other classes, especially the cropland class. Many deforested areas are used as perennial pastures which should be classified as grassland. These two types of agriculture are difficult to differentiate. Favouring grassland over cropland tends to improve the accuracy of the map, although this is not always correct, as shown in Figure 13.

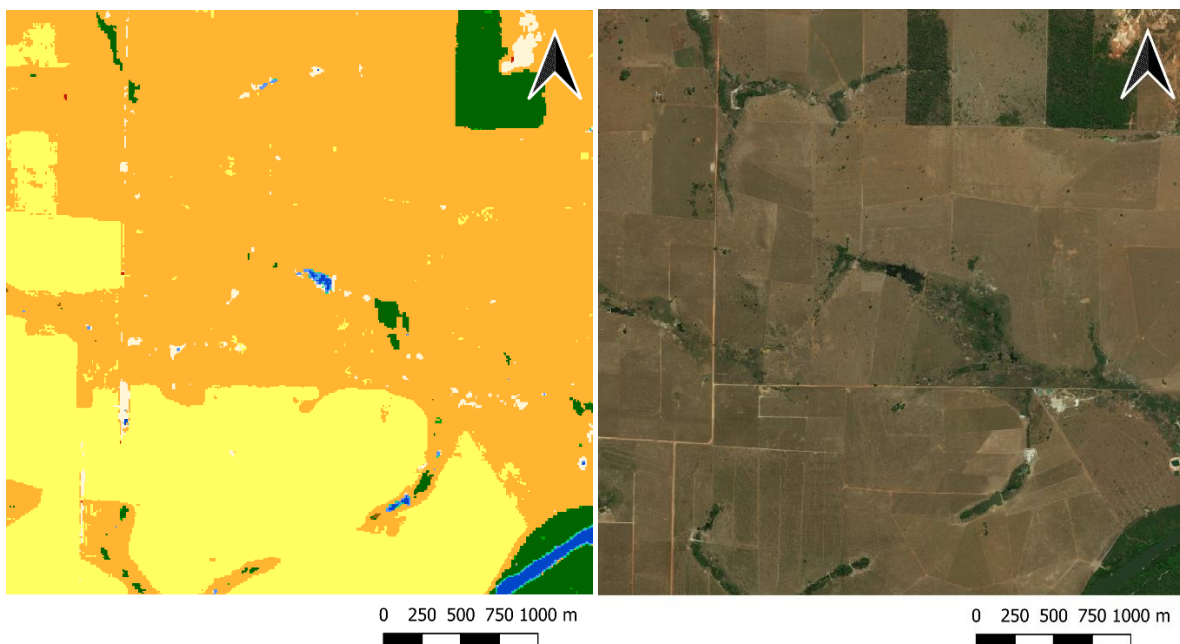


Figure 13. Contamination of crops by grassland (WGS84, -55.12, -10.14).

Much of the mangroves are well classified. The most common error is confusion with the category “Tree cover evergreen broadleaf”.

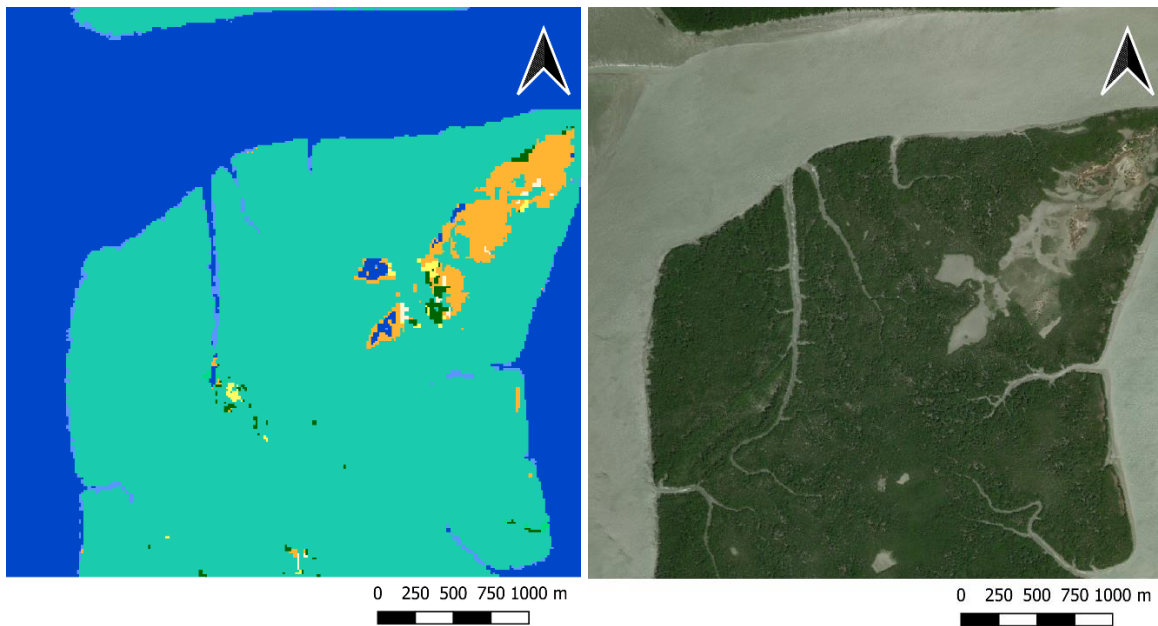


Figure 14. Mangroves are well detected (-45.11, -1.48 EPSG4326).

A small part of the map is filled with an unexpected cover of evergreen needle-leaved trees. The area covered by this class is equal to 0.07% of the map. This class is only present in the lower right corner of the extent and corresponds to tree plantations as shown in Figure 15.

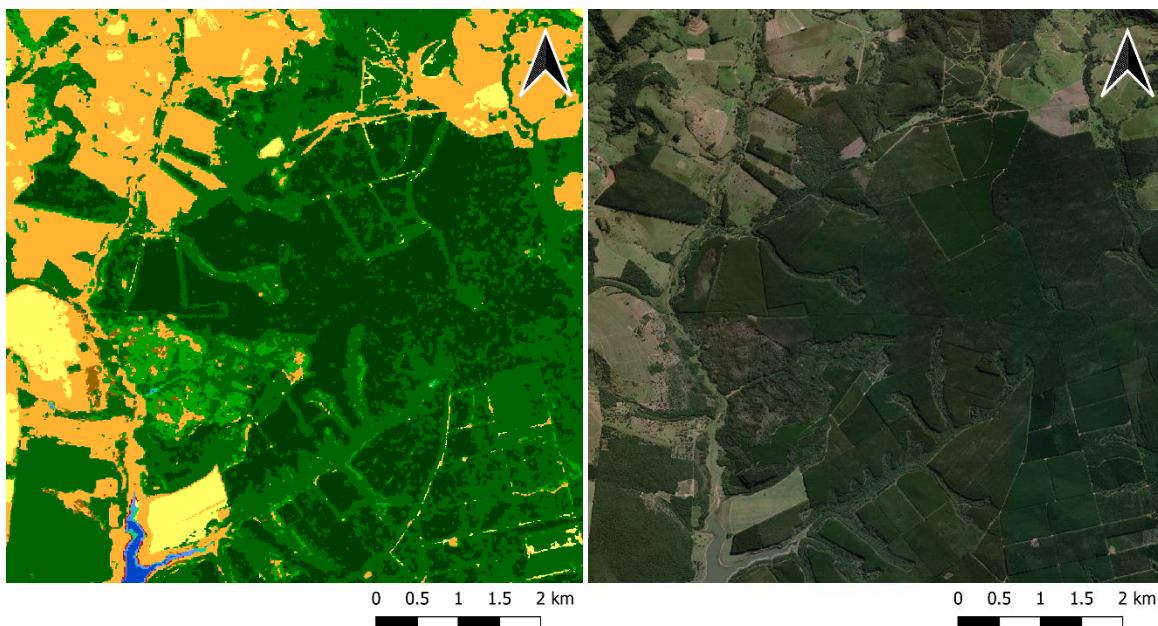
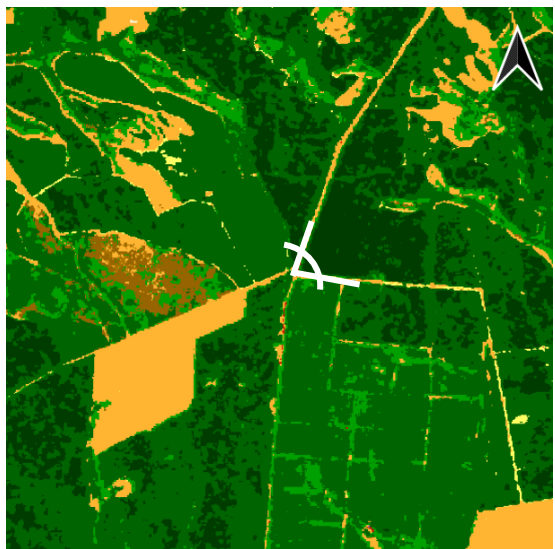


Figure 15. Presence of the class “Tree cover evergreen needleleaf” on the Amazonia static map (WGS84, -48.75, -23.2).

Looking at the VHR images, it is not clear whether these are needle-leaved trees or not. Fortunately, two Google street map views pass by these fields. As we can see from these images (Figure 16), the trees are not needle-leaved and are more likely to be *Eucalyptus sp.* plantations. Almost the entire area covered by the class “Tree cover evergreen broadleaf” should be classified as “Tree cover deciduous broadleaf”, as no VHR image can highlight the presence of needleleaf trees for this area.



0 250 500 750 1000 m



0 0.5 1 1.5 2 km



Figure 16. Two examples of Eucalyptus are classified as needleleaf trees (WGS84, -48.988, -22.728 and -48.677, -23.247).

However, the tree plantation just south of the second example in Figure 21 is classified as deciduous. Yet, the vegetation resembles pine trees and indicates the presence of a "needle-leaved tree cover" (Figure 17).

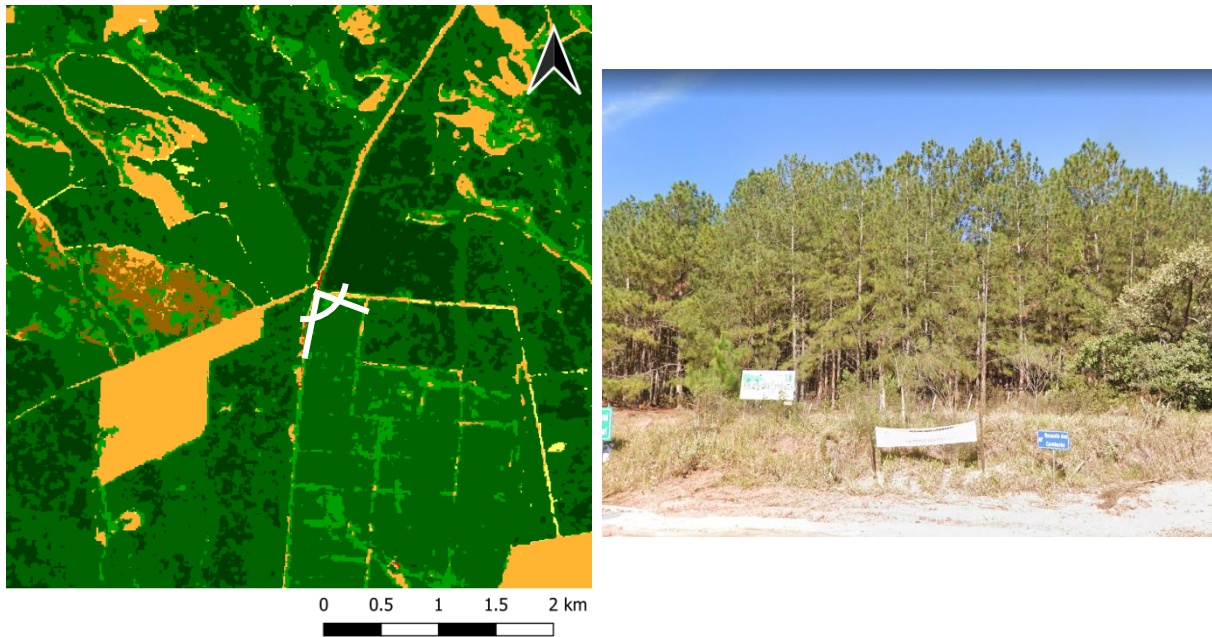


Figure 17. One of the rare needleleaf plantations is classified as broadleaf (WGS84, -48.679, -23.25).

A look at the Sentinel-2 annual composite suggests that the entire area circled is planted with needle-leaved trees and the NDVI profile extracted from Sentinel-2 shows that this area is evergreen.

To summarise, a small part of the map is classified as “Tree cover evergreen needleleaf” but almost none of this area is well classified and is more often “Tree cover evergreen broadleaf”. However, some areas are effectively planted with “Tree cover evergreen needleleaf” but it’s mostly classified as “Tree cover evergreen broadleaf”.

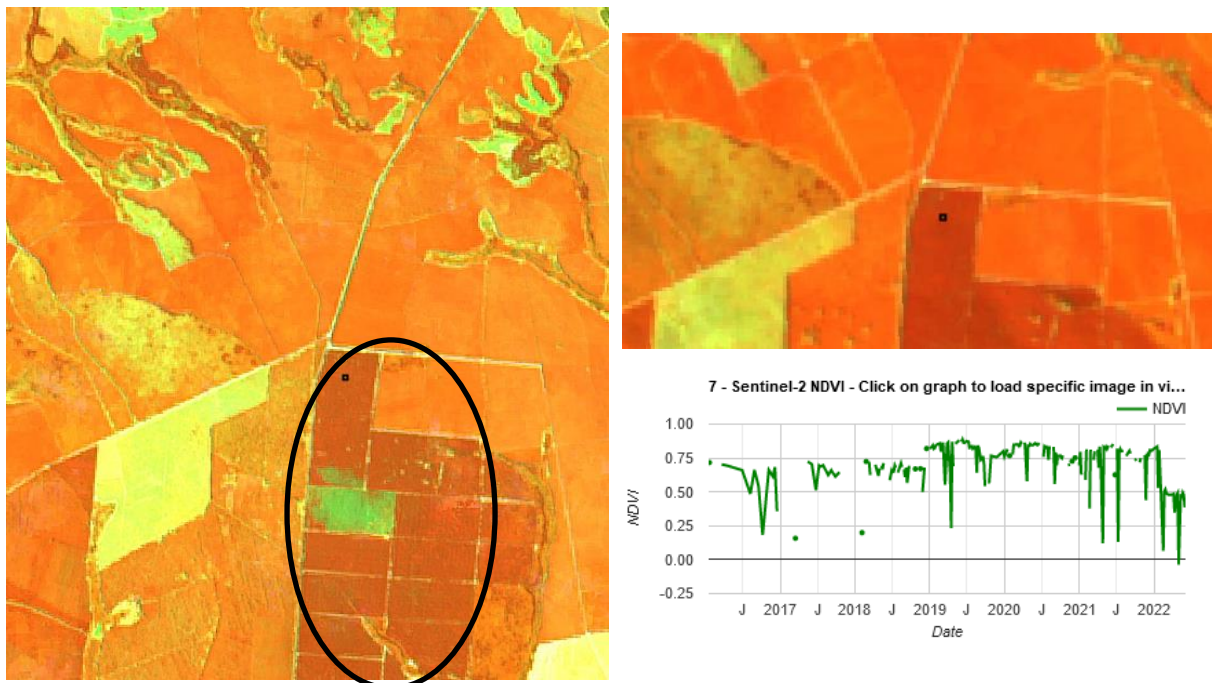


Figure 18. Yearly composite of Sentinel-2 (left) and Landsat (upper right) and the NDVI profile (lower right) of the black square which show the difference between broadleaved and needleleaved evergreen trees.

4.1.2.2 Quantitative assessment

The accuracy estimates of the Amazonia static map were obtained with the 857 homogeneous and certain samples. The map with a grouping of the original legend shows the best of all OA of $81.7 \pm 2.9\%$ (Table 8) across regions while the original map has an OA of $67.9 \pm 3.5\%$ (Table 9). Again, tree classes tend to be mixed with shrub classes. Area-based confusion matrices are detailed in Section 6.

Four classes, “Open Water permanent”, “Built-up”, “Woody vegetation”, and “Croplands” yield high and balanced per-class accuracies, above 90 %, 85 %, 80 %, and 75 %, respectively. The grassland class has an excellent PA of $90.2 \pm 3.9\%$. Contrary to what might be expected, the grassland commission (UA = $61.3 \pm 7.4\%$) is due more to the misclassification of woody vegetation (primarily with evergreen shrub cover, Figure 47) than cropland. Vegetation aquatic or regularly flooded tends to be omitted mostly in favour of the “Tree cover evergreen broadleaf” woody vegetation class.

Table 8. The area-based accuracy estimates of the Amazonia static map v202212 with a grouping of the original legend were derived using 857 homogeneous samples photo-interpreted with certainty. Accuracy figures are reported in % with a 95% confidence interval. OA, PA and UA stand for overall, producer, and user accuracy.

Label	OA (%)	UA (%)	PA (%)
Woody vegetation		94.5 ± 2.4	82.6 ± 3.3
Grassland		61.3 ± 7.4	90.2 ± 3.9
Croplands		81.4 ± 7.6	75.7 ± 9.6
Vegetation aquatic or regularly flooded	81.7 ± 2.9	50 ± 12.9	10.7 ± 5.3
Bare areas		66.7 ± 17.2	56.8 ± 39.2
Built-up		85.7 ± 10.8	100 ± 0.0
Open Water seasonal		8.3 ± 11.4	50.8 ± 59.6
Open Water permanent		97.1 ± 3.9	90.8 ± 2.4

Table 9. The area-based accuracy estimates of the Amazonia static map v202212 in its original legend were derived using 857 homogeneous samples photo-interpreted with certainty. Accuracy figures and their standard errors are reported in % with a 95% confidence interval. OA, PA and UA stand for overall, producer, and user accuracy.

Label	OA (%)	UA	PA
Tree cover evergreen broadleaf		77.6 ± 5.3	89 ± 2.9
Tree cover deciduous broadleaf		50.9 ± 13.3	43.9 ± 10.6
Shrub cover evergreen		26.8 ± 13.7	4.5 ± 2.4
Shrub cover deciduous		6.7 ± 9.0	4 ± 5.5
Grassland		61.3 ± 7.4	91.6 ± 3.3
Croplands		81.4 ± 7.6	76.1 ± 9.6
Woody vegetation aquatic or regularly flooded	67.9 ± 3.5	42.4 ± 17.1	3.1 ± 2.2
Grassland vegetation aquatic or regularly flooded		28 ± 18.0	10.6 ± 9.4
Bare areas		66.7 ± 17.2	56.8 ± 39.2
Built-up		85.7 ± 10.8	100 ± 0.0
Open Water seasonal		8.3 ± 11.4	73.4 ± 46.5
Open Water permanent		97.1 ± 3.9	88.9 ± 2.9

4.1.3 Africa

4.1.3.1 Qualitative assessment

The visual qualitative assessment shows that the Africa static map is of good overall quality with landscape patterns well delineated (Figure 19). The main macroscopic issues concern the tiling or sensor swath effects observed throughout the map that create sharp and unexpected spatial discrepancies between classes (Figure 20), and the absence of the mapping of the swamp forests in the Central cuvette of the Congo Basin (Figure 21).

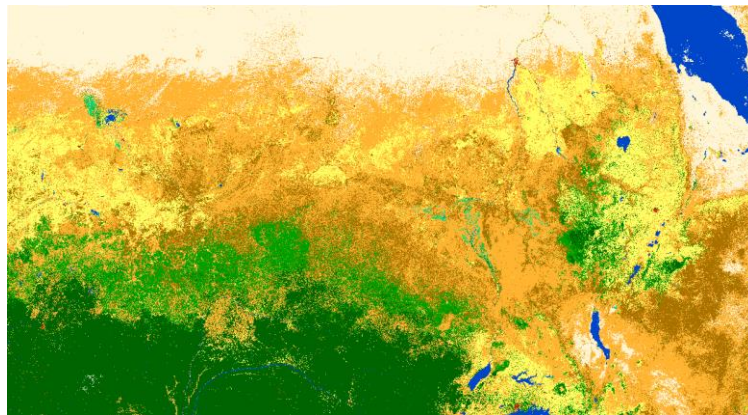


Figure 19. The Africa static map 2019 mosaic.

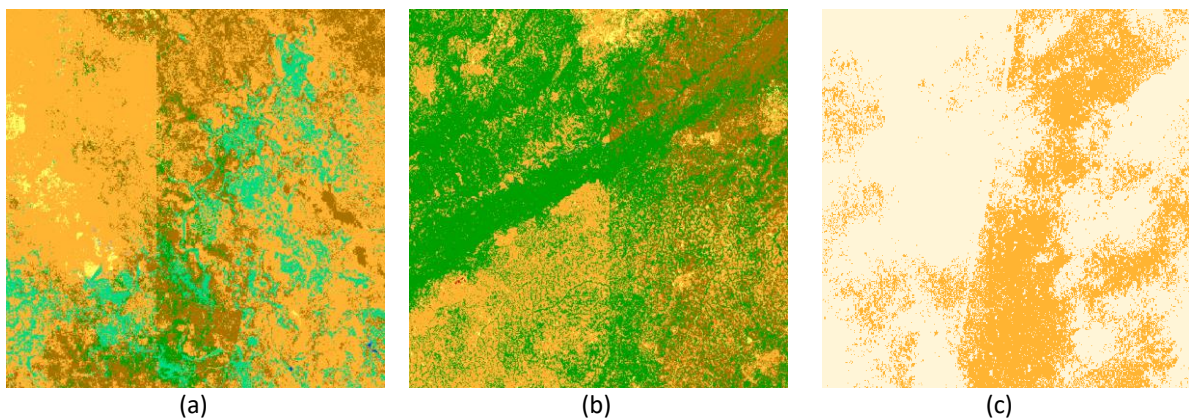


Figure 20. Illustration of the main types of artefacts observed in the Africa static map 2019. (a – c) tiles and sensor swath border effects present throughout the map imply spatial inconsistency in the classification.

Figure 21 illustrates a specific case of macroscopic error related to the absence of “woody vegetation aquatic or regularly flooded” in the place of swamp forests in the Cuvette Centrale, central Congo Basin.

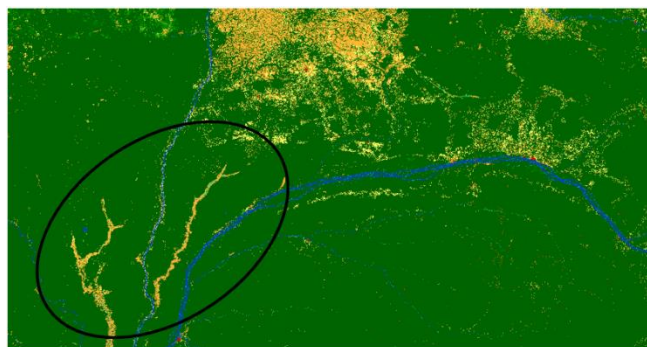


Figure 21. Illustration of a macroscopic error observed in the Africa static map 2019 (v202212): absence of the edaphic forest along the Congo river (18.44° LONG; 0.19° LAT). All coordinates are indicated in EPSG:4326.

4.1.3.2 Quantitative assessment

The accuracy estimates of the Africa static map obtained with the 748 homogeneous and certain samples. The class “Woody vegetation aquatic or regularly flooded” was absent from map and removed from the analysis. The OA with the legend grouping is of $70.7 \pm 3.3 \%$ (Table 10) and of $66.6 \pm 3.5 \%$ (Table 11) with the original legend. The 4.1 % of OA increase brought by the legend grouping demonstrates how little confusion between woody vegetation or wetland classes contributed to the error. Here, the errors mostly relate to overestimated

	Ref	CCI_HRLC_Ph1-D4.1_PVIRb		
	Issue	Date	Page	
	2.rev.2	10/02/2023	23	

grasslands ($44.8 \pm 7.3\%$, Table 10). contaminating all classes but “Open Water seasonal”. Misclassification with the woody deciduous vegetation, bare areas, and the cropland is a common issue for any classification in semi-arid areas. The herbaceous wetlands tend to be omitted in favour of a wide variety of classes ($7.7 \pm 4.1\%$). Area-based confusion matrices are detailed in Section 6.

The “Bare areas”, “Built-up”, “Open Water permanent”, and the “Tree cover evergreen broadleaf” class show the best UA figures about 85 %. Their PA is also high above 70 % except for the “Built-up” class which tends to be omitted. The “Open Water Seasonal” also tends to be omitted mostly in favour of the “Bare areas” and “Open Water permanent” classes. This has a low impact on the OA as it is the least represented class of the map.

Table 10. The area-based accuracy estimates of the Africa static map v202212 with grouping of the original legend were derived using 748 homogeneous samples photo-interpreted with certainty. Accuracy figures are reported in % with a 95% confidence interval. OA, PA and UA stand for overall, producer, and user accuracy.

Label	OA (%)	UA (%)	PA (%)
Woody vegetation		84.2 ± 5.1	78.2 ± 4.7
Grassland		44.8 ± 7.3	70.8 ± 7.3
Croplands		63.8 ± 11.4	66.8 ± 9.8
Vegetation aquatic or regularly flooded	70.7 ± 3.3	58.7 ± 14.3	7.7 ± 4.1
Bare areas		94.9 ± 4.9	70.9 ± 5.9
Built-up		88.9 ± 10.4	15.9 ± 13.3
Open Water seasonal		10 ± 8.4	1 ± 1.2
Open Water permanent		86.7 ± 7.3	77.9 ± 16.9

Table 11. The area-based accuracy estimates of the Africa static map v202212 in its original legend were derived using 748 homogeneous samples photo-interpreted with certainty. Accuracy figures and their standard errors are reported in % with a confidence interval (95% confidence level). OA, PA and UA stand for overall, producer, and user accuracy.

Label	OA (%)	UA (%)	PA (%)
Tree cover evergreen broadleaf		96.2 ± 4.3	92.7 ± 4.9
Tree cover deciduous broadleaf		43.2 ± 14.9	40.9 ± 12.3
Shrub cover evergreen		56.5 ± 20.8	0.2 ± 0.0
Shrub cover deciduous		56.1 ± 12.9	60.1 ± 10.8
Grassland		44.8 ± 7.3	73.2 ± 7.3
Croplands	66.6 ± 3.5	63.8 ± 11.4	67.7 ± 9.8
Grassland vegetation aquatic or regularly flooded		58.7 ± 14.3	7.6 ± 4.1
Bare areas		94.9 ± 4.9	70.9 ± 5.9
Built-up		88.9 ± 10.4	15.9 ± 13.3
Open Water seasonal		10 ± 8.4	1 ± 1.2
Open Water permanent		86.7 ± 7.3	77.9 ± 16.9

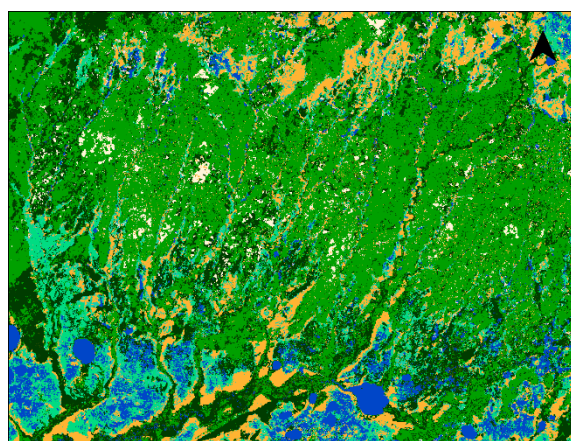
4.2 Historical 30-m regional dynamic LC Best Class and change detection maps

4.2.1 Siberia

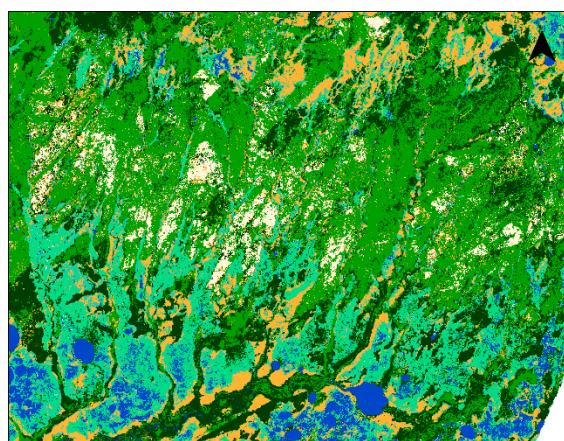
4.2.1.1 Visual quality assessment of the land cover dynamic maps

4.2.1.1.1 Forest fires

Detection of forest fires in Siberia is probably one of the major challenges as it has a strong impact on climate. It was observed that the change from forest to grassland during forest fires was well detected, which is a good point.



1990 Best Class Mosaic



1995 Best Class Mosaic

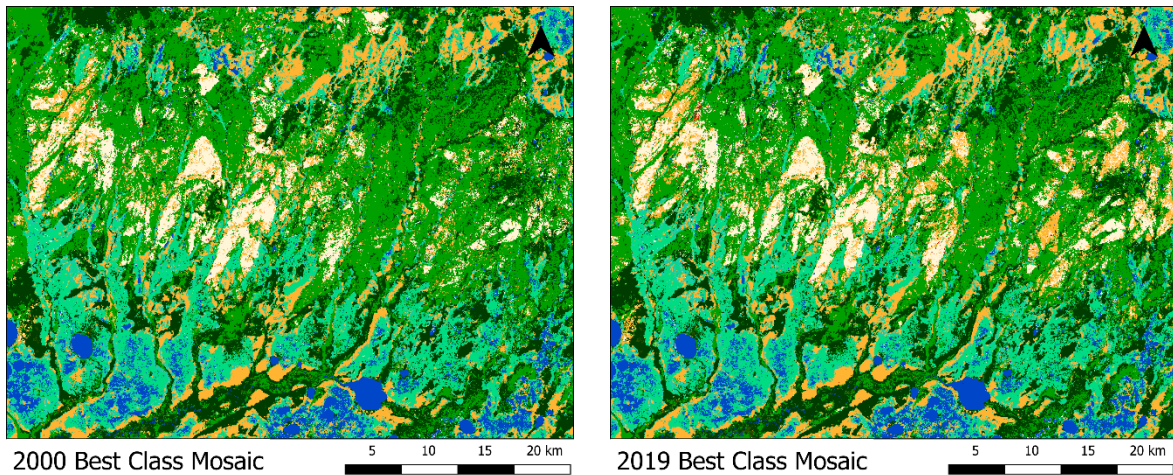


Figure 22. Illustration of the nicely detected fires that induce loss of forest in the district of Khantys-Mansis (83.3168° LONG; 62.3812° LAT).

4.2.1.1.2 Some tiles are missing

Some areas in the Northern part of Siberia were missing in the products covering the years 2000, 2010, 2015, and 2019 (Figure 23). In other years, unmapped areas were found in the Southern east parts of the extent as shown in Figure 24 for 2005, and in Figure 25 for 1990 and 1995.

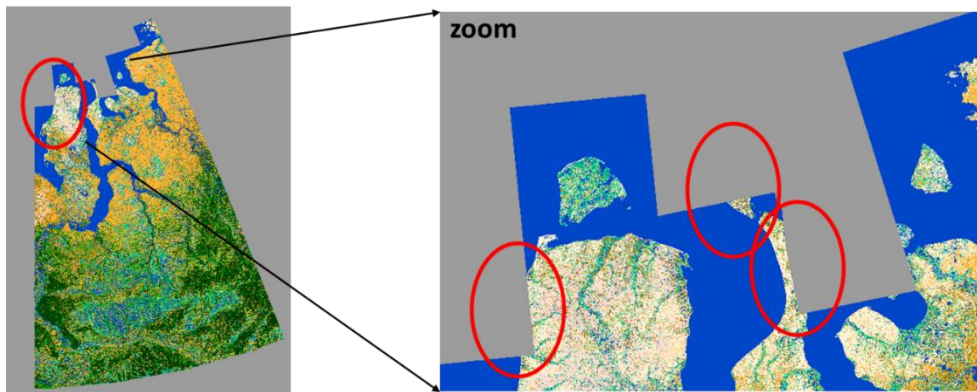


Figure 23. Representative example of the incompleteness of the extent of the “Best Class” layers of the Dynamic LC maps 2000, 2010, 2015, and 2019.

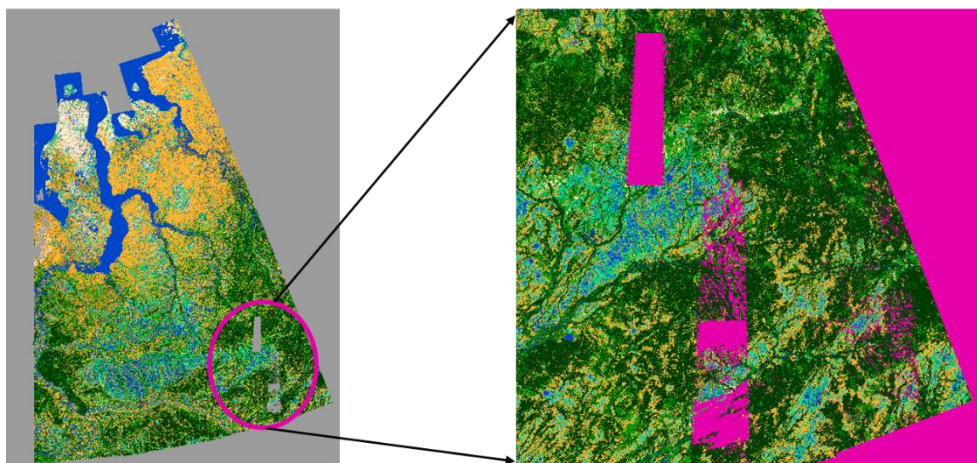


Figure 24. Presence of unmapped areas in the “Best Class” layer of the Dynamic LC map 2005. No data is shown in grey and pink in the left and right-hand side images, respectively.

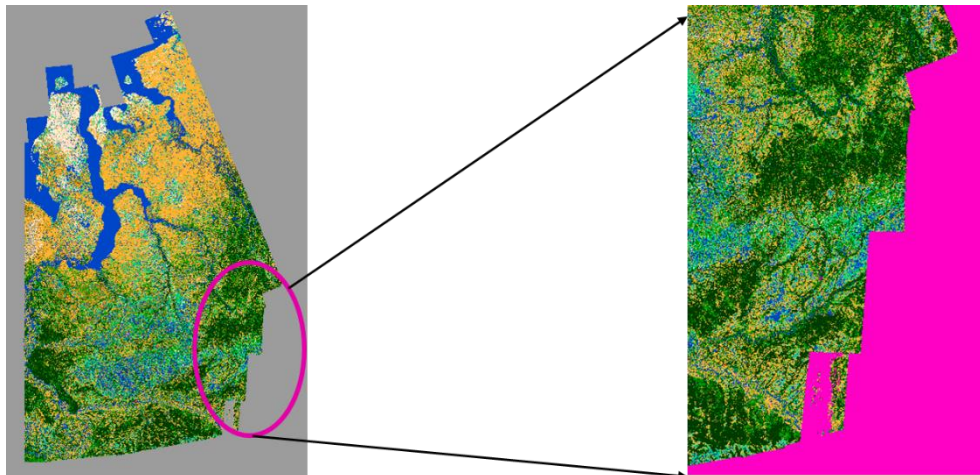


Figure 25. Presence of unmapped areas in the “Best Class” layer of the dynamic LC map 1990 and 1995, respectively. No data is shown in grey and pink in the left and right-hand side images, respectively.

4.2.1.1.3 Detection of energy facilities

Figure 26 shows that several forest areas are being cleared to build energy facilities. These areas are detected correctly in the LC Dynamic Best Class product.

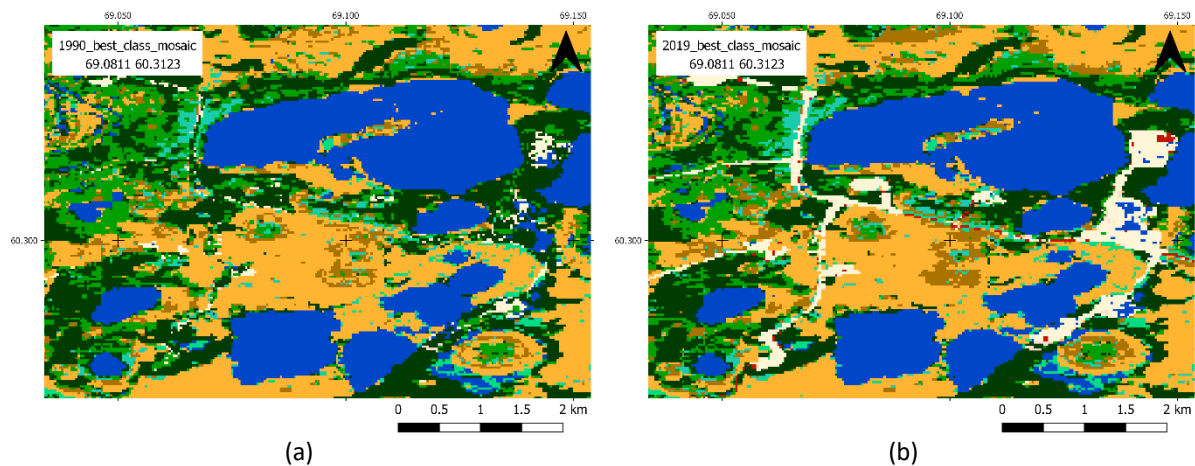


Figure 26. Illustration of the well-detected deforestation into bare areas. (a) Dynamic Land Cover mosaic 1990. (b) Dynamic Land Cover mosaic 2019.

4.2.1.2 Quantitative assessment

Figure 27 summarizes the sample-count discrepancy estimates for the validation of the Siberia historical “Dynamic Land Cover Best Class” mosaic. The main issue is the presence of change where no change was observed in the validation database. The reasons for these discrepancies could be the robustness of the validation database, the amount and uncertainty associated with validation and classification sources, the definition of the change, the minimum mapping unit of the detection of change in the LC change algorithm, etc. These reasons are worth investigating in the future.

Ref\Map	No change	Change	Sum
No change	155	337	492
Change	11	124	135
Sum	166	461	627

Figure 27. Sample-count discrepancy matrix from the validation of the Siberia Dynamic Land Cover Best Class product using the homogeneous and certain validation samples. Rows refer to the reference validation database and columns to the product.

4.2.2 Amazonia

4.2.2.1 Visual quality assessment of the land cover dynamic maps

The map series illustrated for Paraguay (Figure 28) shows that the change in vegetation is well detected when moving from forests to croplands or grasslands. We also see that the other classes are stable over time.

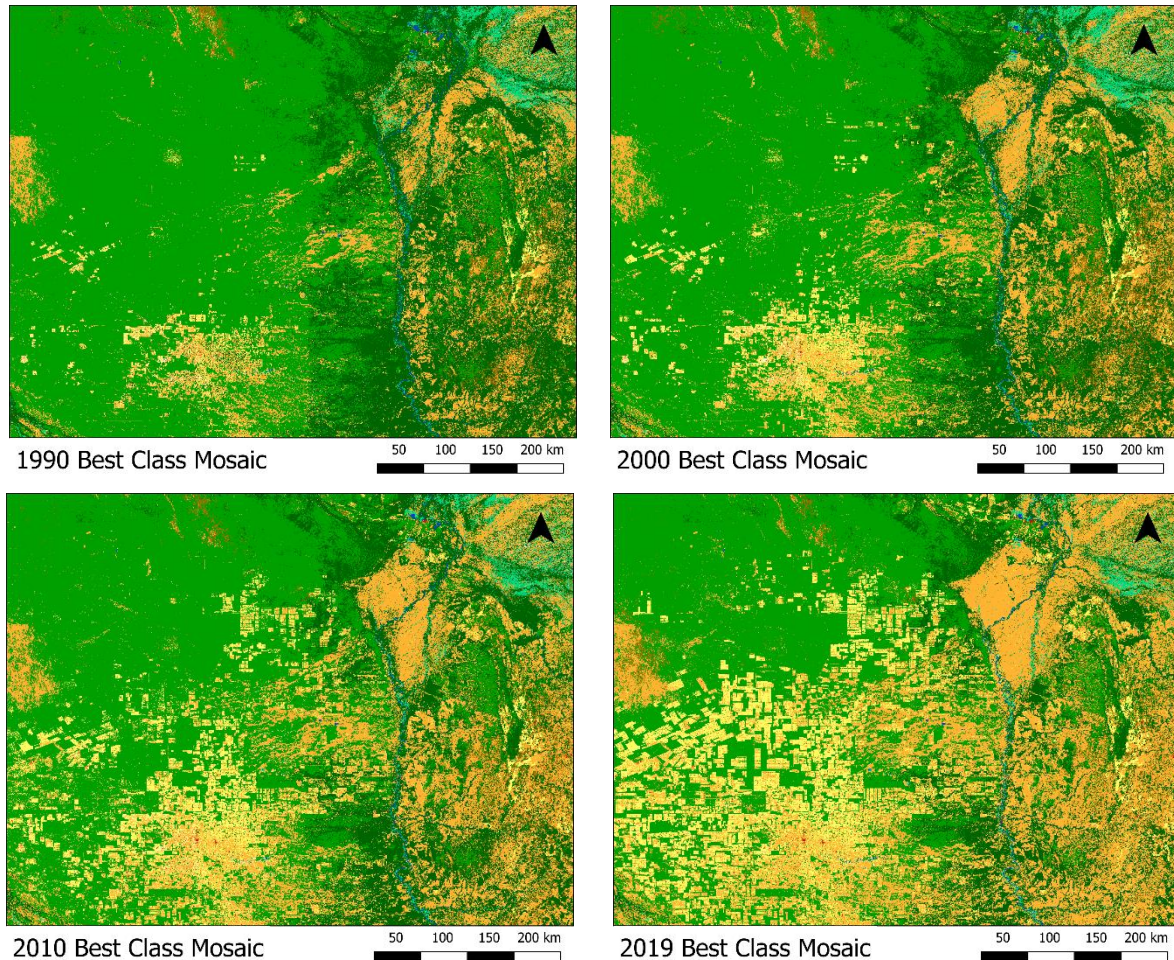


Figure 28. Comparison of four time periods over an area of land cover change in Paraguay. Deforestation patterns are well detected, and land use classes are stable over time, including grassland and cropland (-61.1092; -21.4672 EPSG4326).

Figure 29 shows an example of a permanent dam correctly detected and delineated on the Dynamic Land Cover Best Class maps.

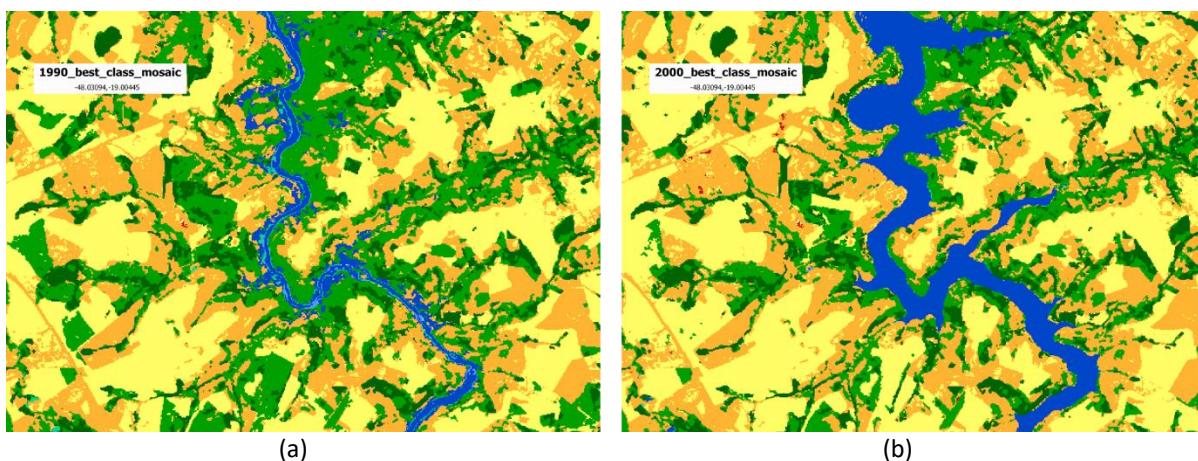


Figure 29. An example of a new dam detected in the Dynamic Land Cover Best Class. (a) Dynamic Land Cover Best Class 1990; (b) Dynamic Land Cover Best Class 2000

4.2.2.2 Differences between the land cover dynamics and change detection maps

LC changes (LCC) present in the « change detection » mosaics were cleaned and thus, the mosaics include less LCC than in the tile version of the Change Detection product (Figure 30).

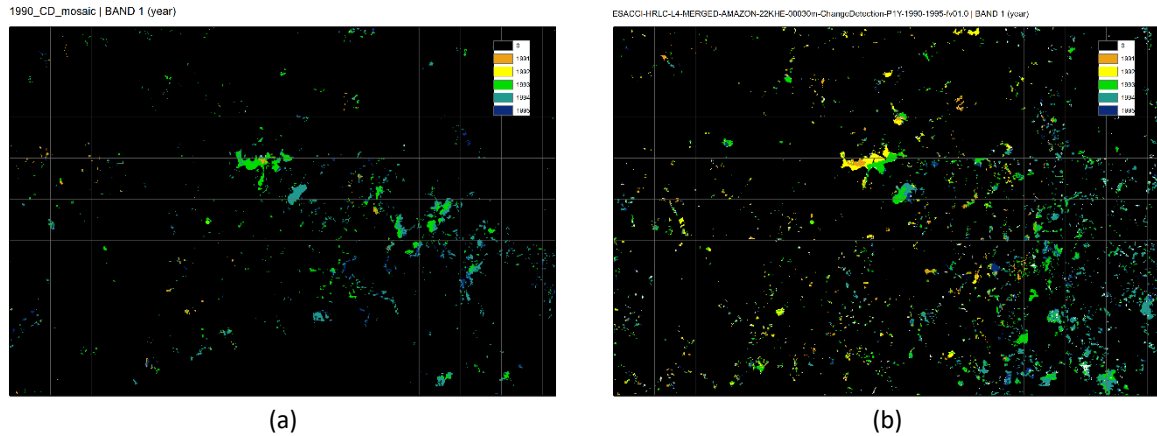


Figure 30. Illustration of the differences of land cover change observed during the 1990-1995 period in (a) the Change Detection mosaic and (b) in the corresponding Change Detection tile. More change is present in the tile version (b).

Yet some land cover change patterns are present in the mosaic and not in the tiled version of the product (Figure 31).

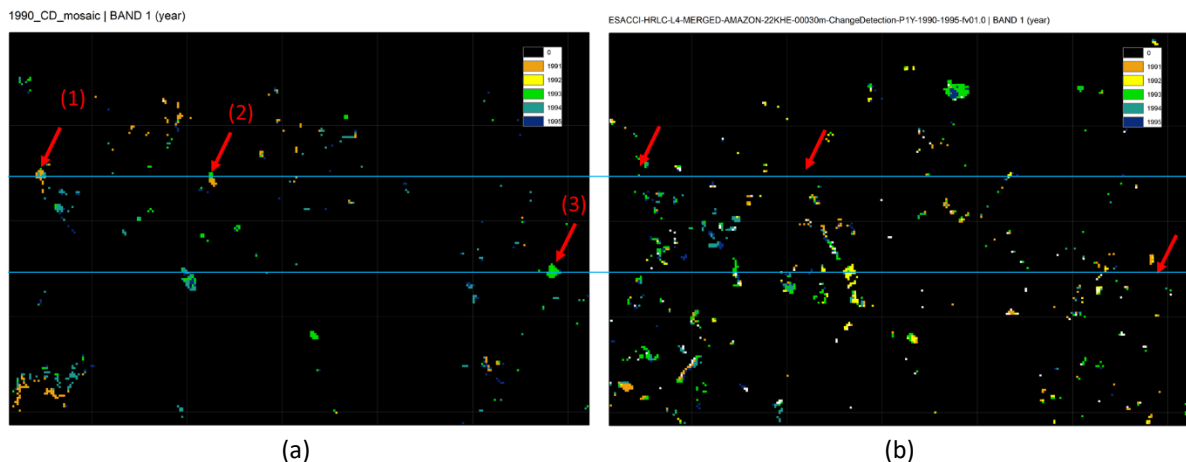


Figure 31. Presence of some land cover change patterns in the Change Detection mosaic which are absent from the tiled version of the Change Detection product.

4.2.2.3 Consistency between the bands inside the change detection product

Few discrepancies were found among the layers in the mosaic stack. It seems that only the highest priority change (class 2) is present in Band1 (year) of the mosaic stack but not always.

Some high-priority LCCs are not included in the mosaic band 1 (see red arrows).

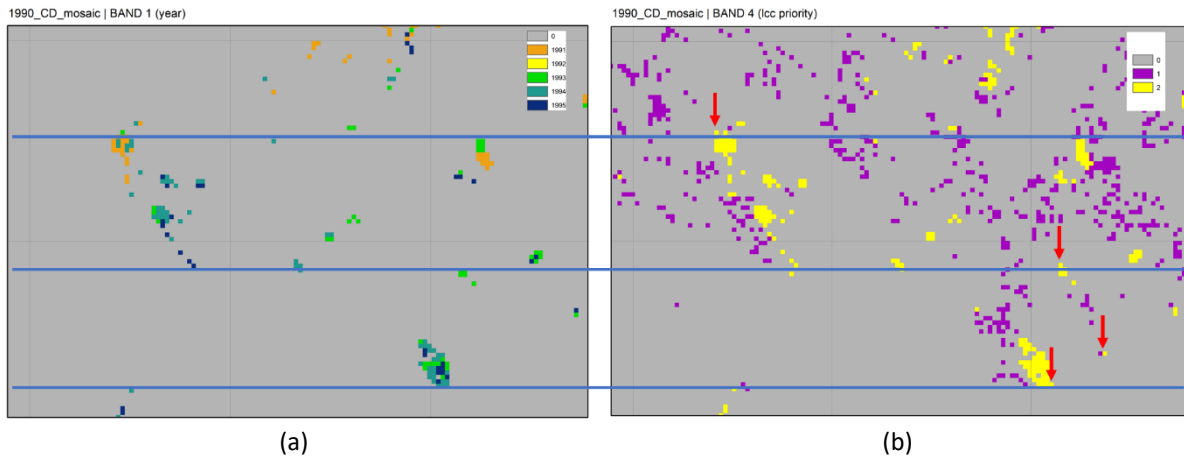


Figure 32. Illustration of the discrepancy between the “year” (a) and “LC change priority” (b) layers of the Change Detection product

The probability associated with the change detection (band 2) is consistent with the year of detection (band 1) (Figure 33). No extra pixels were found at the location of the red arrows, unlike the previous example.

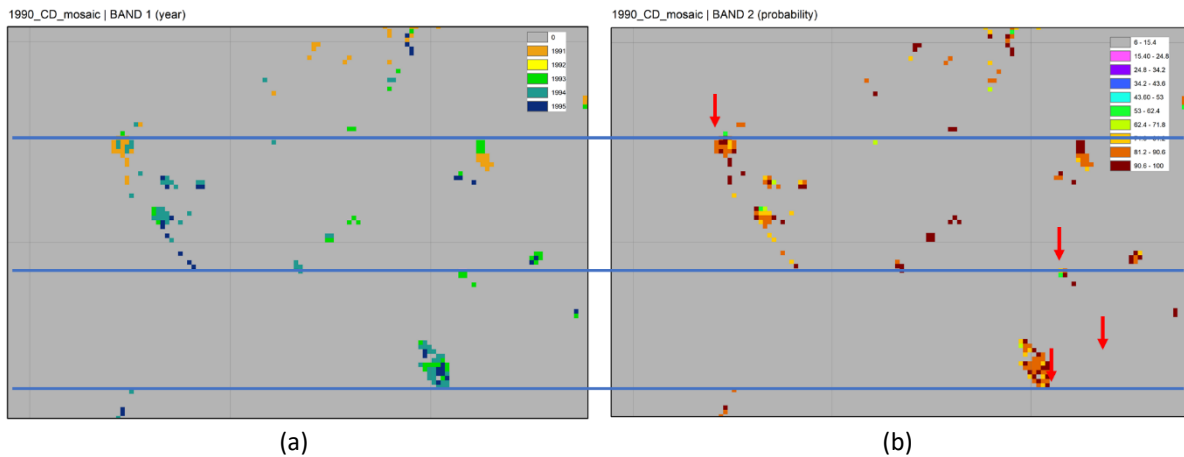


Figure 33. Illustration of the consistency between the “year” (a) and “probability” (b) layers in the Change Detection product.

4.2.2.4 Quantitative assessment

Figure 34 summarizes the sample-count discrepancy estimates for the validation of the Amazonia historical “Dynamic Land Cover Best Class” mosaic. The overall accuracy estimates are good, reaching 71 %.

Contrarily to the other historical products, results show that each per-class accuracy over the changing area is meeting the GCOS target requirements of 35 % of errors for the Dynamic Land Cover Best Class mosaic. Here, the main issue of LC change contamination has a smaller impact on the final estimates.

Ref\Map	No change	Change	Sum	PA
No change	156	277	433	0.36
Change	8	533	541	0.99
Sum	164	810	974	
UA	0.95	0.66		0.71
F1	0.52	0.79		

Figure 34. Sample-count discrepancy matrix from the validation of the Amazonia Dynamic Land Cover Best Class using the homogeneous and certain validation samples. Rows refer to the reference validation database and columns to the product.

4.2.3 Africa

4.2.3.1 Visual quality assessment of the land cover dynamic maps

4.2.3.1.1 Consistent urban extension over time

Overall, the extension of urban areas is well captured with a consistent growing shape through time (Figure 35). Note that the pivot crop circles are also well delineated at the bottom right of the figure.

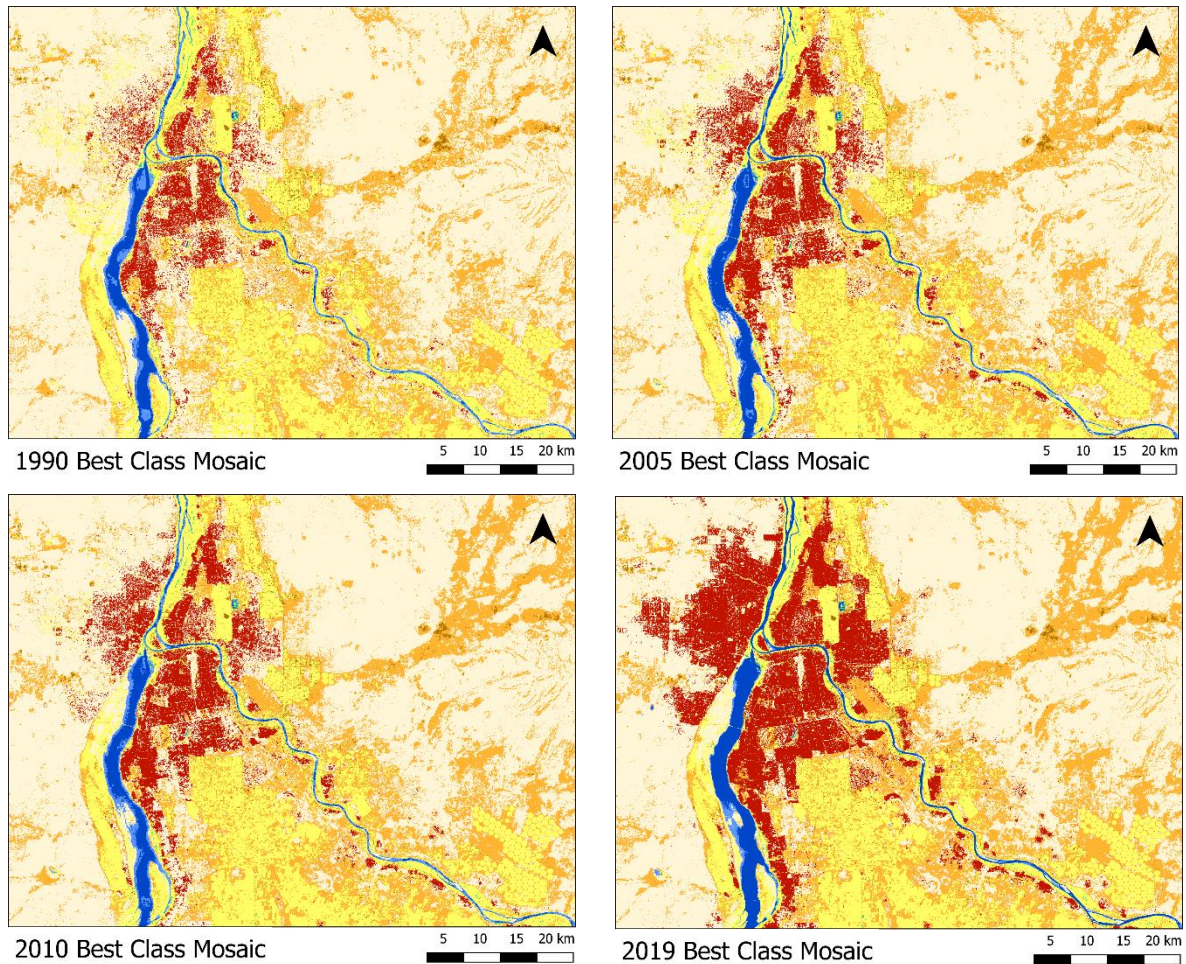


Figure 35. Illustration of the correctly defined urban extension over Khartoum (32.56°LONG; 15.50° LAT).

4.2.3.1.2 New dam detection

New water dams are well detected. Figure 36 shows an example of a permanent dam correctly detected and delineated on the Dynamic Land Cover Best Class maps.

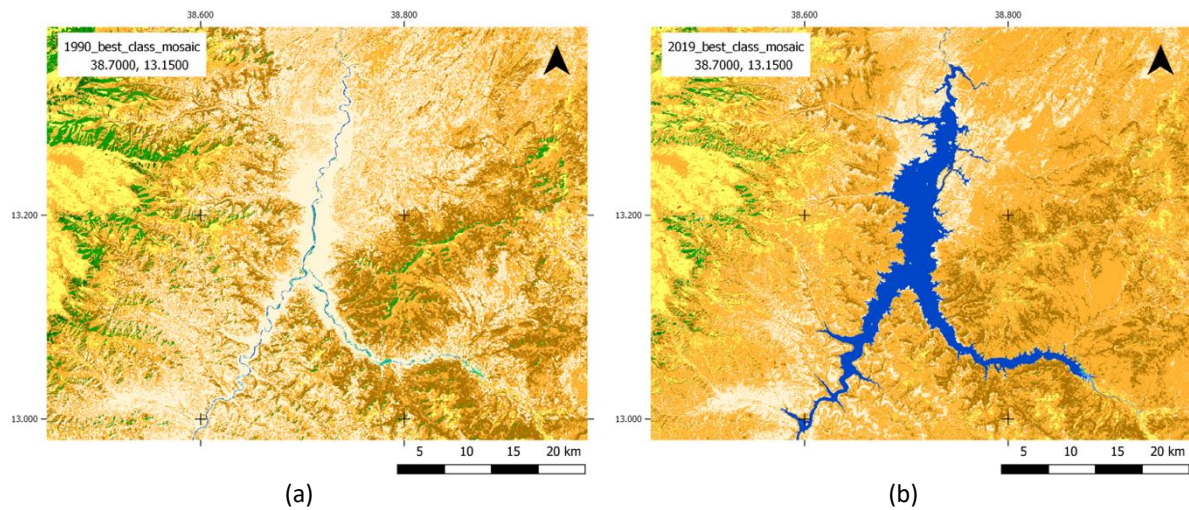
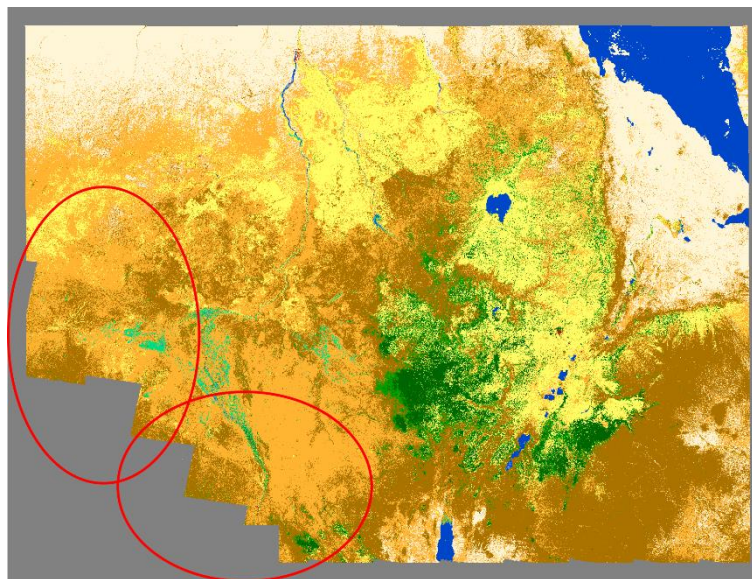


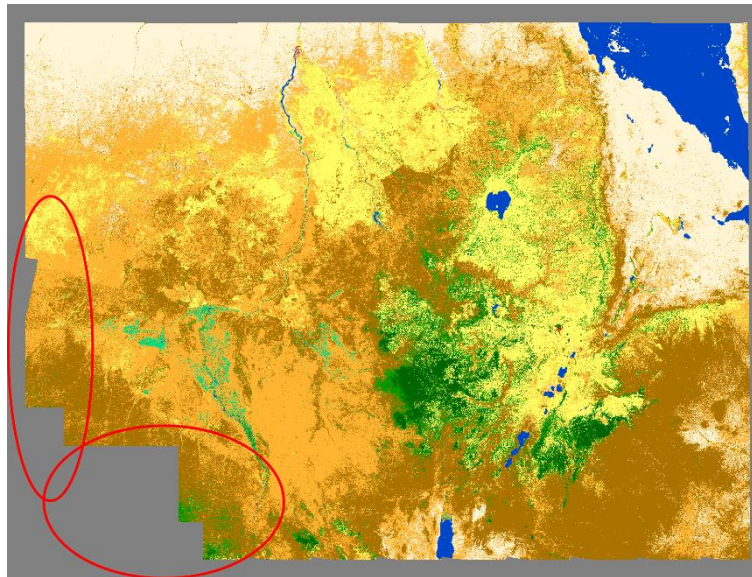
Figure 36. Illustration of an important dam correctly detected as a LC change. (a) Dynamic Land Cover Best Class 1990. (b) Dynamic Land Cover Best Class 2019.

4.2.3.1.3 Some tiles are missing

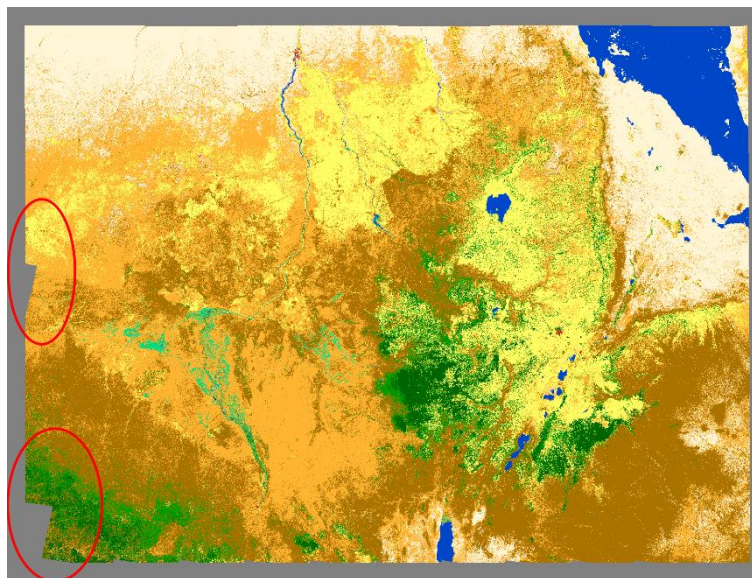
Some areas in the south-western part of Africa were missing from products covering the years 1990, 1995 and 2000 (Figure 37). This problem is solved in 2005, but an unmapped area was found in the north-eastern part of the range as shown in Figure 38. The products appear to be complete as of 2010.



(a)



(b)



(c)

Figure 37. Representative examples of the incompleteness of the extent of the “Best Class” layers of the Dynamic LC maps for the year (a) 1990, (b) 1995, and (c) 2000.

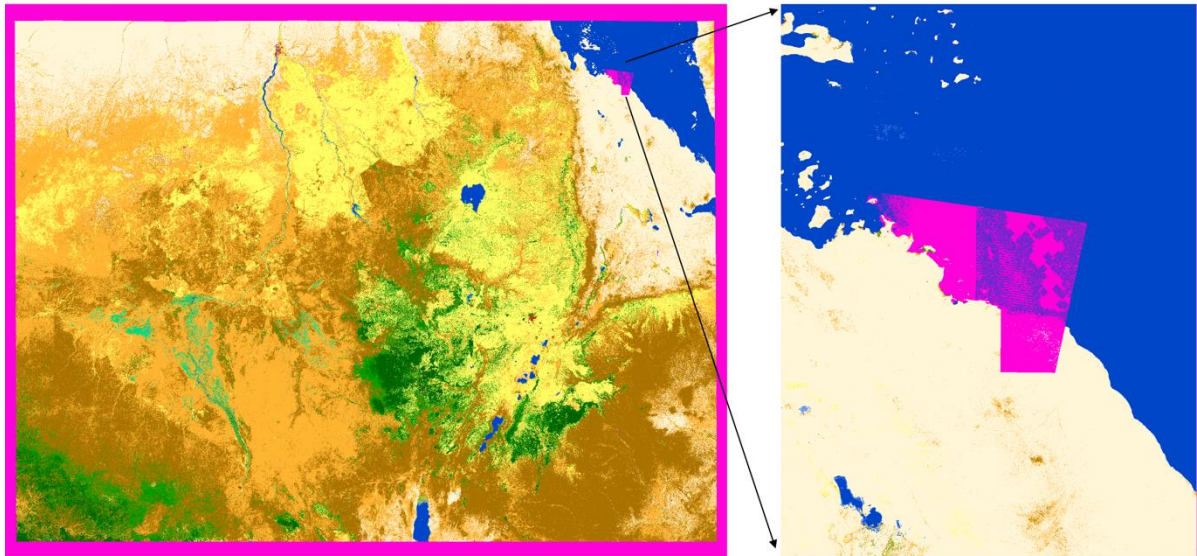
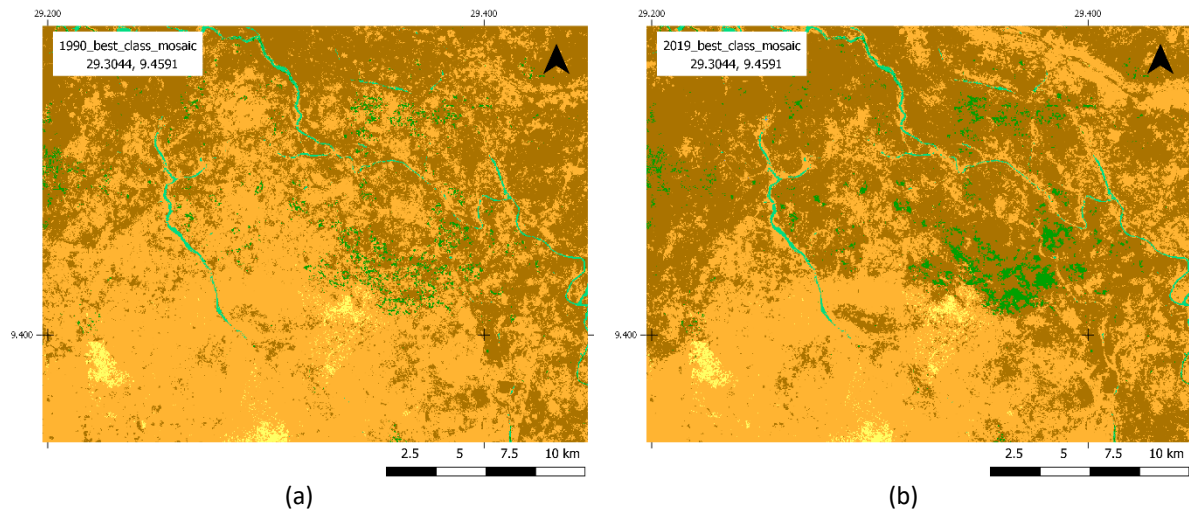


Figure 38. Presence of unmapped areas in the “Best Class” layer of the Dynamic LC map 2005. No data is shown in pink.

4.2.3.1.4 Recurrent fires and change detection

During validation, many points proved problematic to assess due to bushfire dynamics. Some areas seem to burn every year and grow back the following year. Other areas burn at a particular time and take several years to regenerate.

Figure 39 shows an example of a savannah that burns almost every year, so care should be taken with this transition from grassland to shrubland. Earth Timelapse makes it possible to [visualise these dynamics](#) in the area under consideration.



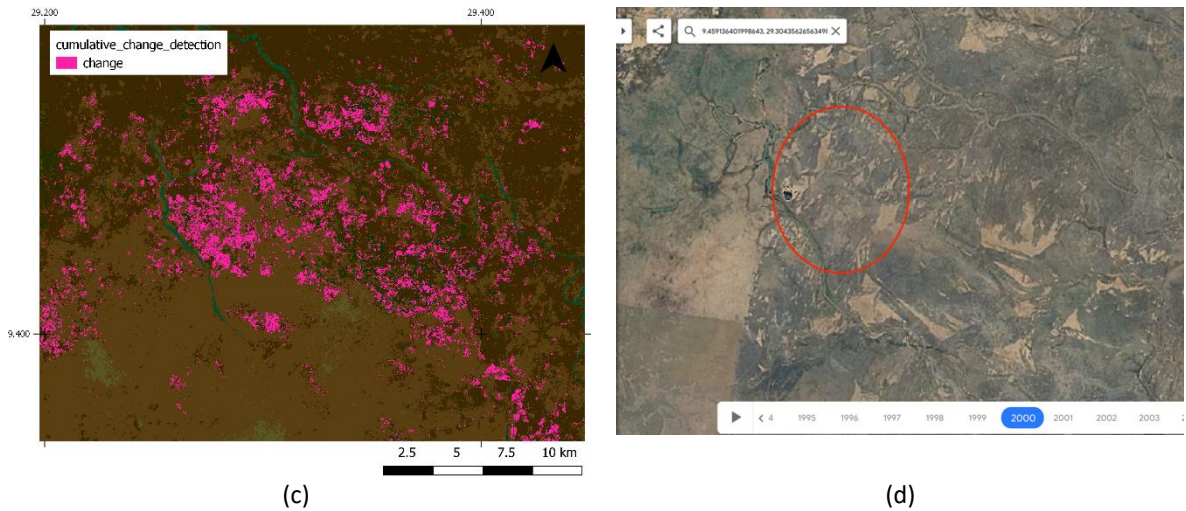


Figure 39. Illustration of a land cover change detection in the savannah due to bushfires. Fires occur almost every year, so the land cover cannot change from grassland to shrubland. (a) Land cover mosaic in 1990. (b) Land cover mosaic in 2019. (c) Cumulative change detection is calculated as the union of all changes observed in the Dynamic Land Cover products. (d) Presence of fires each year with Earth Timelapse: the year 2000.

It is also important to point out that some dynamics are well-identified. Figure 40 shows an area affected by fire, where there has been a change in land cover from shrubland to grassland.

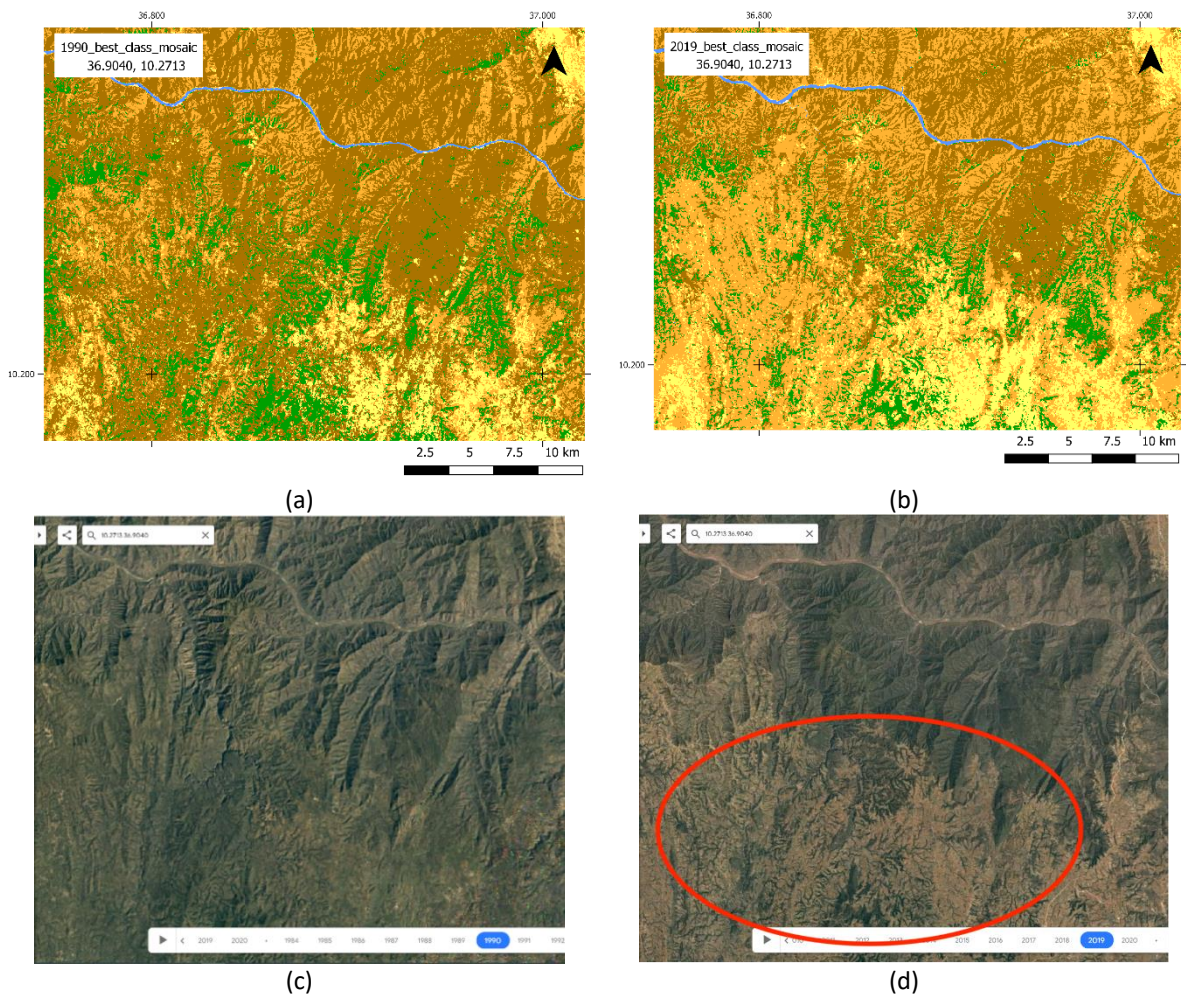


Figure 40. Illustration of a well-detected change related to the issue of fires. (a) Dynamic Land Cover mosaic 1990. (b) Dynamic Land Cover mosaic 2019. (c) Earth Timelapse: no disturbance in 1990. (d) Earth Timelapse: environment was degraded by consecutive fires in 2019.

4.2.3.1.5 Change overestimation on slopes

A very large number of validation sample points were located on shaded slopes, which drew attention to land cover that was stable over time but incorrectly considered to be changing. (Figure 41) Earth Timelapse [shows that the cover does not change](#).

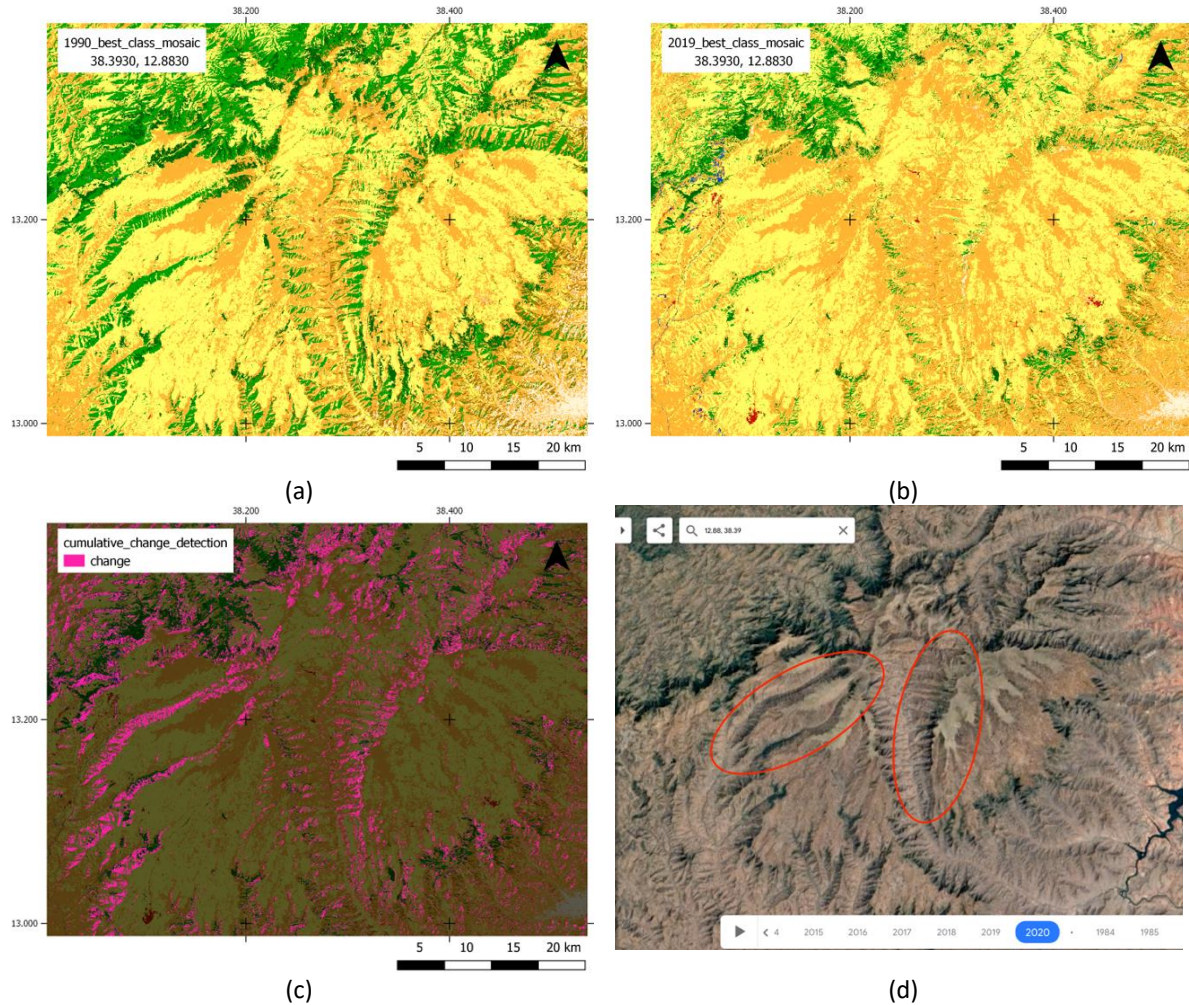


Figure 41. Illustration of land cover change detected on shaded slopes. (a) Dynamic Land Cover mosaic 1990. (b) Dynamic Land Cover mosaic 2019. (c) Cumulative change detection is calculated as the union of all changes observed in the Dynamic Land Cover products. (d) Visualisation of the presence of shadow on Earth Timelapse.

4.2.3.2 Quantitative assessment

Figure 42 summarizes the sample-count discrepancy estimates for the validation of the Africa historical “Dynamic Land Cover Best Class” mosaic. Similar to the feedback provided for the Siberia historical products, further investigations are needed to fully understand the discrepancies between the validation reference and the products.

Ref\Map	No change	Change	Sum
No change	236	464	700
Change	23	72	95
Sum	259	536	795

Figure 42. Sample-count discrepancy matrix from the validation of the Africa Dynamic Land Cover Best Class product using the homogeneous and certain validation samples. Rows refer to the reference validation database and columns to the product.

5 ANNEX –The CCI HRLC hierarchical approach of the legend

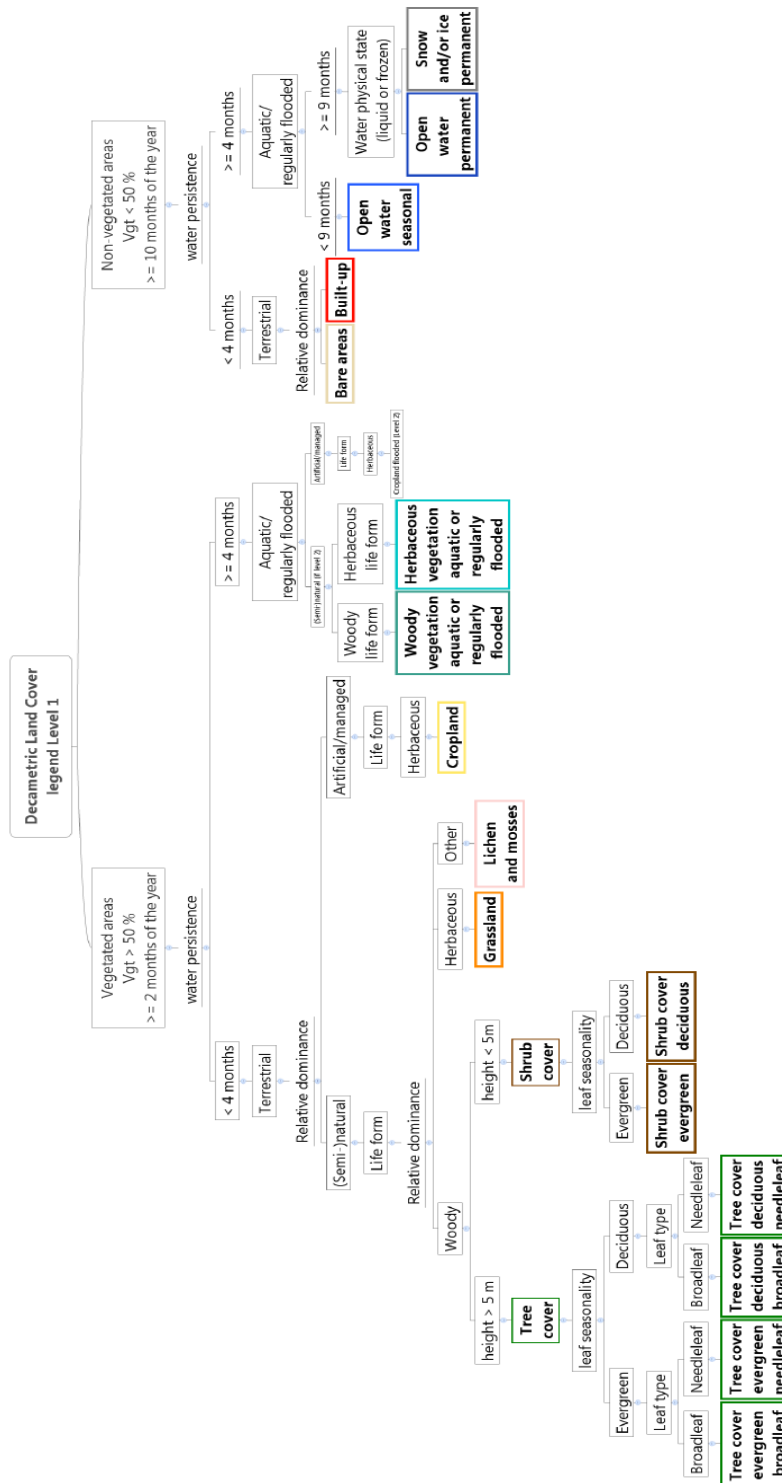


Figure 43. A hierarchical approach to determine the land cover class.

6 ANNEX – Area-based confusion matrices for the static LC maps v202212

6.1 Siberia

MAP\REF	Woody vegetation	Grassland	Croplands	Vegetation aquatic or regularly flooded	Lichen and mosses	Bare areas	Built-up	Open Water	sum	UA	SE_UA
Woody vegetation	0.34128	0.03043	0.00217	0.00869	0.00217				0.38475	88.7	2.4
Grassland	0.05134	0.16608	0.02416	0.00906	0.00906	0.0302	0.00604	0.00302	0.29895	55.6	5
Croplands	0.0027	0.00811	0.07025	0.00135			0.00405		0.08647	81.2	4.9
Vegetation aquatic or regularly flooded	0.04505	0.02896		0.02252	0.00804	0.00161		0.00322	0.1094	20.6	4.9
Lichen and mosses	0.00148	0.00444			0.00593	0.00037			0.01222	48.5	8.8
Bare areas	0.00516	0.00147			0.00147	0.00479	0.00074	0.00037	0.014	34.2	7.8
Built-up	9e-05	9e-05				9e-05	0.00165		0.00192	85.7	7.8
Open Water	0.00188			0.00188				0.08852	0.09229	95.9	2.9
sum	0.44897	0.23959	0.09658	0.04351	0.02668	0.03706	0.01248	0.09513	1		
PA	76	69.3	72.7	51.8	22.2	12.9	13.2	93.1		70.1	OA
SE_PA	2.3	3.6	6.5	10.4	6.4	4.1	5.3	3.7		1.9	SE_OA

Figure 44. Area-based confusion matrix of the Siberia static map v202212 with grouping of the original legend. Class-related cells are expressed in terms of proportions of area (range 0 – 1). The accuracy estimates were derived using 549 homogeneous samples photo-interpreted with certainty. Accuracy figures are reported in % with their standard error. OA, PA and UA stand for overall, producer, and user accuracy, and SE for standard error.

MAP\REF	Tree cover evergreen needleleaf	Tree cover deciduous broadleaf	Tree cover deciduous needleleaf	Shrub cover	Grassland	Croplands	Woody vegetation aquatic or regularly flooded	Grassland vegetation aquatic or regularly flooded	Lichen and mosses	Bare areas	Built-up	Open Water permanent	sum	UA	SE_UA
Tree cover evergreen needleleaf	0.1224	0.01469	0.03182	0.0049	0.00245				0.00245				0.17871	68.5	5.5
Tree cover deciduous broadleaf	0.01894	0.07788	0.01684	0.00631	0.01684	0.0021	0.00421						0.14313	54.4	6.1
Tree cover deciduous needleleaf	0.01754		0.01503		0.00251								0.03508	42.9	13.7
Shrub cover	0.00127	0.00253		0.01645	0.00506			0.00253					0.02784	59.1	10.7
Grassland	0.00604	0.00604		0.03926	0.16608	0.02416	0.00302	0.00604	0.00906	0.0302	0.00604	0.00302	0.29895	55.6	5
Croplands		0.00135		0.00135	0.00811	0.07025		0.00135			0.00405		0.08647	81.2	4.9
Woody vegetation aquatic or regularly flooded	0.00167			0.02839	0.01002		0.00167	0.01336	0.00167	0.00167			0.05845	2.9	2.9
Grassland vegetation aquatic or regularly flooded	0.00154			0.01389	0.01853			0.00772	0.00618			0.00309	0.05095	15.2	6.3
Lichen and mosses				0.00148	0.00444				0.00593	0.00037			0.01222	48.5	8.8
Bare areas				0.00516	0.00147				0.00147	0.00479	0.00074	0.00037	0.014	34.2	7.8
Built-up	9e-05				9e-05					9e-05	0.00165		0.00192	85.7	7.8
Open Water				0.00188				0.00188				0.08852	0.09229	95.9	2.9
sum	0.16949	0.10249	0.0637	0.11908	0.2356	0.09652	0.0089	0.03288	0.02675	0.03712	0.01248	0.095	1		
PA	72.2	76	23.6	13.8	70.5	72.8	18.8	23.5	22.2	12.9	13.2	93.2		57.8	OA
SE_PA	4.2	5.9	6.8	2.7	3.5	6.5	17.7	8.9	6.4	4.1	5.3	3.7		2.2	SE_OA

Figure 45. Area-based confusion matrix of the Siberia static map v202212 with grouping of the shrubs classes. Class-related cells are expressed in terms of proportions of area (range 0 – 1). The accuracy estimates were derived using 549 homogeneous samples photo-interpreted with certainty. Accuracy figures are reported in % with their standard error. OA, PA and UA stand for overall, producer, and user accuracy, and SE for standard error.

6.2 Amazonia

	Woody vegetation	Grassland	Croplands	Vegetation aquatic or regularly flooded	Bare areas	Built-up	Open Water seasonal	Open Water permanent	sum	UA	SE_UA
Woody vegetation	0.49617	0.01013	0.00145	0.01736					0.5251	94.5	1.2
Grassland	0.09497	0.2038	0.02374	0.00791	0.00198				0.33241	61.3	3.8
Croplands	0.00775	0.01065	0.08038						0.09878	81.4	3.9
Vegetation aquatic or regularly flooded	0.00095	0.00032		0.00308			0.00011	0.0017	0.00615	50	6.6
Bare areas	0.00033	0.00066	0.00066		0.00331				0.00496	66.7	8.8
Built-up	0.00017	0.00025			8e-05	0.00299			0.00349	85.7	5.5
Open Water seasonal		5e-05		5e-05	5e-05		0.00011	0.00104	0.00131	8.3	5.8
Open Water permanent				4e-04	4e-04			0.027	0.02779	97.1	2
sum	0.60034	0.22586	0.10623	0.0288	0.00582	0.00299	0.00022	0.02974	1		
PA	82.6	90.2	75.7	10.7	56.8	100	50.8	90.8		81.7	OA
SE_PA	1.7	2	4.9	2.7	20	0	30.4	1.2		1.5	SE_OA

Figure 46. Area-based confusion matrix of the Amazonia static map v202212 with grouping of the original legend. Class-related cells are expressed in terms of proportions of area (range 0 – 1). The accuracy estimates were derived using 857 homogeneous samples photo-interpreted with certainty. Accuracy figures are reported in % with their standard error. OA, PA and UA stand for overall, producer, and user accuracy, and SE for standard error.

MAP/REF	Tree cover evergreen broadleaf	Tree cover deciduous broadleaf	Shrub cover evergreen	Shrub cover deciduous	Grassland	Croplands	Woody vegetation aquatic or regularly flooded	Grassland vegetation aquatic or regularly flooded	Bare areas	Built-up	Open Water seasonal	Open Water permanent	sum	UA	SE_UA
Tree cover evergreen broadleaf	0.31348	0.046	0.02215	0.00341	0.0017		0.01704						0.40378	77.6	2.7
Tree cover deciduous broadleaf	0.01106	0.03872	0.00553	0.01798				0.00277					0.07606	50.9	6.8
Shrub cover evergreen	0.01225	0.00098	0.00539	0.00098	0.00049								0.02009	26.8	7
Shrub cover deciduous	0.00839	0.00252	0.00755	0.00168	0.00419	0.00084							0.02517	6.7	4.6
Grassland	0.00594		0.07321	0.01583	0.2038	0.02374		0.00791	0.00198				0.33241	61.3	3.8
Croplands			0.00581	0.00194	0.01065	0.08038							0.09878	81.4	3.9
Woody vegetation aquatic or regularly flooded	0.00024						0.00055	0.00028			4e-05	2e-04	0.00131	42.4	8.7
Grassland vegetation aquatic or regularly flooded	0.00039		0.00019		0.00058		0.00019	0.00136				0.00213	0.00485	28	9.2
Bare areas	0.00017		0.00017		0.00066	0.00066			0.00331				0.00496	66.7	8.8
Built-up	0.00017				0.00025				8e-05	0.00299			0.00349	85.7	5.5
Open Water seasonal					5e-05			5e-05	5e-05		0.00011	0.00104	0.00131	8.3	5.8
Open Water permanent								4e-04	4e-04			0.027	0.02779	97.1	2
sum	0.35208	0.08822	0.12	0.04181	0.22239	0.10563	0.01778	0.01277	0.00582	0.00299	0.00015	0.03037	1		
PA	89	43.9	4.5	4	91.6	76.1	3.1	10.6	56.8	100	73.4	88.9		67.9	OA
SE_PA	1.5	5.4	1.2	2.8	1.7	4.9	1.1	4.8	20	0	23.7	1.5		1.8	SE_OA

Figure 47. Area-based confusion matrix of the Amazonia static map v202212 in its original legend. The accuracy estimates were derived using 857 homogeneous samples photo-interpreted with certainty. Class-related cells are expressed in terms of proportions of area (range 0 – 1). Accuracy figures are reported in % with their standard error. OA, PA and UA stand for overall, producer, and user accuracy, and SE for standard error.

6.3 Africa

	Woody vegetation	Grassland	Croplands	Vegetation aquatic or regularly flooded	Bare areas	Built-up	Open Water seasonal	Open Water permanent	sum	UA	SE_UA
Woody vegetation	0.28696	0.04195	0.00671	0.00503					0.34066	84.2	2.6
Grassland	0.06222	0.14578	0.032	0.01422	0.06222	0.00533		0.00356	0.32533	44.8	3.7
Croplands	0.01775	0.01775	0.07812	0.00178	0.0071				0.12251	63.8	5.8
Vegetation aquatic or regularly flooded	7e-05	0.00044		0.00197	0.00015		0.00022	0.00051	0.00335	58.7	7.3
Bare areas				0.00229	0.16917	0.00229	0.00229	0.00229	0.17832	94.9	2.5
Built-up	4e-05	9e-05	4e-05			0.00144			0.00162	88.9	5.3
Open Water seasonal	1e-05	1e-05	1e-05	1e-05	3e-05		6e-05	0.00044	0.00058	10	4.3
Open Water permanent				0.00033			0.00333	0.02397	0.02763	86.7	3.7
sum	0.36707	0.20602	0.11689	0.02563	0.23868	0.00906	0.00589	0.03076	1		
PA	78.2	70.8	66.8	7.7	70.9	15.9	1	77.9		70.7	OA
SE_PA	2.4	3.7	5	2.1	3	6.8	0.6	8.6		1.7	SE_OA

Figure 48. Area-based confusion matrix of the Africa static map v202212 with grouping of the original legend. The accuracy estimates were derived using 857 homogeneous samples photo-interpreted with certainty. Class-related cells are expressed in terms of proportions of area (range 0 – 1). Accuracy figures are reported in % with their standard error. OA, PA and UA stand for overall, producer, and user accuracy, and SE for standard error.

MAP/REF	Tree cover evergreen broadleaf	Tree cover deciduous broadleaf	Shrub cover evergreen	Shrub cover deciduous	Grassland	Croplands	Grassland vegetation aquatic or regularly flooded	Bare areas	Built-up	Open Water seasonal	Open Water permanent	sum	UA	SE_UA
Tree cover evergreen broadleaf	0.1519		0.002				0.002		0.002			0.1579	96.2	2.2
Tree cover deciduous broadleaf	0.00807	0.03068	0.00646	0.00969	0.00969	0.00323	0.00323					0.07106	43.2	7.6
Shrub cover evergreen	1e-05		5e-05		2e-05	0						9e-05	56.5	10.6
Shrub cover deciduous	0.00196	0.01762	0.00392	0.06266	0.0235	0.00196						0.11162	56.1	6.6
Grassland	0.00177	0.02122	0.01414	0.02475	0.14145	0.03183	0.01414	0.06188	0.01061		0.00354	0.32533	43.5	3.7
Croplands		0.00525	0.00525	0.007	0.0175	0.07701	0.00175	0.007	0.00175			0.12251	62.9	5.8
Grassland vegetation aquatic or regularly flooded	7e-05				0.00044		0.00197	0.00015		0.00022	0.00051	0.00335	58.7	7.3
Bare areas							0.00226	0.16703	0.00451	0.00226	0.00226	0.17832	93.7	2.8
Built-up	4e-05				9e-05	4e-05			0.00144			0.00162	89.2	5.2
Open Water seasonal			1e-05		1e-05	1e-05	1e-05	3e-05		6e-05	0.00044	0.00058	10	4.3
Open Water permanent							0.00033			0.00333	0.02397	0.02763	86.7	3.7
sum	0.16383	0.07477	0.03183	0.10411	0.1927	0.11408	0.02569	0.2361	0.02032	0.00586	0.03071	1		
PA	92.7	41	0.2	60.2	73.4	67.5	7.7	70.7	7.1	1	78		65.8	OA
SE_PA	2.5	6.3	0	5.5	3.7	5	2.1	3.1	2.1	0.6	8.6		1.8	SE_OA

Figure 49. Area-based confusion matrix of the Africa static map v202212 in its original legend. The accuracy estimates were derived using 857 homogeneous samples photo-interpreted with certainty. Class-related cells are expressed in terms of proportions of area (range 0 – 1). Accuracy figures are reported in % with their standard error. OA, PA and UA stand for overall, producer, and user accuracy, and SE for standard error.

7 ANNEX – Results of the previous validation exercises

The quality assessments included in this section were first made on **RR prototypes** whose areas correspond to one S2 tile for Africa (T37PCP), two for Amazonia (21KUQ and 21KXT) and one for Siberia (42WXS). The first delivery was done in July 2020 but the SAR S1 prototypes for Siberia and Amazonia had a smaller extent than other prototypes. Therefore, these prototypes were updated on 02/10/2020 and 09/10/2020 respectively. While

fusion products were updated on 10/10/2020 for the MRF algorithm, and 15/10/2020 for the LOGP algorithm. Some of the analyses were already done by the time the problem with SAR S1 size was noticed and was not repeated. In this version of the PVIR, the quality of all RR prototypes has been evaluated qualitatively and the Africa RR prototypes were quantitatively assessed.

Second, **static land cover maps over a “zoom area”** were made available on 21/10/2020 for Amazonia and Siberia. This version of the PVIR includes their qualitative assessment and reports about the improvements brought from the RR stage to these LC maps classified at a larger extent.

Finally, the first version of the **historical map of Amazonia** was received and qualitatively assessed.

7.1 RR prototypes

The first production of the static map was received through RR prototypes (Table 2) on 30/07/2020. The areas of the prototypes correspond to one S2 tile for Africa (T37PCP), two for Amazonia (21KUQ and 21KXT), and one for Siberia (42WXS). SAR S1 prototypes for Siberia and Amazonia had smaller extents than other prototypes, so these prototypes were updated on 02/10/2020 and 09/10/2020 respectively. While fusion products were updated on 10/10/2020 for the MRF algorithm, and 15/10/2020 for the LOGP algorithm. Some of the analyses were already done by the time the problem with SAR S1 size was noticed, therefore they are not repeated. It will be specified in the following text when the updated version was not considered.

Table 12: Summary of the RR prototypes received for validation

	Production		
	Optical S2	SAR S1	Fused
Africa (1 tile)	LSTM-Monthly Composite Received LSTM-Time Series Received SVM Received	Received	MRF Received LOGP Received
Amazonia (2 tiles)	LSTM-Monthly Composite Received LSTM-Time Series Received SVM Received	Received	MRF Received LOGP Received
Siberia (1 tile)	LSTM-Time Series Received SVM Received	Received	MRF Received LOGP Received

7.1.1 Visual quality assessment

The following sections consist of a visual evaluation of the quality of the RR prototypes through snapshots and comparison with google imagery and auxiliary LC maps.

7.1.1.1 Africa - T37PCP

7.1.1.1.1 SVM Map

In general, the SVM Map over Africa overestimates the built-up class (Figure 2).

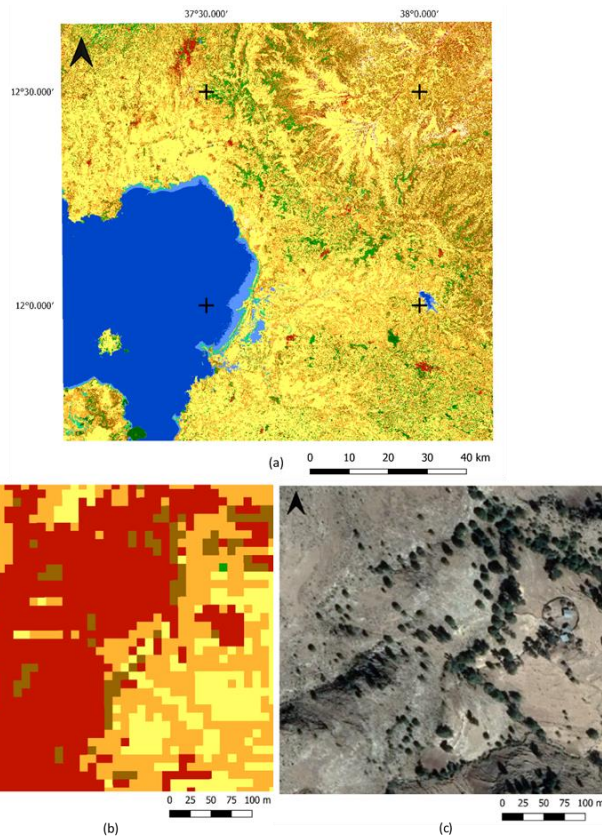


Figure 50. Illustration of the full extent of the CCI-HRLC RR prototypes SVM Map over Africa (a), an example of the overestimation of the built-up class ($37^{\circ}84.40$, $12^{\circ}22.75$, WGS 84) (b) and the corresponding google imagery (c).

Besides, the SVM map suffers from water overestimation. Bare soil and mountains' shadows are often misclassified as water (Figure 3).

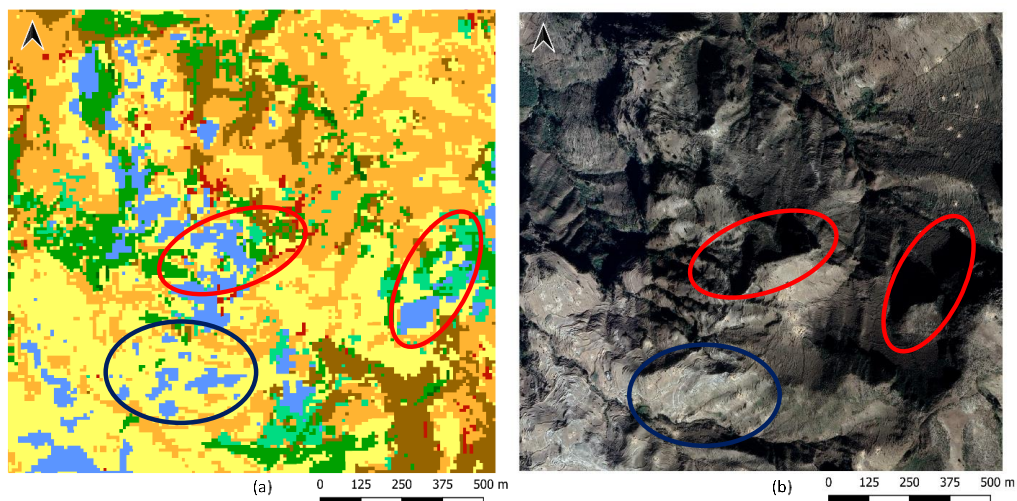


Figure 51. Illustration of the open seasonal water class and the vegetation regularly flooded class detected in the place of shadows (circled in red) and contaminating the map (circled in blue), presented on the CCI-HRLC RR prototypes African SVM map (a) and Google Imagery (b) ($37^{\circ}83.52$, $12^{\circ}25.03$, WGS 84).

Finally, some linear features such as water tracks are not classified although they have a width greater than 10 m, which corresponds to the spatial resolution of the map, and a contrasting spectral signature against the background (here: cropland). Water is confused with bare areas, cropland, and grasslands (Figure 4).

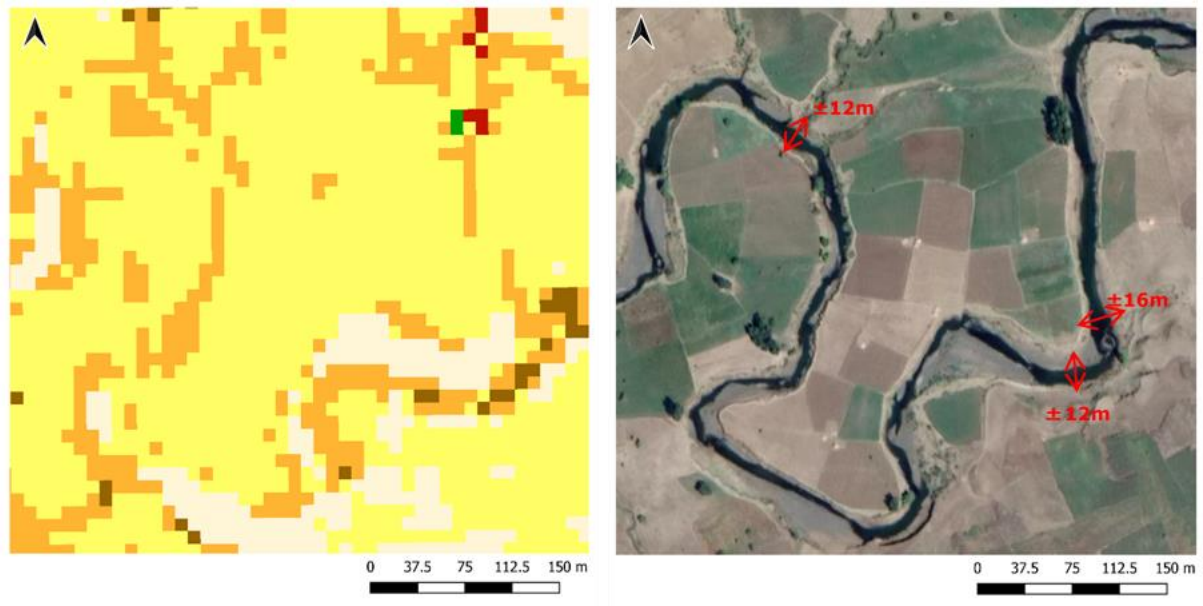
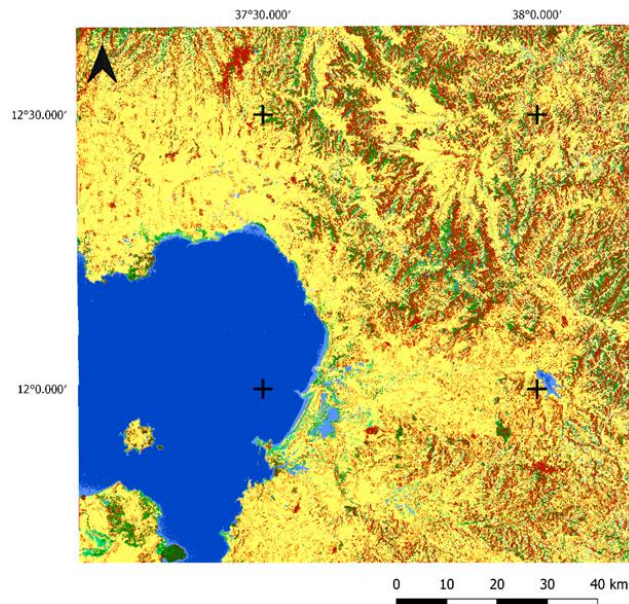


Figure 52. Illustration of a water track partially detected as bare areas on the CCI-HRLC RR prototypes African SVM map (a) and Google Imagery (b) (37°63.89, 12°18.75, WGS 84).

7.1.1.1.2 SAR Map

Compared to the SVM Map, the SAR Map is less accurate in distinguishing finer landscape features such as water streams (circled in red). Although the SAR Map prototype is delivered at a spatial resolution of 10m, the minimum mapping unit is coarser. Moreover, it contains many more thematic errors, especially a huge overestimation of the built-up class (Figure 5).



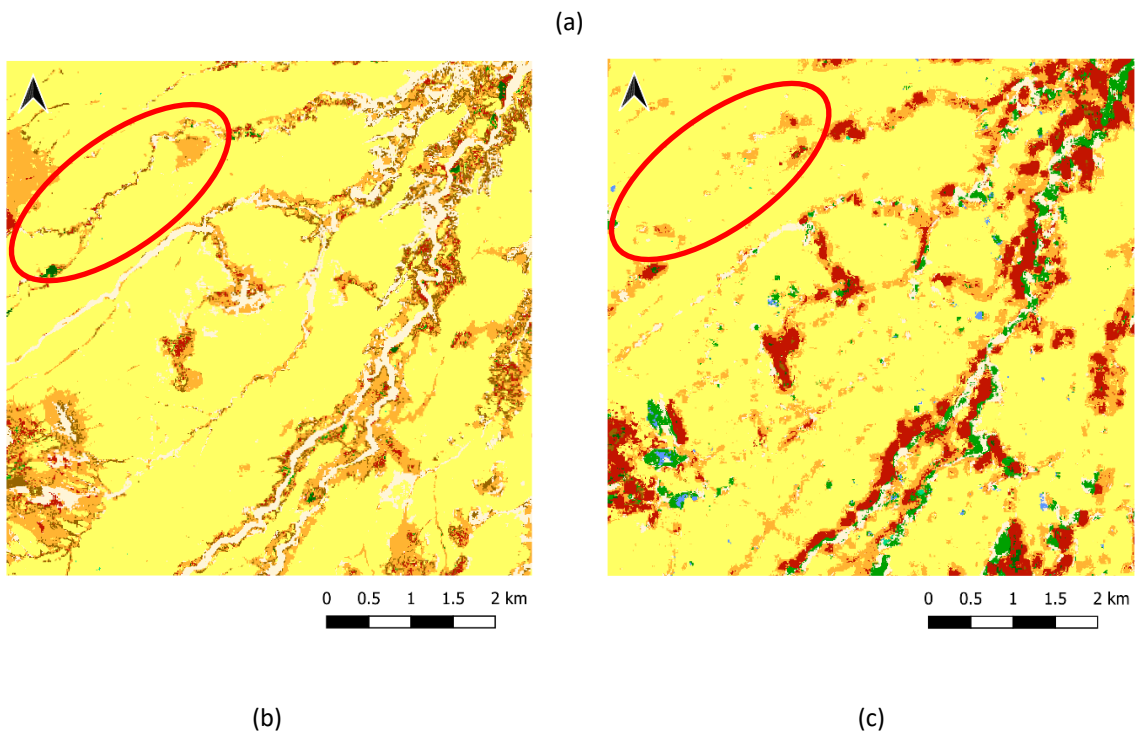


Figure 53. Illustration of the full extent of the CCI-HRLC RR prototypes SAR map over Africa (a), an example of the detection of a landscape feature on the CCI-HRLC RR prototypes SVM Map (b) and the SAR map (c), (37°83.89', 12°.38.91, WGS 84)

The SAR Map is contaminated by the open Water Seasonal class and the grassland aquatic or regularly flooded class (Figure 6)

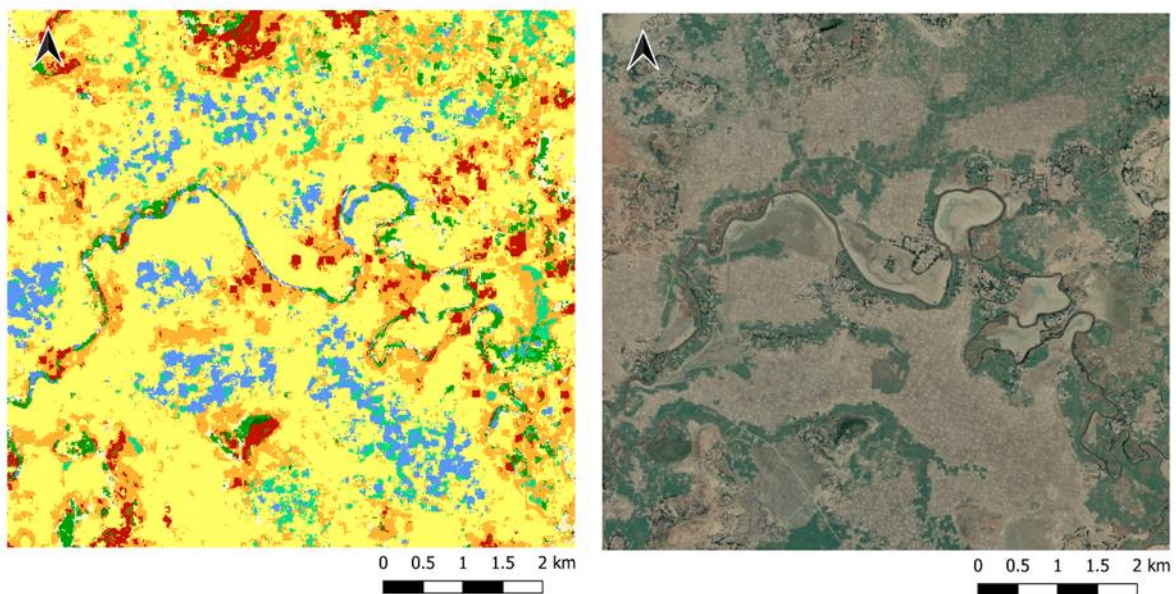


Figure 54. Illustration of the open water seasonal class and the grassland aquatic or regularly flooded class over Africa on the CCI-HRLC RR prototypes SVM Map (a) compared to Google Imagery (b), (37°76.06', 11°.78.67').

7.1.1.1.3 LSTM Composite and Time Series Maps

Both LSTM maps seem to have higher overestimation issues of some classes than the SVM Map. One example shown in Figure 7 is the shrubs class that seems highly overestimated on the LSTM time-series map. The LSTM composite map has the same issue but not as much.

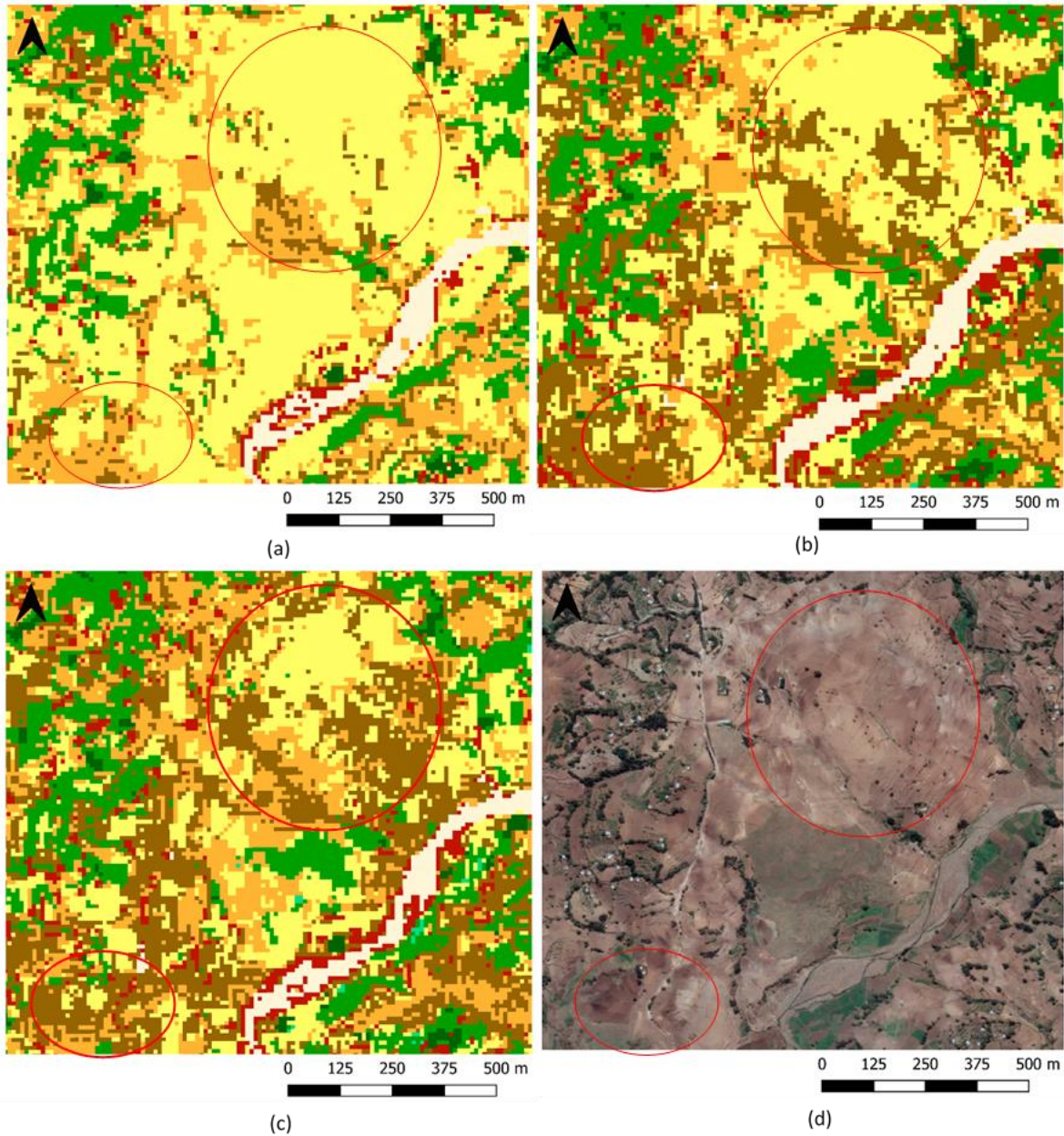


Figure 55. Illustration of the shrubs class classification over Africa on the CCI-HRLC RR prototypes SVM Map (a), LSTM composite map (b), the LSTM time series map (c), and the Google imagery base map (d).

Figure 8 shows shrubland contaminations in the SVM and LSTM Time-series prototypes in cropland areas where shrubs are scarce or absent as demonstrated by the VHR SPOT6 image. This classification heterogeneity should not appear on the map, especially considering the established definitions of each class.

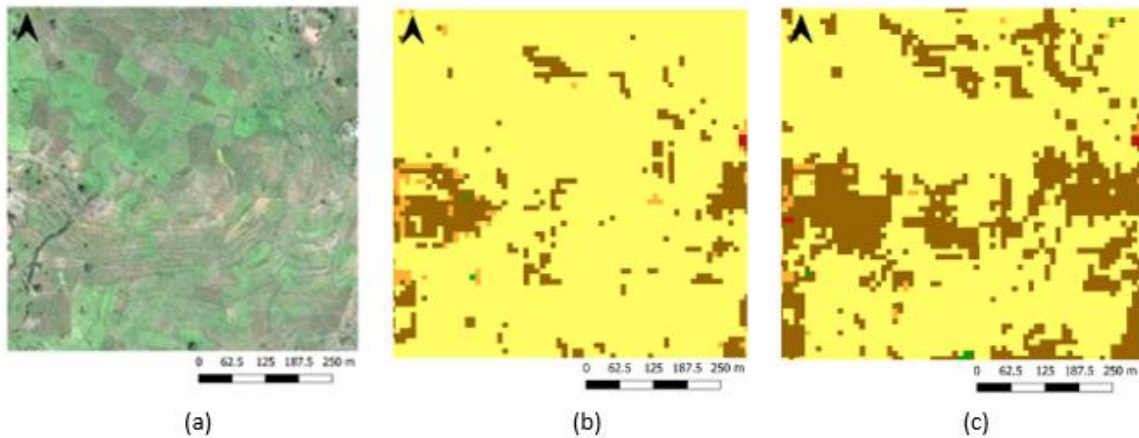


Figure 56. Illustration of the misclassification of the shrub class over Africa on the CCI-HRLC RR prototypes SVM Map (b), LSTM time series map (c), and the corresponding extent of a VHR SPOT6 image of 24.10.2019 (c), (37.67.11, 12.07.06, WGS84).

Both LSTM Maps overestimate the bare area class (especially the LSTM composite) and have a higher overestimation of the built-up class than the SVM Map (Figure 9).

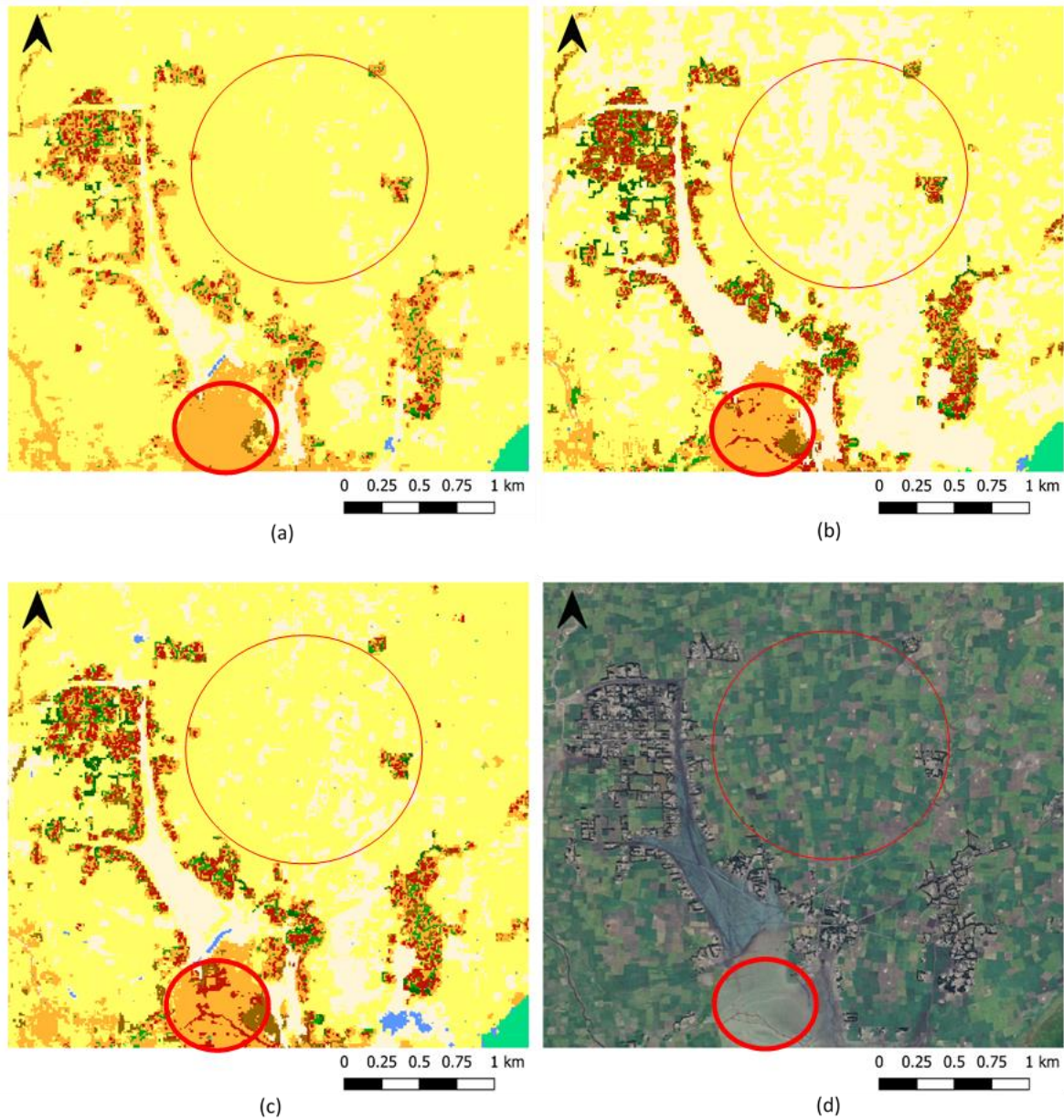


Figure 57. Illustration of the bare area and built-up classes overestimation over Africa comparing the CCI-HRLC RR prototypes SVM Map (a) LSTM composite (b) the LSTM time series (c) and the Google imagery base layer (d) ($37^{\circ}46.72', 12^{\circ}.32.28'$).

Finally, the LSTM maps, particularly the time series one, seem to detect more grassland regularly flooded on cropland areas (Figure 10).

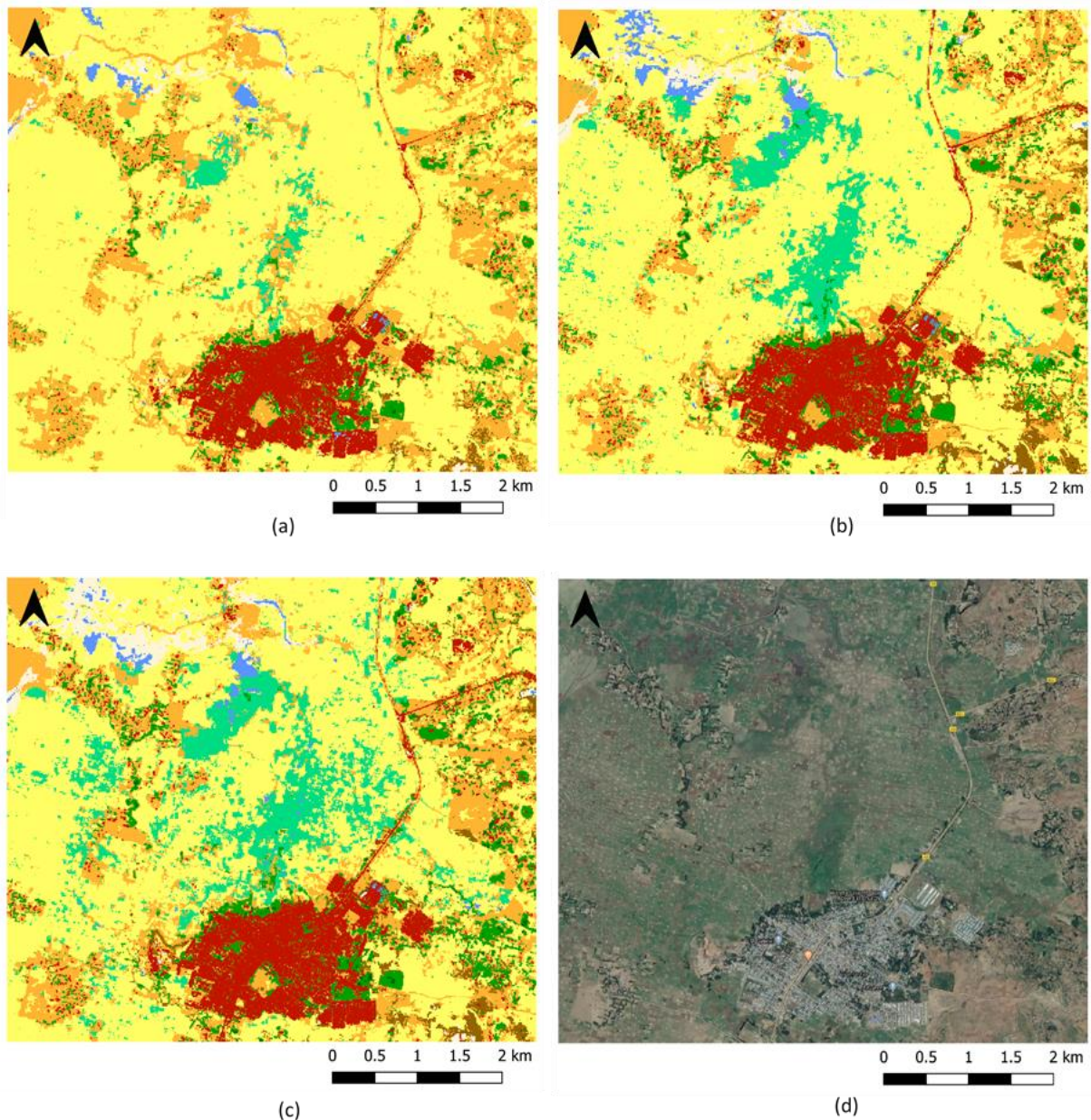


Figure 58. Illustration of the grassland regularly flooded class over Africa comparing the CCI-HRLC RR prototypes SVM Map (a) LSTM composite (b) the LSTM time series (c) and the Google imagery base layer (d) (37°70.06, 11°.94.08, WGS 84).

7.1.1.1.4 Fused maps: LOGP & MRF

The salt and pepper effect is reduced on the MRF map compared to the LOGP and SVM maps. However, some artefacts are visible on the MRF map (Figure 11). The same issues (Built-up overestimation, shadows in the mountains detected as water and features bigger than 10m not detected and some) encountered on the SVM Map can be reported on the fused maps. The fusion enhances the heterogeneity within a class encountered on the S2 maps but still contains thematical errors.

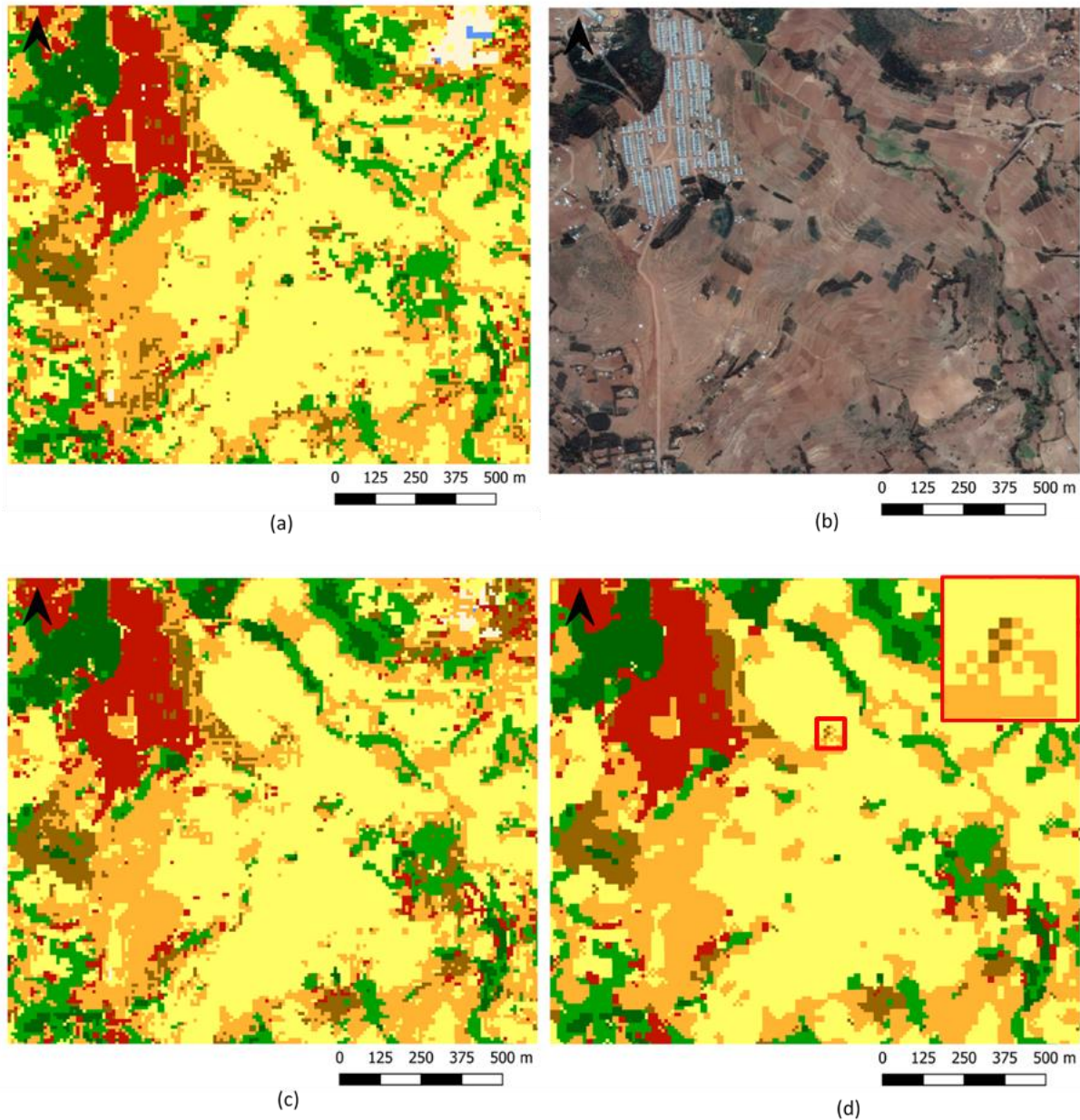
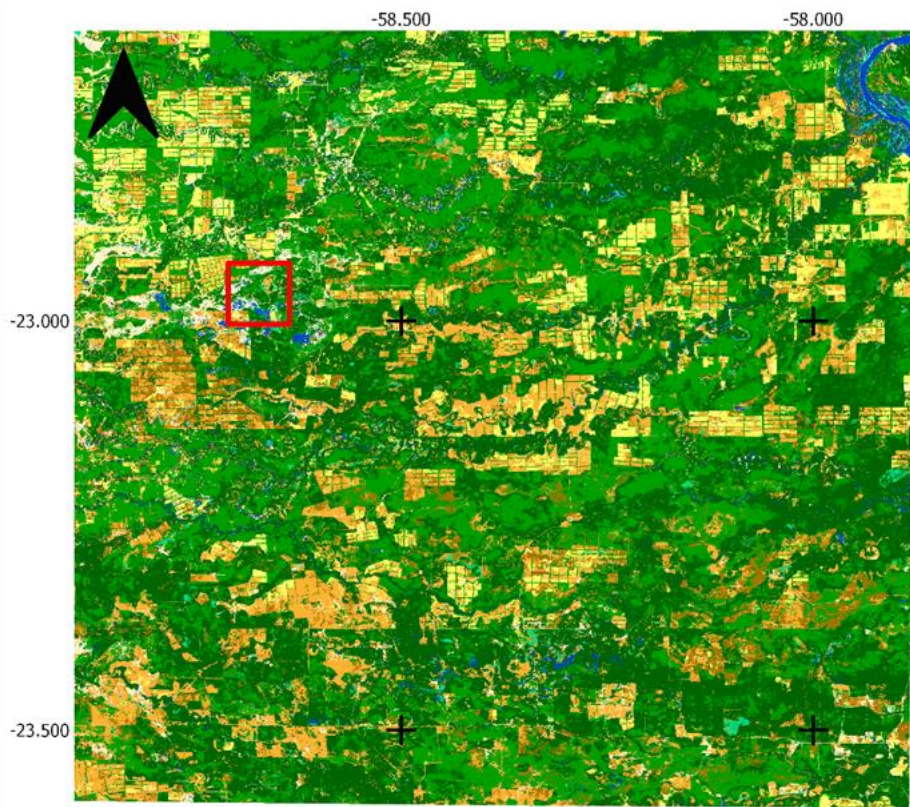


Figure 59. Illustration of the salt and pepper effect on the African CCI-HRLC RR prototypes SVM Map (a), LOGP fused map (c), and MRF fused map (d) with a Google image base map (b) (38°02.89, 11°.84.01, WGS 84).

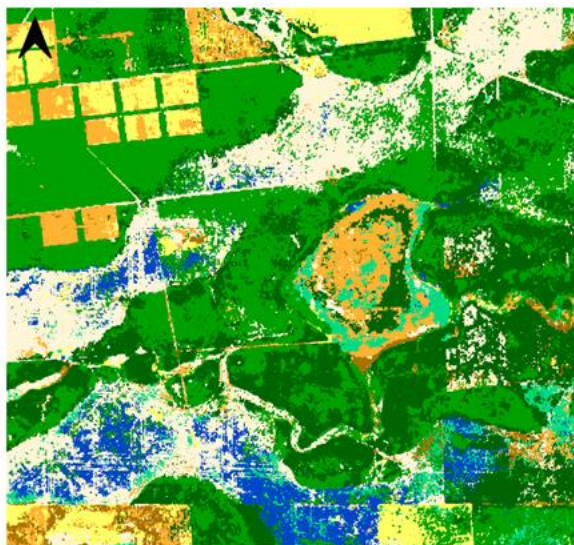
7.1.1.2 Amazonia – 21KUQ

7.1.1.2.1 SVM Map

The Amazonian KUQ SVM Map (Figure 12) seems to overestimate the bare soil class in an area conducive to abundant vegetation. Moreover, one can notice the contamination of the open Water Permanent class and the grassland regularly flooded class. There also seems to be confusion between cropland and grassland at the parcel level.



(a) 0 5 10 15 20 km



(b) 0 0.5 1 1.5 2 km



(c) 0 0.5 1 1.5 2 km

Figure 60. Illustration of the full extent (21KUQ S2 tile) of the CCI-HRLC RR prototypes SVM Map over the Amazonia (a), an example of the overestimation of the bare areas, open water permanent and grassland regularly flooded classes (-58°66.36, -22°93.81, WGS 84).

There is also an overall confusion/contamination between evergreen and deciduous tree cover classes (Figure 13).



Figure 61. Illustration of the confusion between evergreen and deciduous tree cover classes over Amazonia on the CCI-HRLC RR prototypes SVM Map (a) compared to the Google Imagery base map (b) (-58°00.70', -22° 71.04', WGS 84).

7.1.1.2.2 SAR Map

The SAR map seems to have an overall poorer quality due to a higher overestimation of bare soil class and more confusion between evergreen and deciduous tree cover classes (circled in red in Figure 14). When comparing the SAR map with the SVM Map, one can notice disagreements between classes (circled in blue in Figure 14): grassland/shrubs with evergreen tree cover and grassland with cropland.

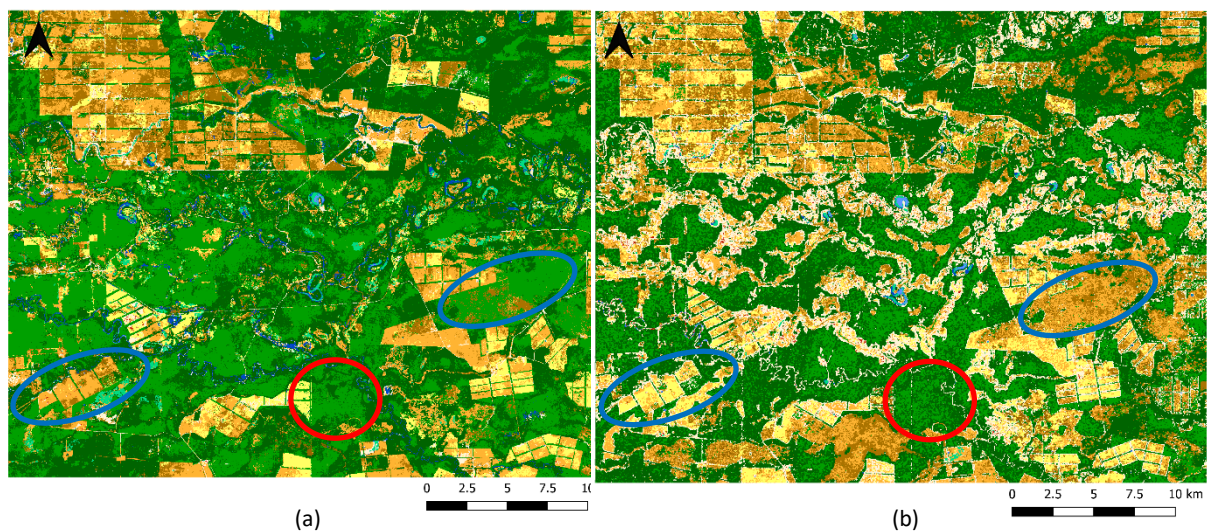


Figure 62. Comparison of the CCI-HRLC RR prototypes over Amazonia, SVM Map (a) and SAR map (b). Illustration of the confusion between evergreen and deciduous tree cover classes (circled in red) and classification disagreement between the two maps (circled in blue) (-58°56.10, -23° 21.08, WGS 84)

7.1.1.2.3 LSTM Composite and Time Series Maps

Both LSTM maps contain contaminations of the built-up and shrub classes (circled in red and dark blue respectively in Figure 15). However, the LSTM composite map seems to better detect water tracks (circled in light blue in Figure 15).

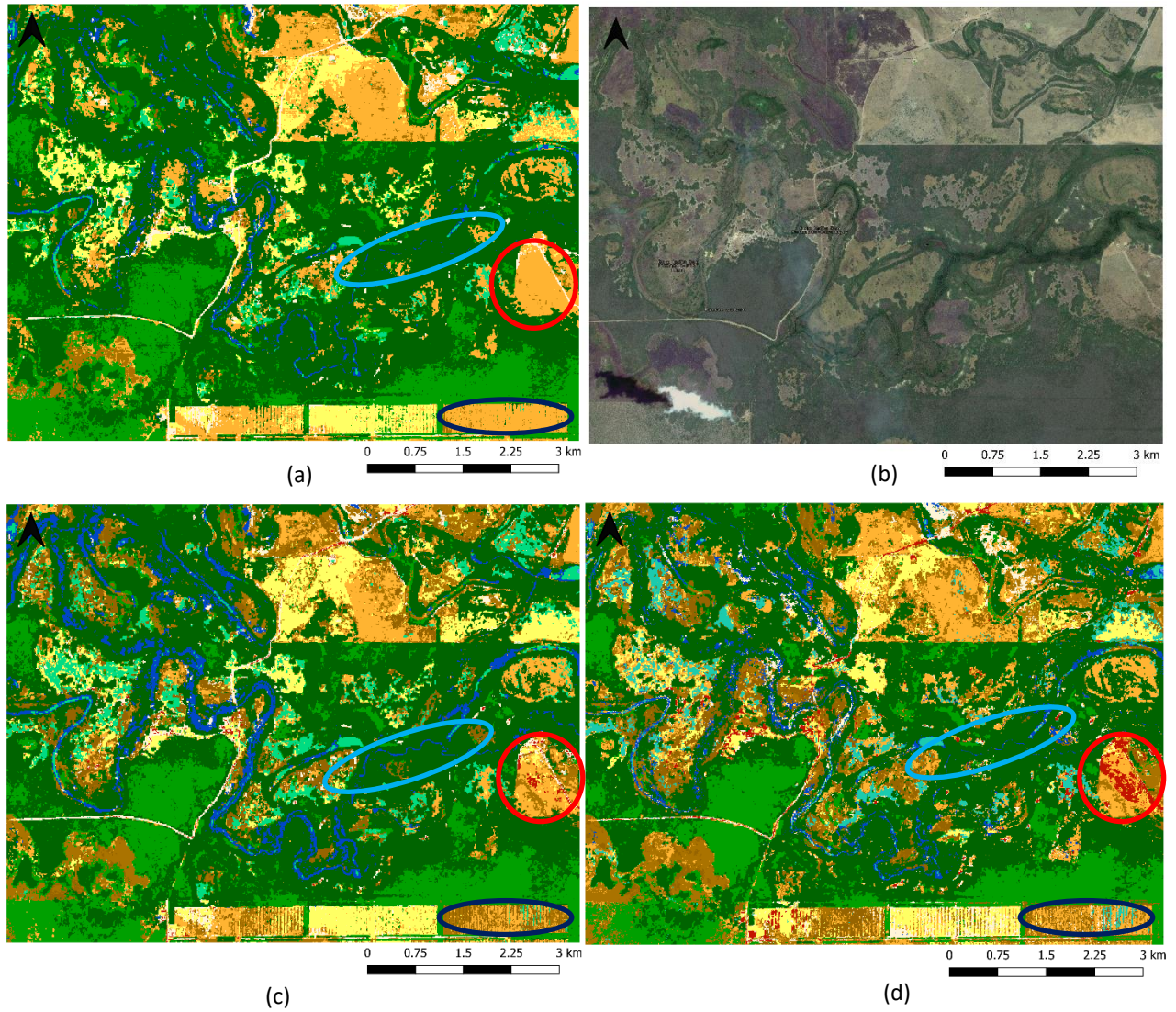


Figure 63. Illustration of the built-up and shrub classes (circled in red and dark blue) contamination and the water tracks detection (circled in light blue) over Amazonia comparing the CCI-HRLC RR prototypes SVM Map (a) LSTM composite (c) LSTM time series (d) and the corresponding extent of Google Imagery (b) (-58°50.00, -23° .13.98, WGS 84)

One improvement visible in the LSTM time series map (Figure 16) is the decrease in the mixing between evergreen and deciduous tree cover classes compare to the SVM Map.

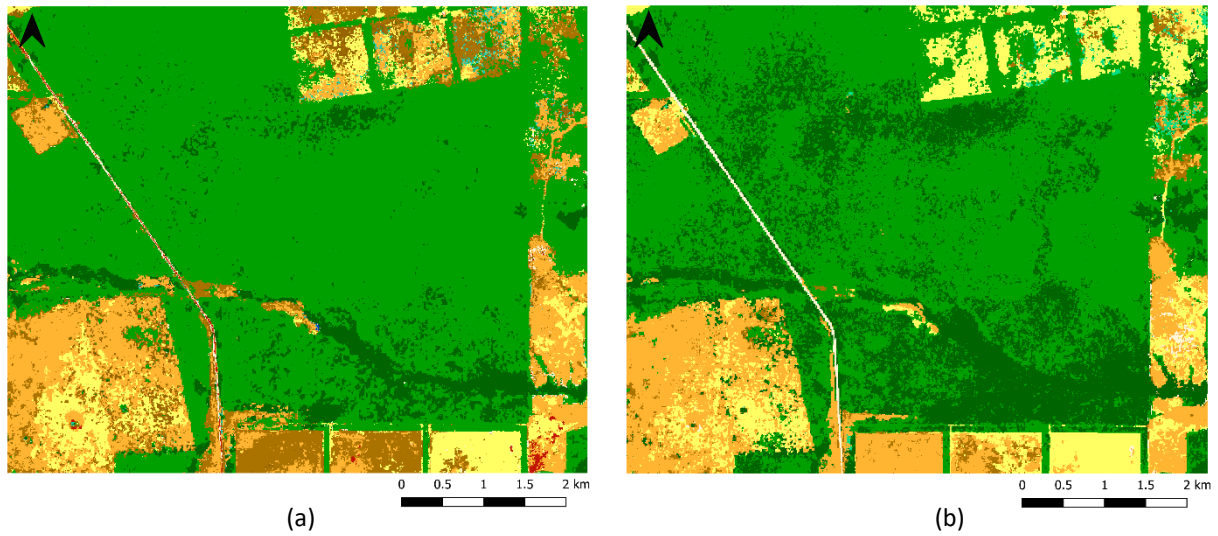


Figure 64. Illustration of the confusion between evergreen and deciduous tree cover classes over Amazonia on the CCI-HRLC RR prototypes LSTM Time series map (a) and the SVM Map (b), (-58°00.70', -22° .71.04', WGS 84).

7.1.1.2.4 Fused maps: LOGP & MRF

Both fused maps do not seem to contain the permanent open water class contamination encountered in the SVM Map (Figure 17).

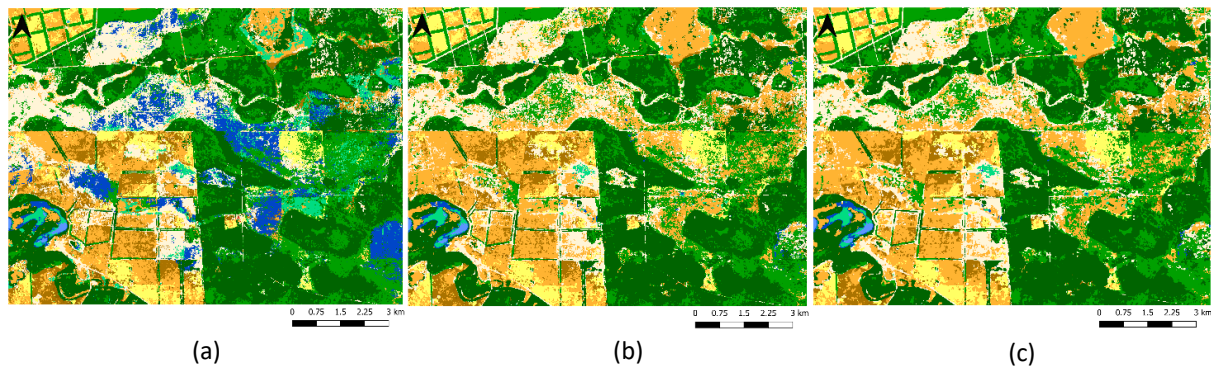


Figure 65. Illustration of open water permanent class over Amazonia comparing the CCI-HRLC RR prototypes SVM Map (a), LOGP fused map (b) and MRF fused map (c) (-58°66.36, -22° .93.81, WGS 84)

The salt and pepper effect diminishes from the SVM Map to the LOGP and finally MRF (circled in red in Figure 18). However, by doing so, the MRF map loses features such as river tracks. The heterogeneity of shrubs, grass, and crop at the parcel level (red arrow in Figure 18) is not relevant to the spatial resolution of the map and the defined legend for each class.

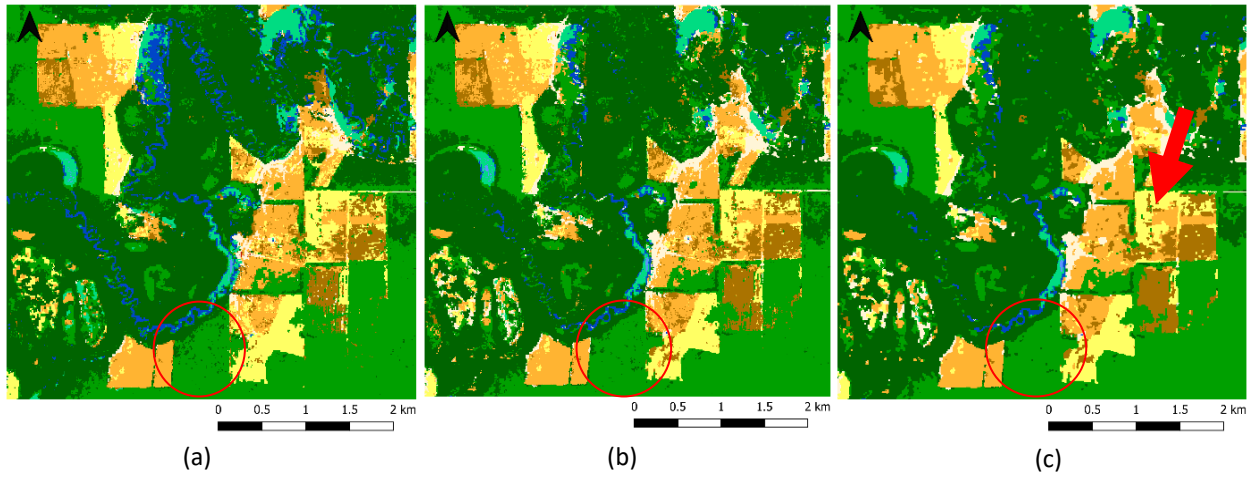


Figure 66. Illustration of the salt and pepper effect (circled in red) over Amazonia comparing the CCI-HRLC RR prototypes SVM Map (a), LOGP fused map (b) and MRF fused map (c) (-58.1686, -23.0475, WGS 84).

7.1.1.3 Amazonia - 21KXT

7.1.1.3.1 SVM Map

Figure 19 shows the same errors encountered on the KUQ tile can be observed on the KXT one. There is an overestimation of the bare area class (red capture), confusion between evergreen and deciduous tree cover classes (orange frame), and confusion between grassland and cropland at the parcel level (blue frame).

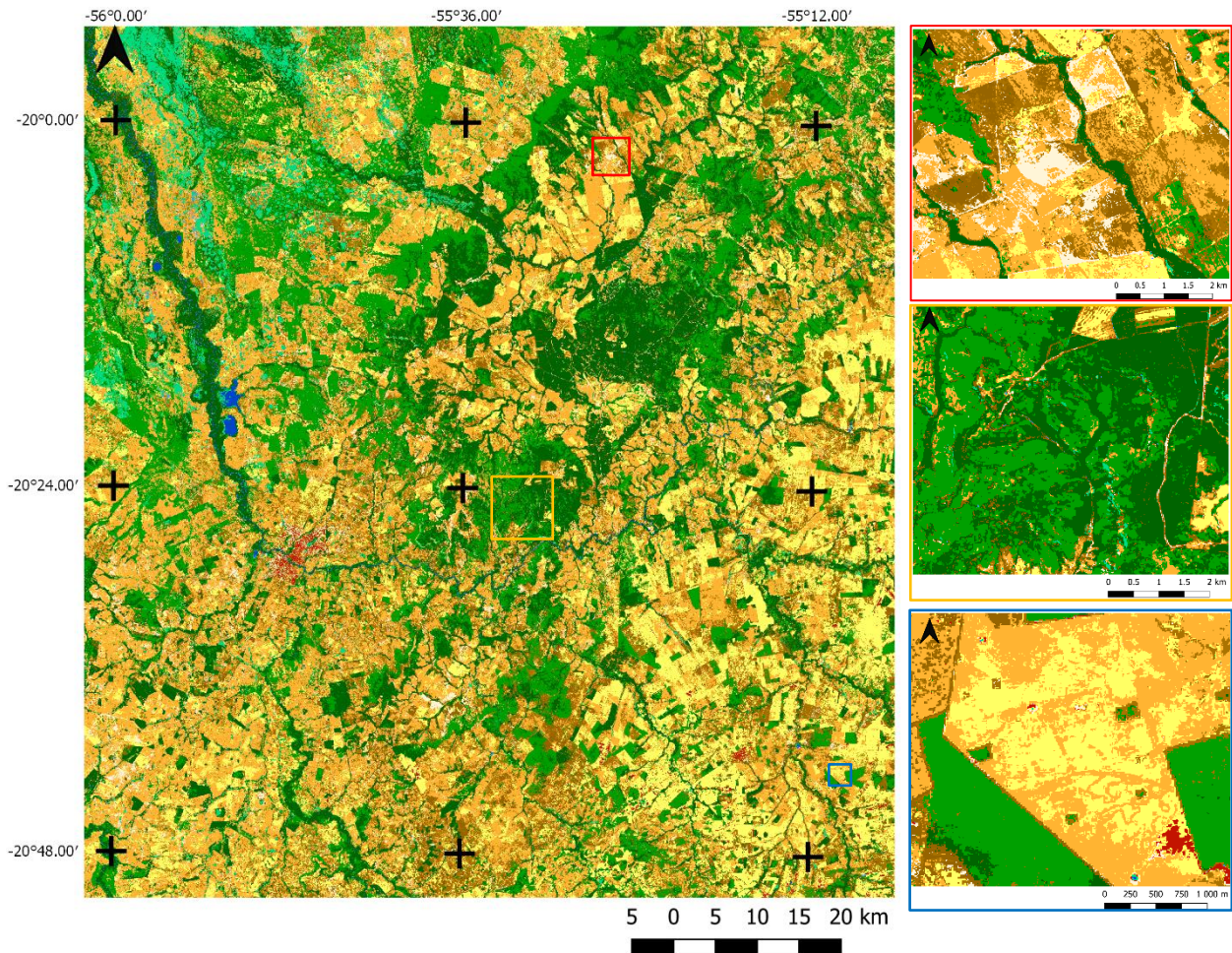


Figure 67. Illustration of the full extent (21KXT S2 tile) of the CCI-HRLC RR prototypes SVM Map over the Amazonia (a) and an example of the overestimation of the bare areas (red frame), a confusion between evergreen and deciduous tree cover classes (orange frame) and a confusion between grassland and cropland at the parcel level (blue frame) (-58°66.36, -22°93.81, WGS 84) (b)

Shadows in the mountain are detected as vegetation regularly flooded (Figure 20).

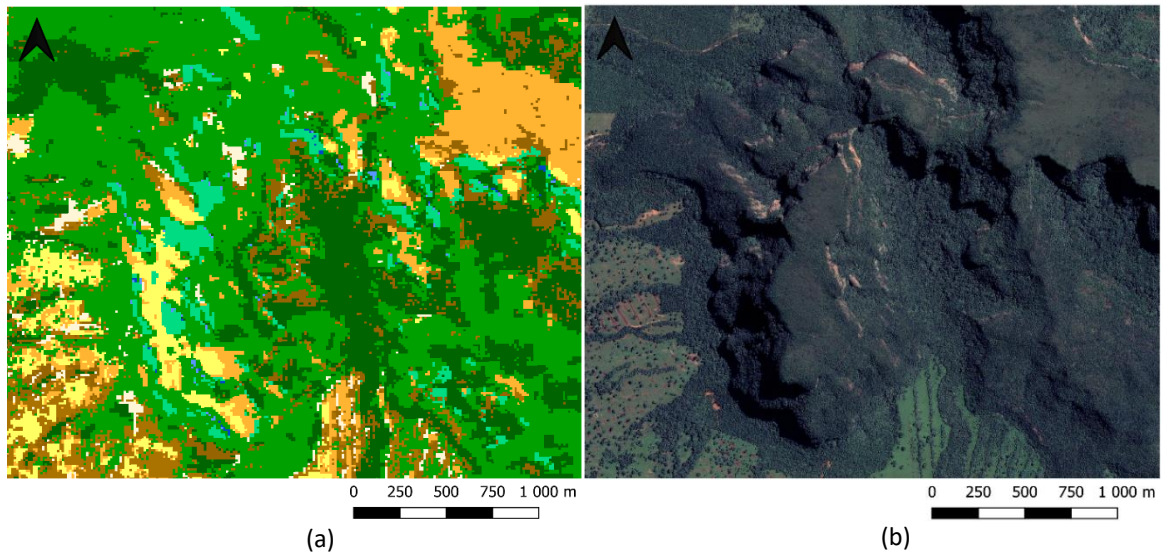


Figure 68. Illustration of the detection of shadows as vegetation regularly flooded on the CCI-HRLC RR prototypes SVM Map over the Amazonia (a) and the corresponding Google imagery base map (b) (-55°32.64, -20°06.61, WGS 84)

7.1.1.3.2 SAR Map

The SAR map seems of poorer quality than the SVM Map as it has an overall higher overestimation of built-up, bare soil, and shrub classes (Figure 21). A disagreement between evergreen and deciduous tree cover classes (circled in red in Figure 21) and cropland-grassland classes (circled in blue in Figure 21) appear between the SAR map and SVM Map.

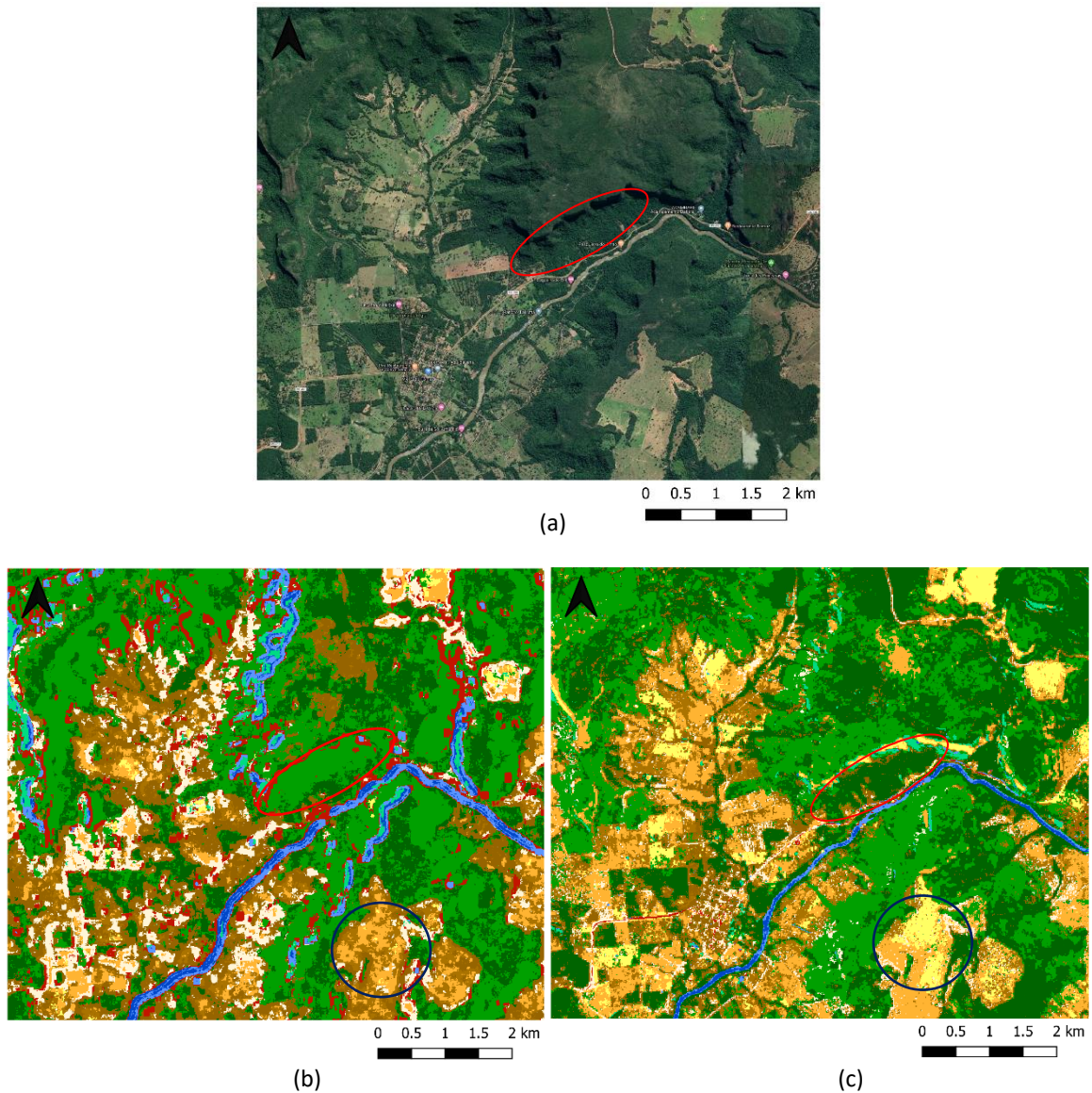


Figure 69. Illustration of the CCI-HRLC RR prototypes SAR map (b), SVM Map (c) over Amazonia and the corresponding Google Imagery base map (a). Disagreements between the two maps are circled in red and blue (-55°52.47, -20°46.30, WGS 84)

7.1.1.3.3 LSTM Composite and Time Series Maps

Both LSTM maps, especially the time series one, have an overall higher overestimation of bare soil, built-up, and shrub classes than SVM Map (Figure 22).

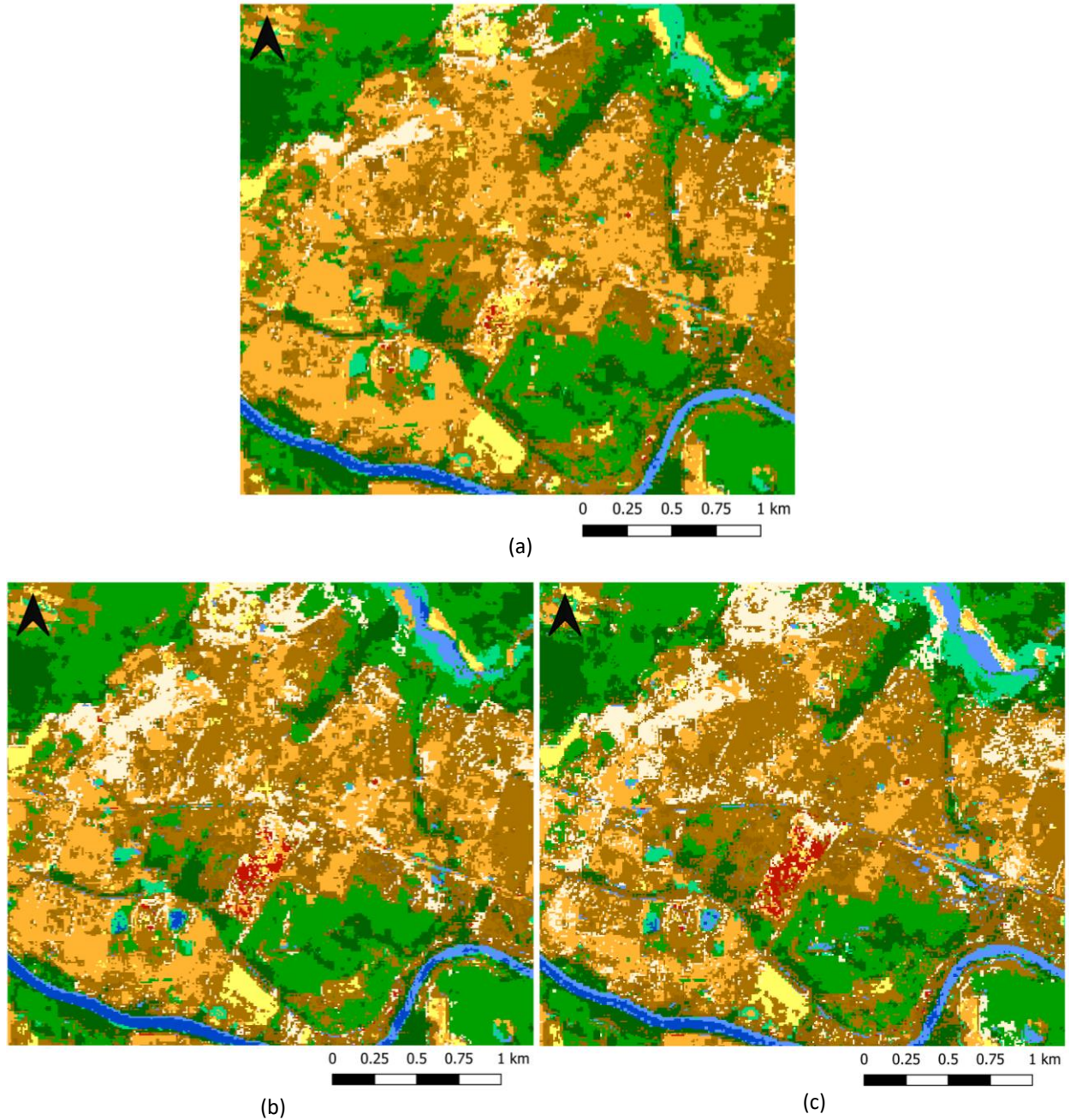


Figure 70. Illustration of the overestimation of the bare soil, built-up and shrub classes over Amazonia comparing the CCI-HRLC RR prototypes SVM Map (a) LSTM composite (b) and the LSTM time series (c) (-55.65.75, -20. 47.67, WGS 84)

7.1.1.3.4 Fused maps: LOGP & MRF

The salt and pepper effect diminish from the SVM Map to the LOGP fused map and finally the MRF fused map. However, as noticed in the fused maps of the other areas, features such as water tracks are lost in the MRF map (Figure 23).

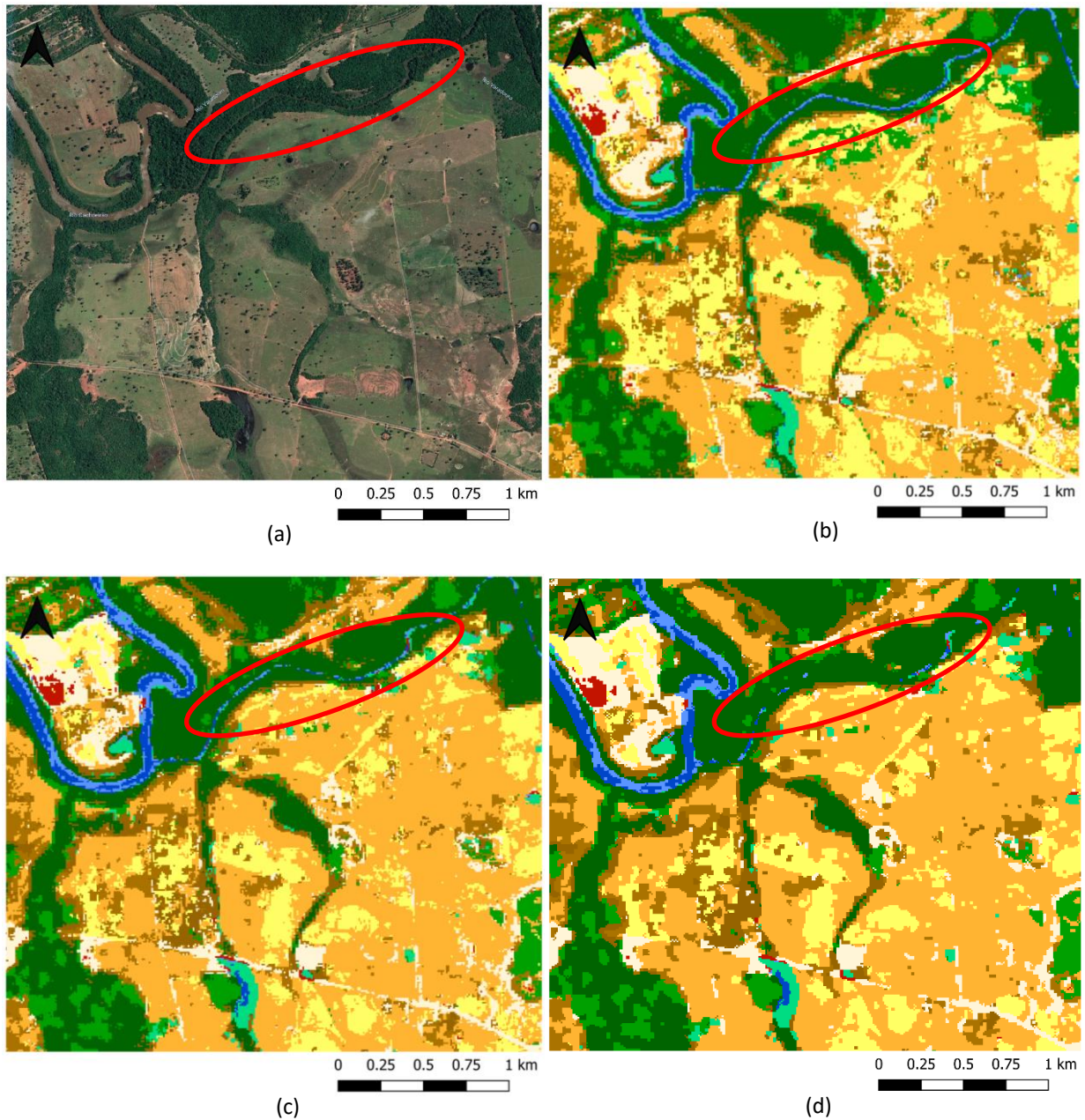


Figure 71. Illustration of the detection of water tracks (circled in red) over Amazonia comparing Google Imagery base map (a), the CCI-HRLC RR prototypes SVM Map (b), LOGP fused map (c) and MRF fused map (d) (-58.38.08, -20.44.48, WGS 84)

7.1.1.4 Siberia – 42WXS

7.1.1.4.1 SVM Map

A first general look at the SVM Map and ESA GlobPermafrost [RD2] existing map (Figure 24) shows good quality and resemblance between the two. Most comparable classes seem to agree between the two maps. The lichen and mosses class from the CCI map does not exist in the ESA GlobPermafrost map but seems to match its “disturbed class”.

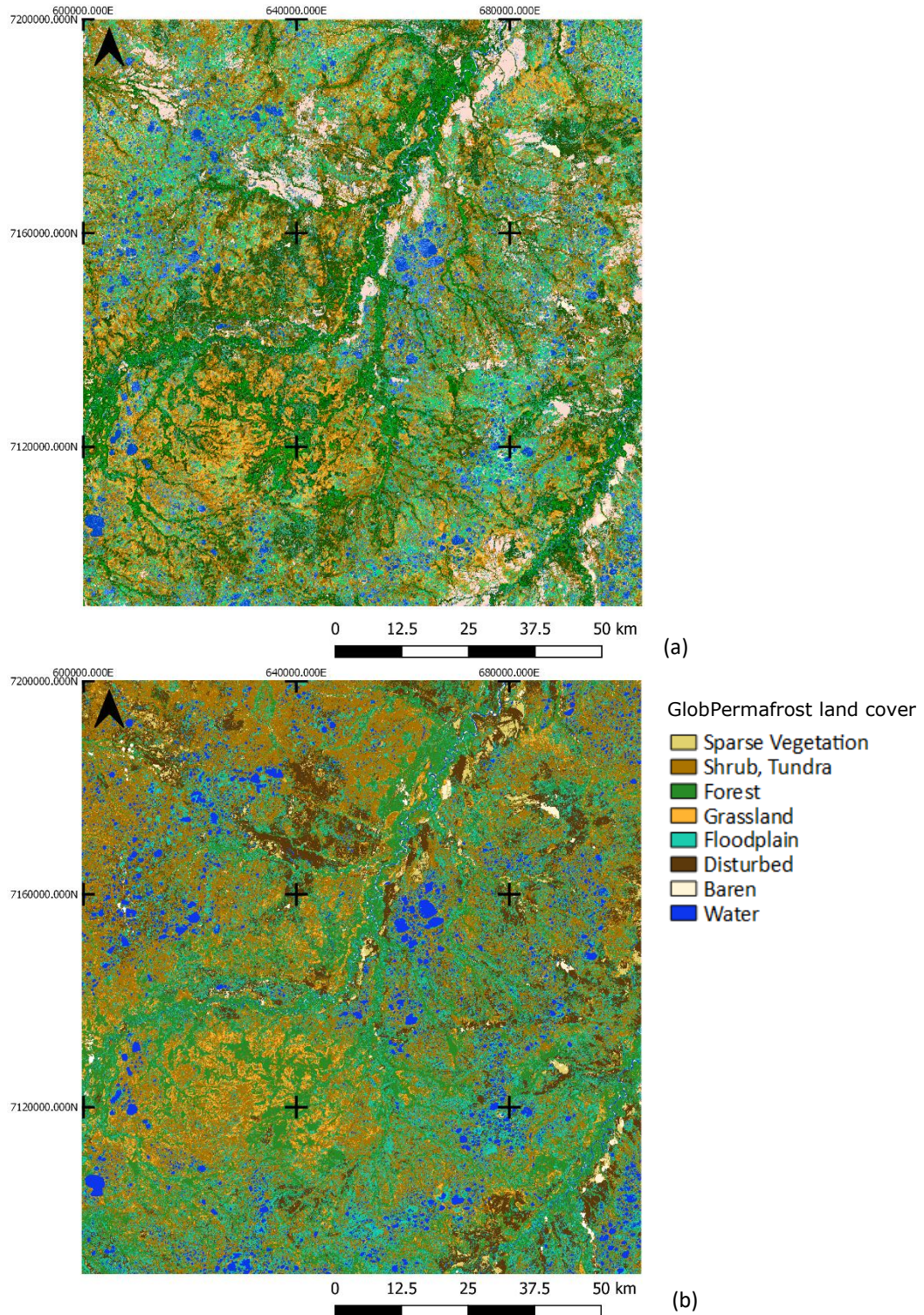


Figure 72. Illustration of the full extent (42WXS S2 tile) of the CCI-HRLC RR prototypes SVM Map over the Amazonia (a) and the corresponding extent of the GlobPermafrost map [RD2] (b)

One major disagreement between the two maps is the presence of circles of the open Water Seasonal and woody vegetation aquatic classes over patches of forests as shown in Figure 25.

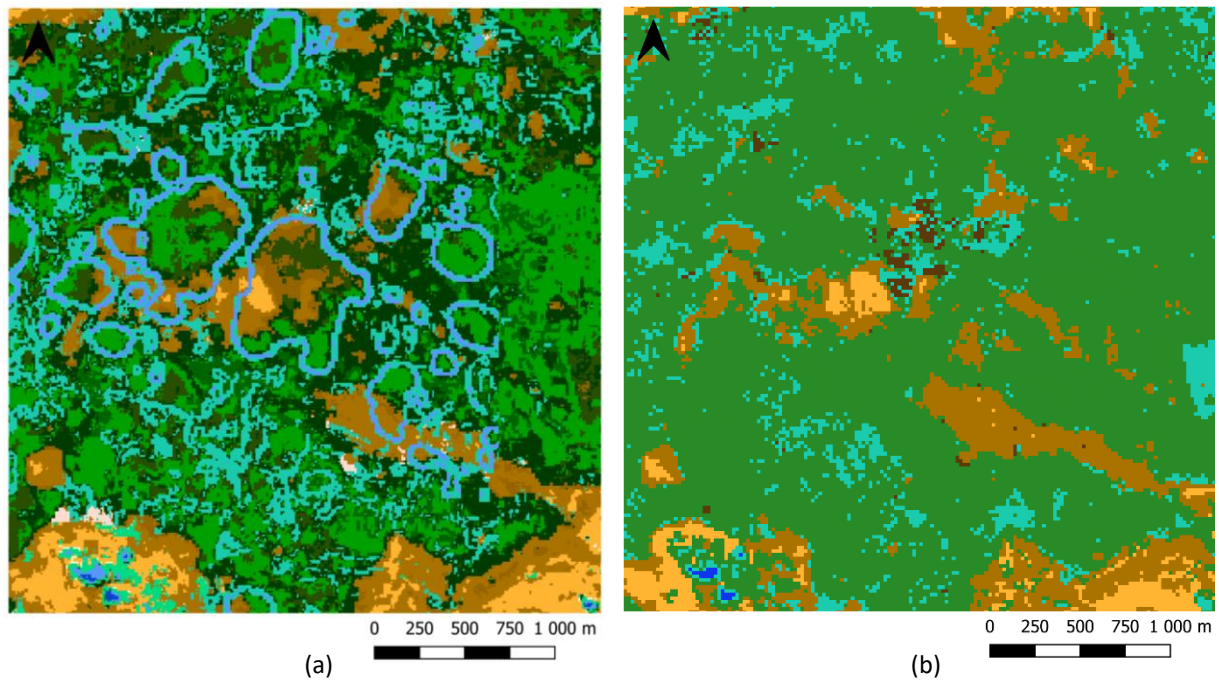


Figure 73. Illustration of the open water seasonal and woody vegetation aquatic classes comparing the CCI-HRLC RR prototypes SVM Map over the Amazonia (a) and the corresponding extent of the GlobPermafrost map [RD2] (b) (686001,7109667, WGS84/UTM Zone 42N)

Those circles found all over the map seem to be an error as they cannot be found in the landscape as shown in the VHR SPOT6 image of Figure 26.

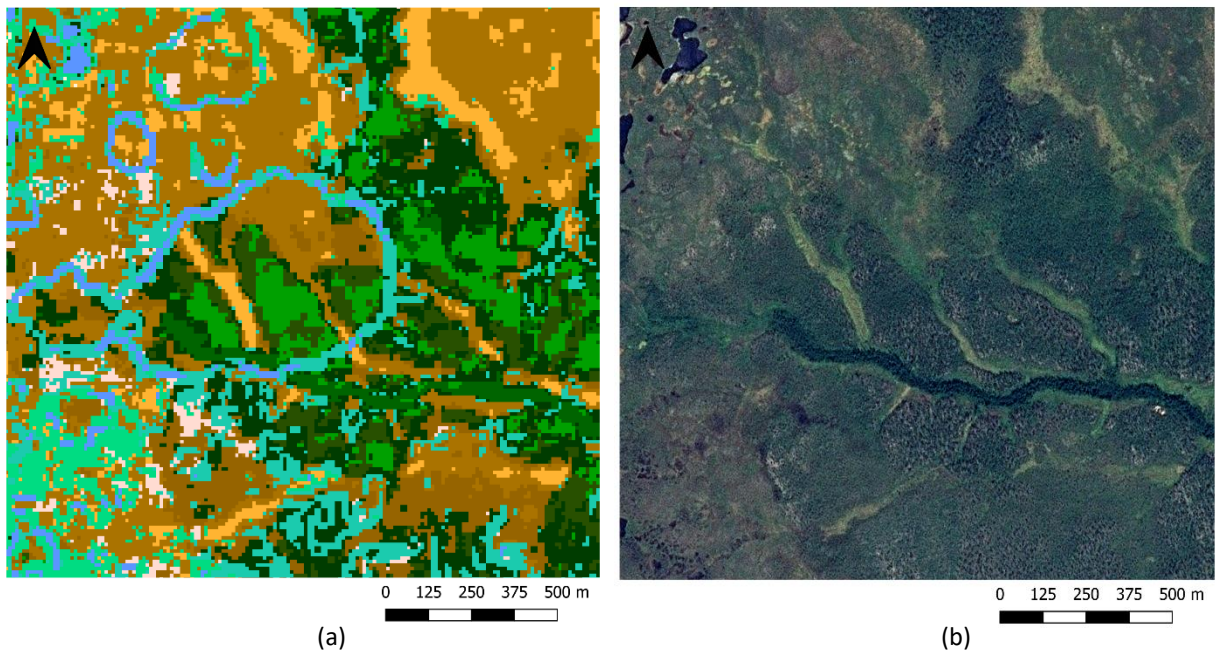


Figure 74. Illustration of the open water seasonal and woody vegetation aquatic classes comparing the CCI-HRLC RR prototypes SVM Map over the Amazonia (a) and the corresponding extent of VHR image SPOT6 from 14.07.19 (b), (686001,7109667, WGS84/UTM Zone 42N)

7.1.1.4.2 SAR Map

The SAR map has an overall overestimation of the grassland regularly flooded class compared to the ESA GlobPermafrost map (Figure 27).

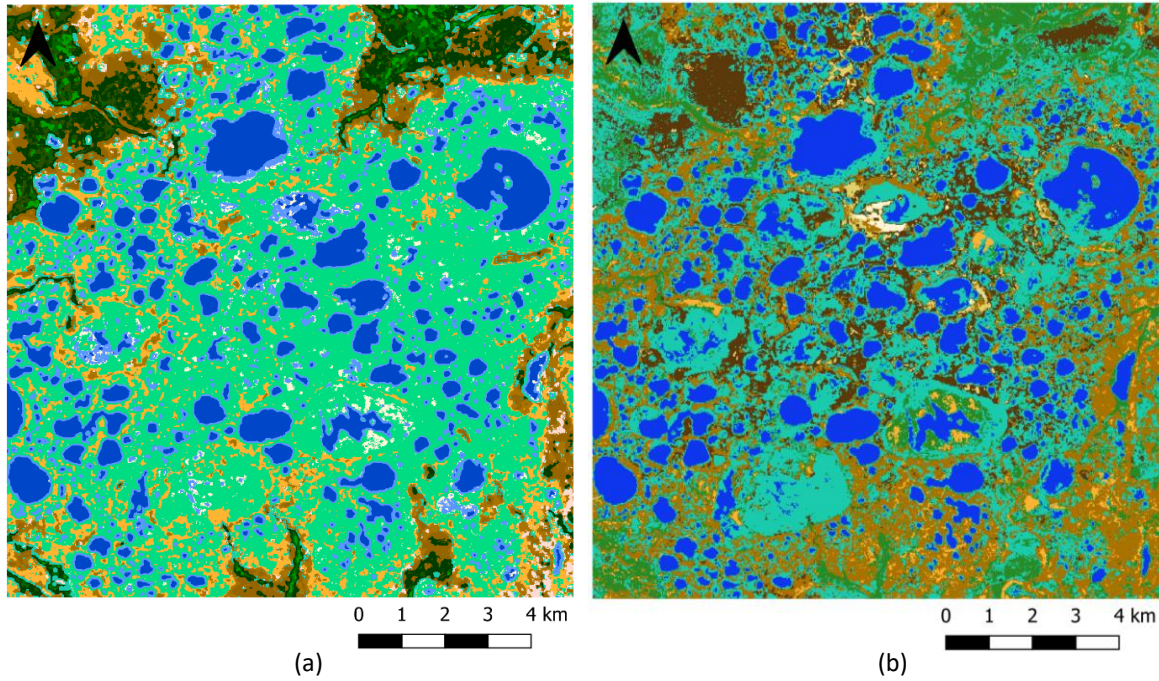


Figure 75: Illustration of the grassland regularly flooded class comparing the CCI-HRLC RR prototypes SAR map over the Amazonia (a) and the corresponding extent of the GlobPermafrost map [RD2] (b) (678817,7116460, WGS84/UTM Zone 42N)

Another disagreement appears between the two maps in Figure 28 with the grassland class that seems to take over in the SAR map where it is classified as shrubs/tundra in the ESA GlobPermafrost map.

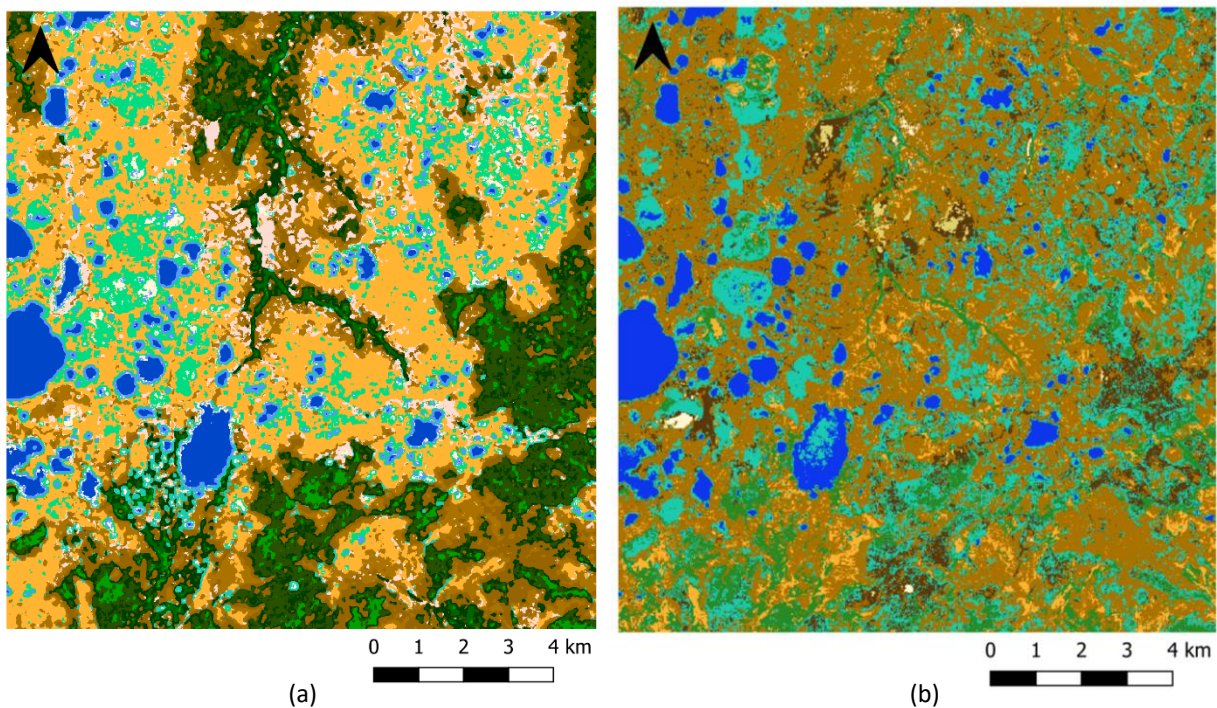


Figure 76. Illustration of the grassland class comparing the CCI-HRLC RR prototypes SAR map over the Amazonia (a) and the corresponding extent of the GlobPermafrost map [RD2] (b) (627857,7155440, WGS84/UTM Zone 42N)

7.1.1.4.3 LSTM Time Series Map

The LSTM Time Series map seems to fit the ESA GlobPermafrost map even better than the SVM Map as it does not contain the patches of open seasonal water and woody vegetation aquatic classes (Figure 29).

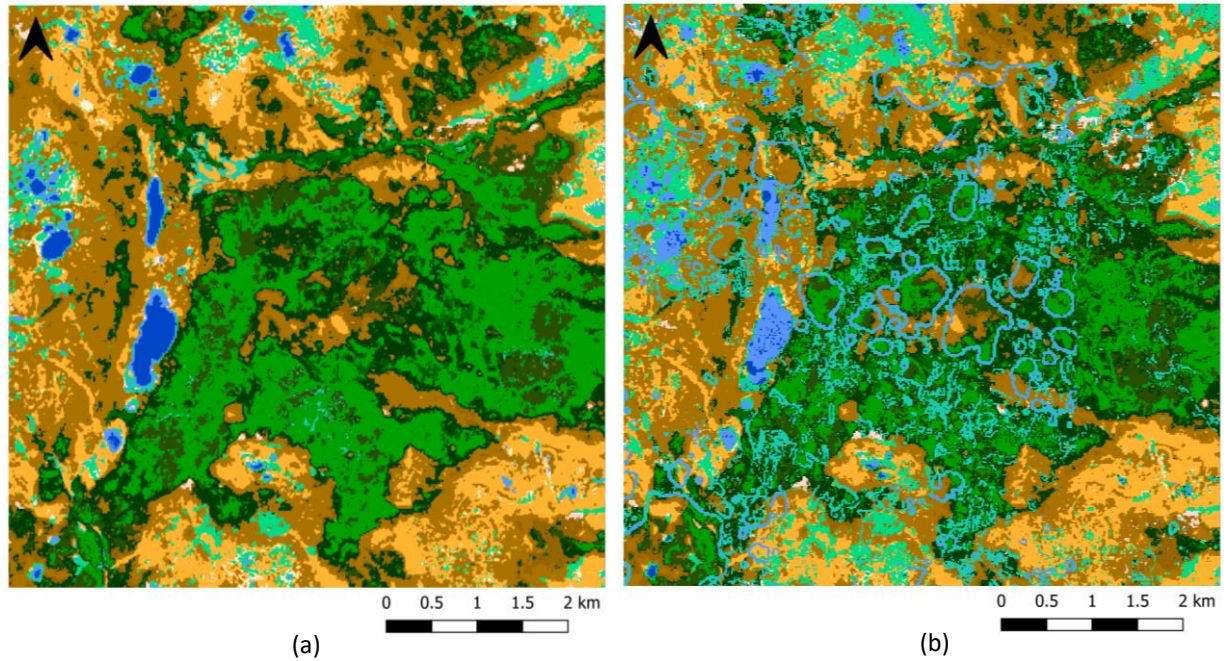


Figure 77. Illustration of the open water seasonal and woody vegetation aquatic classes comparing the CCI-HRLC RR prototypes LSTM Time Series map over the Amazonia (a) and the SVM Map (b) (686001,7109667, WGS84/UTM Zone 42N)

7.1.1.4.4 Fused maps: LOGP & MRF

It can be noticed in the MRF fused prototype (Figure 30) that the errors of the SAR map were propagated naming the overestimation of the grassland regularly flooded class and the confusion of the grassland class instead of the shrub one (red frame in Figure 30). Also, since the SAR map does not have the same extent as the SVM Map and there were disagreements between the two maps, one can see the linkage areas and the resulting discrepancies (Figure 31). Finally, the MRF fused map has a reduced salt and pepper effect compared to the LOGP map (Figure 31).

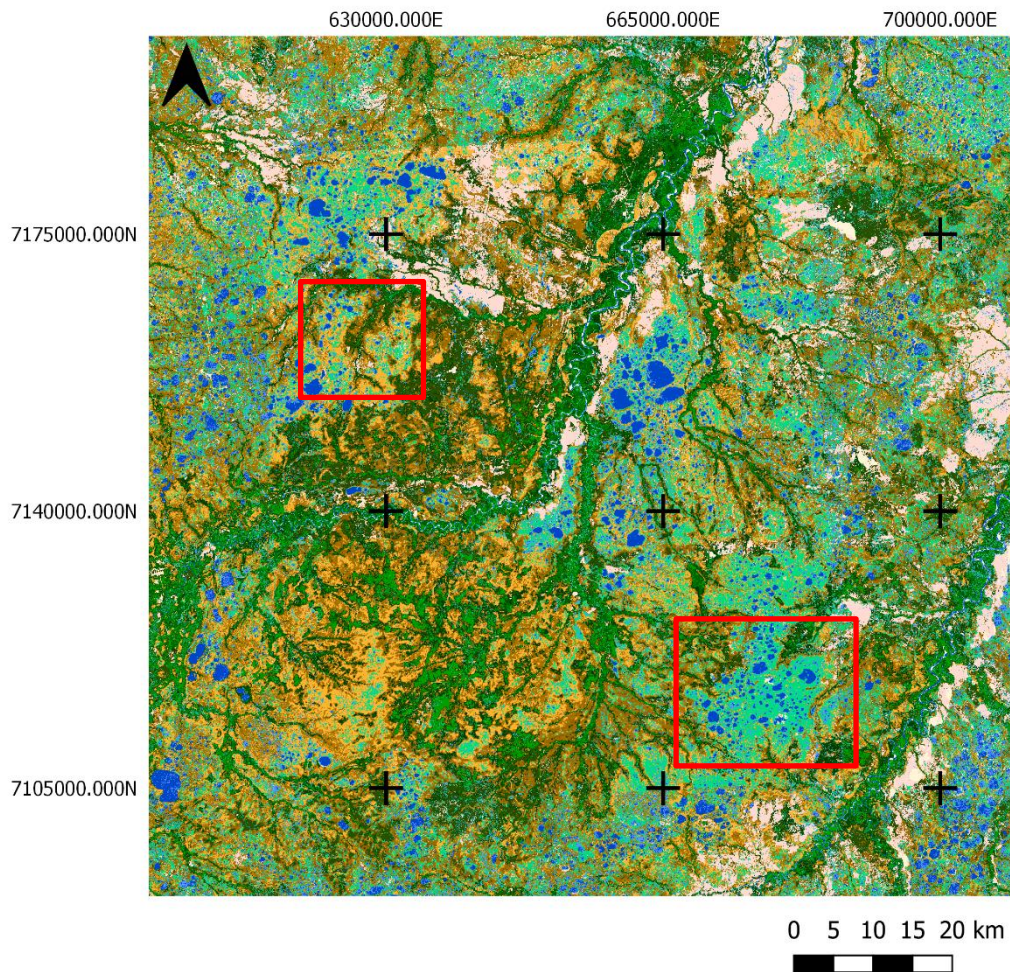


Figure 78. Illustration of the CCI-HRLC RR prototypes MRF fused map full extent over Siberia (42WXS S2 tile) and the propagated errors from the SAR fusion (red frames)

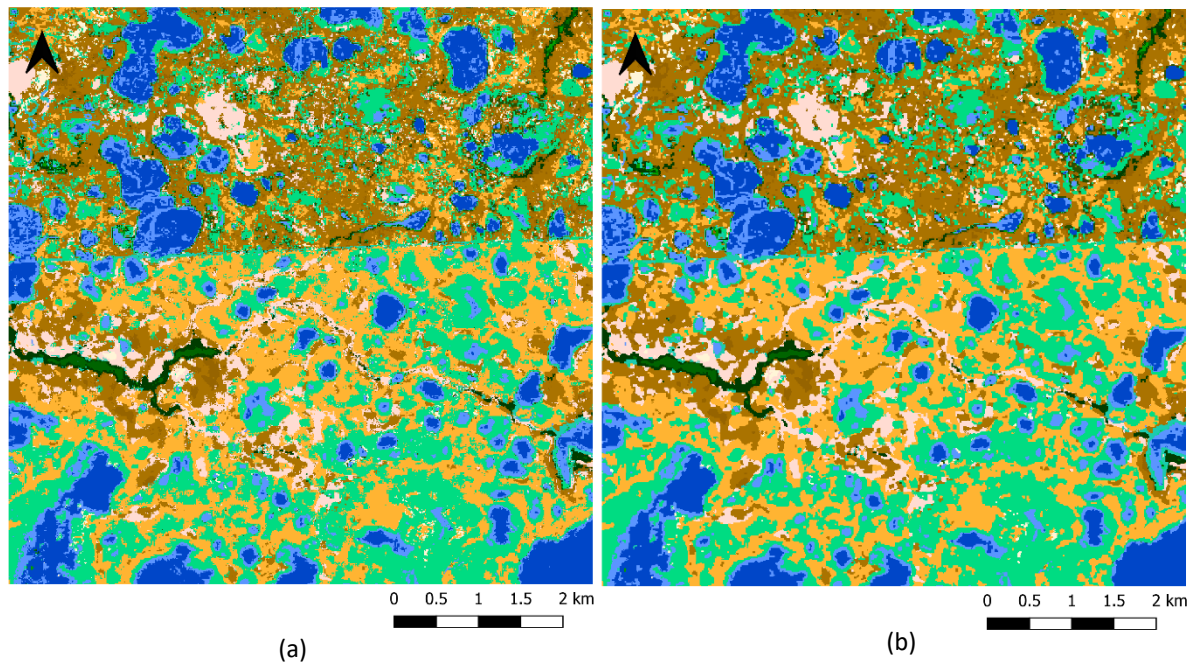


Figure 79. Illustration of the linkage area between the CCI-HRLC RR prototypes SVM Map and the SAR map on the fused products, LOGP (a) and MRF (b) (624314, 7185403, WGS84/UTM Zone 42N)

7.1.1.5 Concluding remarks

Table 13 summarizes the main observations for each type of product per area.

Table 13: Main observations obtained through a visual quality assessment of the RR prototypes

Africa	
S2 Static (SVM – LSTM Composite – LSTM TS)	The SVM Map is the one that detects best the delineation of the landscape features and that fits best the reality. Nevertheless, it contains thematic errors that should not appear considering the expected 10-m spatial resolution of the map. The two LSTM products have an even higher heterogeneity with a large overestimation of shrubs, bare areas, and regularly flooded grassland classes.
SAR	The SAR product is overall of poorer quality. Some landscape features are lost which decreases the spatial resolution of the map. Moreover, the map contains too many thematic errors with an overestimation of the built-up, open Water Seasonal, and grassland regularly flooded classes.
FUSED (LOGP – MRF)	The fused product, more specifically the MRF, has a significant reduction of the salt and pepper effect which reduces the heterogeneity within the classes and corresponds better to reality. However, it produces “chess-board effect” artefacts all over the map.
Amazonia	
S2 Static (SVM – LSTM Composite – LSTM TS)	The static maps have a generally better quality than the other products (SAR and fused). The map contains several thematic errors (wrong LC labels). A fusion between the best classes of these 3 products could be considered as the composite seems to better detect water tacks and the time series decrease the heterogeneity of the tree cover classes.
SAR	The SAR map has poor quality compared to the other prototypes in terms of spatial resolution and thematic errors.

FUSED (LOGP – MRF)	The fused products, especially the MRF, have a reduced salt and pepper effect but at the cost of losing some landscape features such as water tracks.
	Siberia
S2 Static (SVM – LSTM TS)	The SVM Map has a generally good quality and resemblance with the ESA GlobPermafrost map [RD2]. One major issue is the presence of circles of open Water Seasonal and woody vegetation aquatic classes over patches of forests all over the map. The time series product does not have that issue but has a higher overestimation of some classes. A fusion between the best classes of the two maps could be considered.
SAR	The SAR map is of poorer quality with a high overestimation of grassland and grassland regularly flooded classes.
FUSED (LOGP – MRF)	The fused products have poor quality due to the fusion with the SAR map.

A general conclusion of the quality of the prototypes is to say that the SVM map has generally better quality than the other products in terms of landscape feature delineation and thematic errors. The fused products have a reduction of the salt and pepper effect but with the loss of landscape features. The fusion between the SAR and S2 prototypes over Siberia results in a poorer quality map due to the poor performance of the SAR prototype. A solution could be to make the fusion between products, only where necessary (i.e. at locations or for classes where the S2 SVM map is not satisfactory).

7.1.2 Quantitative quality assessment

The following sections consist of a quantitative evaluation of the Round Robin processing chains. As detailed in the Product Validation Plan [AD6], two reporting methods are used to enhance processing chain discrimination: one per stratum and one unbiased for the whole tile.

The stratification method includes two strata that highlight areas with disagreements between the RR processing chains (stratum 1 – discrepancy) and areas where the classifications of all RR processing chains yield the same LC class (stratum 2 – coherence). A general confusion matrix is computed for the coherence stratum and one for each processing chain in the discrepancy stratum.

7.1.2.1 Africa – T37PCP

7.1.2.1.1 The validation database in the perspective of the confidence-based stratification

In total, the validation database includes 490 samples whose distribution varies according to the strata included in the confidence-based stratification (Figure 32).

350 samples were randomly selected in the discrepancy stratum and 140 samples were randomly sampled with an even distribution among LC classes (i.e. 14 samples per class) in the coherence stratum according to the specifications described in the Product Validation Plan [AD6]. Among the 490 samples, no sample was qualified as “totally uncertain” by the photointerpreters, and only 72 of them (14,7 %) as “doubtful”. Given this small number of “doubtful” samples and their distribution among classes, all samples were retained to robustly compute accuracy figures. The case-specific weights allowing to unbiased the accuracy figures by taking the actual LC class surfaces into account are detailed in Table 4.

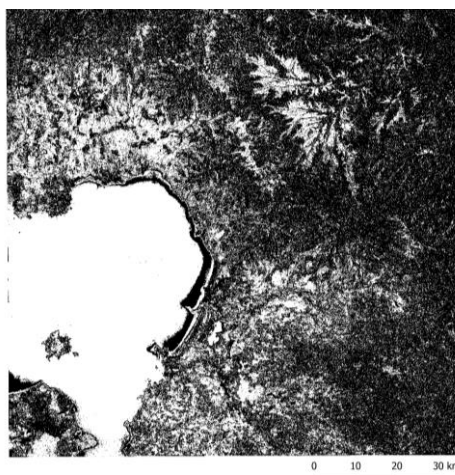


Figure 80. Stratification of the Africa T37PCP tile. In white, the coherence strata (all six RR processing chains agree, in black the discrepancy strata (at least one of the RR processing chains disagree with the others).

Table 14. Stratification specifications including area and sample number.

Stratum	Area (km ²)	Sample number
Discrepancy (stratum 1)	7106	350
Coherence (stratum 2)	5070	140

7.1.2.1.2 Unbiased accuracy figures

7.1.2.1.2.1 SVM Map

The SVM processing chain presents the highest OA of all six processing chains, with high accuracy for the largely present “cropland” class (8) (Table 5).

Table 15. SVM processing chain RR unbiased confusion matrix with PA, UA, and OA.

Ref\Pred	1	3	5	7	8	10	12	13	14	15	SUM	Prod Acc
1	0.21	0.00	0.00	0.00	0.00	0.00	0.00	0.00	0.00	0.00	0.21	1.00
3	0.02	0.14	0.09	0.09	0.00	0.00	0.00	0.00	0.00	0.00	0.34	0.42
5	0.06	1.89	3.29	2.00	0.46	0.00	0.09	0.15	0.00	0.00	7.94	0.41
7	0.00	0.07	0.96	5.84	2.88	0.05	0.28	0.30	0.04	0.00	10.43	0.56
8	0.00	0.23	1.13	3.84	16.41	0.01	0.14	0.07	0.11	0.00	21.95	0.75
10	0.00	0.00	0.00	0.00	0.00	0.16	0.00	0.00	0.38	0.00	0.54	0.30
12	0.00	0.00	0.00	0.14	0.00	0.00	0.19	0.15	0.00	0.00	0.47	0.40
13	0.00	0.00	0.00	0.00	0.00	0.00	0.00	0.30	0.00	0.00	0.30	1.00
14	0.00	0.00	0.00	0.00	0.00	0.00	0.05	0.00	0.00	0.00	0.05	0.00
15	0.00	0.00	0.00	0.00	0.00	0.00	0.05	0.00	0.08	9.69	9.81	0.99
SUM	0.30	2.34	5.47	11.90	19.75	0.23	0.80	0.96	0.61	9.69		
User Acc	0.71	0.06	0.60	0.49	0.83	0.71	0.24	0.31	0.00	1.00	OA =	70%

7.1.2.1.2.2 SAR Map

The SAR processing chain RR presents poor results (Table 6), with an OA of 55%, making it the lowest result of the six processing chains. Classes such as “grassland” (7) and “shrubland evergreen” (5) perform poorly compared to other processing chains, especially knowing that they are widely present in the tile area.

Table 16. SAR processing chain RR unbiased confusion matrix with PA, UA, and OA.

Ref\Pred	1	3	5	7	8	10	12	13	14	15	SUM	Prod Acc
1	0.21	0.00	0.00	0.00	0.00	0.00	0.00	0.00	0.00	0.00	0.21	1.00
3	0.02	0.14	0.09	0.09	0.00	0.00	0.00	0.00	0.00	0.00	0.34	0.42
5	0.06	1.89	3.29	2.00	0.46	0.00	0.09	0.15	0.00	0.00	7.94	0.41
7	0.00	0.07	0.96	5.84	2.88	0.05	0.28	0.30	0.04	0.00	10.43	0.56
8	0.00	0.23	1.13	3.84	16.41	0.01	0.14	0.07	0.11	0.00	21.95	0.75
10	0.00	0.00	0.00	0.00	0.00	0.16	0.00	0.00	0.38	0.00	0.54	0.30
12	0.00	0.00	0.00	0.14	0.00	0.00	0.19	0.15	0.00	0.00	0.47	0.40
13	0.00	0.00	0.00	0.00	0.00	0.00	0.00	0.30	0.00	0.00	0.30	1.00
14	0.00	0.00	0.00	0.00	0.00	0.00	0.05	0.00	0.00	0.00	0.05	0.00
15	0.00	0.00	0.00	0.00	0.00	0.00	0.05	0.00	0.08	9.69	9.81	0.99
SUM	0.30	2.34	5.47	11.90	19.75	0.23	0.80	0.96	0.61	9.69		
User Acc	0.71	0.06	0.60	0.49	0.83	0.71	0.24	0.31	0.00	1.00	OA =	55%

1	0.17	0.06	0.00	0.00	0.00	0.00	0.00	0.01	0.00	0.00	0.24	0.70
3	0.02	0.00	0.00	0.11	0.00	0.00	0.00	0.05	0.00	0.00	0.18	0.00
5	0.10	1.01	2.28	1.29	1.11	0.00	0.34	0.83	0.00	0.00	6.97	0.33
7	0.02	0.42	1.16	2.46	4.85	0.02	0.14	0.41	0.06	0.00	9.55	0.26
8	0.02	0.38	0.70	4.79	11.03	0.06	0.21	0.76	0.10	0.00	18.06	0.61
10	0.00	0.00	0.00	0.11	0.00	0.16	0.02	0.00	0.27	0.00	0.56	0.28
12	0.00	0.06	0.00	0.11	0.00	0.00	0.06	0.03	0.00	0.00	0.26	0.24
13	0.00	0.00	0.00	0.00	0.00	0.00	0.00	0.06	0.00	0.00	0.06	1.00
14	0.00	0.02	0.00	0.00	0.00	0.00	0.00	0.00	0.00	0.00	0.02	0.00
15	0.00	0.00	0.00	0.00	0.11	0.00	0.00	0.00	0.12	8.27	8.50	0.97
SUM	0.33	1.95	4.14	8.86	17.10	0.24	0.78	2.16	0.56	8.27		
User Acc	0.50	0.00	0.55	0.28	0.65	0.66	0.08	0.03	0.00	1.00	OA =	55%

7.1.2.1.2.3 LSTM Composite and Time Series Maps

The LSTM Composite and LSTM Time Series processing chain RR present very similar results, with both obtaining an OA of 67% (Table 7, Table 8).

Table 17. LSTM composite processing chain RR unbiased confusion matrix with PA, UA, and OA.

Ref\Pred	1	3	5	7	8	10	12	13	14	15	SUM	Prod Acc
1	0.15	0.00	0.00	0.00	0.00	0.00	0.00	0.00	0.00	0.00	0.15	1.00
3	0.02	0.16	0.02	0.00	0.00	0.00	0.00	0.00	0.00	0.00	0.19	0.84
5	0.05	1.36	2.50	0.78	0.23	0.00	0.05	0.14	0.00	0.00	5.11	0.49
7	0.00	0.10	1.04	3.87	2.85	0.05	0.28	0.35	0.02	0.00	8.57	0.45
8	0.00	0.14	1.86	3.49	13.36	0.03	0.22	0.04	0.11	0.00	19.25	0.69
10	0.00	0.00	0.00	0.00	0.01	0.10	0.02	0.00	0.16	0.00	0.29	0.33
12	0.00	0.00	0.00	0.09	0.00	0.00	0.11	0.10	0.00	0.00	0.30	0.38
13	0.00	0.00	0.00	0.00	0.00	0.00	0.00	0.21	0.00	0.00	0.21	1.00
14	0.00	0.00	0.00	0.00	0.00	0.00	0.02	0.00	0.00	0.00	0.02	0.00
15	0.00	0.00	0.00	0.00	0.00	0.00	0.02	0.00	0.18	7.85	8.05	0.97
SUM	0.21	1.76	5.41	8.23	16.45	0.18	0.74	0.84	0.47	7.85		
User Acc	0.71	0.09	0.46	0.47	0.81	0.55	0.16	0.24	0.00	1.00	OA =	67%

Table 18. LSTM time-series processing chain RR unbiased confusion matrix with PA, UA, and OA.

Ref\Pred	1	3	5	7	8	10	12	13	14	15	SUM	Prod Acc
1	0.17	0.00	0.00	0.00	0.00	0.00	0.00	0.00	0.00	0.00	0.17	1.00
3	0.02	0.14	0.02	0.00	0.00	0.00	0.00	0.00	0.00	0.00	0.17	0.81
5	0.07	1.49	2.31	1.19	0.05	0.00	0.08	0.13	0.00	0.00	5.31	0.43
7	0.00	0.23	1.48	3.98	2.20	0.06	0.41	0.44	0.05	0.00	8.84	0.45
8	0.00	0.19	2.25	3.86	15.35	0.04	0.34	0.13	0.12	0.00	22.28	0.69
10	0.00	0.00	0.00	0.00	0.00	0.09	0.04	0.00	0.21	0.00	0.34	0.25
12	0.00	0.00	0.00	0.09	0.00	0.00	0.19	0.09	0.00	0.00	0.37	0.52
13	0.00	0.00	0.00	0.00	0.00	0.00	0.00	0.17	0.00	0.00	0.17	1.00
14	0.00	0.00	0.00	0.00	0.00	0.00	0.04	0.00	0.00	0.00	0.04	0.00

15	0.00	0.00	0.00	0.00	0.00	0.00	0.04	0.00	0.17	8.67	8.87	0.98
SUM	0.25	2.05	6.06	9.13	17.60	0.18	1.12	0.95	0.54	8.67		
User Acc	0.67	0.07	0.38	0.44	0.87	0.46	0.17	0.18	0.00	1.00	OA =	67%

7.1.2.1.2.4 Fused maps: LOGP & MRF

The Fused LOGP and Fused MRF processing chain RR present little difference in terms of UA and PA, obtaining overall accuracies of respectively 68% and 69% (Table 9, Table 10).

Table 19. Fused LOGP processing chain RR unbiased confusion matrix with PA, UA, and OA.

Ref\Pred	1	3	5	7	8	10	12	13	14	15	SUM	Prod Acc
1	0.21	0.00	0.00	0.00	0.00	0.00	0.00	0.00	0.00	0.00	0.21	1.00
3	0.02	0.12	0.08	0.08	0.00	0.00	0.00	0.00	0.00	0.00	0.31	0.38
5	0.08	1.87	3.10	2.25	0.19	0.00	0.11	0.22	0.00	0.00	7.82	0.40
7	0.00	0.14	1.21	5.04	3.43	0.04	0.35	0.32	0.04	0.00	10.58	0.48
8	0.00	0.25	0.85	3.83	16.59	0.01	0.11	0.29	0.24	0.00	22.16	0.75
10	0.00	0.00	0.00	0.00	0.00	0.17	0.00	0.00	0.36	0.00	0.53	0.33
12	0.00	0.00	0.00	0.08	0.00	0.00	0.27	0.13	0.00	0.00	0.48	0.56
13	0.00	0.00	0.00	0.00	0.00	0.00	0.00	0.26	0.00	0.00	0.26	1.00
14	0.00	0.00	0.00	0.00	0.00	0.00	0.05	0.00	0.00	0.00	0.05	0.00
15	0.00	0.00	0.00	0.00	0.00	0.00	0.05	0.00	0.07	9.73	9.86	0.99
SUM	0.32	2.38	5.25	11.28	20.21	0.23	0.94	1.21	0.70	9.73		
User Acc	0.67	0.05	0.59	0.45	0.82	0.75	0.28	0.21	0.00	1.00	OA =	68%

Table 20. Fused MRF processing chain RR unbiased confusion matrix with PA, UA, and OA.

Ref\Pred	1	3	5	7	8	10	12	13	14	15	SUM	Prod Acc
1	0.21	0.00	0.00	0.00	0.00	0.00	0.00	0.00	0.00	0.00	0.21	1.00
3	0.00	0.15	0.10	0.09	0.00	0.00	0.00	0.00	0.00	0.00	0.33	0.45
5	0.15	1.89	3.33	2.18	0.19	0.00	0.10	0.12	0.00	0.00	7.96	0.42
7	0.00	0.15	1.22	5.05	3.41	0.04	0.29	0.31	0.04	0.00	10.50	0.48
8	0.00	0.26	0.87	3.86	16.89	0.01	0.10	0.18	0.14	0.00	22.31	0.76
10	0.00	0.00	0.00	0.00	0.00	0.17	0.00	0.00	0.36	0.00	0.54	0.33
12	0.00	0.00	0.00	0.09	0.00	0.00	0.24	0.12	0.00	0.00	0.45	0.53
13	0.00	0.00	0.00	0.00	0.00	0.00	0.00	0.24	0.00	0.00	0.24	1.00
14	0.00	0.00	0.00	0.00	0.00	0.00	0.05	0.00	0.00	0.00	0.05	0.00
15	0.00	0.00	0.00	0.00	0.00	0.00	0.05	0.00	0.07	9.77	9.89	0.99
SUM	0.36	2.44	5.51	11.27	20.49	0.23	0.81	0.98	0.61	9.77		
User Access	0.59	0.06	0.60	0.45	0.82	0.75	0.29	0.25	0.00	1.00	OA =	69%

7.1.2.1.3 Discrepancy stratum accuracy figures

7.1.2.1.3.1 SVM Map

The SVM processing chain presents the highest OA of all six processing chains, with good accuracy for the largely present grassland class (8) (Table 11).

Table 21. SVM processing chain RR unbiased confusion matrix with PA, UA, and OA.

Ref\Pred	1	3	5	7	8	10	12	13	14	15	SUM	Prod Acc
----------	---	---	---	---	---	----	----	----	----	----	-----	----------

1	0	0	0	0	0	0	0	0	0	0	0	N/A
3	0	1	1	1	0	0	0	0	0	0	3	0.33
5	1	15	30	21	4	0	0	1	0	0	72	0.42
7	0	0	11	57	22	1	3	2	1	0	97	0.59
8	0	3	11	35	112	1	2	1	0	0	165	0.68
10	0	0	0	0	0	1	0	0	1	0	2	0.50
12	0	0	0	0	0	0	1	0	0	0	1	1.00
13	0	0	0	0	0	0	0	0	0	0	0	N/A
14	0	0	0	0	0	0	1	0	0	0	1	0.00
15	0	0	0	0	0	0	1	0	0	8	9	0.89
SUM	1	19	53	114	138	3	8	4	2	8	350	
User Access	0.00	0.05	0.57	0.50	0.81	0.33	0.13	0.00	0.00	1.00	OA =	60%

7.1.2.1.3.2 SAR Map

The SAR processing chain RR presents poor results (Table 12), with an OA of 31%, making it the lowest result of the six processing chains. Classes such as “grassland” (7) and “shrubland evergreen” (5) perform poorly compared to other processing chains, especially knowing that they are widely present in the tile area.

Table 22. SAR processing chain RR unbiased confusion matrix with PA, UA, and OA.

Ref\Pred	1	3	5	7	8	10	12	13	14	15	SUM	Prod Acc
1	0	0	0	0	0	0	0	0	0	0	0	N/A
3	0	0	0	1	0	0	0	2	0	0	3	0.00
5	3	13	2	13	10	0	10	21	0	0	72	0.03
7	1	7	3	18	41	0	4	21	2	0	97	0.19
8	0	6	4	44	84	5	8	14	0	0	165	0.51
10	0	0	0	1	0	0	1	0	0	0	2	0.00
12	0	1	0	0	0	0	0	0	0	0	1	0.00
13	0	0	0	0	0	0	0	0	0	0	0	N/A
14	0	1	0	0	0	0	0	0	0	0	1	0.00
15	0	0	0	0	1	0	0	0	2	6	9	0.67
SUM	4	28	9	77	136	5	23	58	4	6	350	
User Acc	0.00	0.00	0.22	0.23	0.62	0.00	0.00	0.00	0.00	1.00	OA =	31%

7.1.2.1.3.3 LSTM Composite and Time Series Maps

The LSTM Composite and LSTM Time Series processing chain RR present very similar results, obtaining an OA of 49% and 46% respectively (Table 13 and Table 14).

Table 23. LSTM composite processing chain RR unbiased confusion matrix with PA, UA, and OA.

Ref\Pred	1	3	5	7	8	10	12	13	14	15	SUM	Prod Acc
1	0	0	0	0	0	0	0	0	0	0	0	N/A
3	0	2	1	0	0	0	0	0	0	0	3	0.67
5	1	15	43	10	2	0	0	1	0	0	72	0.60
7	0	1	20	38	22	3	7	5	1	0	97	0.39
8	0	2	31	31	87	3	7	1	3	0	165	0.53

10	0	0	0	0	0	1	1	0	0	0	2	0.50
12	0	0	0	0	0	0	1	0	0	0	1	1.00
13	0	0	0	0	0	0	0	0	0	0	0	N/A
14	0	0	0	0	0	0	1	0	0	0	1	0.00
15	0	0	0	0	0	0	1	0	8	0	9	0.00
SUM	1	20	95	79	111	7	18	7	12	0	350	
User Acc	0.00	0.10	0.45	0.48	0.78	0.14	0.06	0.00	0.00	N/A	OA =	49%

Table 24. LSTM time-series processing chain RR unbiased confusion matrix with PA, UA, and OA.

Ref\Pred	1	3	5	7	8	10	12	13	14	15	SUM	Prod Acc
1	0	0	0	0	0	0	0	0	0	0	0	N/A
3	0	2	1	0	0	0	0	0	0	0	3	0.67
5	2	20	35	13	1	0	0	1	0	0	72	0.49
7	0	4	22	38	15	5	5	6	2	0	97	0.39
8	0	3	30	36	82	6	4	2	2	0	165	0.50
10	0	0	0	0	0	1	1	0	0	0	2	0.50
12	0	0	0	0	0	0	1	0	0	0	1	1.00
13	0	0	0	0	0	0	0	0	0	0	0	N/A
14	0	0	0	0	0	0	1	0	0	0	1	0.00
15	0	0	0	0	0	0	1	0	5	3	9	0.33
SUM	2	29	88	87	98	12	13	9	9	3	350	
User Acc	0.00	0.07	0.40	0.44	0.84	0.08	0.08	0.00	0.00	1.00	OA =	46%

7.1.2.1.3.4 Fused maps: LOGP & MRF

The Fused LOGP and Fused MRF processing chain RR present little difference in terms of UA and PA, obtaining both overall accuracies of 57% (Table 15, Table 16).

Table 25. Fused LOGP processing chain RR unbiased confusion matrix with PA, UA, and OA.

Ref\Pred	1	3	5	7	8	10	12	13	14	15	SUM	Prod Acc
1	0	0	0	0	0	0	0	0	0	0	0	N/A
3	0	1	1	1	0	0	0	0	0	0	3	0.33
5	1	20	23	25	2	0	0	1	0	0	72	0.32
7	0	1	11	51	27	0	3	3	1	0	97	0.53
8	0	3	7	36	114	1	1	2	1	0	165	0.69
10	0	0	0	0	0	1	0	0	1	0	2	0.50
12	0	0	0	0	0	0	1	0	0	0	1	1.00
13	0	0	0	0	0	0	0	0	0	0	0	N/A
14	0	0	0	0	0	0	1	0	0	0	1	0.00
15	0	0	0	0	0	0	1	0	0	8	9	0.89
SUM	1	25	42	113	143	2	7	6	3	8	350	
User Acc	0.00	0.04	0.55	0.45	0.80	0.50	0.14	0.00	0.00	1.00	OA =	57%

Table 26. Fused MRF processing chain RR unbiased confusion matrix with PA, UA, and OA.

Ref\Pred	1	3	5	7	8	10	12	13	14	15	SUM	Prod Acc
1	0	0	0	0	0	0	0	0	0	0	0	N/A
3	0	1	1	1	0	0	0	0	0	0	3	0.33
5	2	19	24	25	2	0	0	0	0	0	72	0.33
7	0	1	11	51	27	0	3	3	1	0	97	0.53
8	0	3	7	36	115	1	1	1	1	0	165	0.70
10	0	0	0	0	0	1	0	0	1	0	2	0.50
12	0	0	0	0	0	0	1	0	0	0	1	1.00
13	0	0	0	0	0	0	0	0	0	0	0	N/A
14	0	0	0	0	0	0	1	0	0	0	1	0.00
15	0	0	0	0	0	0	1	0	0	8	9	0.89
SUM	2	24	43	113	144	2	7	4	3	8	350	
User Acc	0.00	0.04	0.56	0.45	0.80	0.50	0.14	0.00	0.00	1.00	OA =	57%

7.1.2.1.4 Coherence stratum accuracy figure

The coherence stratum presents an OA of 56% (Table 17). This area of agreement between all six processing chains presents good PA and UA for the “tree cover broadleaf evergreen” class (1) and good UA for “evergreen shrubland” (5) and “grassland” (7). The “cropland” class reaches high UA (94%) but low PA (50%).

Table 27 - Confusion matrix for the coherence stratum with PA, UA, and OA.

Ref\Pred	1	3	5	7	8	10	12	13	14	15	SUM	Prod Acc
1	10	0	0	0	0	0	0	0	0	0	10	1.00
3	1	1	0	0	0	0	0	0	0	0	2	0.50
5	3	11	11	1	0	0	2	2	0	0	30	0.37
7	0	1	2	8	1	3	3	2	0	0	20	0.40
8	0	0	2	7	16	0	1	2	3	0	31	0.52
10	0	0	0	0	0	11	0	0	9	0	20	0.55
12	0	0	0	1	0	0	4	2	0	0	7	0.57
13	0	0	0	0	0	0	0	4	0	0	4	1.00
14	0	0	0	0	0	0	0	0	0	0	0	N/A
15	0	0	0	0	0	0	0	0	2	14	16	0.88
SUM	14	13	15	17	17	14	10	12	14	14	140	
User Acc	0.71	0.08	0.73	0.47	0.94	0.79	0.40	0.33	0.00	1.00	OA =	56%

7.1.2.1.5 Comparison

A confidence-based stratification was used for the validation sampling scheme to highlight differences between processing chains, along with an unbiased OA computation on the whole tile.

The range of unbiased overall accuracies is large, from 55% to 70% (Table 18), with the SVM presenting the highest OA score of 70%, closely followed by the Fused MRF (69%) and LOGP (68%) processing chains. Those three processing chains are of similar quality with close PA, UA, and OA. The LSTM composite and LSTM Time-Series follow closely with overall accuracies of 67%. The SAR RR processing chain has the lowest OA with 55%.

Table 28. Comparison of the Unbiased Overall Accuracies of each RR processing chain

RR	SVM	SAR	LSTM composite	LSTM TS	Fused LOGP	Fused MRF
----	-----	-----	----------------	---------	------------	-----------

Unbiased OA	70%	55%	67%	67%	68%	69%
-------------	-----	-----	-----	-----	-----	-----

The results of the stratified validation do not change the ranking of overall accuracies but allow highlighting the lower accuracies of both LSTM processing chains over the discrepancy area compared to SVM, Fused MRF and Fused LOGP which are confirmed as best-performing processing chains. Only those three processing chains reach higher accuracies than the coherence stratum.

Table 29. Comparison of the Overall Accuracies of each RR processing chain according to the stratification

RR	SVM	SAR	LSTM composite	LSTM TS	Fused LOGP	Fused MRF
Discrepancy stratum OA	60%	31%	49%	46%	57%	57%
Coherence stratum OA	56%					

7.1.2.1.6 Local misclassifications from discrepancies in the legend interpretation

Along the shores of Lake Tana, floating vegetation or algae covers the water several months a year. According to the hierarchical approach of HRLC legend rules, this should correspond to the “herbaceous vegetation aquatic or regularly flooded (10)” class. Indeed, the area is covered by vegetation for more than 2 months a year, but with a water persistence of more than 4 months, and a herbaceous life form (Annex 1, Figure 68). However, it has been detected as “Open water temporary” in all six processing chains (Figure 32). This can be seen in the high NDVI seasonality with around 6 months of high NDVI and 6 months of water (Figure 33).

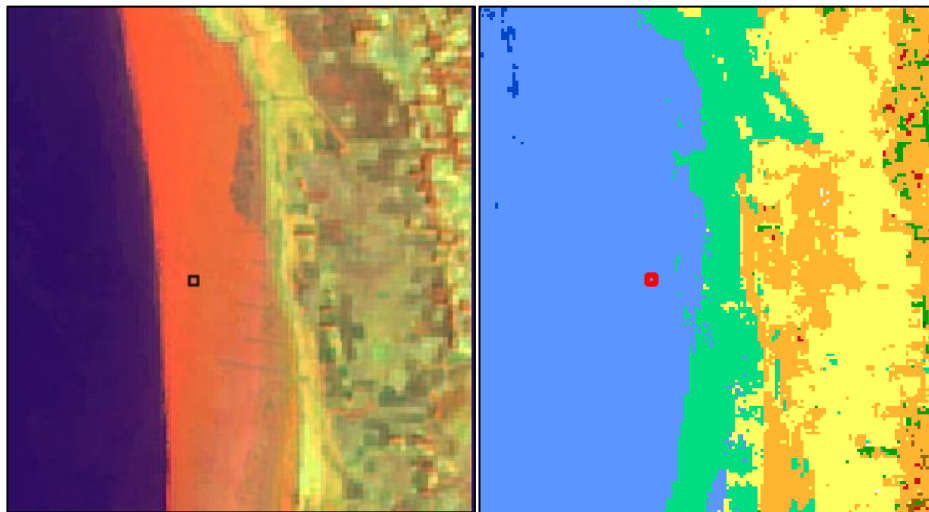


Figure 81. Sentinel 2 annual composite (left) and corresponding Fused LOGP RR (right). The area in orange on the left represents the extent of the floating algae along the shore of Lake Tana. The area close to the shore is well detected as “grassland vegetation aquatic or regularly flooded”, while the rest of it is detected as “Open water seasonal”.

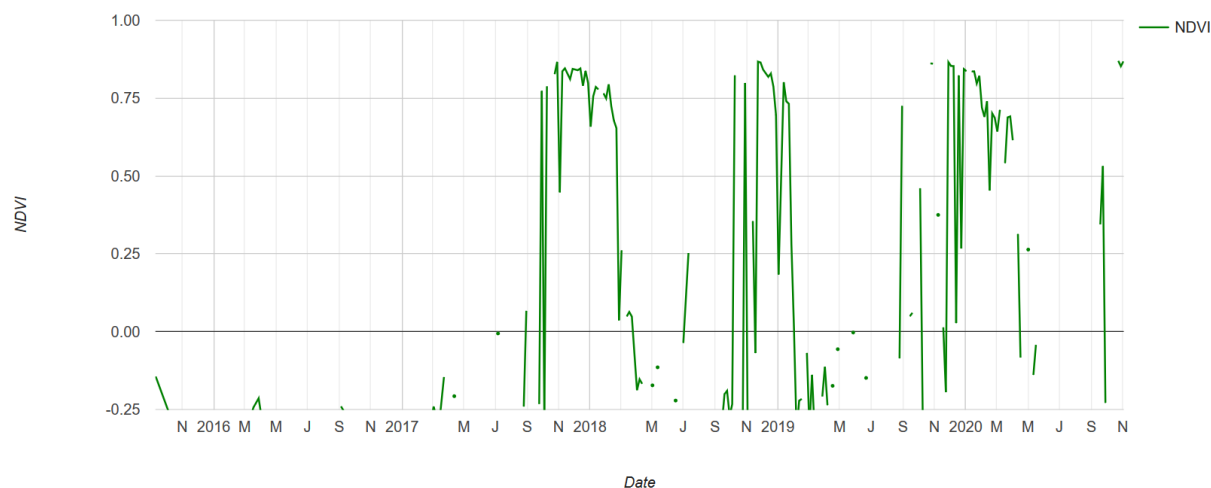


Figure 82. NDVI Time Series of the sample presented in the previous figure. The floating algae is a recent phenomenon starting in 2018, with high NDVI values during the November–April 6 months period. Negative NDVI values indicate the presence of water for the rest of the year.

7.1.2.1.7 Conclusion

In terms of OA, the SVM processing chain reach the highest score in both validation strategies, closely followed by the Fused MRF and LOGP processing chains.

Overall, most classes behave similarly in all RR processing chains and a general analysis concerning all six processing chains can be made.

In terms of accurate classes, the “Open water permanent (15)” class has the best scores, with almost 100% PA and UA, which was expected since its spectral characteristics are very specific compared to other classes. The second-best class is the “Cropland (8)”, with UA around 80% in most RR processing chains but with a PA varying from around 50% to 70%, indicating that some processing chains omit some cropland areas. This is a positive result since this class is widely present in the area.

When looking at moderately accurate classes, the “bare areas (12)” and the “built-up (13)” classes score a high PA but a very low UA, which indicates large commission errors. These errors mainly occur over grassland and cropland classes. It can be due to an incorrect capture of the duration of the bare soil period defining the cropland class or the low intensity of vegetation over natural herbaceous areas in the context of a dry climate like Ethiopia where the RR site was selected.

In terms of the least accurate classes, the “Grassland (7)” class, which is largely represented in this landscape, yields UA and PA of just 50 %. This is due to a large confusion with close life forms like cropland and shrubland.

Finally, in each processing chain, woody classes (“Tree cover evergreen broadleaf (1)”, “Tree cover deciduous broadleaf (3)”, and “Shrub cover evergreen (5)”) present very low accuracies due to general confusion between themselves.

Specifically, a large confusion occurs between the “tree cover deciduous broadleaf (3)” and the “shrub cover deciduous (5)” classes. Misclassification between trees and shrubs can be expected since the difference mostly lies in the height of the arbustive vegetation.

However, confusion between evergreen and deciduous vegetation was not expected. Validation samples interpreted as the “Tree cover evergreen broadleaf (1)” class are badly detected in all six processing chains, where they are labelled as “Shrub cover evergreen (5)”.

7.1.2.2 Amazonia – T21KXT & T21KUQ

7.1.2.2.1 The validation database in the perspective of the confidence-based stratification

In total, the validation database includes 485 samples split between both tiles on a 2/3 (T21KXT)– 1/3 (T21KUQ) basis whose distribution varies according to the strata included in the confidence-based stratification (Figure 35).

350 samples were randomly selected in the discrepancy stratum and 135 samples were randomly sampled with an even distribution among LC classes (i.e. 13 samples per class) in the coherence stratum according to the specifications described in the Product Validation Plan [AD6]. Among the 485 samples, 3 samples were qualified as “totally uncertain” by the photointerpreters, and only 40 of them (8,2 %) as “doubtful”. Given this small number of “doubtful” samples and their distribution among classes, all samples were retained to robustly compute accuracy figures. The stratum areas and sample number per tile are detailed in Table 20. Stratification specifications of Amazonia T21KXT tile, including area and sample number. and Table 21. Stratification specifications of Amazonia T21KUQ tile, including area and sample number.

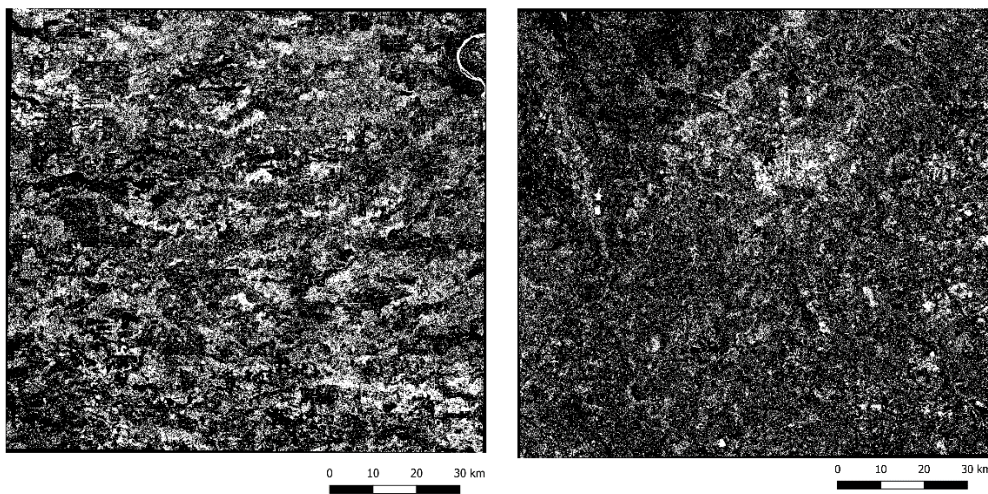


Figure 83. Stratification of the Amazonia T21KXT (left) and T21KUQ (right). In white, the coherence strata (all six RR processing chains agree, in black the discrepancy strata (at least one of the RR processing chains disagree with the others).

Table 30. Stratification specifications of Amazonia T21KXT tile, including area and sample number.

Stratum	Area (km ²)	Sample number
Discrepancy (stratum 1)	9605	233
Coherence (stratum 2)	2671	90

Table 31. Stratification specifications of Amazonia T21KUQ tile, including area and sample number.

Stratum	Area (km ²)	Sample number
Discrepancy (stratum 1)	8470	117
Coherence (stratum 2)	3823	45

7.1.2.2.2 Unbiased accuracy figures

7.1.2.2.2.1 SVM Map

The SVM processing chain presents a low OA of 33%. The “built-up” class (13) reaches high UA and PA (Table 22).

Table 32. SVM processing chain RR unbiased confusion matrix with PA, UA, and OA.

Ref\Pred	1	3	5	6	7	8	9	10	12	13	14	15	SUM	Prod Acc
1	8.81	8.88	1.12	1.79	3.91	0.57	0.00	0.20	0.49	0.00	0.02	0.02	25.80	0.34
3	0.00	0.00	0.00	0.11	0.00	0.00	0.00	0.00	0.00	0.00	0.00	0.00	0.11	0.00

5	0.17	0.38	0.73	0.63	0.39	0.00	0.00	0.00	0.21	0.00	0.00	0.00	2.51	0.29
6	0.34	0.38	0.22	0.00	0.00	0.00	0.00	0.00	0.14	0.00	0.00	0.00	1.08	0.00
7	0.84	1.39	2.58	5.39	10.01	8.72	0.00	0.13	0.76	0.06	0.00	0.01	29.89	0.33
8	0.17	0.00	0.00	0.00	0.00	0.38	0.00	0.00	0.00	0.00	0.00	0.00	0.54	0.69
9	0.00	0.00	0.00	0.00	0.00	0.00	0.00	0.00	0.00	0.00	0.00	0.00	0.00	N/A
10	0.17	0.00	0.00	0.00	0.11	0.19	0.00	0.00	0.07	0.00	0.02	0.00	0.55	0.00
12	0.00	0.00	0.00	0.00	0.00	0.00	0.00	0.01	0.07	0.08	0.00	0.01	0.17	0.42
13	0.00	0.00	0.00	0.00	0.00	0.00	0.00	0.00	0.07	0.47	0.01	0.00	0.55	0.86
14	0.00	0.00	0.00	0.00	0.00	0.00	0.00	0.00	0.00	0.00	0.00	0.00	0.00	N/A
15	0.18	0.00	0.11	0.11	0.00	0.00	0.00	0.01	0.00	0.00	0.05	0.10	0.55	0.18
SUM	10.67	11.03	4.76	8.03	14.41	9.85	0.00	0.34	1.81	0.61	0.09	0.13		
User Acc	0.83	0.00	0.15	0.00	0.69	0.04	N/A	0.00	0.04	0.77	0.00	0.73	OA =	33%

7.1.2.2.2 SAR Map

The SVM processing chain presents a low OA of 33% (Table 23).

Table 33. SAR processing chain RR unbiased confusion matrix with PA, UA, and OA.

Ref\Pred	1	3	5	6	7	8	9	10	12	13	14	15	SUM	Prod Acc
1	10.67	6.76	2.57	1.59	2.42	0.25	0.13	0.00	2.00	0.00	0.08	0.05	26.52	0.40
3	0.00	0.00	0.00	0.00	0.00	0.00	0.00	0.00	0.11	0.00	0.00	0.00	0.11	0.00
5	0.39	0.19	0.61	0.49	0.23	0.12	0.00	0.00	0.53	0.00	0.00	0.00	2.56	0.24
6	0.20	0.30	0.21	0.00	0.12	0.00	0.00	0.00	0.40	0.00	0.00	0.00	1.22	0.00
7	1.56	1.16	2.71	3.48	6.77	3.68	0.25	0.00	3.58	0.31	0.01	0.00	23.51	0.29
8	0.00	0.00	0.10	0.00	0.00	0.25	0.00	0.00	0.00	0.00	0.00	0.00	0.35	0.71
9	0.00	0.00	0.00	0.00	0.00	0.00	0.00	0.00	0.00	0.00	0.00	0.00	0.00	N/A
10	0.39	0.58	0.00	0.00	0.12	0.12	0.00	0.00	0.21	0.00	0.02	0.00	1.44	0.00
12	0.00	0.00	0.00	0.00	0.00	0.00	0.00	0.00	0.11	0.35	0.02	0.01	0.48	0.22
13	0.00	0.00	0.00	0.00	0.12	0.00	0.00	0.00	0.00	0.41	0.01	0.00	0.53	0.76
14	0.00	0.00	0.00	0.00	0.00	0.00	0.00	0.00	0.00	0.00	0.00	0.00	0.00	N/A
15	0.00	0.19	0.21	0.00	0.00	0.00	0.00	0.00	0.00	0.00	0.04	0.08	0.52	0.16
SUM	13.20	9.18	6.41	5.56	9.78	4.42	0.38	0.00	6.94	1.06	0.18	0.13		
User Acc	0.81	0.00	0.09	0.00	0.69	0.06	0.00	N/A	0.02	0.38	0.00	0.61	OA =	33%

7.1.2.2.3 LSTM Composite and Time Series Maps

The LSTM Composite and LSTM Time Series processing chain RR present very similar results, with low accuracies of 33% and 30%.

Table 34. LSTM composite processing chain RR unbiased confusion matrix with PA, UA, and OA.

Ref\Pred	1	3	5	6	7	8	9	10	12	13	14	15	SUM	Prod Acc
1	11.35	11.32	1.25	1.50	2.37	0.28	0.00	0.00	0.83	0.00	0.02	0.38	29.30	0.39
3	0.00	0.00	0.00	0.08	0.00	0.00	0.00	0.00	0.00	0.00	0.00	0.00	0.08	0.00
5	0.25	0.38	0.23	0.64	0.31	0.00	0.00	0.00	0.27	0.00	0.00	0.00	2.08	0.11
6	0.75	0.31	0.15	0.00	0.00	0.00	0.00	0.00	0.18	0.00	0.00	0.00	1.39	0.00

7	1.26	1.87	1.92	4.58	6.10	5.27	0.00	0.16	1.07	0.10	0.00	0.04	22.36	0.27
8	0.25	0.00	0.07	0.00	0.00	0.12	0.00	0.00	0.00	0.00	0.00	0.00	0.44	0.27
9	0.00	0.00	0.00	0.00	0.00	0.00	0.00	0.00	0.00	0.00	0.00	0.00	0.00	N/A
10	0.25	0.00	0.00	0.00	0.08	0.12	0.00	0.00	0.09	0.00	0.02	0.00	0.56	0.00
12	0.00	0.00	0.00	0.00	0.00	0.00	0.00	0.00	0.09	0.10	0.01	0.04	0.25	0.36
13	0.00	0.00	0.00	0.00	0.00	0.00	0.00	0.00	0.09	0.37	0.01	0.00	0.47	0.79
14	0.00	0.00	0.00	0.00	0.00	0.00	0.00	0.00	0.00	0.00	0.00	0.00	0.00	N/A
15	0.07	0.00	0.07	0.08	0.00	0.00	0.00	0.00	0.00	0.00	0.06	0.53	0.82	0.65
SUM	14.18	13.89	3.69	6.88	8.86	5.78	0.00	0.16	2.61	0.58	0.13	0.99		
User Acc	0.80	0.00	0.06	0.00	0.69	0.02	N/A	0.00	0.03	0.64	0.00	0.53	OA =	33%

Table 35. LSTM time-series processing chain RR unbiased confusion matrix with PA, UA, and OA.

Ref\Pred	1	3	5	6	7	8	9	10	12	13	14	15	SUM	Prod Acc
1	10.29	10.42	1.69	1.83	1.72	0.35	0.47	0.00	1.38	0.02	0.15	0.50	28.83	0.36
3	0.00	0.00	0.00	0.09	0.00	0.00	0.00	0.00	0.00	0.00	0.00	0.00	0.09	0.00
5	0.23	0.80	0.37	0.60	0.28	0.00	0.00	0.00	0.18	0.00	0.00	0.00	2.46	0.15
6	0.23	0.26	0.29	0.09	0.00	0.00	0.00	0.00	0.18	0.00	0.00	0.00	1.05	0.08
7	0.94	2.00	2.06	6.04	5.25	3.99	0.23	0.00	1.27	0.15	0.00	0.07	22.00	0.24
8	0.23	0.00	0.00	0.00	0.00	0.23	0.00	0.00	0.00	0.00	0.00	0.00	0.47	0.50
9	0.00	0.00	0.00	0.00	0.00	0.00	0.00	0.00	0.00	0.00	0.00	0.00	0.00	N/A
10	0.23	0.00	0.00	0.09	0.00	0.12	0.00	0.00	0.09	0.00	0.03	0.00	0.57	0.00
12	0.00	0.00	0.00	0.00	0.00	0.00	0.00	0.00	0.09	0.18	0.02	0.03	0.33	0.28
13	0.00	0.00	0.00	0.00	0.00	0.00	0.00	0.00	0.09	0.39	0.00	0.00	0.48	0.81
14	0.00	0.00	0.00	0.00	0.00	0.00	0.00	0.00	0.00	0.00	0.00	0.00	0.00	N/A
15	0.08	0.00	0.08	0.09	0.00	0.00	0.00	0.00	0.00	0.00	0.15	0.38	0.77	0.49
SUM	12.25	13.48	4.49	8.82	7.24	4.69	0.70	0.00	3.29	0.73	0.36	0.98		
User Acc	0.84	0.00	0.08	0.01	0.72	0.05	0.00	N/A	0.03	0.53	0.00	0.38	OA =	30%

7.1.2.2.4 Fused maps: LOGP & MRF

The Fused LOGP and Fused MRF processing chain RR present little differences in terms of UA and PA and obtain both overall accuracies of respectively 38% and 40%, making them the best-performing processing chains (Table 26, Table 27).

Table 36. Fused LOGP processing chain RR unbiased confusion matrix with PA, UA, and OA.

Ref\Pred	1	3	5	6	7	8	9	10	12	13	14	15	SUM	Prod Acc
1	11.65	10.30	1.01	0.82	2.78	0.35	0.00	0.15	0.45	0.00	0.02	0.01	27.54	0.42
3	0.00	0.00	0.00	0.05	0.00	0.00	0.00	0.00	0.00	0.00	0.00	0.00	0.05	0.00
5	0.25	0.43	0.33	0.38	0.25	0.00	0.00	0.08	0.24	0.00	0.00	0.00	1.96	0.17
6	0.49	0.43	0.10	0.00	0.00	0.00	0.00	0.00	0.16	0.00	0.00	0.00	1.19	0.00
7	1.23	1.62	0.67	2.42	7.47	5.69	0.08	0.15	0.81	0.02	0.00	0.00	20.17	0.37
8	0.25	0.00	0.00	0.00	0.00	0.23	0.00	0.00	0.00	0.00	0.00	0.00	0.47	0.48
9	0.00	0.00	0.00	0.00	0.00	0.00	0.00	0.00	0.00	0.00	0.00	0.00	0.00	N/A
10	0.00	0.00	0.00	0.05	0.12	0.11	0.00	0.45	0.00	0.00	0.25	0.00	1.00	0.45
12	0.00	0.00	0.00	0.00	0.00	0.00	0.00	0.00	0.08	0.03	0.00	0.00	0.11	0.71

13	0.00	0.00	0.00	0.00	0.00	0.00	0.00	0.00	0.08	0.19	0.00	0.00	0.28	0.69
14	0.00	0.00	0.00	0.00	0.00	0.00	0.00	0.00	0.00	0.00	0.00	0.00	0.00	N/A
15	0.25	0.00	0.05	0.05	0.00	0.00	0.00	0.00	0.00	0.00	0.02	0.05	0.43	0.12
SUM	14.12	12.79	2.16	3.78	10.62	6.38	0.08	0.83	1.84	0.24	0.30	0.07		
User Acc	0.83	0.00	0.15	0.00	0.70	0.04	0.00	0.55	0.04	0.81	0.00	0.72	OA =	38%

Table 37. Fused MRF processing chain RR unbiased confusion matrix with PA, UA, and OA.

Ref\Pred	1	3	5	6	7	8	9	10	12	13	14	15	SUM	Prod Acc
1	13.79	12.23	0.14	1.02	3.14	0.42	0.00	0.23	0.44	0.00	0.02	0.05	31.48	0.44
3	0.00	0.00	0.00	0.06	0.00	0.00	0.00	0.00	0.00	0.00	0.00	0.00	0.06	0.00
5	0.29	0.50	0.21	0.38	0.29	0.00	0.00	0.08	0.26	0.00	0.00	0.00	2.00	0.10
6	0.58	0.50	0.00	0.00	0.09	0.00	0.00	0.00	0.09	0.00	0.00	0.00	1.26	0.00
7	1.44	1.68	0.19	2.58	8.94	6.85	0.00	0.23	0.78	0.02	0.00	0.02	22.74	0.39
8	0.29	0.00	0.00	0.00	0.00	0.28	0.00	0.00	0.00	0.00	0.00	0.00	0.57	0.49
9	0.00	0.00	0.00	0.00	0.00	0.00	0.00	0.00	0.00	0.00	0.00	0.00	0.00	N/A
10	0.29	0.00	0.00	0.00	0.14	0.14	0.00	0.47	0.09	0.00	0.01	0.00	1.13	0.41
12	0.00	0.00	0.00	0.00	0.00	0.00	0.00	0.00	0.09	0.03	0.00	0.02	0.14	0.62
13	0.00	0.00	0.00	0.00	0.00	0.00	0.00	0.00	0.09	0.18	0.00	0.00	0.27	0.66
14	0.00	0.00	0.00	0.00	0.00	0.00	0.00	0.00	0.00	0.00	0.00	0.00	0.00	N/A
15	0.29	0.00	0.00	0.06	0.00	0.00	0.00	0.00	0.00	0.00	0.03	0.30	0.68	0.44
SUM	16.96	14.92	0.54	4.10	12.59	7.68	0.00	1.01	1.83	0.22	0.06	0.40		
User Acc	0.81	0.00	0.38	0.00	0.71	0.04	N/A	0.46	0.05	0.79	0.00	0.75	OA =	40%

7.1.2.2.3 Discrepancy stratum accuracy figures

7.1.2.2.3.1 SVM Map

The SVM processing chain presents an OA of 30% (Table 28).

Table 38. SVM processing chain RR unbiased confusion matrix with PA, UA, and OA.

Ref\Pred	1	3	5	6	7	8	9	10	12	13	14	15	SUM	Prod Acc
1	42	57	6	14	16	3	0	4	3	0	1	0	146	0.29
3	0	0	0	1	0	0	0	0	0	0	0	0	1	0.00
5	1	4	4	5	2	0	0	0	1	0	0	0	17	0.24
6	2	3	0	0	0	0	0	0	0	0	0	0	5	0.00
7	5	10	14	35	46	35	0	5	4	2	0	0	156	0.29
8	1	0	0	0	0	1	0	0	0	0	0	0	2	0.50
9	0	0	0	0	0	0	0	0	0	0	0	0	0	N/A
10	1	0	0	0	1	0	0	6	1	0	0	0	9	0.67
12	0	0	0	0	0	0	0	0	0	2	0	0	2	0.00
13	0	0	0	0	0	0	0	0	1	4	1	0	6	0.67
14	0	0	0	0	0	0	0	0	0	0	0	0	0	N/A
15	2	0	0	1	0	0	0	1	0	0	0	2	6	0.33
SUM	54	74	24	56	65	39	0	16	10	8	2	2	350	
User Acc	0.78	0.00	0.17	0.00	0.71	0.03	N/A	0.38	0.00	0.50	0.00	1.00	OA =	30%

7.1.2.2.3.2 SAR Map

The SAR processing chain RR presents an OA of 29% (Table 29).

Table 39. SAR processing chain RR unbiased confusion matrix with PA, UA, and OA.

Ref\Pred	1	3	5	6	7	8	9	10	12	13	14	15	SUM	Prod Acc
1	40	25	20	15	16	2	2	0	16	0	5	5	146	0.27
3	0	0	0	0	0	0	0	0	1	0	0	0	1	0.00
5	2	1	4	4	2	1	0	0	3	0	0	0	17	0.24
6	1	2	0	0	1	0	0	0	1	0	0	0	5	0.00
7	8	4	15	24	49	21	2	0	29	3	1	0	156	0.31
8	0	0	1	0	0	1	0	0	0	0	0	0	2	0.50
9	0	0	0	0	0	0	0	0	0	0	0	0	0	N/A
10	2	3	0	0	1	0	0	0	2	0	1	0	9	0.00
12	0	0	0	0	0	0	0	0	0	1	1	0	2	0.00
13	0	0	0	0	1	0	0	0	0	4	1	0	6	0.67
14	0	0	0	0	0	0	0	0	0	0	0	0	0	N/A
15	0	1	1	0	0	0	0	0	0	0	1	3	6	0.50
SUM	53	36	41	43	70	25	4	0	52	8	10	8	350	
User Acc	0.75	0.00	0.10	0.00	0.70	0.04	0.00	N/A	0.00	0.50	0.00	0.38	OA =	29%

7.1.2.2.3.3 LSTM Composite and Time Series Maps

The LSTM Composite and LSTM Time Series processing chain RR present very similar results, with both obtaining an OA of 23% (Table 30, Table 31).

Table 40. LSTM composite processing chain RR unbiased confusion matrix with PA, UA, and OA.

Ref\Pred	1	3	5	6	7	8	9	10	12	13	14	15	SUM	Prod Acc
1	34	60	11	16	13	1	0	2	6	0	1	2	146	0.23
3	0	0	0	1	0	0	0	0	0	0	0	0	1	0.00
5	1	2	3	7	2	0	0	1	1	0	0	0	17	0.18
6	3	2	0	0	0	0	0	0	0	0	0	0	5	0.00
7	5	10	19	44	31	34	0	3	7	3	0	0	156	0.20
8	1	0	1	0	0	0	0	0	0	0	0	0	2	0.00
9	0	0	0	0	0	0	0	0	0	0	0	0	0	N/A
10	1	0	0	0	1	0	0	6	1	0	0	0	9	0.67
12	0	0	0	0	0	0	0	0	0	2	0	0	2	0.00
13	0	0	0	0	0	0	0	0	1	4	1	0	6	0.67
14	0	0	0	0	0	0	0	0	0	0	0	0	0	N/A
15	1	0	0	1	0	0	0	0	0	0	1	3	6	0.50
SUM	46	74	34	69	47	35	0	12	16	9	3	5	350	
User Acc	0.74	0.00	0.09	0.00	0.66	0.00	N/A	0.50	0.00	0.44	0.00	0.60	OA =	23%

Table 41. LSTM time-series processing chain RR unbiased confusion matrix with PA, UA and OA.

Ref\Pred	1	3	5	6	7	8	9	10	12	13	14	15	SUM	Prod Acc
1	32	52	13	19	8	3	4	0	9	1	3	2	146	0.22
3	0	0	0	1	0	0	0	0	0	0	0	0	1	0.00
5	1	5	3	6	2	0	0	0	0	0	0	0	17	0.18
6	1	1	1	1	0	0	0	0	1	0	0	0	5	0.20
7	4	10	20	54	30	23	2	0	10	2	0	1	156	0.19
8	1	0	0	0	0	1	0	0	0	0	0	0	2	0.50
9	0	0	0	0	0	0	0	0	0	0	0	0	0	N/A
10	1	0	0	1	0	0	0	6	1	0	0	0	9	0.67
12	0	0	0	0	0	0	0	0	0	2	0	0	2	0.00
13	0	0	0	0	0	0	0	0	1	4	1	0	6	0.67
14	0	0	0	0	0	0	0	0	0	0	0	0	0	N/A
15	1	0	0	1	0	0	0	0	0	0	2	2	6	0.33
SUM	41	68	37	83	40	27	6	6	22	9	6	5	350	
User Acc	0.78	0.00	0.08	0.01	0.75	0.04	0.00	1.00	0.00	0.44	0.00	0.40	OA =	23%

7.1.2.2.3.4 Fused maps: LOGP & MRF

The Fused LOGP and Fused MRF processing chain RR present little difference in terms of UA and PA, obtaining both overall accuracies of respectively 31% (Table 32, Table 33).

Table 42. Fused LOGP processing chain RR unbiased confusion matrix with PA, UA, and OA.

Ref\Pred	1	3	5	6	7	8	9	10	12	13	14	15	SUM	Prod Acc
1	38	59	8	12	18	3	0	2	3	0	3	0	146	0.26
3	0	0	0	1	0	0	0	0	0	0	0	0	1	0.00
5	1	3	4	5	2	0	0	1	1	0	0	0	17	0.24
6	2	3	0	0	0	0	0	0	0	0	0	0	5	0.00
7	5	10	7	33	53	38	1	2	5	2	0	0	156	0.34
8	1	0	0	0	0	1	0	0	0	0	0	0	2	0.50
9	0	0	0	0	0	0	0	0	0	0	0	0	0	N/A
10	0	0	0	1	1	0	0	6	0	0	1	0	9	0.67
12	0	0	0	0	0	0	0	0	0	2	0	0	2	0.00
13	0	0	0	0	0	0	0	0	1	4	1	0	6	0.67
14	0	0	0	0	0	0	0	0	0	0	0	0	0	N/A
15	1	0	0	1	0	0	0	0	0	0	1	3	6	0.50
SUM	48	75	19	53	74	42	1	11	10	8	6	3	350	
User Acc	0.79	0.00	0.21	0.00	0.72	0.02	0.00	0.55	0.00	0.50	0.00	1.00	OA =	31%

Table 43. Fused MRF processing chain RR unbiased confusion matrix with PA, UA, and OA.

Ref\Pred	1	3	5	6	7	8	9	10	12	13	14	15	SUM	Prod Acc
1	36	61	7	13	17	3	0	3	3	0	3	0	146	0.25
3	0	0	0	1	0	0	0	0	0	0	0	0	1	0.00

5	1	3	4	5	2	0	0	1	1	0	0	0	17	0.24
6	2	3	0	0	0	0	0	0	0	0	0	0	5	0.00
7	5	8	11	29	56	37	1	3	4	2	0	0	156	0.36
8	1	0	0	0	0	1	0	0	0	0	0	0	2	0.50
9	0	0	0	0	0	0	0	0	0	0	0	0	0	N/A
10	1	0	0	0	1	0	0	6	1	0	0	0	9	0.67
12	0	0	0	0	0	0	0	0	0	2	0	0	2	0.00
13	0	0	0	0	0	0	0	0	1	4	1	0	6	0.67
14	0	0	0	0	0	0	0	0	0	0	0	0	0	N/A
15	1	0	0	1	0	0	0	0	0	0	1	3	6	0.50
SUM	47	75	22	49	76	41	1	13	10	8	5	3	350	
User Acc	0.77	0.00	0.18	0.00	0.74	0.02	0.00	0.46	0.00	0.50	0.00	1.00	OA =	31%

7.1.2.2.4 Coherence stratum accuracy figure

The coherence stratum presents an OA of 34% (Table 34).

Table 44. Confusion matrix for the coherence stratum with PA, UA and OA.

Ref\Pred	1	3	5	6	7	8	9	10	12	13	14	15	SUM	Prod Acc
1	19	12	4	2	5	0	0	0	3	0	1	2	48	0.40
3	0	0	0	0	0	0	0	0	0	0	0	0	0	N/A
5	0	0	1	1	0	0	0	0	2	0	0	0	4	0.25
6	0	0	2	0	0	0	0	0	2	0	0	0	4	0.00
7	0	2	6	11	10	12	0	0	5	2	0	1	49	0.20
8	0	0	0	0	0	1	0	0	0	0	0	0	1	1.00
9	0	0	0	0	0	0	0	0	0	0	0	0	0	N/A
10	0	0	0	0	0	1	0	0	0	0	1	1	3	0.00
12	0	0	0	0	0	0	0	0	1	3	1	1	6	0.17
13	0	0	0	0	0	0	0	0	0	4	0	0	4	1.00
14	0	0	0	0	0	0	0	0	0	0	0	0	0	N/A
15	0	0	1	0	0	0	0	0	0	0	5	10	16	0.63
SUM	19	14	14	14	15	14	0	0	13	9	8	15	135	
User Acc	1.00	0.00	0.07	0.00	0.67	0.07	N/A	N/A	0.08	0.44	0.00	0.67	OA =	34%

7.1.2.2.5 Comparison

A confidence-based stratification was used for the validation sampling scheme to highlight differences between processing chains. However, it appears that all processing chains reach similar low accuracies, ranging from 30% to 40% for the Unbiased OA and from 23% to 31% for the discrepancy stratum. In both strategies, the Fused MRF processing chain performs best, and the LSTM TS performs the worse.

It appears that the stratification sampling strategy does not lead to improved discrimination between processing chains. This is mainly due to the initial rationale of processing chains reaching good accuracy in most LC classes that are not met in the Round Robin processing chains.

Table 45. Comparison of the Overall Accuracies of each RR processing chain

RR	SVM	SAR	LSTM composite	LSTM TS	Fused LOGP	Fused MRF
----	-----	-----	----------------	---------	------------	-----------

Unbiased OA	33%	33%	33%	30%	38%	40%
-------------	-----	-----	-----	-----	-----	-----

Table 46. Comparison of the Stratified Overall Accuracies of each RR processing chain

RR	SVM	SAR	LSTM composite	LSTM TS	Fused LOGP	Fused MRF
Discrepancy stratum OA	30%	29%	23%	23%	31%	31%
Coherence stratum OA	34%					

7.1.2.2.6 Analysis of main misclassifications

Although all processing chains present low accuracy values, these are related to two main misclassification issues.

The first main misclassification is the detection of one-third to half of the large “tree cover evergreen broadleaf” area (1) as “tree cover deciduous broadleaf” (3), and to a lesser extent as shrub cover classes (5, 6). This is represented by the 100% UA but 40% PA of the “tree cover evergreen broadleaf” class (1).

The second main misclassification issue is the detection of around two-thirds of the large grassland areas (7) as cropland (8) and as shrubland classes (6). Although some cropland is present in the area, most of the low vegetation is pasture. This is represented by the 67% UA and 20% PA scores for the “grassland” class (7).

Therefore, solving those two issues would rapidly increase the accuracy. In the case of the coherence stratum, an OA of 69% could be reached, along with a PA of 77% for the “tree cover evergreen broadleaf” class (1) and 80% for the “grassland” class (7) (Table 37).

Table 47. Hypothetical confusion matrix for the coherence stratum if the two main classification issues were solved. Red values are taken into account for the OA computation.

Ref\Pred	1	3	5	6	7	8	9	10	12	13	14	15	SUM	Prod Acc
1	19	12	4	2	5	0	0	0	3	0	1	2	48	0.77
3	0	0	0	0	0	0	0	0	0	0	0	0	0	N/A
5	0	0	1	1	0	0	0	0	2	0	0	0	4	0.25
6	0	0	2	0	0	0	0	0	2	0	0	0	4	0.00
7	0	2	6	11	10	12	0	0	5	2	0	1	49	0.80
8	0	0	0	0	0	1	0	0	0	0	0	0	1	1.00
9	0	0	0	0	0	0	0	0	0	0	0	0	0	N/A
10	0	0	0	0	0	1	0	0	0	0	1	1	3	0.00
12	0	0	0	0	0	0	0	0	1	3	1	1	6	0.17
13	0	0	0	0	0	0	0	0	0	4	0	0	4	1.00
14	0	0	0	0	0	0	0	0	0	0	0	0	0	N/A
15	0	0	1	0	0	0	0	0	0	0	5	10	16	0.63
SUM	19	14	14	14	15	14	0	0	13	9	8	15	135	
User Acc	1.00	0.00	0.07	0.00	0.67	0.07	N/A	N/A	0.08	0.44	0.00	0.67	OA =	69%

7.1.2.2.7 Conclusion

All processing chains present low OA scores ranging from 23% to 40% including both validation strategies. Although low, these scores are mainly due to two main classification errors. If these were solved, higher OA values would be reached.

7.1.2.3 Siberia – T42WXS

7.1.2.3.1 The validation database in the perspective of the confidence-based stratification

In total, the validation database includes 493 samples whose distribution varies according to the strata included in the confidence-based stratification (Figure 36).

350 samples were randomly selected in the discrepancy stratum and 143 samples were randomly sampled with an even distribution among LC classes (i.e., 11 samples per class) in the coherence stratum according to the specifications described in the Product Validation Plan [AD6].

Among the 493 samples, no samples were qualified as “totally uncertain” by the photo-interpreters but 112 of them (22,8 %) as “doubtful”. This larger proportion of “doubtful” interpretations is mainly due to the low availability of VHR imagery on Google Earth, along with an 8–9-month snow period on the whole area which makes NDVI yearly profiles difficult to interpret. The stratum areas and sample number per tile are detailed in Table 38.

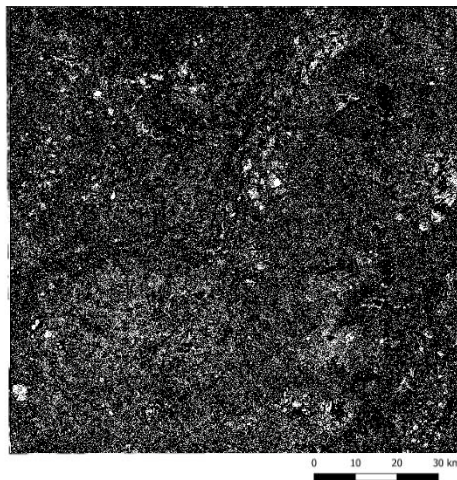


Figure 84. Stratification of the Africa T37PCP tile. In white, the coherence strata (all six RR processing chains agree, in black the discrepancy strata (at least one of the RR processing chains disagree with the others).

Table 48. Stratification specifications including area and sample number.

Stratum	Area (km ²)	Sample number
Discrepancy (stratum 1)	10962	350
Coherence (stratum 2)	2317	143

7.1.2.3.2 Unbiased accuracy figures

7.1.2.3.2.1 SVM Map

The SVM processing chain presents low accuracy scores (Table 39).

Table 49. SVM processing chain RR unbiased confusion matrix with PA, UA and OA.

Ref\Pred	1	2	3	4	5	6	7	9	10	11	12	14	15	SUM	Prod Acc
1	0.00	0.00	0.00	0.00	0.00	0.00	0.00	0.00	0.00	0.00	0.00	0.00	0.00	0.00	N/A
2	1.53	1.98	0.10	2.60	1.30	0.27	0.00	1.40	0.00	2.21	0.04	0.26	0.00	11.70	0.17

5	0.00	0.00	0.00	0.00	0.00	0.00	0.00	0.00	0.00	0.00	0.00	0.00	0.00	0.00	N/A
6	0.11	0.64	0.11	0.21	2.22	8.78	0.00	0.34	2.77	0.99	0.00	0.61	0.09	16.86	0.52
7	0.00	0.10	0.00	0.00	0.00	0.73	1.38	0.00	0.11	0.00	0.12	0.09	0.00	2.52	0.55
9	0.00	0.00	0.00	0.00	0.00	0.00	0.00	0.00	0.43	0.00	0.06	0.19	0.00	0.68	0.00
10	0.00	0.11	0.00	0.10	0.00	0.11	0.00	0.25	0.00	0.00	0.00	0.07	0.00	0.63	0.00
11	0.00	0.00	0.00	0.00	0.00	0.00	0.00	0.00	0.00	0.30	0.00	0.00	0.00	0.30	1.00
12	0.00	0.00	0.00	0.10	0.00	0.00	0.00	0.00	0.00	0.10	0.62	0.00	0.00	0.81	0.76
14	0.00	0.00	0.00	0.00	0.00	0.00	0.00	0.00	0.00	0.00	0.00	0.19	0.00	0.19	1.00
15	0.00	0.00	0.00	0.00	0.00	0.00	0.00	0.09	0.11	0.00	0.00	0.77	2.15	3.11	0.69
SUM	1.17	2.46	0.30	3.63	3.73	10.2	1.38	0.92	3.41	3.18	0.86	2.01	2.23		
User Acc	0.00	0.66	0.00	0.00	0.00	0.86	1.00	0.00	0.00	0.09	0.71	0.10	0.96	OA =	42%

7.1.2.3.2.4 Fused maps: LOGP & MRF

The Fused LOGP and Fused MRF processing chain RR present little difference in terms of accuracies, obtaining overall accuracies of 32% and 30% (Table 42, Table 43).

Table 52. Fused LOGP processing chain RR unbiased confusion matrix with PA, UA, and OA.

Ref\Pred	1	2	3	4	5	6	7	9	10	11	12	14	15	SUM	Prod Acc
1	0.00	0.00	0.00	0.00	0.00	0.00	0.00	0.00	0.00	0.00	0.00	0.00	0.00	0.00	N/A
2	1.74	2.40	1.98	1.71	1.81	0.10	0.00	0.73	0.00	1.25	0.05	0.06	0.00	11.83	0.20
3	0.00	0.00	0.00	0.00	0.00	0.00	0.00	0.00	0.00	0.00	0.00	0.00	0.00	0.00	N/A
4	0.00	0.00	0.00	0.00	0.00	0.00	0.00	0.00	0.00	0.00	0.00	0.00	0.00	0.00	N/A
5	0.00	0.00	0.00	0.00	0.00	0.00	0.00	0.00	0.00	0.00	0.00	0.00	0.00	0.00	N/A
6	0.16	0.40	0.05	0.20	1.36	3.89	3.71	0.00	0.00	0.81	0.50	0.33	0.00	11.40	0.34
7	0.00	0.00	0.00	0.00	0.00	0.10	1.59	0.16	0.46	0.22	0.16	0.00	0.00	2.67	0.59
9	0.00	0.00	0.00	0.00	0.00	0.00	0.00	0.00	0.43	0.00	0.00	0.16	0.00	0.59	0.00
10	0.00	0.12	0.00	0.00	0.00	0.10	0.00	0.11	0.00	0.00	0.05	0.06	0.00	0.43	0.00
11	0.00	0.00	0.00	0.00	0.00	0.00	0.00	0.00	0.00	0.36	0.00	0.00	0.00	0.36	1.00
12	0.05	0.00	0.00	0.00	0.00	0.00	0.00	0.00	0.00	0.00	0.54	0.00	0.00	0.59	0.91
14	0.00	0.00	0.00	0.00	0.00	0.00	0.00	0.05	0.00	0.00	0.05	0.06	0.00	0.16	0.35
15	0.00	0.00	0.00	0.00	0.00	0.00	0.00	0.00	0.11	0.00	0.00	1.11	0.83	2.05	0.41
SUM	1.95	2.92	2.03	1.90	3.17	4.17	5.30	1.05	0.99	2.63	1.34	1.77	0.83		
User Acc	0.00	0.82	0.00	0.00	0.00	0.93	0.30	0.00	0.00	0.14	0.40	0.03	1.00	OA =	32%

Table 53. Fused MRF processing chain RR unbiased confusion matrix with PA, UA, and OA.

Ref\Pred	1	2	3	4	5	6	7	9	10	11	12	14	15	SUM	Prod Acc
1	0.00	0.00	0.00	0.00	0.00	0.00	0.00	0.00	0.00	0.00	0.00	0.00	0.00	0.00	N/A
2	1.83	1.40	3.37	3.47	4.00	0.30	0.00	1.02	0.00	0.12	0.06	0.07	0.00	15.65	0.09
3	0.00	0.00	0.00	0.00	0.00	0.00	0.00	0.00	0.00	0.00	0.00	0.00	0.00	0.00	N/A
4	0.00	0.00	0.00	0.00	0.00	0.00	0.00	0.00	0.00	0.00	0.00	0.00	0.00	0.00	N/A
5	0.00	0.00	0.00	0.00	0.00	0.00	0.00	0.00	0.00	0.00	0.00	0.00	0.00	0.00	N/A
6	0.22	0.27	0.10	0.46	2.75	6.91	0.08	0.00	0.00	0.00	0.40	0.52	0.00	11.71	0.59
7	0.00	0.00	0.00	0.00	0.00	0.53	0.16	0.24	0.31	0.00	0.12	0.00	0.00	1.35	0.11

9	0.00	0.00	0.00	0.00	0.00	0.00	0.00	0.00	0.62	0.00	0.00	0.30	0.00	0.92	0.00
10	0.00	0.00	0.00	0.00	0.00	0.31	0.00	0.31	0.00	0.00	0.06	0.07	0.00	0.75	0.00
11	0.00	0.00	0.00	0.00	0.00	0.00	0.00	0.00	0.00	0.00	0.00	0.00	0.00	0.00	N/A
12	0.00	0.00	0.00	0.00	0.00	0.00	0.00	0.08	0.00	0.00	0.64	0.00	0.00	0.71	0.89
14	0.00	0.00	0.00	0.00	0.00	0.00	0.00	0.08	0.00	0.00	0.06	0.07	0.00	0.21	0.35
15	0.00	0.00	0.00	0.00	0.00	0.00	0.00	0.00	0.16	0.00	0.00	1.48	1.11	2.75	0.40
SUM	2.04	1.67	3.47	3.93	6.76	8.06	0.23	1.73	1.09	0.12	1.33	2.53	1.11		N/A
User Acc	0.00	0.84	0.00	0.00	0.00	0.86	0.66	0.00	0.00	0.00	0.48	0.03	1.00	OA =	30%

7.1.2.3.3 Discrepancy stratum accuracy figures

7.1.2.3.3.1 SVM Map

The SVM processing chain presents low accuracy scores (Table 44).

Table 54. SVM processing chain RR unbiased confusion matrix with PA, UA and OA.

Ref\Pred	1	2	3	4	5	6	7	9	10	11	12	14	15	SUM	Prod Acc
1	0	0	0	0	0	0	0	0	0	0	0	0	0	0	N/A
2	20	25	15	34	10	3	0	22	0	10	1	4	0	144	0.17
3	0	0	0	0	0	0	0	0	0	0	0	0	0	0	N/A
4	0	0	0	0	0	0	0	0	0	0	0	0	0	0	N/A
5	0	0	0	0	0	0	0	0	0	0	0	0	0	0	N/A
6	3	11	0	4	21	52	14	13	26	4	0	5	0	153	0.34
7	2	0	0	0	1	5	4	1	2	0	1	0	0	16	0.25
9	0	0	0	0	0	0	0	0	5	0	0	0	0	5	0.00
10	0	1	1	0	3	0	0	0	3	0	0	1	0	9	0.33
11	0	0	0	0	0	0	0	0	0	1	0	0	0	1	1.00
12	0	0	0	0	0	0	0	0	0	1	3	0	0	4	0.75
14	0	1	0	0	0	0	0	0	0	0	0	1	1	3	0.33
15	0	0	0	0	0	0	0	0	0	0	0	10	5	15	0.33
SUM	25	38	16	38	35	60	18	36	36	16	5	21	6	350	
User Acc	0.00	0.66	0.00	0.00	0.00	0.87	0.22	0.00	0.08	0.06	0.60	0.05	0.83	OA =	27%

7.1.2.3.3.2 SAR Map

The SAR processing chain presents low accuracy scores (Table 45).

Table 55. SAR processing chain RR unbiased confusion matrix with PA, UA, and OA.

Ref\Pred	1	2	3	4	5	6	7	9	10	11	12	14	15	SUM	Prod Acc
1	0	0	0	0	0	0	0	0	0	0	0	0	0	0	N/A
2	26	48	13	14	27	4	1	8	0	2	1	0	0	144	0.33
3	0	0	0	0	0	0	0	0	0	0	0	0	0	0	N/A
4	0	0	0	0	0	0	0	0	0	0	0	0	0	0	N/A
5	0	0	0	0	0	0	0	0	0	0	0	0	0	0	N/A
6	3	9	2	1	16	22	42	13	24	14	4	3	0	153	0.14
7	1	2	0	0	1	0	5	0	5	1	1	0	0	16	0.31

9	0	0	0	0	0	0	2	0	1	0	0	2	0	5	0.00
10	0	1	0	0	0	1	1	1	4	0	1	0	0	9	0.44
11	0	0	0	0	0	0	0	0	0	0	1	0	0	1	0.00
12	0	0	0	0	0	0	0	2	0	1	0	1	0	4	0.00
14	0	0	0	0	0	0	0	1	0	0	0	2	0	3	0.67
15	0	0	0	0	0	0	0	1	0	0	0	8	6	15	0.40
SUM	30	60	15	15	44	27	51	26	34	18	8	16	6	350	
User Acc	0.00	0.80	0.00	0.00	0.00	0.81	0.10	0.00	0.12	0.00	0.00	0.13	1.00	OA =	25%

7.1.2.3.3 LSTM Time Series Map

The LSTM Time Series processing chain presents low accuracy scores, with an OA of 31% which makes it the best of all 6 processing chains (Table 46).

Table 56. LSTM time-series processing chain RR unbiased confusion matrix with PA, UA, and OA.

Ref\Pred	1	2	3	4	5	6	7	9	10	11	12	14	15	SUM	Prod Acc
1	0	0	0	0	0	0	0	0	0	0	0	0	0	0	N/A
2	10	22	33	48	13	5	0	0	0	11	1	1	0	144	0.15
3	0	0	0	0	0	0	0	0	0	0	0	0	0	0	N/A
4	0	0	0	0	0	0	0	0	0	0	0	0	0	0	N/A
5	0	0	0	0	0	0	0	0	0	0	0	0	0	0	N/A
6	2	10	1	4	20	62	11	2	20	8	6	6	1	153	0.41
7	0	2	0	0	0	5	5	0	1	0	2	1	0	16	0.31
9	0	0	0	0	0	0	0	0	3	0	1	1	0	5	0.00
10	0	1	0	1	0	1	0	2	3	0	0	1	0	9	0.33
11	0	0	0	0	0	0	0	0	0	1	0	0	0	1	1.00
12	0	0	0	1	0	0	0	0	0	1	2	0	0	4	0.50
14	0	1	0	0	0	0	0	0	0	0	0	2	0	3	0.67
15	0	0	0	0	0	0	0	0	0	0	0	2	13	15	0.87
SUM	12	36	34	54	33	73	16	4	27	21	12	14	14	350	
User Acc	0.00	0.61	0.00	0.00	0.00	0.85	0.31	0.00	0.11	0.05	0.17	0.14	0.93	OA =	31%

7.1.2.3.4 Fused maps: LOGP & MRF

The Fused LOGP and Fused MRF processing chain RR present little difference in terms of accuracies, obtaining overall accuracies of respectively 24% and 21% (Table 47, Table 48).

Table 57. Fused LOGP processing chain RR unbiased confusion matrix with PA, UA, and OA.

Ref\Pred	1	2	3	4	5	6	7	9	10	11	12	14	15	SUM	Prod Acc
1	0	0	0	0	0	0	0	0	0	0	0	0	0	0	N/A
2	20	32	23	25	28	1	0	9	0	4	1	1	0	144	0.22
3	0	0	0	0	0	0	0	0	0	0	0	0	0	0	N/A
4	0	0	0	0	0	0	0	0	0	0	0	0	0	0	N/A
5	0	0	0	0	0	0	0	0	0	0	0	0	0	0	N/A
6	3	6	1	4	17	32	25	15	34	5	6	5	0	153	0.21

7	0	0	0	0	0	0	6	3	3	2	2	0	0	16	0.38
9	0	0	0	0	0	0	0	0	3	0	0	2	0	5	0.00
10	0	1	0	0	0	1	0	1	4	0	1	1	0	9	0.44
11	0	0	0	0	0	0	0	0	0	1	0	0	0	1	1.00
12	1	0	0	0	0	0	0	0	0	0	3	0	0	4	0.75
14	0	0	0	0	0	0	0	1	0	0	1	1	0	3	0.33
15	0	0	0	0	0	0	0	0	0	0	0	11	4	15	0.27
SUM	24	39	24	29	45	34	31	29	44	12	14	21	4	350	
User Acc	0.00	0.82	0.00	0.00	0.00	0.94	0.19	0.00	0.09	0.08	0.21	0.05	1.00	OA =	24%

Table 58. Fused MRF processing chain RR unbiased confusion matrix with PA, UA, and OA.

Ref\Pred	1	2	3	4	5	6	7	9	10	11	12	14	15	SUM	Prod Acc
1	0	0	0	0	0	0	0	0	0	0	0	0	0	0	N/A
2	17	20	30	32	29	2	0	9	0	3	1	1	0	144	0.14
3	0	0	0	0	0	0	0	0	0	0	0	0	0	0	N/A
4	0	0	0	0	0	0	0	0	0	0	0	0	0	0	N/A
5	0	0	0	0	0	0	0	0	0	0	0	0	0	0	N/A
6	3	4	2	6	17	38	17	15	39	2	4	6	0	153	0.25
7	0	0	0	0	0	3	6	3	2	0	2	0	0	16	0.38
9	0	0	0	0	0	0	0	0	3	0	0	2	0	5	0.00
10	0	0	0	0	0	2	0	3	2	0	1	1	0	9	0.22
11	0	0	0	0	0	0	0	0	0	1	0	0	0	1	1.00
12	0	0	0	0	0	0	0	1	0	0	3	0	0	4	0.75
14	0	0	0	0	0	0	0	1	0	0	1	1	0	3	0.33
15	0	0	0	0	0	0	0	0	0	0	0	11	4	15	0.27
SUM	20	24	32	38	46	45	23	32	46	6	12	22	4	350	
User Acc	0.00	0.83	0.00	0.00	0.00	0.84	0.26	0.00	0.04	0.17	0.25	0.05	1.00	OA =	21%

7.1.2.3.4 Coherence stratum accuracy figure

The coherence stratum (common for all processing chains) presents a low accuracy value, with an OA just above the best processing chain of the discrepancy stratum (Table 49).

Table 59. Confusion matrix for the coherence stratum with PA, UA, and OA.

Ref\Pred	1	2	3	4	5	6	7	9	10	11	12	14	15	SUM	Prod Acc
1	0	0	0	0	0	0	0	0	0	0	0	0	0	0	N/A
2	10	10	12	11	5	0	0	4	0	7	0	0	0	59	0.17
3	0	0	0	0	0	0	0	0	0	0	0	0	0	0	N/A
4	0	0	0	0	0	0	0	0	0	0	0	0	0	0	N/A
5	0	0	0	0	0	0	0	0	0	0	0	0	0	0	N/A
6	0	1	0	0	7	9	4	6	7	2	3	1	0	40	0.23
7	0	0	0	0	0	1	6	0	1	0	0	0	0	8	0.75
9	0	0	0	0	0	0	0	0	1	0	0	1	0	2	0.00
10	0	0	0	0	0	0	0	1	2	0	0	0	0	3	0.67

11	0	0	0	0	0	0	0	0	0	2	0	0	0	2	1.00
12	0	0	0	0	0	0	0	0	0	0	8	0	0	8	1.00
14	0	0	0	0	0	0	0	0	0	0	0	0	0	0	N/A
15	0	0	0	0	0	0	0	0	1	0	0	9	11	21	0.52
SUM	10	11	12	11	12	10	10	11	12	11	11	11	11	143	
User Acc	0.00	0.91	0.00	0.00	0.00	0.90	0.60	0.00	0.17	0.18	0.73	0.00	1.00	OA =	34%

7.1.2.3.5 Comparison

A confidence-based stratification was used for the validation sampling scheme to highlight differences between processing chains. However, it appears that all processing chains reach low accuracies, ranging from 18% to 42% for the Unbiased OA (Table 50) and from 21% to 31% for the discrepancy stratum (Table 51). In both strategies, the LSTM Time-series processing chain performs best.

It appears that the stratification sampling strategy does not lead to improved discrimination between processing chains. This is mainly due to the initial rationale of processing chains reaching good accuracy in most LC classes that are not met in the Round Robin processing chains.

Table 60. Comparison of the Unbiased Overall Accuracies of each RR processing chain

RR	SVM	SAR	LSTM TS	Fused LOGP	Fused MRF
Unbiased OA	18%	38%	42%	32%	30%

Table 61. Comparison of the Stratified Overall Accuracies of each RR processing chain

RR	SVM	SAR	LSTM TS	Fused LOGP	Fused MRF
Discrepancy stratum OA	27%	25%	31%	24%	21%
Coherence stratum OA	34%				

7.1.2.3.6 Analysis of main misclassifications

Although all processing chains present low accuracy values, these are related to three main misclassification problems.

The first main misclassification is the detection of the large “tree cover evergreen needleleaf” area (2) as all four tree cover classes (broadleaf/needleleaf, deciduous/evergreen) equally. This is represented by the 91% UA but 17% PA of the “tree cover evergreen needleleaf” class (2).

The second main misclassification issue is the detection of the large low vegetation areas which are mainly “shrub cover deciduous” class (6) as “shrub cover evergreen” (5) and as “grassland” classes (6). This is represented by the 90% UA and 23% PA scores for the “shrub cover deciduous” class (6). This is a common misclassification error since those classes are hard to discriminate in such a landscape with a short positive NDVI period along the year due to the 8-9 months snow period. The seasonality of shrub cover was also challenging to interpret in the validation dataset, and the samples interpreted as “doubtful” in the dataset are mainly present in this class.

The last main misclassification error is the confusion between the “open water seasonal” and “open water permanent” classes (14 and 15).

Therefore, solving those issues would rapidly increase the accuracy. In the case of the coherence stratum, an Overall Accuracy of 71% could potentially be reached (Table 60. Comparison of the Unbiased Overall Accuracies of each RR processing chain Table 62).

Table 62. Hypothetical confusion matrix for the coherence stratum if the two main classification issues were solved. Red values are taken into account for the OA computation.

Ref\Pred	1	2	3	4	5	6	7	9	10	11	12	14	15	SUM	Prod Acc
1	0	0	0	0	0	0	0	0	0	0	0	0	0	0	N/A
2	10	10	12	11	5	0	0	4	0	7	0	0	0	59	0.17
3	0	0	0	0	0	0	0	0	0	0	0	0	0	0	N/A
4	0	0	0	0	0	0	0	0	0	0	0	0	0	0	N/A
5	0	0	0	0	0	0	0	0	0	0	0	0	0	0	N/A
6	0	1	0	0	7	9	4	6	7	2	3	1	0	40	0.23
7	0	0	0	0	0	1	6	0	1	0	0	0	0	8	0.75
9	0	0	0	0	0	0	0	0	1	0	0	1	0	2	0.00
10	0	0	0	0	0	0	0	1	2	0	0	0	0	3	0.67
11	0	0	0	0	0	0	0	0	0	2	0	0	0	2	1.00
12	0	0	0	0	0	0	0	0	0	0	8	0	0	8	1.00
14	0	0	0	0	0	0	0	0	0	0	0	0	0	0	N/A
15	0	0	0	0	0	0	0	0	1	0	0	9	11	21	0.52
SUM	10	11	12	11	12	10	10	11	12	11	11	11	11	143	
User Acc	0.00	0.91	0.00	0.00	0.00	0.90	0.60	0.00	0.17	0.18	0.73	0.00	1.00	OA =	71%

7.1.2.3.7 Conclusion

All processing chains present low OA scores ranging from 18% to 42% including both validation strategies. Although low, these scores are mainly due to three main classification errors. If these were solved, higher OA values would be reached.

7.2 Preliminary HRLC static LC map 2019 over a zoom area

A second production of the static map was received through zoom areas (Table 63) which all include the area covered by the RR prototype of the same region. The zoom area over Africa contains 282 S2 tiles, the one over Amazonia contains 266 tiles and the one over Siberia contains 204 S2 tiles.

A mosaic was created for each region after checking the integrity of each file/tile.

Table 63: Zoom area received for qualitative validation

Africa, Sahel	Received 23/12/2020
Amazonia	Received 21/10/2020
Siberia	Received 22/10/2020

7.2.1 Visual quality assessment

The following figures present a visual evaluation of the quality of the Zoom area products. First, a comparison between the Zoom area products and the RR prototypes is performed to evaluate potential improvements. Then, outside the overlapping extent between both RR and Zoom areas, the zoom area will be evaluated through snapshots and visual comparison with Google imagery and other existing maps.

7.2.1.1 Africa

7.2.1.1.1 Comparison with the African RR prototype

The issue of the contaminating built-up area is considerably reduced inside the RR prototype extent, being mostly replaced by bare soil as shown in Figure 37.

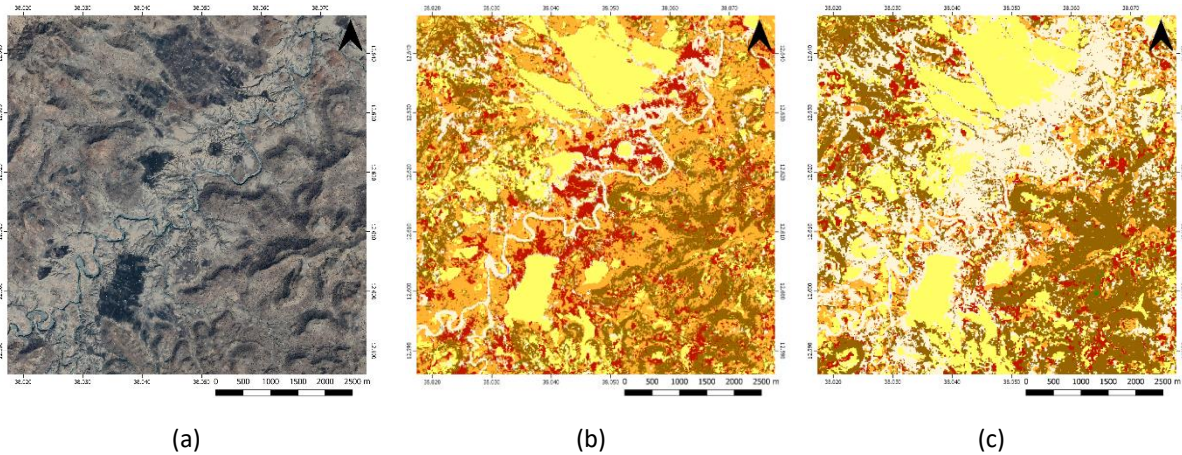


Figure 85. Illustration of the locally solved built-up class contamination from the CCI HRLC RR SVM prototype Africa T37PCP (b) and the zoom area Africa (c), with Google imagery as reference (a).

The comparison with the SVM RR prototype shows us that many cropland areas that were well detected on the RR prototype are now commissioned by shrub cover on the zoom area (Figure 38)

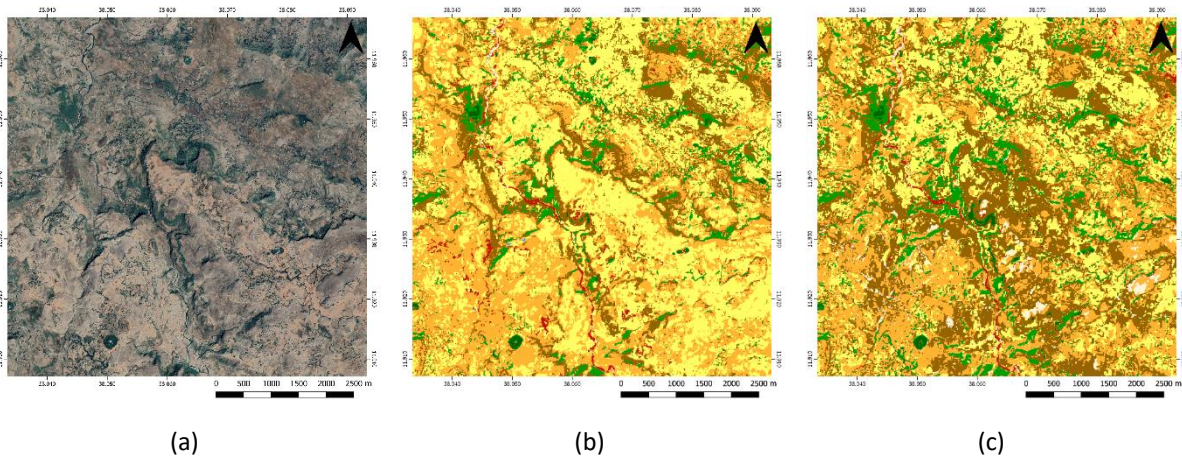
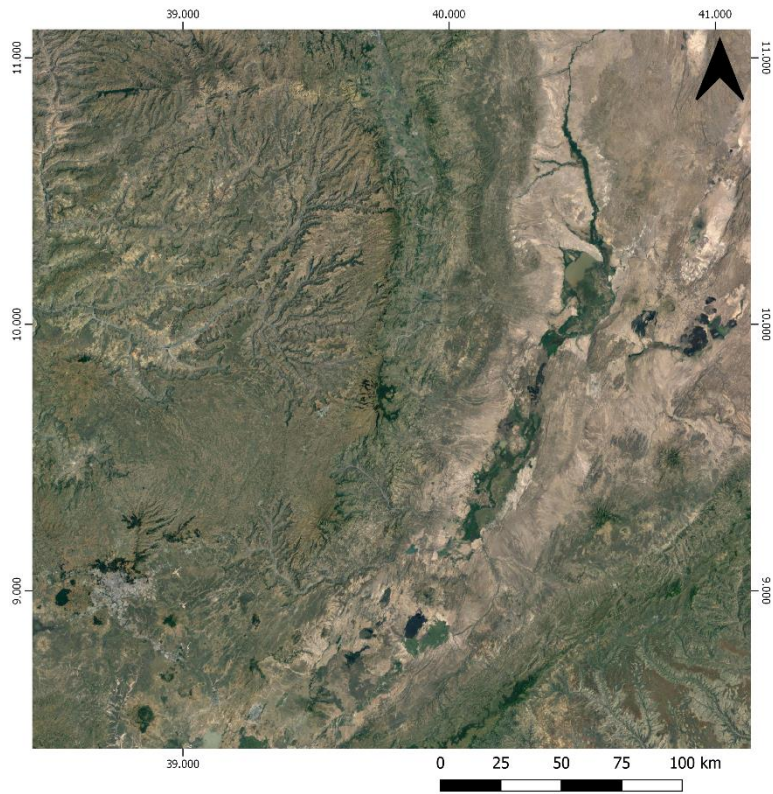


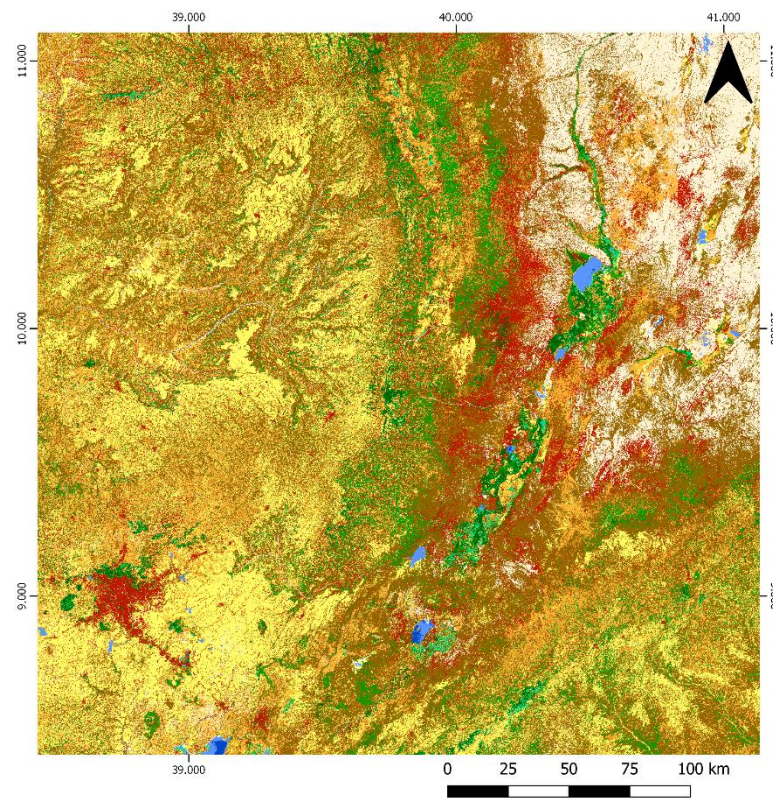
Figure 86. Illustration of the shrub cover class commission over cropland on the zoom area (c) compared to the RR prototype (b), with Google imagery as reference (a).

7.2.1.1.2 Qualitative assessment of the rest of the zoom area

Although improved over the RR prototype extent, the built-up class contamination problem is not solved in the rest of the zoom area. It is noticeable in various areas of the map that the built-up class is contaminating the other classes. As shown in Figure 39, large regions of bare soil are contaminated east of the zoom area.



(a)



(b)

Figure 87. Illustration of the large built-up class contamination over the bare areas east of the zoom area by comparing Google imagery (a) and the zoom area Africa.

The built-up class also contaminates large cropland areas (Figure 40). Cropland areas are also commissioned by bare soil, grassland and grassland vegetation flooded class (Figure 41).

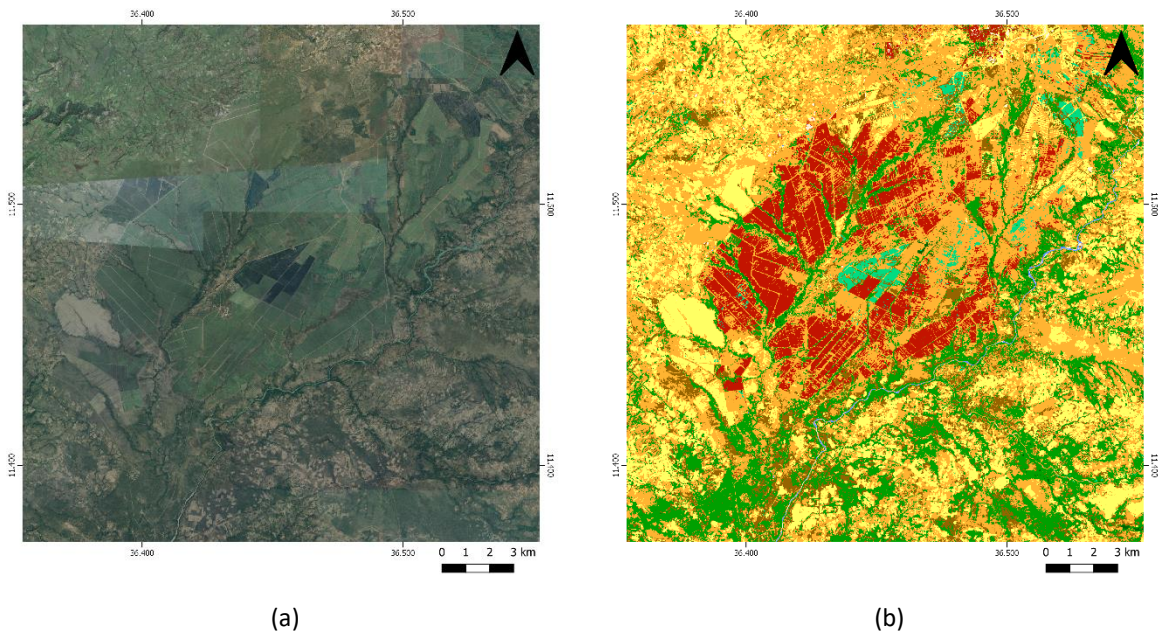


Figure 88. Illustration of the built-up class contamination over cropland area by comparing Google imagery (a) and the zoom area Africa (b).

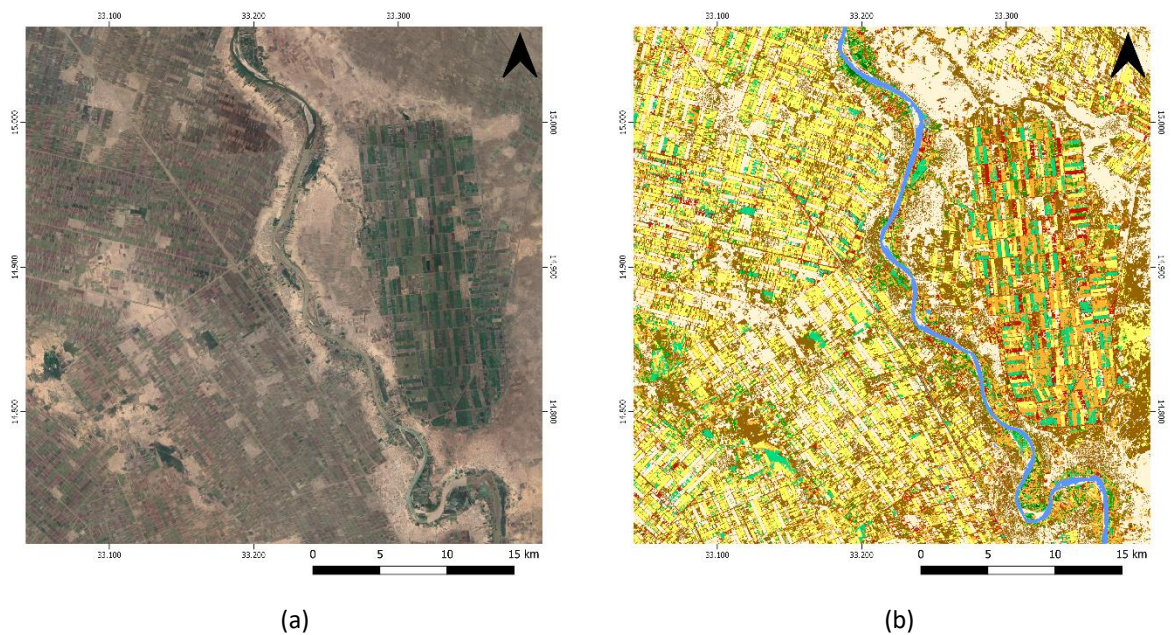


Figure 89. Illustration of the built-up, bare soil and grassland vegetation flooded class contamination over cropland area by comparing Google imagery (a) and the zoom area Africa (b).

The other main LC class commissioning the area is the grassland vegetation flooded class, which is commissioning large areas of tree cover deciduous broadleaf (Figure 42) and locally follows swath band.

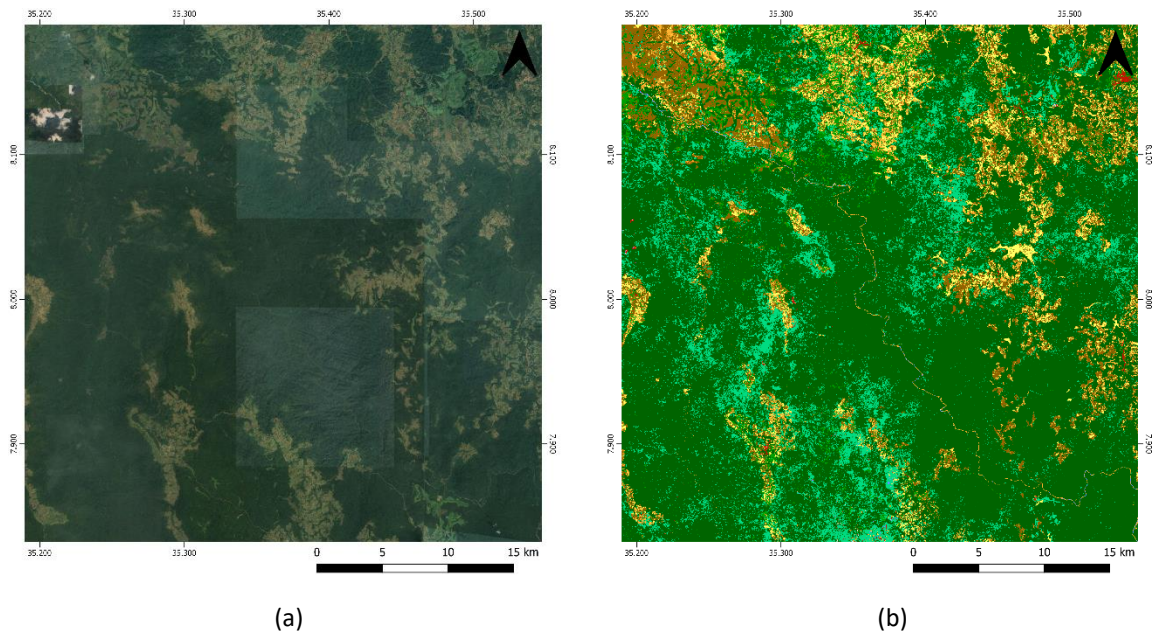


Figure 90. Illustration of the grassland flooded class contamination over tree cover evergreen broadleaf area by comparing Google imagery (a) and the zoom area Africa (b).

Finally, some artefacts related to the processing have to be mentioned, namely tile effects due to erroneous tiles or sharp differences in tiles classification, and some swath effects resulting in large stripping bands of grassland vegetation flooded commission (Figure 43).

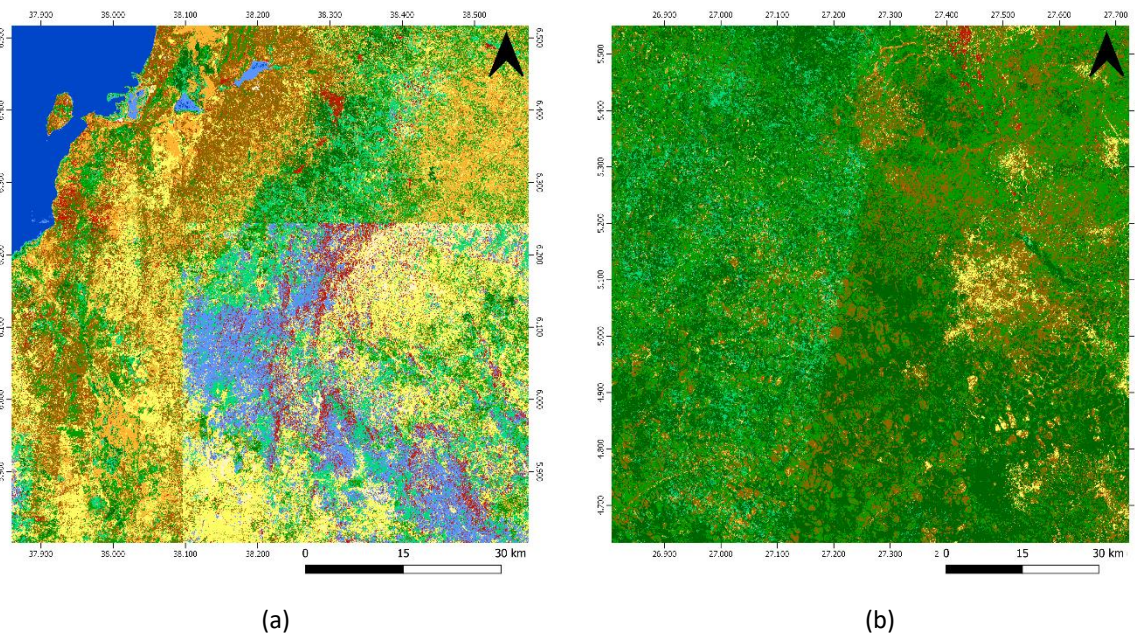


Figure 91. Illustration of processing artefacts; tile effect due to an erroneous tile (a) and swath effect (b).

7.2.1.1.3 Concluding remarks

The African zoom area map encounters several misclassification issues that are not consistent with the targeted 10 m spatial resolution:

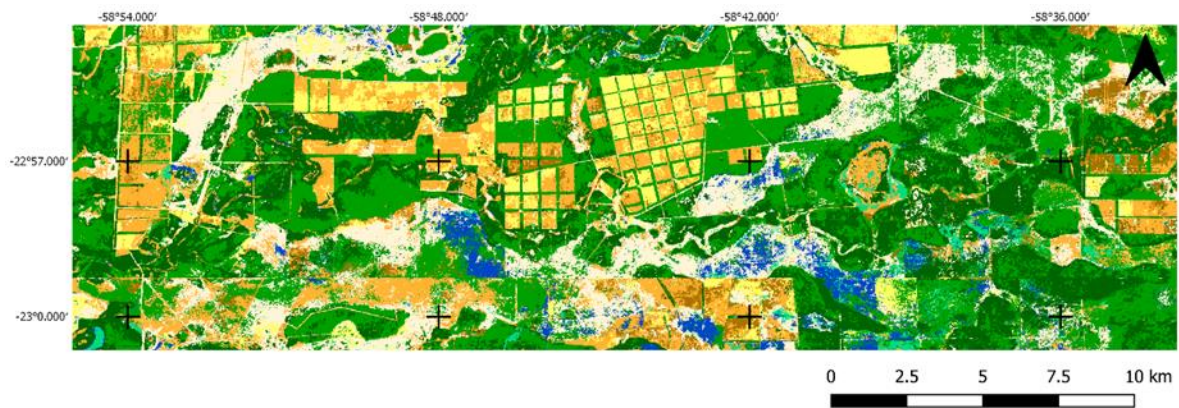
- The major thematic errors (wrong LC labels) are the contamination of built-up and grassland vegetation flooded classes over large areas of bare soil and tree cover evergreen broadleaf, respectively.
- Cropland areas are contaminated with built-up, shrub cover, bare soil, and grassland vegetation flooded classes.
- Some processing artefacts are visible such as tiles and swath effects.

Although improvements have been noticed in the overlapping area between the RR prototypes and the zoom area, some other issues remain in the rest of the zoom area.

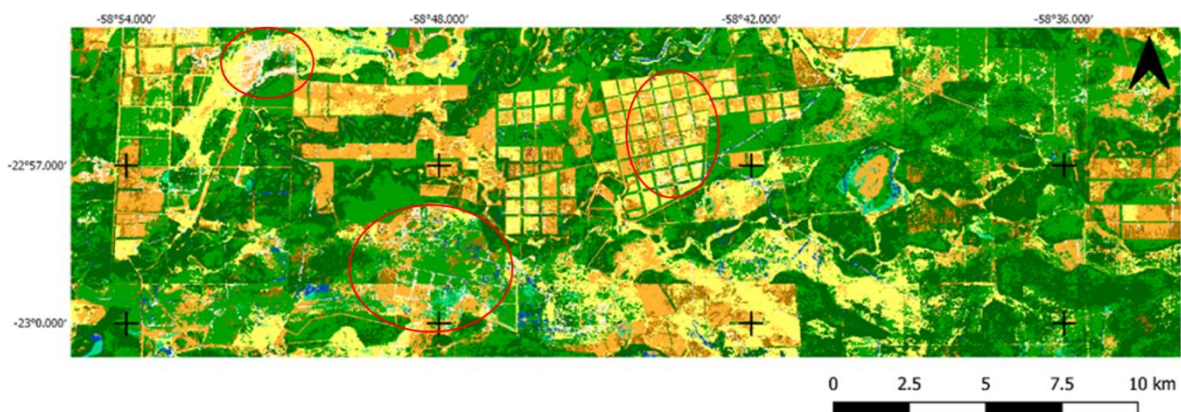
7.2.1.2 Amazonia

7.2.1.2.1 Comparison with the RR prototype Amazonia KUQ

The issue of the contaminating bare area is considerably reduced as shown in Figure 37. However, patterns in various regions of the map, and overestimation of the presence of bare soil remain (Figure 37 (b)).



(a)



(b)

Figure 92. Comparison of the bare area class from the CCI HRLC RR prototype Amazonia KUQ (a) and the zoom area Amazonia (b)

The comparison with the SVM RR prototype shows us that the zoom area encounters some issues when classifying water. We can see in Figure 38 that the water track is lost in the zoom area (circled in red) and unwanted patterns and contaminations appear on other regions of the map (one example is framed in red).

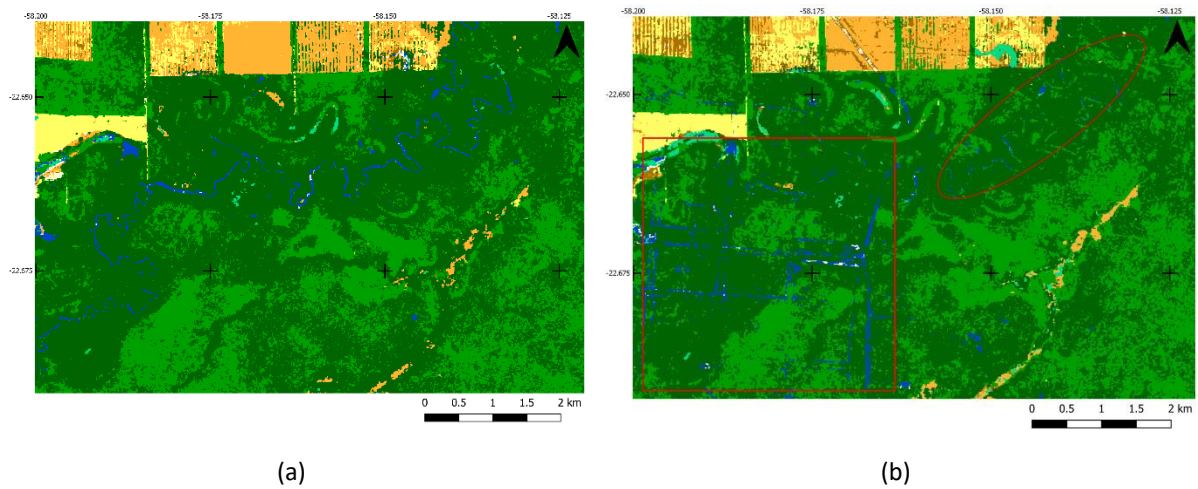
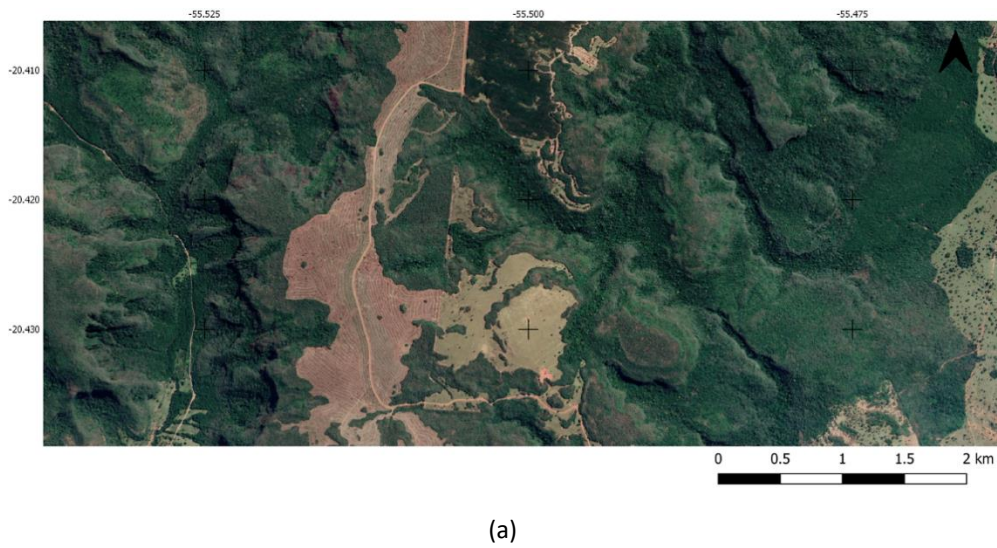
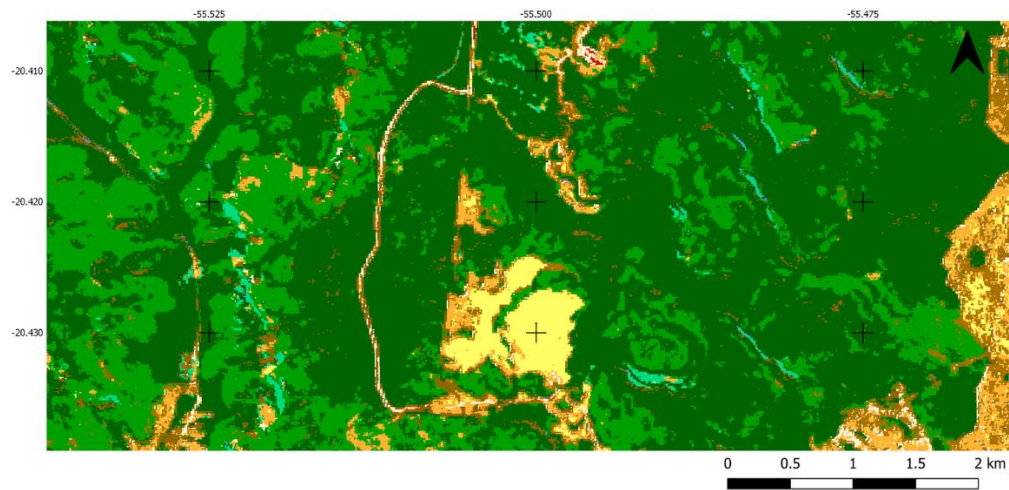


Figure 93. Comparison of the classification of the open water permanent class on the CCI HRLC RR prototype Amazonia KUQ (a) and the Amazonia Zoom area (b)

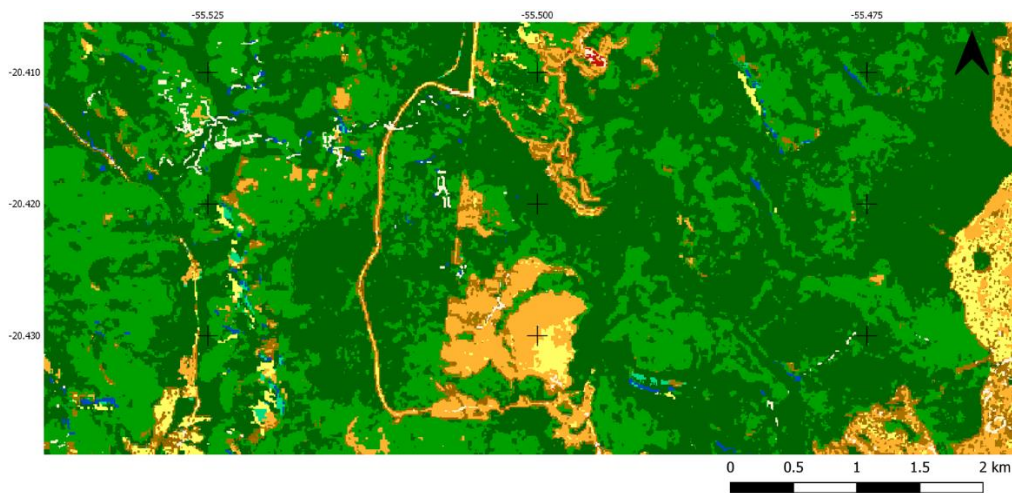
7.2.1.2.2 Comparison with the RR prototype Amazonia KXT

As mentioned for the RR prototype Amazonia KXT, shadows in mountains were detected as vegetation regularly flooded Figure 39 (b). In the case of the zoom area, shadows are detected as a mix of vegetation regularly flooded and open permanent water. This class is also contaminating other regions of the map Figure 39 (c).





(b)



(c)

Figure 94. Illustration of the detection of shadows as vegetation regularly flooded and open permanent water in google imagery (a), in the CCI-HRLC RR prototype Amazonia KXT (b) and the zoom area Amazonia (c)

Another issue remains with the built-up class. As shown in Figure 40, some areas that were contaminated by the built-up class on the RR prototype (b) disappeared (c). However, at some other places on the map, built-up contamination appeared (Figure 41). The contamination often appears on parcels of crops or grassland which, at a 10m spatial resolution, should be avoided. There is therefore a built-up class issue to be corrected.

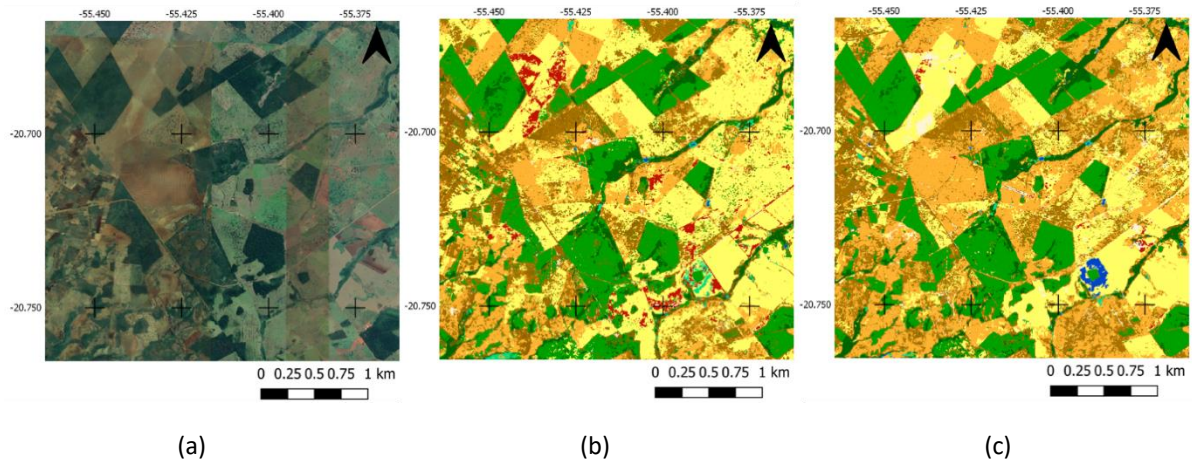


Figure 95. Illustration of an improvement of the built-up contamination on google imagery (a), CCI HRLC RR prototype Amazonia KXT (b), and zoom area Amazonia (c)

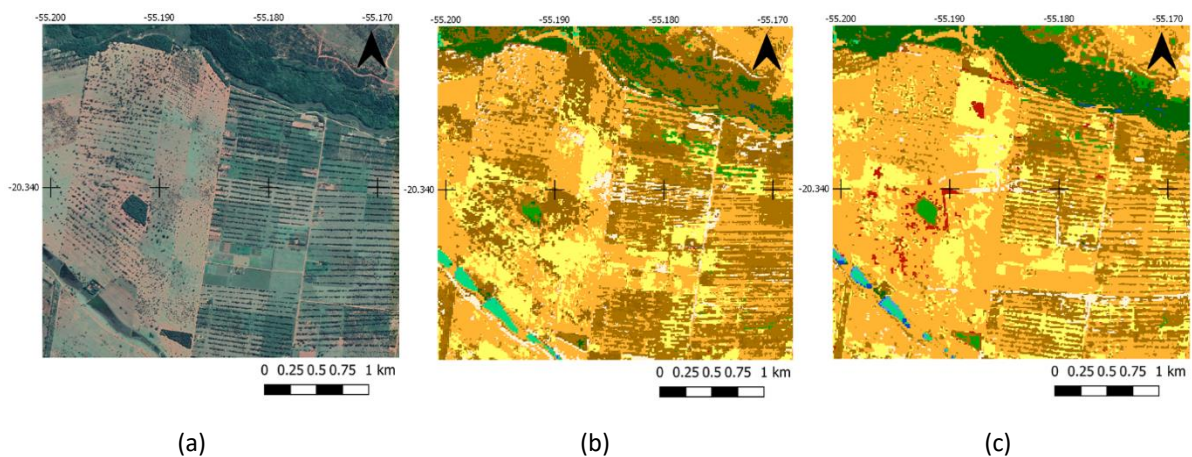


Figure 96. Illustration of built-up contamination appearance on the CCI HRLC zoom area (c) compared to the RR prototype Amazonia KXT (b) and google imagery (a).

7.2.1.2.3 Qualitative assessment of the rest of the zoom area

First, it is noticeable in various areas of the map that the built-up class is contaminating the other classes. As shown in Figure 42, pure grassland or cropland areas are contaminated by built-up.

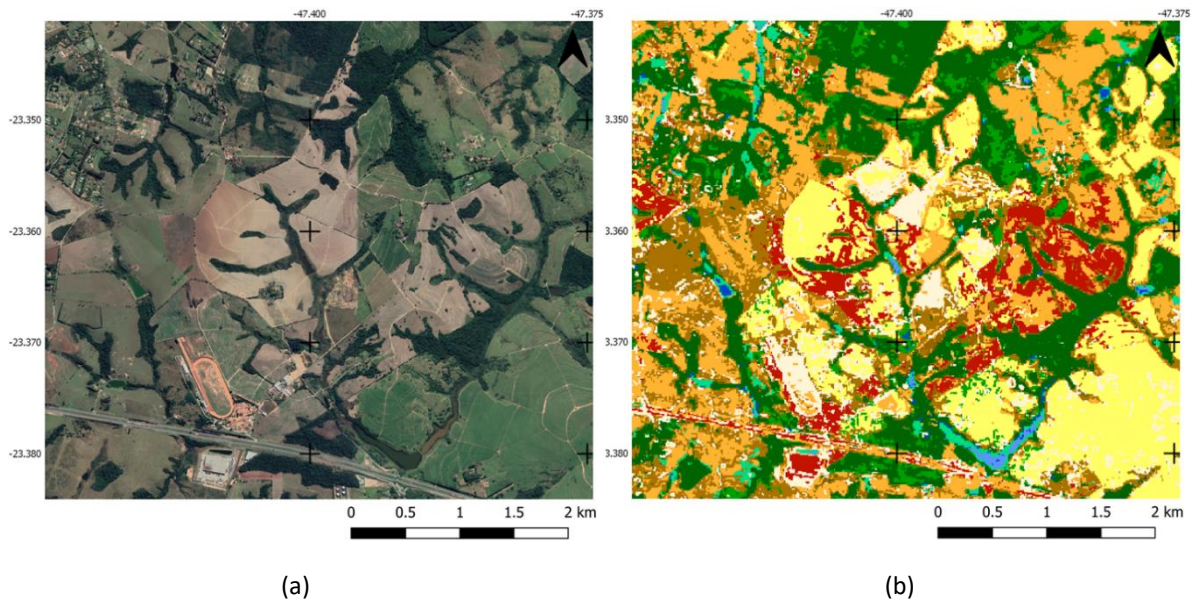


Figure 97. Illustration of built-up contamination by comparing google imagery (2020) (a) and the CCI HRLC Amazonia Zoom area (b).

Another classification error visible in various places on the map is the contamination of the bare area class. As shown in Figure 43, some roads, as well as pixels inside crop fields or grassland, are classified as bare areas.

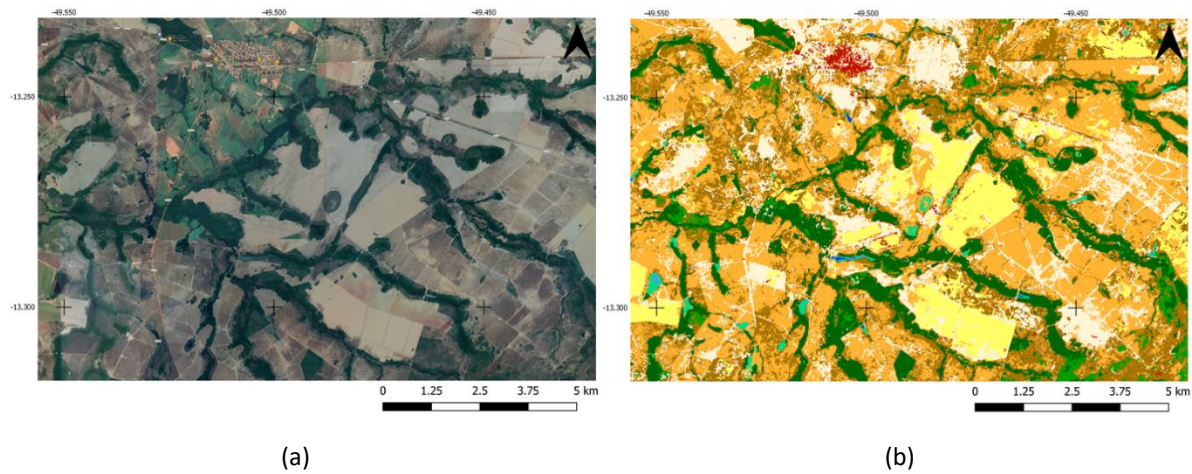


Figure 98. Illustration of misclassification of the bare area class by comparing google imagery (2020) (a) and the CCI HRLC Amazonia zoom area (b)

One can notice in Figure 44 the presence of misclassified, isolated pixels over wide patches of tree cover. The phenomenon occurs in various areas of the map. Figure 45 shows in more detail the presence of pixels classified as cropland, bare areas, and evergreen tree cover over a dense patch of deciduous tree cover.

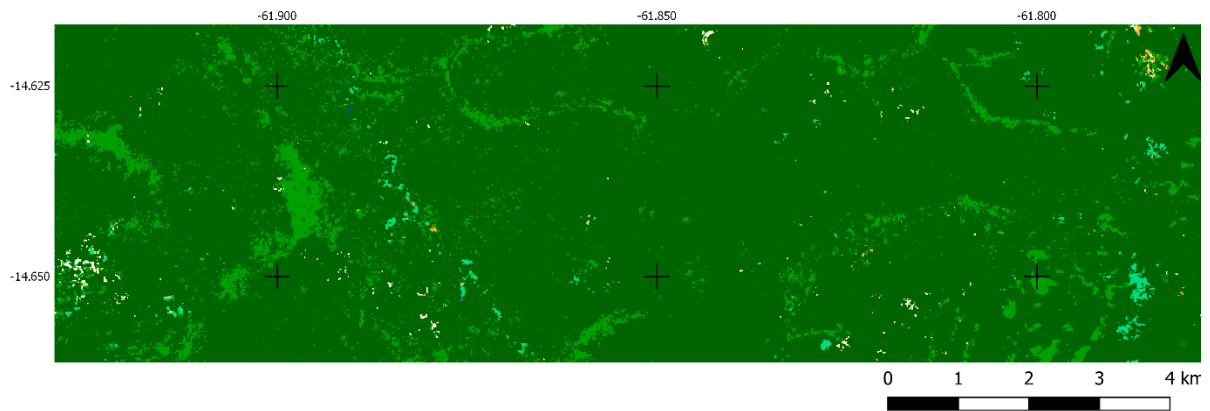


Figure 99. Illustration of misclassified isolated pixels on the CCI HRLC Amazonia zoom area

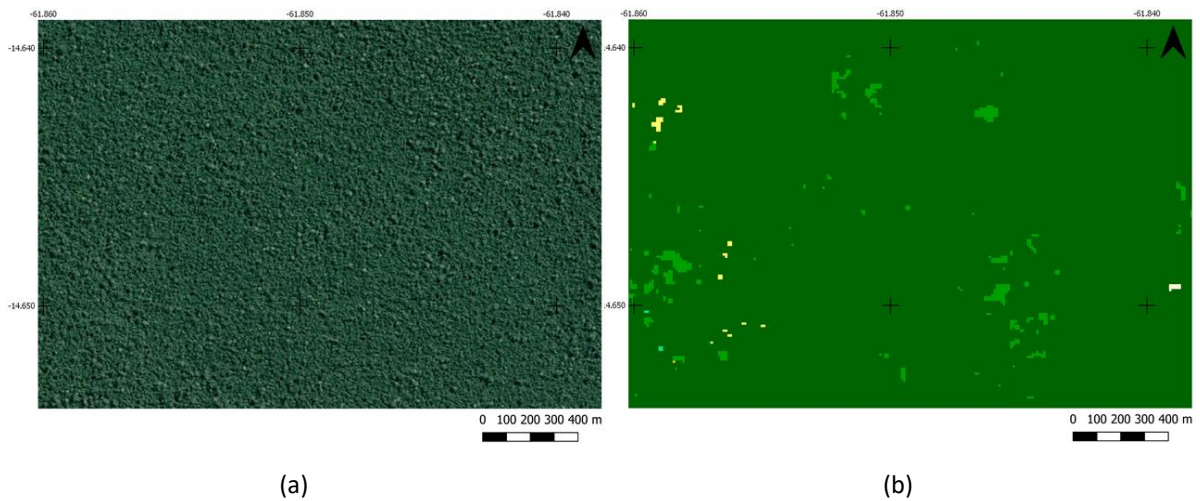


Figure 100. Illustration of misclassified cropland, bare areas, and evergreen tree cover pixels by comparing google imagery (a) and the CCI HRLC Amazonia zoom area (b)

Figure 46 shows that almost all roads, including highways, are classified as grassland. This is a recurring issue noticeable on the map. Confusion also sometimes appears with bare areas. Although some narrow roads or paths might indeed be classified as bare soil or grassland, this issue should not appear especially for highways (as pointed out by the red arrow) since their width is bigger than the 10 m spatial resolution of the map.

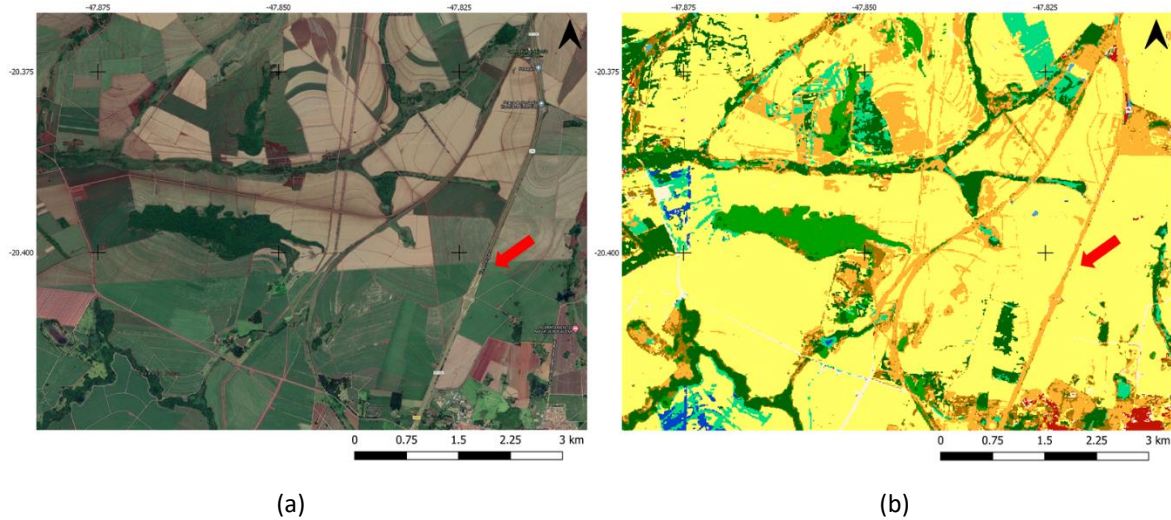


Figure 101. Illustration of roads detected as grassland by comparing google imagery (2020) (a) and the CCI HRLC Amazonia zoom area

Another noticeable issue is the presence of patterns of regularly flooded vegetation across wide permanent open water (Figure 47). This should be further investigated in light of the CCI HRLC legend.

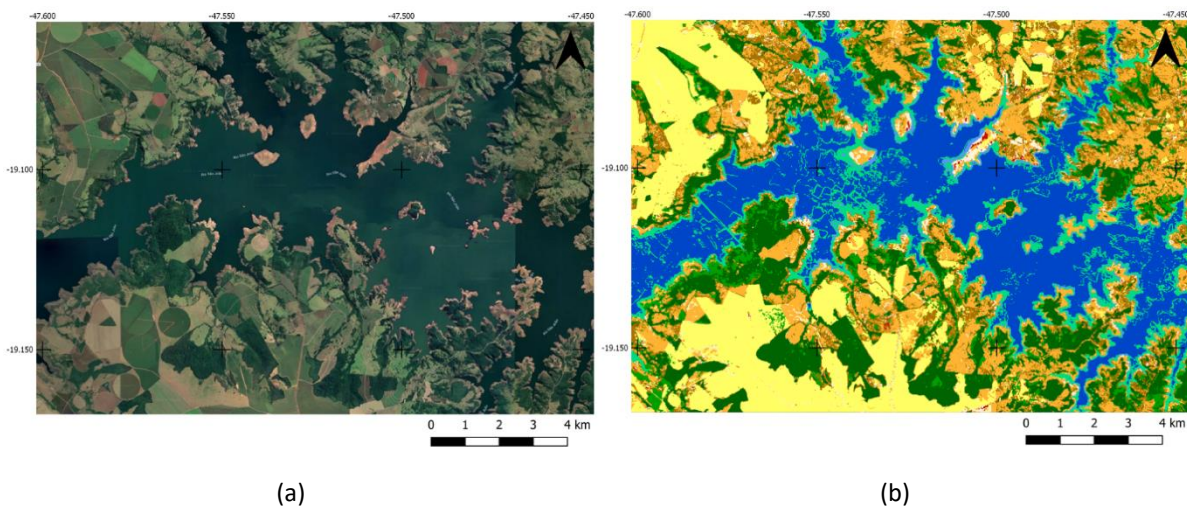


Figure 102. Illustration of contaminating grassland regularly flooded class by comparing google imagery (2020) (a) and the CCI HRLC Amazonia zoom area.

Some problems encountered in natural areas are reported in Figure 48 and Figure 49. First, we noticed an overestimation of the cropland class. In another area, we could notice an overestimation of the grassland regularly flooded class in the form of non-logical patterns.

Besides, one can also notice on the right of Figure 49 the confusion/mixing between cropland and grassland at the parcel level.

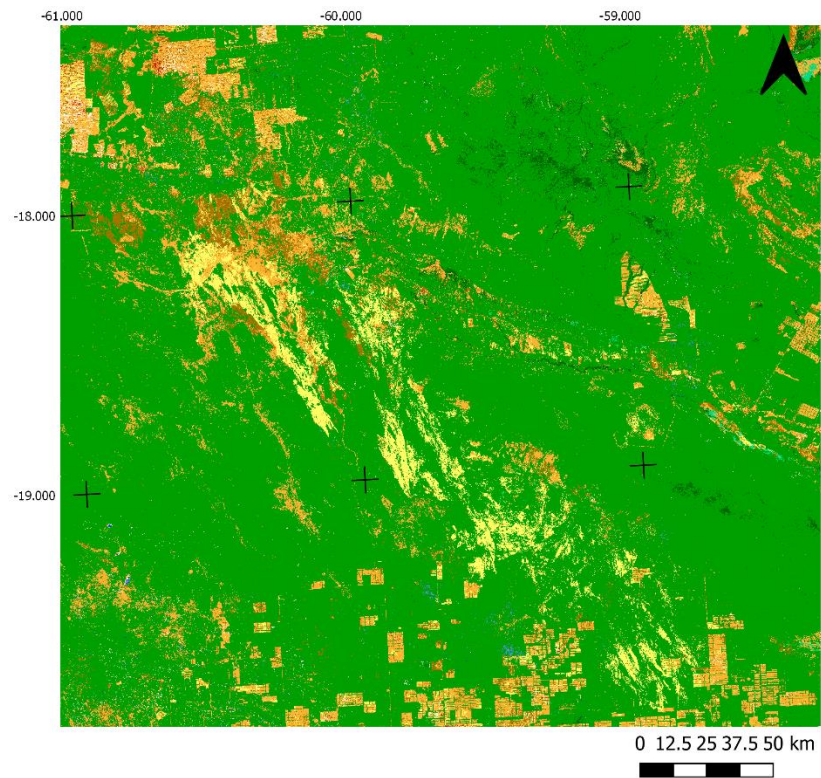


Figure 103. Illustration of cropland overestimation in natural areas on the CCI HRLC Amazonia zoom area.

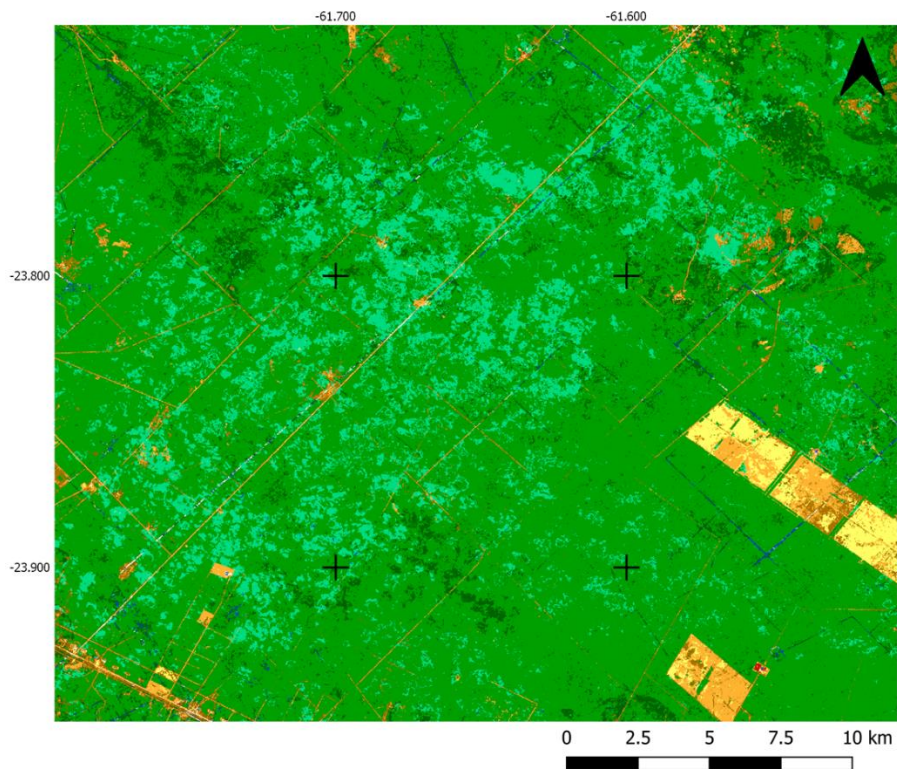


Figure 104. Illustration of grassland regularly flooded overestimation on the CCI HRLC Amazonia zoom area

Figure 50 shows the contamination of the water and wetland classes in urban areas.



Figure 105. Illustration of water and wetland contamination in urban areas in the CCI HRLC Amazonia zoom area

Finally, Figure 51 illustrates an issue that can be found in various regions of the map which is a processing artefact (pointed out by the red arrow).

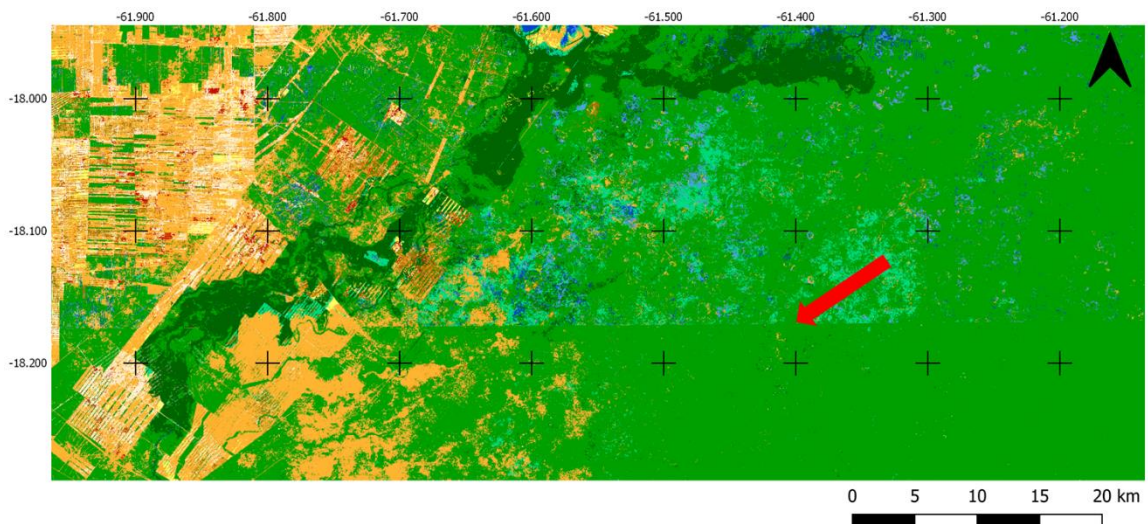


Figure 106. Illustration of processing artefact on the CCI HRLC Amazonia zoom area

7.2.1.2.4 Concluding remarks

The Amazonia zoom area map encounters several misclassification issues that are not consistent with the targeted 10 ms' spatial resolution:

- the major thematic errors (wrong LC labels) are the contamination of built-up and bare areas classes.

- most of the roads are detected either as grassland or bare area.
- isolated pixels are noticeable over a wide patch of homogenous land cover class.
- some shadows are detected as grassland regularly flooded or open permanent water.
- some water tracks are not detected, and unwanted patterns of permanent open water are visible on various areas of the map
- some natural areas are contaminated with cropland and wetland overestimations
- wetland and water classes are contaminating some urban areas
- some processing artefacts are visible

Although improvements have been noticed in the overlapping area between the RR prototypes and the zoom area, some other issues remain in the rest of the zoom area.

7.2.1.3 Siberia

7.2.1.3.1 Comparison with the Siberian RR prototype

An improvement can be noticed when comparing the overlapping area between the zoom area and the fused MRF RR prototype. First, as shown in Figure 52, there is a reduced overestimation of wetlands which is more consistent with the ESA GlobPermafrost map. Similarly, one can notice a reduction of the grassland overestimation in Figure 53.

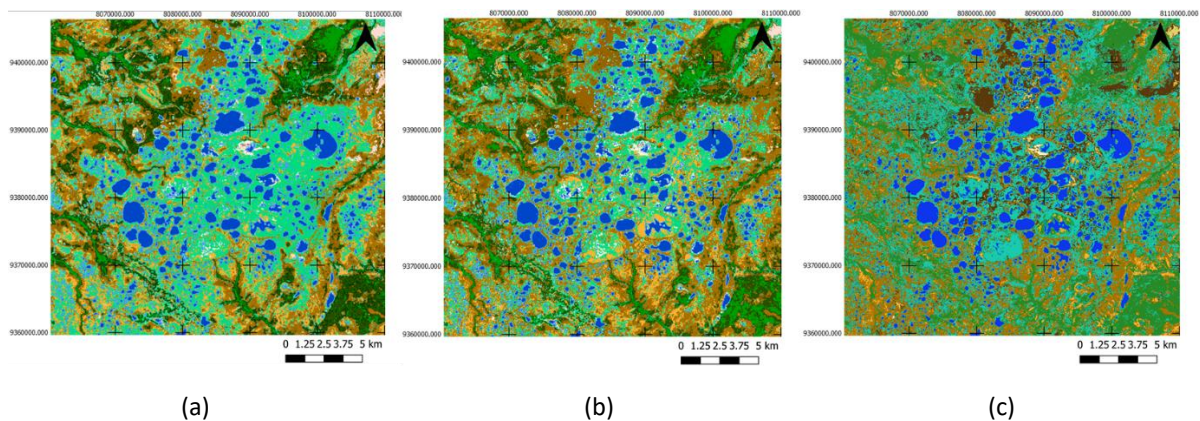


Figure 107. Illustration of reduced overestimation of wetland area by comparing the CCI HRLC Siberia RR prototype fused MRF (a) with the zoom area (b) and the ESA GlobPermafrost map (c)

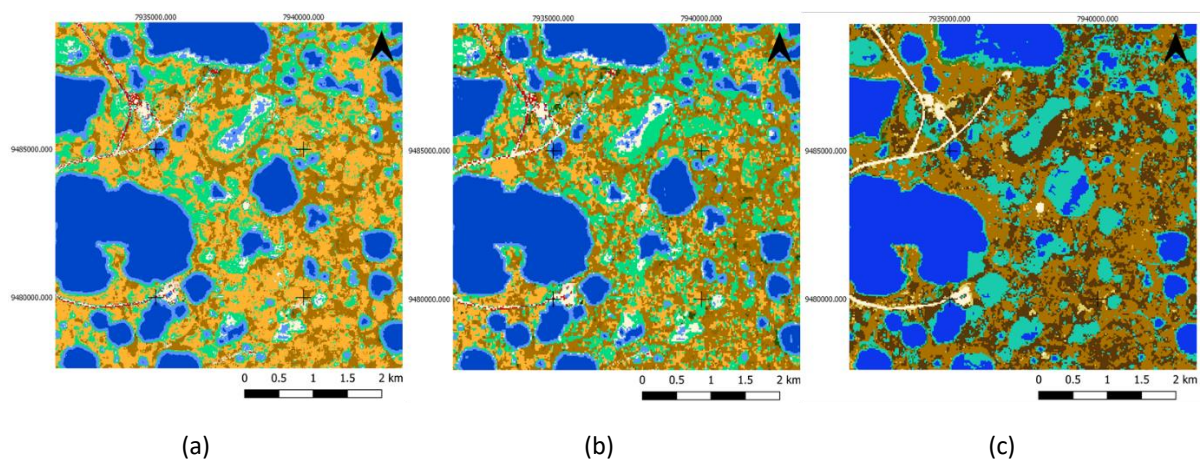


Figure 108. Illustration of reduced overestimation of grassland area by comparing the CCI HRLC Siberia RR prototype fused MRF (a) with the zoom area (b) and the ESA GlobPermafrost map (c)

7.2.1.3.2 Comparison with the ESA GlobPermafrost map [RD2]

When comparing the Siberia zoom area with the ESA GlobPermafrost map (Figure 54), one can notice that overall, the south region of the map (framed in red) seems to agree. However, there is a disagreement on the north region of the map (circled in red). The zoom area map seems to detect a good share of wetlands while this class is not represented at all on the ESA GlobPermafrost map.

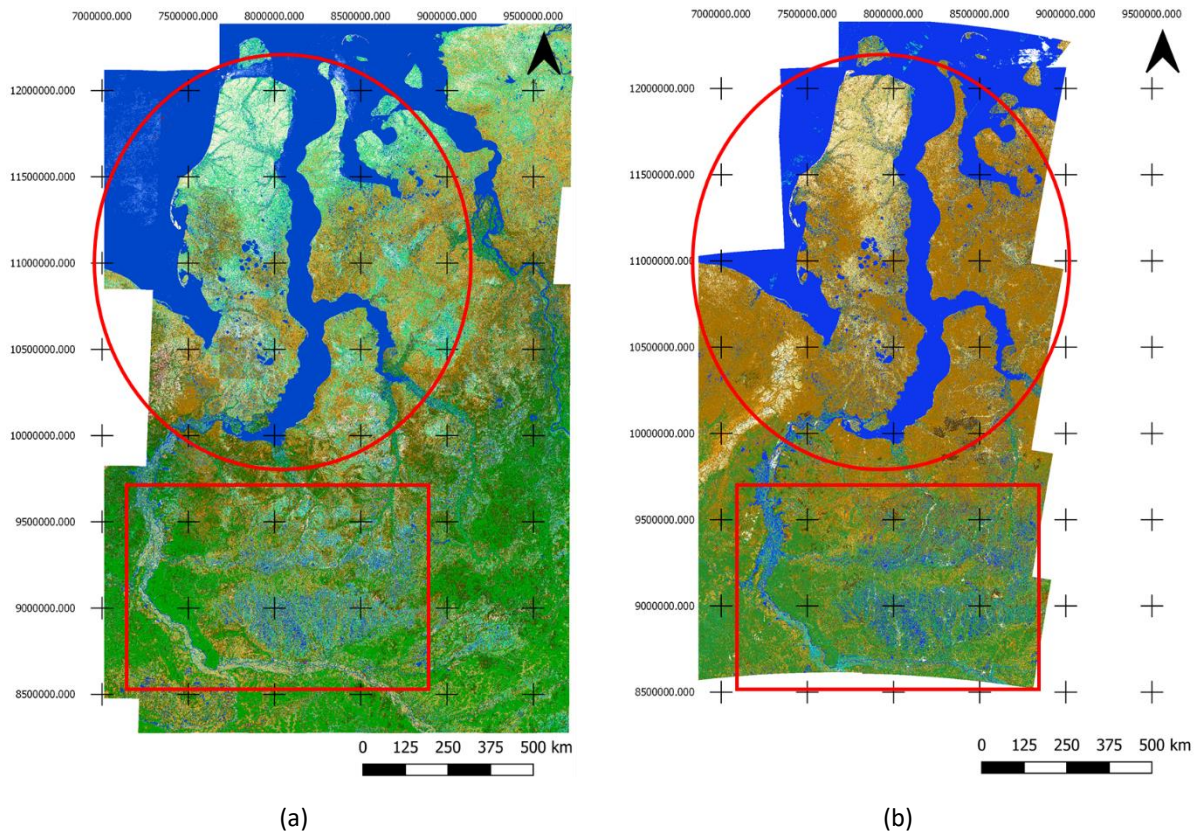


Figure 109. Comparison between the CCI HRLC Siberia zoom area (a) and the ESA GlobPermafrost map (b). Large similarities between both maps are observed in the southern part of the zoom area while divergences increase further North.

Figure 55 shows us that some disagreements between the Siberia zoom area and the ESA GlobPermafrost map are nevertheless noticeable in the southeast region of the map. The presence of bare areas does not seem consistent in an area where many water tracks are shaping the landscape. Besides, the ESA GlobPermafrost map predicts a wide plain of wetland.

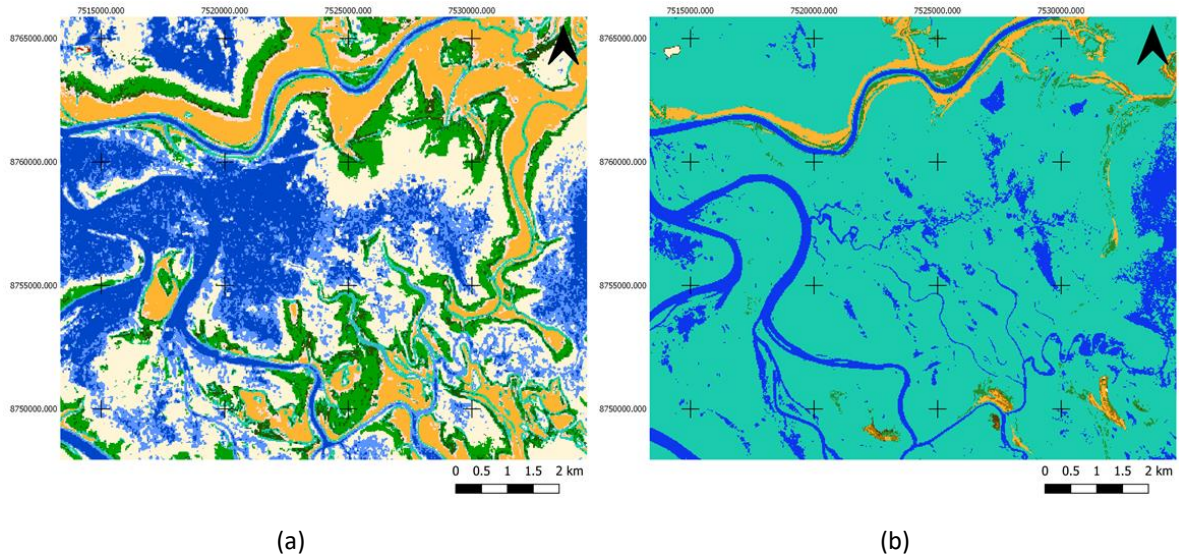
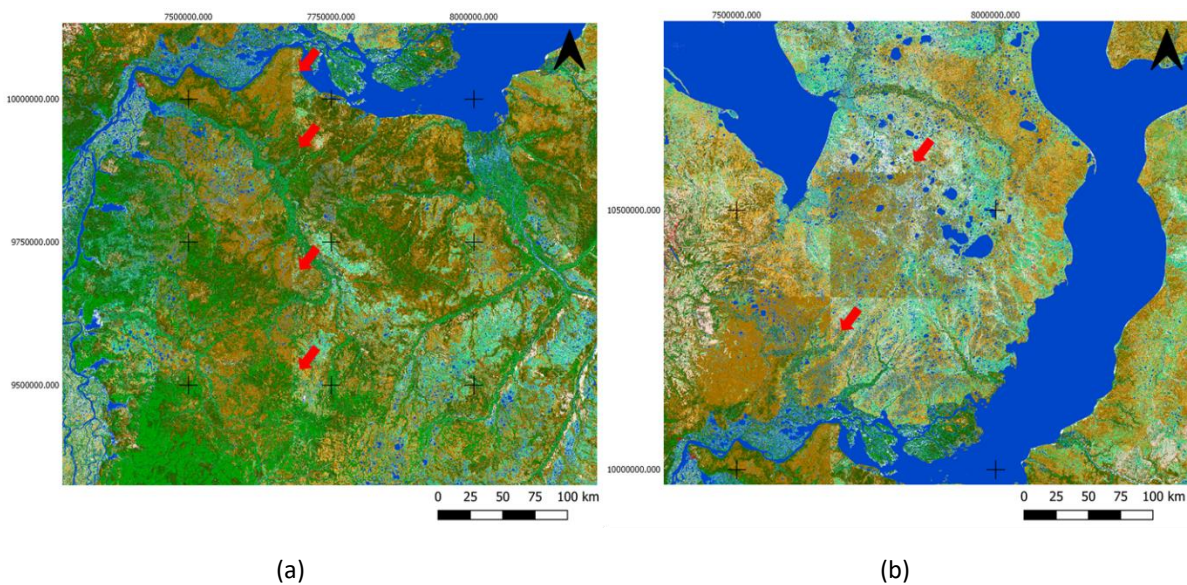
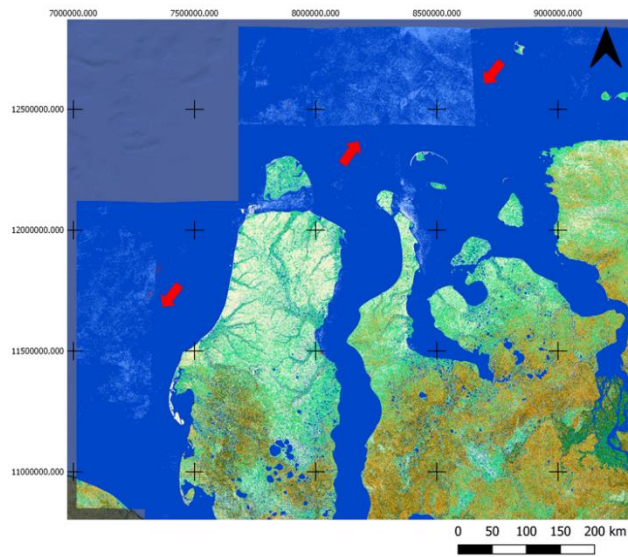


Figure 110. Comparison between the CCI HRLC Siberia zoom area (a) and the ESA GlobPermafrost map (b).

7.2.1.3.3 Qualitative assessment of the rest of the zoom area

On various areas of the map, one can notice a tile processing effect (Figure 56, pointed out by red arrows). Besides, Figure 56 (c) shows the detection of open seasonal water on a large body of open permanent water which is incoherent.

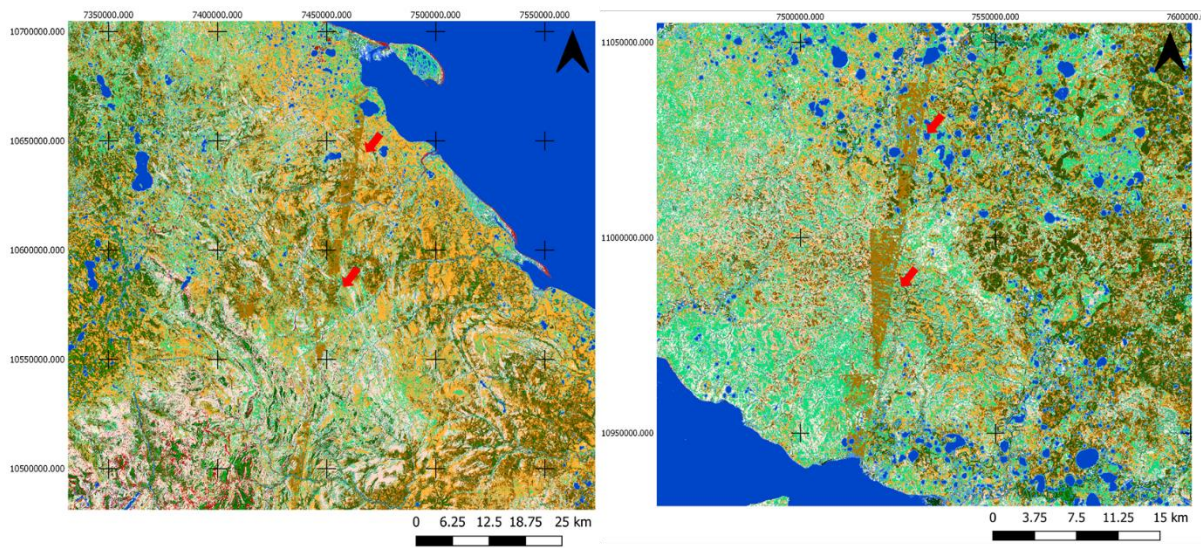




(c)

Figure 111. Illustration of a tile processing effect on various regions of the CCI HRLC Siberia zoom area (a), (b), and (c)

Another processing issue encountered on the map is the presence of remains of orbital tracks that cross the map from north to south (Figure 57).



(a)

(b)

Figure 112. illustration of a processing issue on the CCI HRLC Siberia zoom area (a) and (b).

One last processing issue is the presence of artefacts as one illustrated in Figure 58.

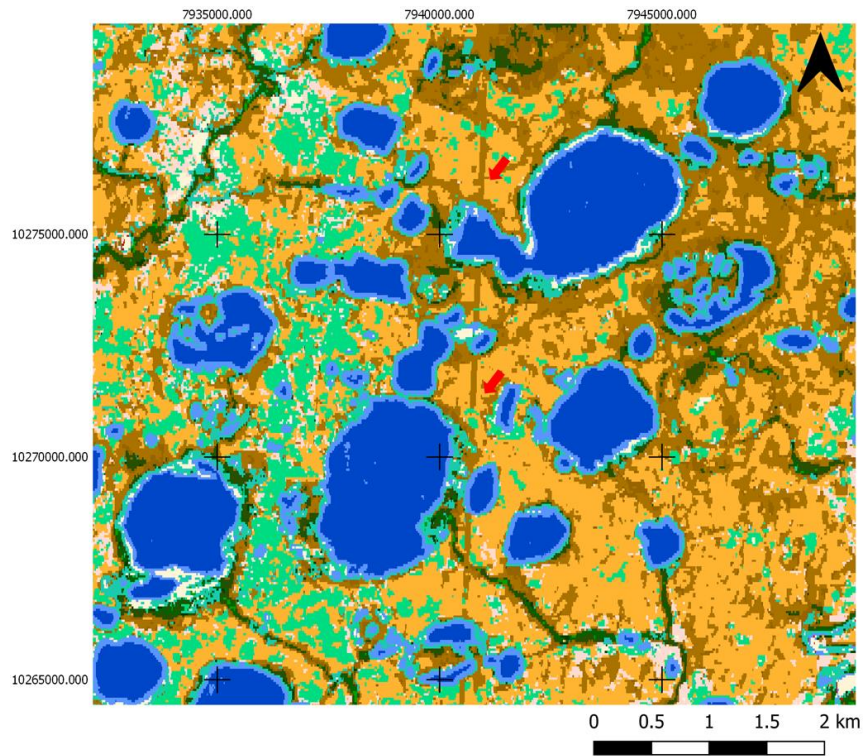


Figure 113. Illustration of an artefact on the CCI HRLC Siberia zoom area.

In terms of thematic errors, one can notice the presence of an overestimation of the built-up class as shown in Figure 59.

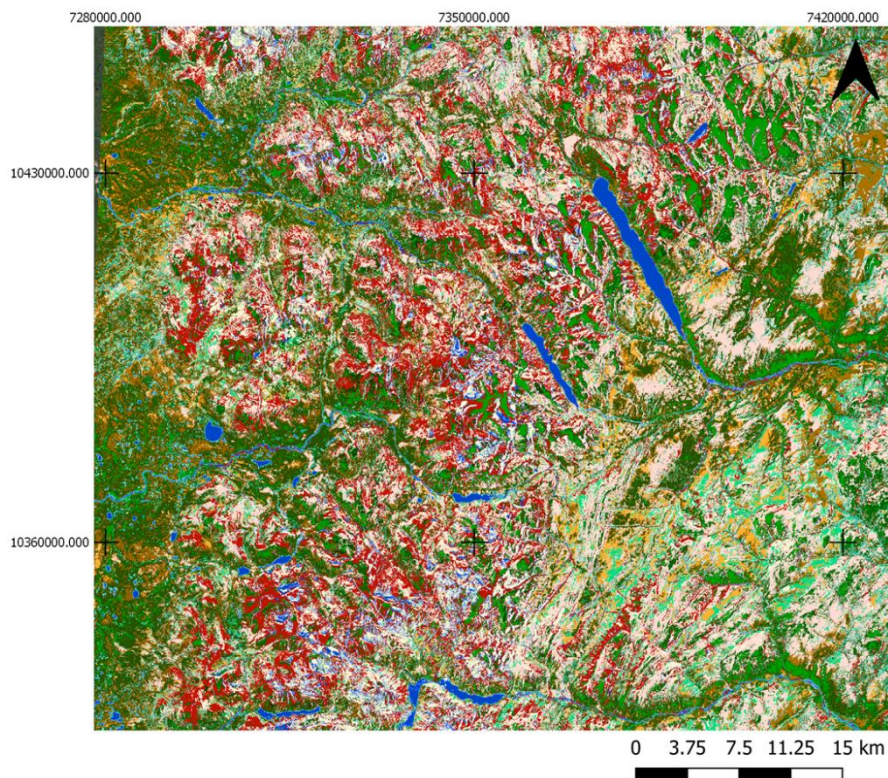


Figure 114. Illustration of built-up overestimation on the CCI HRLC Siberia zoom area.

7.2.1.3.4 Concluding remarks

To conclude, the Siberia zoom area shows improvements compared to the RR prototype fused MRF in terms of grassland and wetland overestimation.

However, when comparing the zoom area map to the ESA GlobPermafrost map, there is an important disagreement for the northern region of the map as well as several regions in the south.

The zoom area map also encounters several processing issues (S2 tiles, orbital tracks, and artefacts) that cause thematic errors (wrong LC label).

Finally, one major thematic error (wrong LC label) encountered on the map is the overestimation of the built-up class.

7.3 Quantitative assessment of the previous LC static maps

7.3.1 Siberia v20220624

MAP/REF	Tree cover evergreen needleleaf	Tree cover deciduous broadleaf	Tree cover deciduous needleleaf	Shrub cover	Grassland	Croplands	Woody vegetation aquatic or regularly flooded	Grassland vegetation aquatic or regularly flooded	Lichen and mosses	Bare areas	Built-up	Open Water	sum	UA	SE_UA
Tree cover evergreen needleleaf	0.10841	0.01314	0.04928	0.00329	0.00329				0.00329				0.18068	60	6.7
Tree cover deciduous broadleaf	0.0246	0.07871	0.01476	0.00492	0.00984	0.00246							0.13528	58.2	6.7
Tree cover deciduous needleleaf	0.01643		0.01095		0.00274		0.00274						0.03285	33.3	14.2
Shrub cover		0.00346		0.01555	0.00346							0.00173	0.02419	64.3	13.3
Grassland		0.0051		0.02548	0.24974	0.04077	0.0051	0.01529	0.01529	0.01529	0.0051	0.0051	0.38226	65.3	5.5
Croplands		0.00138		0.00138	0.00691	0.06771				0.00138	0.00276		0.08153	83.1	4.9
Woody vegetation aquatic or regularly flooded	0.00121			0.00789	0.00303		0.00121	0.00364		0.00061			0.01759	6.9	4.8
Grassland vegetation aquatic or regularly flooded				0.0053	0.01458			0.0053	0.00133			0.00133	0.02783	19	8.8
Lichen and mosses				0.00067	0.00235			0.00034	0.00403	0.00067			0.00806	50	10.4
Bare areas				0.00542	0.00217				0.00163	0.00596		0.00054	0.01571	37.9	9.2
Built-up	0.00012			0.00025	0.00037	0.00025				5e-04	0.00262		0.00412	63.6	8.5
Open Water								0.00187				0.08802	0.08989	97.9	2.1
sum	0.15077	0.10179	0.07498	0.07015	0.29848	0.11119	0.00905	0.02644	0.02556	0.02441	0.01048	0.09671	1		
PA	71.9	77.3	14.6	22.2	83.7	60.9	13.4	20.1	15.8	24.4	25	91		63.8	OA
SE_PA	4.7	6.8	5.8	5.3	2.6	7.8	11.8	10.1	6.5	9.9	13.3	5.2		2.7	SE_OA

Figure 115. Area-based confusion matrix of the Siberia static map v20220624 with grouping of the original legend. Class-related cells are expressed in terms of proportions of area (range 0 – 1). The accuracy estimates were derived using 549 homogeneous samples photo-interpreted with certainty. Accuracy figures are reported in % with their standard error (95% confidence level). OA, PA and UA stand for overall, producer, and user accuracy, and SE for standard error.

MAP/REF	Tree cover evergreen broadleaf	Tree cover deciduous broadleaf	Shrub cover evergreen	Shrub cover deciduous	Grassland	Croplands	Woody vegetation aquatic or regularly flooded	Grassland vegetation aquatic or regularly flooded	Bare areas	Built-up	Open Water seasonal	Open Water permanent	sum	UA	SE_UA
Tree cover evergreen broadleaf	0.31348	0.046	0.02215	0.00341	0.0017		0.01704						0.40378	77.6	2.7
Tree cover deciduous broadleaf	0.01106	0.03872	0.00553	0.01798				0.00277					0.07606	50.9	6.8
Shrub cover evergreen	0.01225	0.00098	0.00539	0.00098	0.00049								0.02009	26.8	7
Shrub cover deciduous	0.00839	0.00252	0.00755	0.00168	0.00419	0.00084							0.02517	6.7	4.6
Grassland	0.00594		0.07321	0.01583	0.2038	0.02374		0.00791	0.00198				0.33241	61.3	3.8
Croplands			0.00581	0.00194	0.01065	0.08038							0.09878	81.4	3.9
Woody vegetation aquatic or regularly flooded	0.00024						0.00055	0.00028			4e-05	2e-04	0.00131	42.4	8.7
Grassland vegetation aquatic or regularly flooded	0.00039		0.00019		0.00058		0.00019	0.00136				0.00213	0.00485	28	9.2
Bare areas	0.00017		0.00017		0.00066	0.00066			0.00331				0.00496	66.7	8.8
Built-up	0.00017				0.00025				8e-05	0.00299			0.00349	85.7	5.5
Open Water seasonal					5e-05			5e-05	5e-05		0.00011	0.00104	0.00131	8.3	5.8
Open Water permanent								4e-04	4e-04			0.027	0.02779	97.1	2
sum	0.35208	0.08822	0.12	0.04181	0.22239	0.10563	0.01778	0.01277	0.00582	0.00299	0.00015	0.03037	1		
PA	89	43.9	4.5	4	91.6	76.1	3.1	10.6	56.8	100	73.4	88.9		67.9	OA
SE_PA	1.5	5.4	1.2	2.8	1.7	4.9	1.1	4.8	20	0	23.7	1.5		1.8	SE_OA

Figure 116. Error matrix of the Amazonia static land cover map 2019 v20220414 expressed in terms of proportions of area (range 0 – 1) with accuracy estimates (%) and their standard errors (%). Rows refer to the map and columns to the reference. PA: producer accuracy, SE: standard error, UA: user accuracy, OA: overall accuracy.

	Tree cover evergreen broadleaf	Tree cover deciduous broadleaf	Shrub cover evergreen	Shrub cover deciduous	Grassland	Croplands	Grassland vegetation aquatic or regularly flooded	Bare areas	Built-up	Open Water seasonal	Open Water permanent	sum	UA	SE_UA
Tree cover evergreen broadleaf	0.15129						0.00204					0.15333	98.7	1.3
Tree cover deciduous broadleaf	0.0085	0.03401	0.0051	0.0102	0.0102	0.0017	0.0017					0.07142	47.6	7.8
Shrub cover evergreen	1e-05		4e-05		2e-05	1e-05		0				8e-05	50	9.3
Shrub cover deciduous	0.00187	0.01682	0.00187	0.06166	0.02429	0.00374						0.11023	55.9	6.5
Grassland	0.00189	0.02082	0.01892	0.0246	0.14571	0.03028	0.01703	0.05677	0.01135			0.32738	44.5	3.8
Croplands		0.00544	0.00362	0.00725	0.01631	0.07791	0.00906	0.00544				0.12501	62.3	5.9
Grassland vegetation aquatic or regularly flooded	7e-05				0.00041		0.00157	2e-04		0.00014	0.00041	0.00279	56.1	7.8
Bare areas					0.00222		0.00222	0.17071	0.00222		0.00222	0.17958	95.1	2.4
Built-up	4e-05				0.00011	4e-05		4e-05	0.00138	4e-05	4e-05	0.00169	81.8	5.9
Open Water seasonal			1e-05		1e-05	3e-05	1e-05	3e-05		6e-05	0.00044	0.00059	10	3.9
Open Water permanent							0.00036			0.00358	0.02397	0.0279	85.9	4
sum	0.16367	0.07707	0.02957	0.10371	0.19928	0.11369	0.03398	0.23319	0.01495	0.00381	0.02707	1		
PA	92.4	44.1	0.1	59.5	73.1	68.5	4.6	73.2	9.2	1.5	88.5		66.8	OA
SE_PA	2.5	6.4	0	5.6	3.7	5.2	1.2	3.2	3.2	0.7	7.3		1.8	SE_OA

Figure 117. Error matrix of the Africa static land cover map 2019 v20221027 expressed in terms of proportions of area (range 0 – 1) with accuracy estimates (%) and their standard errors (%). Rows refer to the map and columns to the reference. PA: producer accuracy, SE: standard error, UA: user accuracy, OA: overall accuracy.

7.4 First visual quality assessment of the Amazonia historic LC maps

This section concerns the validation of an old version of the historical maps of the Amazon dating from January 2021. The different periods are analysed over areas of stable LC and areas of LC change to assess their respective quality.

7.4.1 Processing artefacts

Generally, a larger proportion of processing artefacts are observed over the six periods, compared to the RR prototypes and the zoom area map. These artefacts are located along the western side of the area with part of the tiles missing, but also in large forested areas where swath effects are visible. These artefacts are present in all six periods (Figure 67).

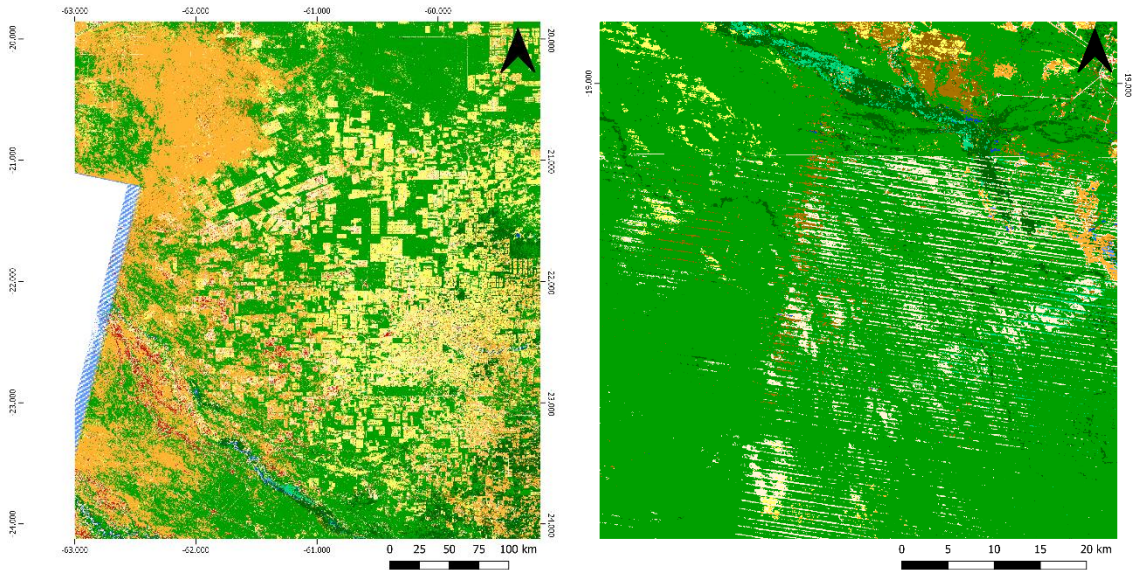
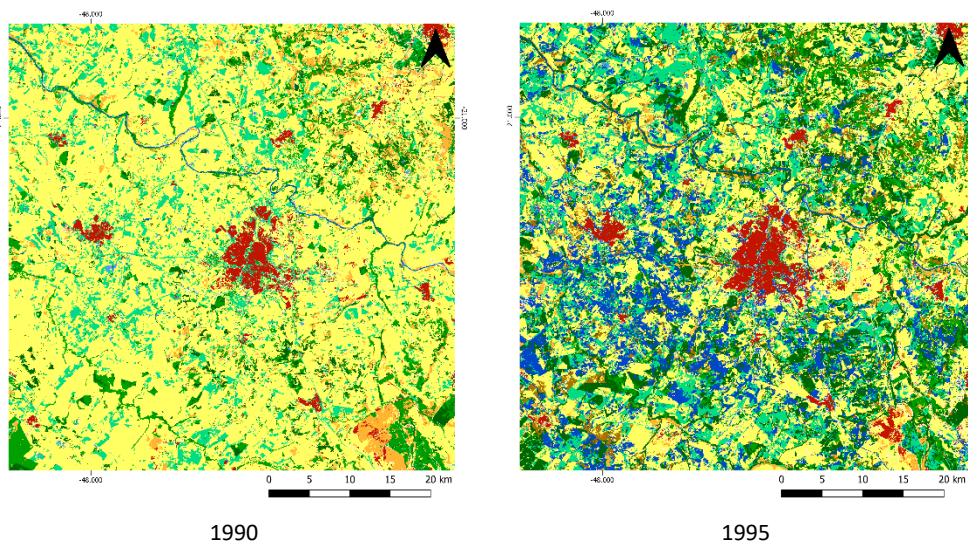


Figure 118. An example of artefacts related to the absence of data at the western edge of the tile (left) and swath effects (right). The example is shown for the 2015 period but these artefacts are present in all six periods.

7.4.2 Area of stable LC

When comparing the six periods over a stable LC area, for example in an open cropland landscape with an urban centre and rivers (few land cover change dynamics), it appears that the different periods present very different results (Figure 68). Large contaminations of open water temporary/permanent and grassland vegetation flooded classes are present in all periods except 2015. Confusion between grassland and cropland is also observed. These observations are largely present over the whole product area.



1990

1995

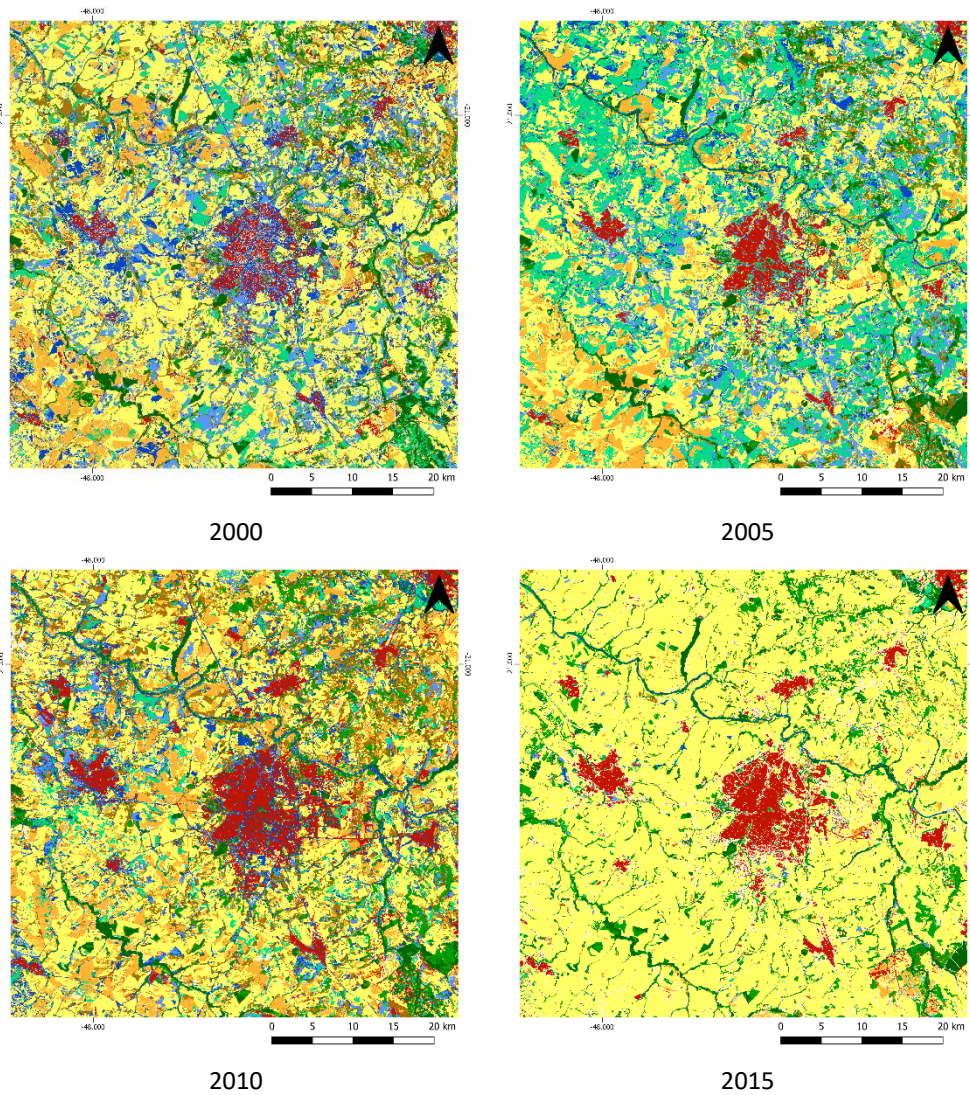


Figure 119. Comparison of the six periods over an area of stable land cover. All six periods present very different results, with contamination of open water permanent and grassland vegetation flooded classes, and a general confusion between grassland and cropland.

7.4.3 Area of LC change

When comparing the six periods over an area of LC change, for example in a deforestation dynamic area, it appears that the change in tree cover is well detected (Figure 69). However, low vegetation areas present instability in the LC class, mainly a confusion of grassland and cropland that do not reflect actual dynamics. Figure 70 shows that while the LC change in water cover is detected, the other LC classes are not consistent in time.

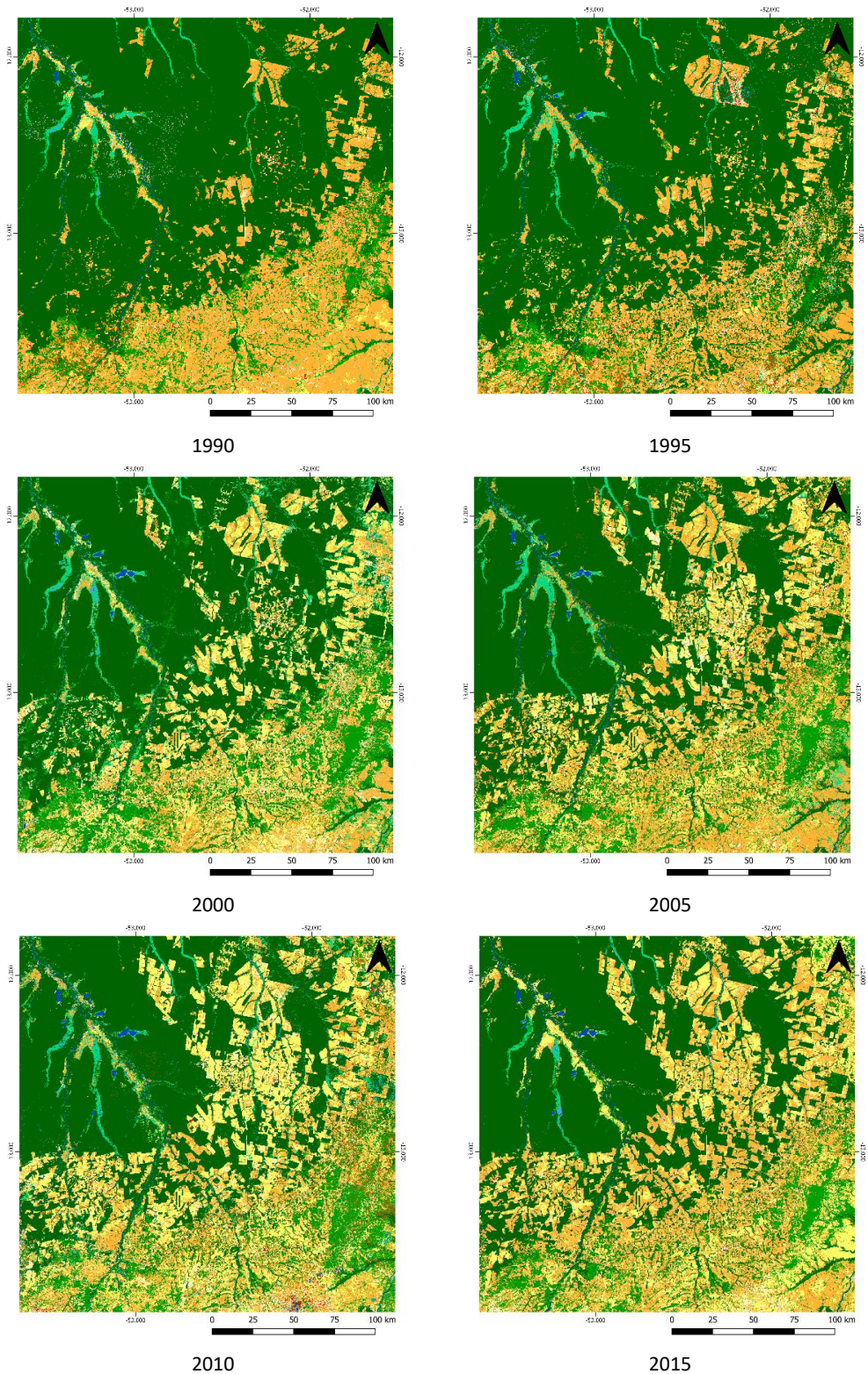


Figure 120. Comparison of the six periods over an area of land cover change. The deforestation patterns are detected, but the land cover classes are not stable over time, especially grassland and cropland.

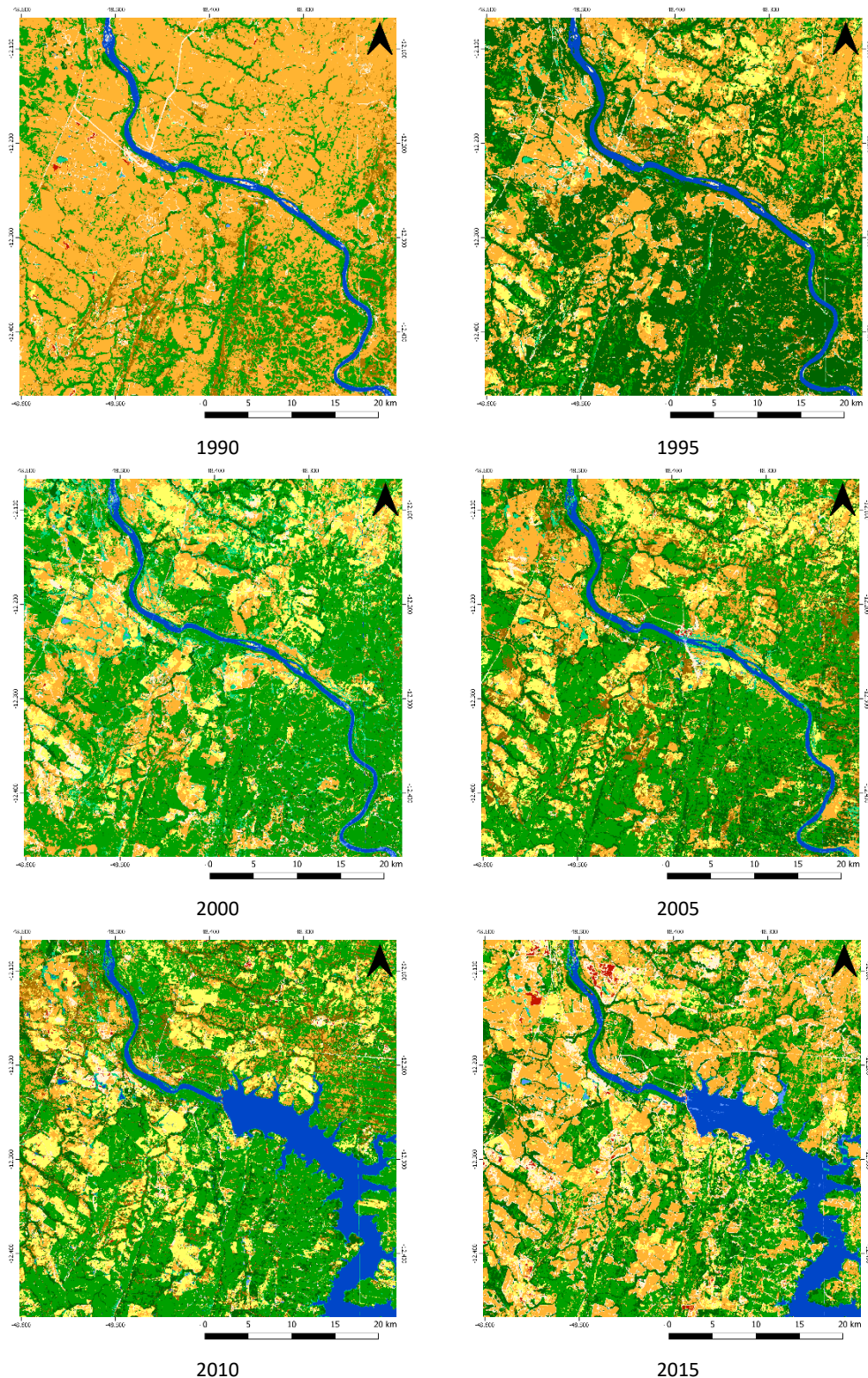


Figure 121. Comparison of the six periods over an area of land cover change. The dam lake formation is detected, but the appearance and disappearance of tree cover areas are not consistent, even more with a change in tree cover class. The confusion between grassland and cropland is also present, along with contamination of the bare soil class.

7.4.4 Concluding remarks

In conclusion, besides some important processing artefacts, the different periods are most often not consistent in time. Although major land cover changes are present, many areas present very different classification results through the different periods, with large contaminations and confusion between classes.

	Ref	CCI_HRLC_Ph1-D4.1_PVIRb		
	Issue	Date	Page	
	2.rev.2	10/02/2023	114	